Contact mechanics and dynamics of frictional systems under oscillation

vorgelegt von

M.Sc. Mikhail Popov

an der Fakultät V – Verkehrs- und Maschinensysteme
der Technischen Universität Berlin
zur Erlangung des akademischen Grades
Doktor der Ingenieurwissenschaften
– Dr.-Ing. –
genehmigte Dissertation

Promotionsausschuss

Vorsitzender:	Prof. Dr.-Ing. Christian Oliver Paschereit
Gutachter:	Prof. Dr. rer. nat. Wolfgang H. Müller
Gutachter:	Prof. Dr. rer. nat. Heinz Sturm
Gutachter:	Prof. Dr.-Ing. habil. Georg-Peter Ostermeyer
Gutachter:	Prof. Dr.-Ing. habil. Sergej Fatikow

Tag der wissenschaftlichen Aussprache: 10. November 2022

Berlin 2022

Acknowledgments

I would like to thank my parents, Elena and Valentin, for the unwavering support they have shown me over the years, and, in the case of my father, for introducing me to the field of tribology in the first place.

Part of this work was completed during my two years in Tomsk, which I remember fondly, and for which I am grateful to the late Prof. Sergey G. Psakhie, who never hesitated to help me in any academic or personal matter, and with whom I enjoyed many interesting discussions. Many others have also helped to make my stay in Tomsk productive and enjoyable, even though not mentioned here by name.

Many thanks are also due to my mentors, Prof. Wolfgang H. Müller and Prof. Heinz Sturm, who took it upon themselves to supervise this work, and have helped me over a number of hurdles. The support of Prof. Georg-Peter Ostermeyer, Prof. Sergej Fatikow and Prof. Oliver C. Paschereit is likewise much appreciated.

Last but not least, I would like to thank my colleagues and co-authors, including those from other research projects and from my xTribo days: Lars Voll, Jasminka Starcevic, Roman Pohrt, Justus Benad, Johannes Thaten, Qiang Li, Andrei Dimaki, Evegeny Shilko, Alexey Tsukanov, among many others.

Abstract

This thesis consists of a series of publications dealing with frictional contacts under the influence of externally applied vibration. The considered cases fall into two large groups: frictional damping and active control of friction through vibration. Phenomenologically, these two cases are quite distinct, but they can also be understood as two sides of the same system—a vibrating frictional couple with or without bulk sliding. A flexible model is presented that is able to describe both of these effects. In this thesis, it is applied to the following variations of the basic problem:

- Static and sliding friction, as well as damping in stationary contacts.
- Normal, longitudinal and transverse vibration, as well as superpositions thereof.
- Passive friction reduction and active frictional drives and ratchets.
- Displacement-controlled and inertial systems.

The proposed model differs from prior art first and foremost in being purely *macroscopic*. It is based on classical contact mechanics and dynamics and does not postulate any micro-scale processes other than Amontons friction. A key role is played by the compliance of the contact. Unlike the many specialized empirical and semi-empirical friction laws currently used to describe transient frictional phenomena, the proposed model is simple, physical, free of fitting parameters and generalizes to a wide variety of situations. The ten publications forming this thesis explore a few of them in detail.

Despite being rooted in the same model framework, multiple distinct mechanisms and behaviors can be identified in the studied systems:

- Damping in the case of combined normal and tangential oscillation leads to the qualitatively new effect of Relaxation Damping, whose asymptotic behavior differs from the classical Mindlin damping: Whereas in Mindlin damping (only in-plane motion) the dissipation depends on the coefficient of friction μ and goes to zero as μ goes to infinity, introducing the normal degree of freedom enables damping even with infinite friction, and has a regime where damping does not depend on μ even if it is finite.
- Normal oscillation reduces sliding friction by inducing a walking-like stick-slip motion, and is only effective up to a certain maximum sliding velocity. However, resonances in the surrounding system can be exploited to reduce friction at any sliding velocity.
- Transverse oscillation redirects the average friction vector away from the sliding direction, while actually increasing the total dissipated energy. Unlike with normal vibration, stick-slip has no special significance.

- Superimposed normal and tangential oscillation cover a continuum from reduction of friction, over asymmetric resistance (frictional ratchets) to active drives.

It is hoped that this work will contribute to better understanding and more precise modeling of friction under complicated and dynamic loading scenarios. Such situations frequently arise in modern applications of tribology, e.g., robotics and high-precision positioning systems. It is also the aim of this thesis to demonstrate the importance of the macro scale in tribology in general. In the opinion of the author, the conception of friction as a localized phenomenon is often inappropriate, and can easily lead to incorrect modeling and measurements. This view is supported with additional examples from the literature.

Zusammenfassung

Die vorliegende Dissertation besteht aus einer Reihe von Publikationen, die sich mit Reibkontakten unter Einfluss von extern angebrachten Schwingungen befassen. Die Publikationen lassen sich thematisch in zwei Gruppen einordnen: Reibungsdämpfung und aktive Reibungsbeeinflussung. Obwohl beide Themengebiete eine eigene Phänomenologie aufweisen, können sie dennoch als verschiedene Aspekte desselben Systems betrachtet werden, nämlich als vibrationsbehaftete Kontakte mit oder ohne makroskopisches Gleiten. Es wird ein flexibles Modell vorgestellt, welches beide Fälle gut beschreiben kann. Im Rahmen dieser Dissertation werden mithilfe dieses Modells verschiedene Variationen des Grundproblems untersucht:

- Haft- und Gleitreibung, sowie stationäre Reibungsdämpfung.
- Einfluss von Vibration in Normalrichtung, Gleitrichtung, orthogonal zur Gleitrichtung in der Kontaktebene, sowie verschiedene Kombinationen davon.
- Reibungsverringerung, richtungsabhängige Reibung und aktive Reibantriebe.
- Weggesteuerte (quasistatische) und massenbehaftete Systeme.

Der vorgestellte Ansatz unterscheidet sich von Vorarbeiten in erster Linie durch seine vollständig *makroskopische* Natur. Er basiert auf der klassischen Kontaktmechanik und Systemdynamik, und macht keine Annahmen über Prozesse auf der Mikroskala, abgesehen von dem einfachen Amontons'schen Reibgesetz. Eine besonders wichtige Rolle wird der endlichen Kontaktsteifigkeit der Verbindung eingeräumt. Im Gegensatz zu den vielen empirischen und semi-empirischen Reibgesetzen, die für die Beschreibung von Reibung unter dynamischer Beanspruchung entwickelt wurden, ist das hier verwendete Modell sehr einfach, physikalisch begründet, enthält keine Fittingparameter, und kann für eine Vielzahl von unterschiedlichen Situationen angepasst werden. In den zehn Publikationen, die die vorliegende Arbeit ausmachen, werden einige dieser Möglichkeiten im Detail untersucht.

Obwohl alle untersuchten Systeme auf denselben Modellvorstellungen beruhen, zeigen sie dennoch recht unterschiedliches Verhalten, und ähnliche Effekte können oft unterschiedlichen Mechanismen zugeschrieben werden. Einige Beispiele dafür sind:

- Dämpfung im Kontakt mit überlagerter Vibration in Normal- und Tangentialrichtung führt zum *Relaxation Damping*, welches sich qualitativ von der klassischen Mindlin-Dämpfung unterscheidet: Bei der Mindlin-Dämpfung (nur Tangentialschwingungen) ist der Energieverlust vom Reibungskoeffizienten μ abhängig, und geht gegen Null, wenn μ sehr groß wird. Wenn aber Schwingungen in Normalrichtung hinzugefügt werden, dann hat der Dämpfungskoeffizient selbst bei vollständigem Haften einen endlichen Wert. Unter bestimmten Bedingungen ist dieser Grenzwert auch bei endlichen Reibkoeffizienten gültig.

- Gleitreibung lässt sich durch Schwingungen in Normalrichtung reduzieren, wobei im Kontakt eine Stick-Slip Bewegung auftritt, die die Energiedissipation im Vergleich zum normalen Gleiten verringert. Dieser Prozess ist grob mit dem Gehen (statt Schleifen) vergleichbar, und is geschwindigkeitsabhängig. Bei gegebenen Frequenz und Amplitude ist die Reduktion der Reibkraft nur bis zu einer Maximalgeschwindigkeit möglich. Allerdings können Resonanzen im System ausgenutzt werden, um Reibung bei einer beliebigen Gleitgeschwindigkeit zu verringern.

- Transversalschwingungen (orthogonal zur Gleitrichtung in der Ebene) können den Reibungskoeffizienten ebenfalls reduzieren, aber auf eine andere Art und Weise: Der Betrag der momentanen Reibkraft bleibt immer konstant, aber die Richtung oszilliert in der Ebene, so dass in der Projektion auf die Bewegungsrichtung die Reibkraft scheinbar kleiner wird. Allerdings steigt gleichzeitig die durch die Reibung insgesamt dissipierte Energie. Bei Transversalschwingungen kann Stick-Slip ebenfalls auftreten, spielt aber keine besondere Rolle. Eine feste Obergrenze für die Gleitgeschwindigkeit gibt es nicht.

- Auch Schwingungen in Gleitrichtung können die Reibung verringern. In Kombination mit Normalschwingungen ist ein Kontinuum von Systemverhalten, angefangen mit verringerter Reibung, über richtungsabhängige Reibung (*Dynamic Ratchets*), bis zu aktiven Reibantrieben realisierbar.

Diese Arbeit stellt hoffentlich einen Beitrag zum besseren Verständnis und Modellierung von dynamischen Reibungsphänomenen dar. Trockene Reibung unter Einfluss von Vibration sowie Kraft-, Geschwindigkeits-, und Richtungsänderungen ist in vielen technischen Anwendungen zu finden, insbesondere in aktuellen Technologien wie der Robotik und in hochpräzisen Positionierungssystemen. Abgesehen von konkreten Anwendungen unterstreicht die vorliegende Dissertation auch die allgemeine Wichtigkeit der Makroskala in der Tribologie. Es wird in der Praxis oft angenommen, dass Systemdynamik und „intrinsische" Reibung mehr oder weniger getrennt betrachtet werden können. Nach Ansicht des Autors ist diese Betrachtung nicht mehr zeitgemäß und kann leicht zu falschen Modellansätzen und unzuverlässigen Messwerten führen. Zusätzliche Beispiele aus der Literatur für mögliche „Skalenfehler" werden im letzten Kapitel diskutiert.

Contents

List of Figures

Nomenclature

Abbreviations

COF	coefficient of friction
MDR	method of dimensionality reduction (in contact mechanics)

Greek symbols

α	dimensionless variable
β	dimensionless variable
γ	damping constant
μ	coefficient of friction
μ_0	intrinsic coefficient of friction
μ_s	static coefficient of friction
$\bar{\mu}$	macroscopic coefficient of friction
ν	Poisson ratio
ρ	fiber aspect ratio
τ	characteristic relaxation time
φ	phase of an oscillation
φ_0	phase difference
Ψ_w	waveform-specific friction reduction function
ω	angular frequency

Latin characters

a	contact radius
A	displacement amplitude
A_F	force amplitude
d	indentation depth

E	elastic modulus
E^*	reduced elastic modulus
f	frequency
F	force
g	dimensionless waveform in force context
G	shear modulus
G^*	reduced shear modulus
$\tilde{G}$	reduced shear modulus for torsional contact
k	stiffness / spring constant
K	complete elliptic integral of the first kind
l_0	average in-plane displacement
m	mass
R	radius of curvature
t	time
T	period of oscillation
u	displacement
$\bar{u}$	average displacement
v_0	bulk sliding velocity
v_c	critical velocity of controllability
w	dimensionless waveform in displacement context
W	work
$\tilde{y}_0$	normalized transverse amplitude

Chapter 1

Introduction

1.1 On Friction and Friction Laws

Dry friction is a deceptively complex phenomenon. Despite its great technological importance and more than two centuries of serious scientific research, it still defies quantitatively accurate, *ab initio* prediction. Upon closer examination, this is not entirely surprising. Most surfaces exhibit roughness and chemical and structural heterogeneity at the microscopic level, and actual contact is usually limited to a few hotspots that account for a small fraction of the apparent contact area [8]. Due to the high stresses encountered in these microcontacts, many nonlinear processes may occur there, including complex elastic and plastic deformation, fracture, phase changes, chemical reactions, interaction with wear particles, etc. [82]. All of this is notoriously difficult to model mathematically. As Wolfgang Pauli put it, "God made the bulk; surfaces were invented by the devil."[1]

It is actually quite remarkable, given all this microscopic complexity, that relatively simple and useful "laws" of friction exist at all. The earliest and still widely used friction law is $F = \mu F_n$, which asserts that the force of friction is proportional to the normal load and mostly independent of other factors. The constant of proportionality μ is known as the coefficient of friction (COF), and is supposed to depend only on the materials of the contacting bodies. This simple equation is widely known as Amontons' law [3], and is only a very rough approximation of real friction. A much more sophisticated view was introduced by Charles-Augustin de Coulomb around 1780 [11, 66]. Through careful measurements, Coulomb found that the coefficient of friction is not really a constant, but rather depends on many factors, such as sliding velocity, normal load, time of rest, cleanliness of surfaces, etc. Many additional factors have since been added to that list, e.g., apparent contact area, surface roughness and patterning, temperature and humidity. The shape of the contact and the stiffness of the measurement apparatus are also known to exert an influence [84].

A number of additional phenomena become relevant when friction occurs under non-steady-state conditions, such as during stick-slip transitions or changes of velocity. One example is the kinetic (explicitly time-dependent) behavior of friction, which was already known to Coulomb at least in principle, and was later studied by Dieterich [15, 16] in the context of rock friction and earthquake dynamics. On the basis of this work, Ruina [69] and Rice [68] formulated the first rate-state friction laws, which depend on time and one or more internal state variables. It is thought that the phenomenon is caused by thermally-activated aging processes at the micro scale.

[1] As quoted by Schroeder in [71].

Rate-state laws have become established in the geological community and are employed, e.g., in the study of earthquake dynamics. They may also be used to explain the detailed dynamics of the stick-slip transition: although such transitions appear to be abrupt in ordinary friction experiments, high-resolution position measurements reveal a continuous and accelerating creeping motion that seamlessly transitions into bulk sliding [28]. This behavior is not compatible with the usual division into static and sliding friction, but may be explained using a combination of rate-state friction and system dynamics [65]. However, an alternative, non-kinetic, explanation for accelerated creep has also been proposed [47].

A somewhat different framework is used for describing similar issues in control systems and robotics. The central phenomenon in this context is the so-called *pre-slip*, which describes the tendency of a frictional contact to experience a small displacement under lateral loading, even before bulk sliding sets in. This displacement is not purely elastic, which also gives rise to the concept of hysteresis of friction under changes of direction. Correct modeling of such effects is essential when exact positioning under stop-and-go conditions is required, e.g., in the control of robotic manipulators and stick-slip-based drives and actuators. Various empirical models have been developed to describe pre-slip. These include, in order of sophistication, the Elastoplastic [17], Dahl [12] and LuGre [14] models. The latter is a semi-empirical law based on the bristle model of friction, which itself can be considered a generalization of the Prandtl-Tomlinson model.

1.1.1 Friction and Oscillation

Another major cluster of dynamic frictional effects is formed by the rich interaction between friction and vibration. On the one hand, there is the well-known tendency of many tribosystems to experience frictional instabilities (stick-slip) and thereby produce oscillations at various frequencies. When the frequency is in the audible range, this is perceived as noise. Typical examples are brake squeal and cornering noise. However, self-excited vibration is not always undesirable, and is deliberately used in musical instruments to produce sound. A comprehensive review of friction-induced noise was compiled by Akay [2].

Going in the other direction, externally applied vibration (usually ultrasonic) is able to significantly reduce friction. This has been known since at least the 1950s [23]. Both static and sliding friction are affected, and vibration applied in any of the three directions (normal to the plane [81]; in the direction of motion or static load [35]; transverse) is known to reduce friction. In the sliding case, the phenomenon is known to be velocity-dependent. It should also be noted that ultrasonic vibration can suppress lower-frequency frictional instabilities and therefore finds use as one of the ways to suppressing brake squeal [34, 44].

Although the influence of vibration on friction has been known for a long time and has found multiple practical applications, there appear to be few experimental studies of the effect, and even fewer credible theoretical models. On the experimental front, the work of Pohlman [51] and Godfrey [27] is notable. These authors measured the electrical resistance in the contact and concluded that the reduction of friction is caused by the breaking of microscopic bridges by the action of ultrasonic vibration. More recent work on friction under the influence of longitudinal vibration was performed by Chowdhury et al. [10] and V. L. Popov et al. [64].

A few models have been proposed as well, for example a Prandtl-Tomlinson-based formulation by Zaloj et al. [85]. This model was somewhat successful in reproducing certain aspects of friction under the influence of vibration, e.g., the suppression of frictional instabilities. However, due to its abstract nature, it is generally difficult to connect back to physical reality and concrete experimental data.

1.1.2 Frictional Damping

The reduction of friction by externally applied vibration forms one of the focus areas of this thesis, with *frictional damping* forming the other.

This kind of damping is generally caused by surfaces sliding relative to each other in a frictional connection. Typically this involves *partial slip* (also called micro-slip), a well-known contact-mechanical phenomenon, first analyzed by Mindlin et al. in 1952 [42]. When a curved (non-conformal) contact is subjected to a lateral load, it does not begin to slide all at once, but rather forms a ring-shaped partial slip zone at the edge of the contact. This slip zone propagates inwards as the lateral load increases. When the partial slip zone reaches the center of the contact, bulk sliding sets in. Under periodic lateral loading (i.e. vibration), microslip thus leads to energy dissipation, even though the contact is nominally at rest, and also produces a characteristic ring-shaped wear track, which is known as fretting wear [32].

In many cases, frictional damping is a desirable characteristic. However, the associated wear is almost always problematic, both from the point of view of structural integrity and the release of wear particles. Frictional damping not only plays a role in macroscopic contacts, but can also affect energy dissipation in bulk materials, e.g., due to the presence of internal cracks or fiber-fiber contacts in composites.

The immediate cause of mirco-slip is periodic loading in the lateral (in-plane) direction, and the original analysis of Mindlin focused on this degree of freedom exclusively. Frictional damping under combined normal and lateral oscillation, on the other hand, was not considered until fairly recently. Putignano, Davies et al. [67, 13] studied this problem using numerical simulation of rough surface contacts, and found that the normal degree of freedom significantly affects the dissipation.

1.1.3 Wear and Long-term Dynamics

Apart from being associated with frictional damping, wear also plays a role in another dynamic aspect of friction—one that occurs on a much longer time scale than the kinetic friction discussed earlier: Friction inevitably leads to wear, and wear modifies the surface at the microscopic level, which in turn affects friction. Especially in rotating or reciprocating tribosystems this produces a variety of long-term effects, which may be either asymptotic (run-in) [36], random, or even periodic. The temporal evolution of friction and its relation to wear processes has been studied extensively by Ostermeyer [49]. The effect of wear particles on the coefficient of friction is also an interesting research topic. Under some circumstances, such particles can act as microscopic ball bearings, and probably contribute to the extremely low coefficients of friction of diamond-like carbon and similar coatings [22].

However, all such long-term phenomena are outside the scope of this thesis.

1.1.4 Some Practical Applications

The phenomena described above have found a large number of practical applications. The reduction of friction forces through ultrasonic vibration is often used to improve the precision and efficiency of metalworking processes. Classical examples include wire drawing [73, 45], press forming [18, 72, 5], cutting and machining [80]. Micro-machining and surgical tools

[21] in particular can benefit from ultrasonic cutting technology. Ultrasonic welding is employed as well, but this involves a level of plastic deformation that puts it well outside the scope of this thesis.

Another major area of application is the stabilization of system dynamics and suppression of frictionally induced noise. Brake squeal [44] and rail-wheel curve squeal [31] stand out, but the potential applications are almost limitless. Another possibility for combating undesirable vibration is the deliberate introduction of suitable frictional connections [26] to increase damping. This is particularly attractive in lightweight metallic structures, e.g., in aerospace. Purposeful design of composite materials with suitable damping properties due to internal friction is also possible [86].

There are also a number of advanced applications that go beyond simple sliding friction, and involve vibration-driven motors, actuators and transporters [61]. The most famous example are traveling wave motors [70, 83, 76], which are used to adjust focus in camera lenses, among many other applications. Similar principles are employed in vibrational conveyors [25, 24, 43]. The ongoing miniaturization in many fields makes vibration-based drives increasingly attractive, since they can be manufactured in much more compact sizes than conventional motors.

Another variation of stick-slip drives is to be found in high-precision positioning systems [74, 20]. These are usually based on some combination of piezoelectric actuation and stick-slip motion, and can reach nanometer precision. Such positioning stages and micro-actuators play an essential role in microelectronics manufacturing and high-precision scientific instruments.

1.2 Beginnings of a Macroscopic View

As described above, there is a rich body of existing research into the detailed phenomenology of friction, including many different environmental and boundary conditions, as well as various dynamic effects from microscopic creep to ultrasonic vibration. However, the predominately empirical nature of the research has, for the most part, prevented the integration of individual results into a coherent and reusable whole. Especially when it comes to physical interpretation and modeling, much work remains to be done.

This is not to say that reasonable explanations for individual phenomena have not been proposed. E.g., the mechanism and model parameters of rate-state laws in the context of rock friction can be plausibly related to thermally activated processes and the characteristic length of microscopic asperities. Another example is the LuGre model, which consists of differential equations for the (statistical) evolution of "microcontacts" in the bristle model. The reduction of friction due to out-of-plane vibration has been attributed to breaking of asperity contacts. Variations of the Prandtl-Tomlinson model have also been used to explain frictional phenomena at the micro scale. However, upon closer examination, explanations of this kind have to be classified as mostly empirical. Many of them are plausible in a post-hoc explanatory fashion, but they do not usually describe *specific* physical mechanisms and often lack quantitative predictive power. In addition, while the model parameters are often at least somewhat physically motivated, they do not reliably correspond to measurable physical quantities and in practice have to be treated as fitting parameters.

Part of the difficulty in making progress towards proper physical understanding might be related to the intuitive expectation that the phenomena in question are intrinsic properties of friction, and are caused primarily by micro-scale processes. However, the complexity of friction at the microscopic level makes it rather difficult to work with full-scale physical models, which greatly increases the appeal of abstract substitutes such as Prandtl-Tomlinson or the bristle model. A possible solution to this is the emerging hypothesis that many supposedly intrinsic properties of friction actually arise from the interaction of "ordinary" (e.g., Amontons) friction and *macroscopic* dynamics. The promise of this approach is that it may result in properly verifiable physical models with physical parameters and at least some degree of unifying power. In this thesis, the viability of this approach is shown in the context of dynamic frictional phenomena, with a particular focus on friction under externally imposed vibration. Hints at the macroscopic nature of other properties of friction will also be discussed.

The idea that friction is partly determined by macro-scale interactions is not new per se, and has been around at least since the 1950s. At tribological conferences and in the literature it is often acknowledged that friction is a "multiscale phenomenon" and that the coefficient of friction is really a "system property", rather than a material-specific constant. Work to put these general principles on a specific, quantitative basis is, on the other hand, fairly recent. One early example is due to Storck et al. [76], who studied the influence of ultrasonic vibration, stemming from an interest in ultrasonic motors. They proposed an extremely simple model consisting of an unstructured contact point sliding with a uniform velocity under constant normal load, and subject to Coulomb (or rather Amontons) friction. In addition, an in-plane displacement-controlled oscillation (in either parallel or transverse directions) is present. This model succeeded in reproducing some features of experimental data quite well, but others remained unaccounted for.

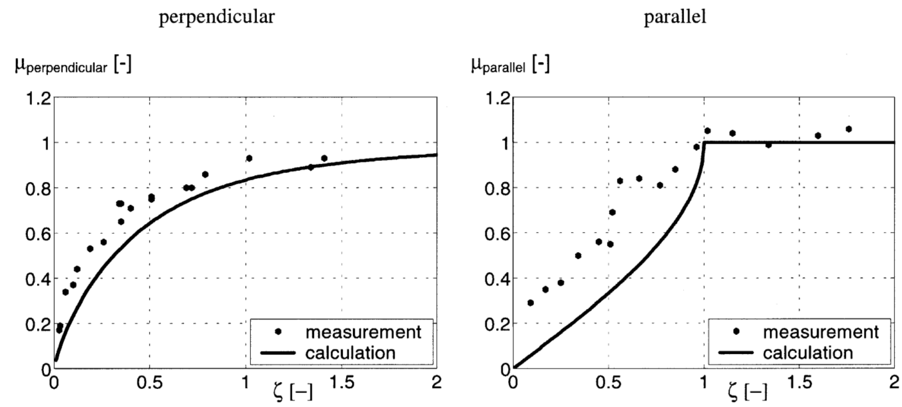

Figure 1.1: Velocity-dependence of the COF under transverse and parallel oscillation, as calculated (solid lines) and measured (dots) by Storck et al. Source: Fig. 5 in [76].

In Figure 1.1, reproduced from [76], one can see that in the case of perpendicular oscillations a convincing fit of theory and experiment is achieved, but in the parallel case the only really good agreement is in the point of cross-over from reduced to constant friction. The shape of the predicted curve is also somewhat implausible (and according to results of this thesis, actually incorrect). The model is also only applicable to sliding friction and is unable to accommodate static friction or out-of-plane vibration.

Another major contribution to the macroscopic point of view arose from a collaboration between Edeler et al. [20] and Teidelt et al. [79, 48]. The work of Edeler concerned the construction of stick-slip microdrives involving spherical ruby micro-contacts. The control of such devices requires accurate modeling of dynamic friction and the previously mentioned pre-slip phenomenon. This was attempted using the LuGre [14] model, which is generally considered to be the best available for such applications. Unfortunately, this approach did not yield the desired accuracy. A much better fit could be achieved by Teidelt [77] based on the idea that *pre-slip* is not an intrinsic frictional effect, but simply partial slip in a curved contact.

Partial slip was already mentioned in the context of damping, but even under non-periodic loading (e.g. during a stick-slip transition), Mindlin slip is macroscopically observable as a small, non-recoverable displacement that precedes sliding. I.e., it has exactly the same characteristics as *pre-slip*. However obvious in retrospect, this connection apparently wasn't made in the 60 years between Mindlin and Teidelt. But when it ultimately arrived, it proved highly successful in quantitative modeling of Edeler's microdrives [20, 19], and did so using only classical contact mechanics, Amontons friction and no additional fitting parameters.

The identity of "intrinsic" pre-slip and macroscopic partial sliding was extensively tested by Teidelt [77] and later Milahin [40], and was experimentally confirmed to hold for a range of normal forces, radii of the contacting spheres, etc. The same was verified numerically for the contact of rough surfaces by Grzemba et al. [29]. In all cases, the characteristic length of *pre-slip* was found to be simply the indentation depth multiplied by the coefficient of friction. Although this work is yet to gain general recognition, in the opinion of the author it presents sufficient evidence to strike *pre-slip* from the list of intrinsic frictional phenomena and to render associated empirical models, including the highly regarded LuGre, more or less obsolete. It not only provides a parsimonious physical explanation, but also good quantitative agreement with experiment and takes into account factors that are not covered by empirical laws (e.g., curvature of the contact and indentation depth).

The idea to apply macroscopic contact mechanics to friction under dynamic loading was also tried in the case of friction under the influence of ultrasonic vibration. This can be seen as an augmentation of the earlier model of the Wallaschek group [76] by a structured contact capable of pre-slip, and in some cases an additional degree of freedom representing the elasticity of the surrounding system. This approach was pursued by Starcevic and Filippov [75], Teidelt [78] and Milahin [39, 41] both theoretically and experimentally. This work removed some of the mentioned limitations of the earlier model (such as the inability to handle static friction and normal oscillations), but was still unable to achieve accurate fit with experimental data in many situations.

1.3 The Role of Contact Stiffness

The present thesis continues and extends the approach outlined in the previous section. The primary difference relative to earlier work by Storck, Starcevic, Teidelt, Milahin and others is explicit consideration of the macroscopic deformation and dynamics of the contact region, which continuously responds to changes in the external load. In terms of model complexity this represents a relatively small addition, but one that turned out to have high impact and successfully resolved the main issues encountered in earlier models.

The promise of this approach, and the importance of the compliance of the contact, was initially demonstrated in the context of frictional damping (Chapter 2, Publications 1-3). In particular, the extension of the Mindlin problem to damping under superimposed in-plane and out-of-plane oscillation was considered. In this context, the simplicity of the model led to the discovery of relaxation damping, an effect that appears to have been missed by earlier investigators [67, 13].

When applied to active control of friction by externally applied vibration, the new model overcame the remaining discrepancies seen in the work of Storck and later authors, and was able to unify the influence of vibration in any of the three possible directions (Chapter 3, Publications 4-10). Static and sliding friction are handled with equal ease, and the peculiarity of the *displacement amplitude* being the determining factor in the former and the *velocity amplitude* in the latter, is easily explained. The velocity-dependence and important cross-over points appear to be described correctly. Both displacement-controlled (quasi-static) and inertial systems can be modeled, as well as superimposed and phase-shifted oscillations, which may result in asymmetric friction and active drives.

It should be noted that in most of the work to be presented here, no calculation of the full contact problem (such as, e.g., the Hertzian contact) is performed. Although this is both possible and advisable where maximum accuracy is required, all the basic mechanisms can be elucidated with a minimal contact model that assumes a constant (with respect to indentation) normal contact stiffness. This assumption is equivalent to a contact of a flat-ended cylinder with a plane, and in the model can be represented with a single spring element with a spring constant equal to the bulk contact's normal and tangential stiffness. Thus, most of the following papers make use of variations of the simple system shown in Figure 1.2, although some publications also treat a curved contact for comparison.

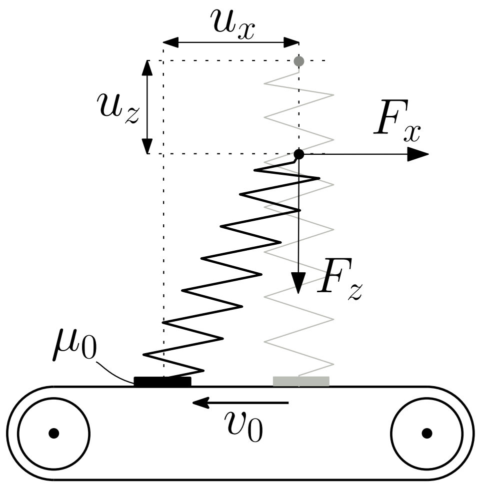

Figure 1.2: Prototype model employed in this thesis, with a single spring representing the normal and tangential compliance of the contact. Variations of this model are employed in the presented publications. The situation represented in this particular example is sliding friction (with a constant velocity v_0) under a displacement-controlled normal oscillation $u_z(t)$.

Even when working within the constant-stiffness approximation, it is important to note that the *actual* contact stiffness at the given average indentation should be used. Since this stiffness is in general a function of contact size, curvature and indentation, it stands to reason that these parameters quantitatively affect friction under vibration. This has been indeed observed experimentally [40].

Interestingly, a large variety of proximate mechanisms of friction control and reduction are observed depending on the specifics of the problem, even though the underlying model is essentially the same. For example, a sliding contact under *normal* oscillation will experience reduced friction due to a type of stick-slip motion that might be described as "pseudo-walking". This process causes a direct reduction of both the apparent COF and the total dissipated energy. In the case of *parallel* oscillation, on the other hand, the "reduction" of friction is caused by shifting some of the work from the slider to the oscillator, and in the case of superimposed normal and parallel oscillation, the work done by the oscillator can even be used to produce a driving force. In the third case, *transverse* oscillation, the apparent reduction of friction is effected by yet another mechanism: the projection of the oscillating friction vector in the direction of sliding, which is essentially the same as in the Storck model [76].

In the immediate contact point, Amontons friction (with a constant coefficient of friction μ_0 applying to both static and sliding cases) is usually assumed. This is done not only for the sake of simplicity, but also because the very premise of this thesis is that complex frictional properties can be decomposed into "featureless" microscopic friction and macroscopic dynamics. In principle, the model allows the use of any other friction law. This is not made use of in the present thesis, but is one of the possibilities for future work.

1.4 Overview of the Thesis

In the sequel, ten publications are presented, which explore frictional contacts under periodic loading using the described macroscopic methodology.

The publications are grouped thematically into two chapters. The three papers making up Chapter 2 are concerned with damping in nominally static contacts under combined normal and lateral oscillation. Of particular note is the phenomenon of *relaxation damping* which occurs in these conditions. The remaining seven papers, grouped in Chapter 3, deal with the primary focus of this thesis—reduction and active control of friction by exterally applied oscillation. This problem is approached in the same general way as frictional damping, but with the addition of bulk sliding, which qualitatively changes its phenomenology. The individual publications introduce and analyze the proposed macroscopic model in some detail and then apply it to a variety of situations, including normal, tangential and transverse oscillation, quasi-static and inertial systems, as well as frictional drives and ratchets. Each paper is preceded by a short introduction providing some context to the reader.

In the final Chapter 4, the main findings of these papers are summarized and some additional commentary is provided. The relation of particular results to the work of other authors is discussed, and an overall synthesis is attempted. Following this, there is a brief review of additional examples from the literature, where frictional properties that are normally considered intrinsic can be plausibly attributed to macroscopic dynamics. The chapter is concluded by a discussion of the presented work and avenues for future research.

Some additional proofs, with particular relevance to Publication 9, can be found in the Appendix.

Chapter 2

Publications: Relaxation Damping

This chapter presents three publications on the topic of relaxation damping:

P1: M. Popov, V. L. Popov, and R. Pohrt. "Relaxation damping in oscillating contacts". *Scientific reports* 5 (2015), p. 16189

P2: M. Popov. "Non-frictional damping in the contact of two fibers subject to small oscillations". *Facta Universitatis, Series: Mechanical Engineering* 13.1 (2015), pp. 21–25

P3: M. Popov and V. L. Popov. "Relaxation damping in contacts under superimposed normal and torsional oscillation". *Physical Mesomechanics* 19.2 (2016), pp. 178–181

Publication 1 forms the core of this chapter. It introduces the phenomenon of relaxation damping in the context of a contact with perfect stick. This would preclude energy dissipation in a traditional fretting-type, tangentially oscillating contact. However, in the paper it is shown that interaction with the normal degree of freedom allows irreversible loss of energy even in the absence of frictional slip.

The two follow-up publications use the methodology established in P1 to extend the analysis to different settings, including the contact of oscillating fibers (P2) and combined torsional and normal oscillation (P3).

Each publication is presented in the original layout, and is preceded with a brief commentary that summarizes the contents and provides some additional perspective.

2.1 Publication 1

Introductory remarks

This paper introduces the concept of relaxation damping, which was so named to contrast it with ordinary frictional damping. When a contact is subjected to periodic loading in the tangential direction *only*, it develops a zone of partial slip at the edge of the contact, where energy is dissipated in every cycle (and which also leads to the well-known fretting wear pattern). It can be shown that the energy dissipated per oscillation cycle is inversely proportional to the coefficient of friction, so that dissipation tends to zero as friction tends to infinity. However, when a contact is periodically loaded in both tangential *and normal* directions, qualitatively new behavior appears. Most importantly, dissipation does *not* tend to zero when the condition of perfect stick is approached. Instead, it reaches a finite value that is determined by the stiffness ratio of the medium, the oscillation parameters and a geometry factor. In this limit, energy is dissipated by radiation of elastic waves, which are eventually thermalized by conventional means. The process can be likened to energy dissipation in a plucked string: elastic potential energy is first converted to vibrational energy—still mechanical, but less available—and is then gradually converted to sound and ultimately to thermal motion.

In retrospect, it is the opinion of the author that the paper puts too much focus on this limiting case of infinite friction and the resulting "elastic dissipation". The presented analysis is also applicable to contacts where the coefficient of friction is merely large, rather than infinite. In that case energy will be dissipated mundanely through friction, although the *amount* will still tend to the value given in the paper. This fact is, unfortunately, only briefly mentioned in the *Discussion* section, but should be kept in mind when considering the main analysis.

Summary

The analysis begins by establishing a simple contact model—based on the Method of Dimensionality Reduction (MDR)—wherein a rigid indenter is pressed into an elastic foundation and subjected to simultaneous normal and tangential oscillation. The indenter is initially assumed to be conical, although this is later relaxed to an arbitrary shape, since the surface slope near the edge of the contact turns out to be the defining factor. The oscillations are assumed to be harmonic and of equal frequency, but with an arbitrary phase shift. The coefficient of friction is assumed to be infinite, so that the springs of the elastic foundation stick to the indenter wherever the local normal force is positive.

Based on this model, it is argued that energy dissipation occurs at all nontrivial phase shifts, because springs of the foundation are "captured" by the indenter in one position and released (by loss of contact) in another, with the accumulated energy being released as elastic waves. The total energy released in this fashion is given in closed form in Eqs. (11, 12).

A different case is then considered, where the frequency of the normal oscillation is much higher than that of the tangential oscillation. The result, given in Eqs. (16, 17), shows that the dissipation is proportional to the square of the tangential amplitude, i.e., the energy of the main oscillation. This implies that the addition of a high-frequency normal oscillation component can convert frictional attenuation from the usual reciprocal to exponential, although this is not explicitly mentioned in the paper.

The main results can be written in a shape-invariant form using only the second derivative of the normal contact force w.r.t. indentation ($\partial^2 F_z/\partial u_z^2$). From this it is argued that the obtained results have nearly universal validity (including rough surfaces, Eq. 18), so long as the amplitudes are not too large. This is confirmed numerically for a number of non-trivial contact configurations using the Boundary Element Method (Fig. 3).

The question of physical interpretation is raised next. The MDR-based model is very convenient for analysis, but it does not make it very clear how a continuous, quasi-static movement of a 3D contact can lead to the discontinuous release of stresses as required by relaxation damping. The explanation is found in a moving stress singularity at the edge of the contact, which is also confirmed numerically (Fig. 4). However, it should be noted that this explanation is only required in the limiting case considered in the paper. With finite friction the stored elastic energy would be dissipated by ordinary frictional sliding in a very brief period prior to detachment.

www.nature.com/scientificreports

SCIENTIFIC REPORTS

OPEN

Relaxation damping in oscillating contacts

M. Popov[1,2], V.L. Popov[1,2,3] & R. Pohrt[1]

Received: 07 April 2015
Accepted: 07 October 2015
Published: 09 November 2015

If a contact of two purely elastic bodies with no sliding (infinite coefficient of friction) is subjected to superimposed oscillations in the normal and tangential directions, then a specific damping appears, that is not dependent on friction or dissipation in the material. We call this effect "relaxation damping". The rate of energy dissipation due to relaxation damping is calculated in a closed analytic form for arbitrary axially-symmetric contacts. In the case of equal frequency of normal and tangential oscillations, the dissipated energy per cycle is proportional to the square of the amplitude of tangential oscillation and to the absolute value of the amplitude of normal oscillation, and is dependent on the phase shift between both oscillations. In the case of low frequency tangential oscillations with superimposed high frequency normal oscillations, the dissipation is proportional to the ratio of the frequencies. Generalization of the results for macroscopically planar, randomly rough surfaces as well as for the case of finite friction is discussed.

It is well known that oscillating tangential contacts exhibit frictional damping due to slip in parts of the contact. Solutions for this behavior in the case of spherical surfaces were given by Mindlin *et al.*[1] in 1952. This contact damping plays an important role in numerous applications in structural mechanics[2], tribology[3] and materials science[4]. Since this damping arises due to partial slip in the contact of bodies with curved surfaces, when the coefficient of friction tends towards infinity, slip disappears, frictional losses are eliminated, and the oscillation damping becomes zero[1]. However, when a contact oscillates in *both normal and tangential* directions, there is another, purely elastic loss mode that we refer to as "relaxation damping". To our knowledge this phenomenon has not yet been discussed in the literature. Damping due to a combination of normal and tangential oscillations has been studied recently by Davies *et al.*[5] for smooth two-dimensional profiles and by Putignano *et al.*[6] for rough surfaces. However, the fact that dissipation exists even in the limiting case of an infinite coefficient of friction, when relative frictional movement of contacting bodies does not occur, went unnoticed. This effect is an example of purely "non-dissipative" damping, like the Landau damping in a collisionless plasma[7].

In its essence the proposed loss mechanism is similar to a spring that is deflected and abruptly released, converting the stored energy into elastic waves that are eventually dissipated. If we consider a body that is pressed into a plane, then moved tangentially (with "stick" conditions in the contact), and finally lifted in the normal direction, the accumulated shear energy will eventually be lost even if there is no slip in the contact area and the material is purely elastic. Thus, an apparently non-dissipative system shows dissipation. The same will also happen in contacts that oscillate normally and tangentially at the same time, even if the motion is very slow (quasi-static.) At first glance it seems contradictory that a slowly moving, non-dissipative system shows dissipation. The physical reason for this dissipation is the infinite stress concentration at the borders of a tangential contact. Due to the stress singularity, infinitely rapid movements occur in the material even in the case of quasi-static macroscopic movement of the contacting bodies, similar to the dissipation from elastic instabilities in the Prandtl-Tomlinson-model[8,9,10]. The physical nature of relaxation damping can be understood and analyzed very simply in the framework of the method of dimensionality reduction (MDR). For small oscillation amplitudes, the dissipation rate can be calculated analytically.

[1]Berlin University of Technology, 10623 Berlin, Germany. [2]National Research Tomsk State University, 634050 Tomsk, Russia. [3]National Research Tomsk Polytechnic University, 634050 Tomsk, Russia. Correspondence and requests for materials should be addressed to M.P. (email: mikhail.popov@tu-berlin.de)

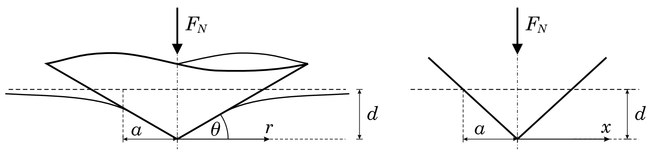

Figure 1. (**a**) Contact of a cone with a half-space and (**b**) the corresponding MDR-transformed one-dimensional profile.

Results

Preliminary remarks. Consider a contact between two axially-symmetric elastic bodies with moduli of elasticity of E_1 and E_2, Poisson's numbers of ν_1 and ν_2, and shear moduli of G_1 and G_2, accordingly. We denote the difference between the profiles of the bodies as $\tilde{z} = f(r)$, where $\tilde{z}$ is the coordinate normal to the contact plane, and r is the in-plane polar radius. The profiles are brought into contact and are subjected to a superposition of normal and tangential oscillation with small amplitudes. This contact problem can be reduced to the contact of a rigid profile $\tilde{z} = f(r)$ with an elastic half-space, Fig. 1a.

In our analysis we use the method of dimensionality reduction, MDR[11]. MDR is based on the solutions for the normal contact by Galin[12] and Sneddon[13] as well as their extensions for tangential contacts by Cattaneo[14], Mindlin[15], Jäger[16] and Ciavarella[17]. In the framework of the MDR, two preliminary steps are performed[11]: First, the three-dimensional elastic half-space is replaced by a one-dimensional linearly elastic foundation consisting of an array of independent springs, with a sufficiently small separation distance Δx and normal and tangential stiffness Δk_z and Δk_x defined according to the rules

$$\Delta k_z = E^* \Delta x \quad \text{with} \quad \frac{1}{E^*} = \frac{1-\nu_1^2}{E_1} + \frac{1-\nu_2^2}{E_2}, \tag{1}$$

$$\Delta k_x = G^* \Delta x \quad \text{with} \quad \frac{1}{G^*} = \frac{2-\nu_1}{4G_1} + \frac{2-\nu_2}{4G_2}. \tag{2}$$

In the second step, the three-dimensional profile $\tilde{z} = f(r)$ is transformed into a one-dimensional profile according to

$$g(x) = |x| \int_0^{|x|} \frac{f'(r)}{\sqrt{x^2 - r^2}} \mathrm{d}r. \tag{3}$$

If the MDR-transformed profile $g(x)$ is indented into the elastic foundation and is moved normally and tangentially according to an arbitrary law, the contact radius and the force-displacement relations of the one-dimensional system will exactly reproduce those of the initial three-dimensional contact problem (proofs have been done in[18] and[11]). The MDR solution is as accurate as the solutions of Cattaneo[14] and Mindlin[1]: the solution contains an inaccuracy, which has been shown to be generally quite small[19]. From the correctness of the force-displacement relations, it follows that the work and the dissipated energy will be reproduced correctly as well.

In the following, we consider, without loss of generality, a rigid conical indenter

$$\tilde{z} = f(r) = r \tan \theta \tag{4}$$

in contact with a half-space, Fig. 1a.

The one-dimensional MDR image of the conical profile (4), according to (3), is

$$g(x) = |x| \frac{\pi}{2} \tan \theta = c|x|, \tag{5}$$

where $c = (\pi/2)\tan \theta$ is the slope of the one-dimensional equivalent profile, Fig. 1b. The generalization for an arbitrary axis-symmetrical shape can be made very easily: if the amplitude of normal oscillation is sufficiently small compared to the indentation depth of the indenter, the shape of the edge of the contact will always be approximately linear. For determining the energy dissipated during one cycle of oscillation, only the zone near the edge of contact (of one-dimensional MDR model) must be considered because dissipation can only take place where the surfaces come in and out of contact. In this case, all axially-symmetric indenters will behave like conical indenters and the slope c at the edge of the contact of the one-dimensional MDR-transformed profile will be the only shape-related parameter. For example, for a parabolic indenter $\tilde{z} = r^2/(2R)$, the MDR-transformed profile is $\tilde{z} = g(x) = x^2/R$ and the edge slope is $c = 2a/R$ where a is the contact radius. The parameter c can also be represented in a universal

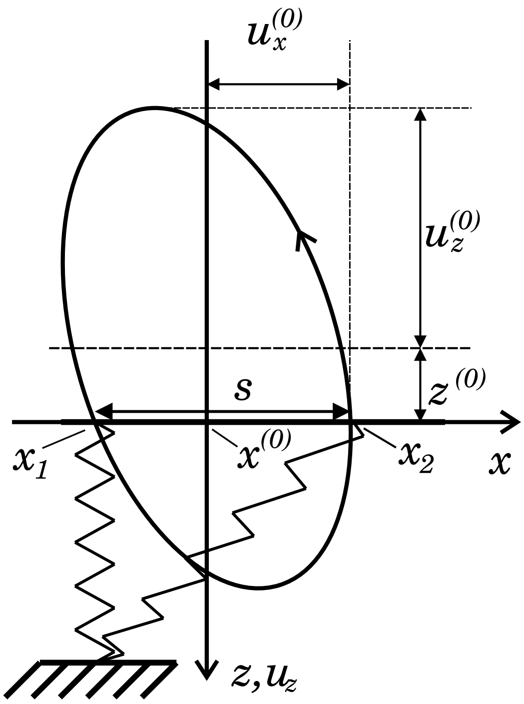

Figure 2. A point of the rigid surface with the initial coordinate z=−z$^{(0)}$ oscillates around this position. It comes into contact with a spring in point x_1 and loses contact in point x_2.

form that does not depend on the profile shape: The incremental contact stiffness is known to be equal to $\partial F_N / \partial d = 2aE^*$, see [20]. Deriving this equation once more gives $\partial^2 F_N / \partial d^2 = 2E^* \partial a / \partial d = 2E^*/c$. Thus, the slope of the MDR-transformed profile can be calculated as

$$\frac{1}{c} = \frac{1}{2E^*} \frac{\partial^2 F_N}{\partial d^2}. \tag{6}$$

In the following, we consider energy dissipation in two cases: (a) oscillations in the normal and tangential direction with equal frequencies, (b) oscillation in the normal direction with much higher frequency than in the tangential direction.

Normal and tangential oscillations with equal frequencies. Let the profile oscillate harmonically with a normal amplitude $u_z^{(0)}$, a tangential amplitude $u_x^{(0)}$ and a phase difference φ_0. To study the effect of relaxation damping in the pure, we assume an infinite friction coefficient between both bodies. Since the springs of elastic foundation in the MDR model are independent, it is sufficient to analyze the energy dissipation of a single spring (Fig. 2), and then to sum over all springs which come into contact during an oscillation cycle. Consider a point of the rigid indenter with the initial coordinates $x^{(0)}$, $z^{(0)}$. Its coordinates during the oscillatory motion can be written as $z(t) = -z^{(0)} + u_z^{(0)} \cos \omega t$ and $x(t) = x^{(0)} + u_x^{(0)} \cos(\omega t + \varphi_0)$. If $|u_z^{(0)}| > z^{(0)}$, the point of the rigid surface will come into contact with one of the springs of the elastic foundation in point x_1 and will drag it along to point x_2, where contact is lost and the spring relaxes over the distance $s = x_2 - x_1$. The coordinates x_1 and x_2 are determined by setting $z = 0$. After simple calculations we get

$$s = x_2 - x_1 = 2u_x^{(0)} \sqrt{1 - \left(z^{(0)}/u_z^{(0)}\right)^2} \ \sin \ \varphi_0. \tag{7}$$

The energy dissipated by a single spring during one cycle is equal to the energy stored in the stressed spring at the time of its release:

$$\Delta W = \frac{1}{2} \Delta k_x s^2 = \frac{1}{2} G^* s^2 \Delta x. \tag{8}$$

Energy dissipation occurs only if the point of the surface was in contact with the substrate during only a part of the cycle. This is the case for all points which satisfy the condition

$$-|u_z^{(0)}| < z^{(0)} < |u_z^{(0)}|. \tag{9}$$

Substituting $\Delta x = \Delta z^{(0)}/c$ in (8) and integrating over the interval (9), we obtain the total dissipated energy per cycle:

$$W = 2\frac{1}{2}\frac{G^*}{c}\int_{-|u_z^{(0)}|}^{|u_z^{(0)}|} s^2 dz^{(0)}. \tag{10}$$

The factor "2" takes into account that there are two symmetric regions on both sides of the contact giving equal contributions to dissipation (this complete symmetry is only valid in the standard half-space-approximation used in this paper). Substitution of (7) into (10) and evaluation of the integral finally gives

$$W = \frac{16}{3}\frac{G^*}{c}u_x^{(0)2}|u_z^{(0)}|\sin^2\varphi_0 \tag{11}$$

or in the shape invariant form, using (6),

$$W = \frac{8}{3}\frac{G^*}{E^*}\frac{\partial^2 F_N}{\partial d^2}u_x^{(0)2}|u_z^{(0)}|\sin^2\varphi_0. \tag{12}$$

Low frequency tangential oscillation with high frequency normal oscillation. If the frequency of normal oscillation ω_z is much larger than ω_x, the frequency of tangential oscillation, the body will move tangentially with an approximately constant velocity $v_x^{(0)}$ during any given cycle of normal oscillation. Let the x-coordinate of a point of the indenter be $x = x^{(0)} + v_x^{(0)}t$, while the z-coordinate is defined by $z = -z^{(0)} + u_z^{(0)}\cos\omega_z t$ as before. The times at which a spring is coming into contact with the indenter (t_1) and is released (t_2) are given by the condition $z = 0$, from which it follows that $t_{1,2} = \mp\,(1/\omega_z)\arccos(z^{(0)}/u_z^{(0)})$. For the distance s, we get the following result:

$$s = x_2 - x_1 = 2\frac{v_x^{(0)}}{\omega_z}\arccos(z^{(0)}/u_z^{(0)}). \tag{13}$$

Substituting into (10) and evaluating the integral, we get the energy dissipated per normal oscillation cycle:

$$W_1 = 4(\pi^2 - 4)\frac{G^*}{c}|u_z^{(0)}|\frac{v_x^{(0)2}}{\omega_z^2} \tag{14}$$

from which we obtain the average dissipated power in a normal oscillation cycle:

$$P_1 = 2\frac{(\pi^2 - 4)}{\pi}\frac{G^*}{c}|u_z^{(0)}|\frac{v_x^{(0)2}}{\omega_z}. \tag{15}$$

By defining $v_x^{(0)} = \omega_x u_x^{(0)}\cos\omega_x t$ and integrating over one cycle of tangential oscillation (from 0 to $2\pi/\omega_x$) we find the dissipated energy to be:

$$W = 2(\pi^2 - 4)\frac{G^*}{c}|u_z^{(0)}|u_x^{(0)2}\frac{\omega_x}{\omega_z}. \tag{16}$$

In the shape-invariant form, the energy dissipation per cycle of tangential oscillation is:

$$W = (\pi^2 - 4)\frac{G^*}{E^*}\frac{\partial^2 F_N}{\partial d^2}|u_z^{(0)}|u_x^{(0)2}\frac{\omega_x}{\omega_z}, \tag{17}$$

which is nearly identical to (12), save for the different constant and a dependence on the ratio of frequencies, instead of the phase difference. As stated before, this result is only valid if $\omega_z \gg \omega_x$.

Further generalization. We would like to stress that in spite of the fact that the relaxation losses (11)–(12) and (16)–(17) have been derived in a one-dimensional model, they represent, due to the MDR theorems, the exact three-dimensional results for axis-symmetric profiles. In the shape invariant form (12) and (17) they are even applicable to multi-contact systems with independent contacts, as e.g. represented by the Greenwood and Williamson model of contact of rough surfaces[21]. This follows directly from the linearity of the energy losses with respect to the normal force. The shape invariance of the results (12) and (17) suggests that these may even be exact relations applicable to any three-dimensional contact topography*.

To illustrate this universality and to provide additional numerical validation of the general equations (12) and (17), we carried out a series of three-dimensional, full-Cerruti-type numerical simulations of oscillating contacts using the methods described in detail in[23] and[25], with some modifications. We assumed that normal and tangential deformation are uncoupled i.e. tangential stresses do not alter the normal contact solution. This is strictly valid only when both materials are identical, or one is incompressible and the other one is either incompressible or perfectly rigid. In order to handle the case of infinite friction, the boundary conditions were altered to force all contact points into an individual horizontal deformation depending on their time of entering into contact.

The essential findings related to these simulations are summarized in Fig. 3: For 4 different surface topographies (left column), the minimum and maximum contact areas are shown (middle column) as well as the time plots of the work done by the external force in the x-direction (right column). The total work done during one period (values reached at $\omega t = 2\pi$) is the dissipated energy. The horizontal dotted line shows the unity-normalization according to Eq. (12). One can see that the three-dimensional results coincide with the analytical prediction not only for axis-symmetrical profiles, but also for profiles having an "arbitrary" different form. We thus can conclude that Eq. (12) can be universally applied to contacts of arbitrarily shaped bodies. The same will be valid of course for Eq. (17).

Let us apply Eq. (12) to an important class of nominally flat rough surfaces (surfaces having a long wavelength cut-off of the power spectrum of roughness) in contact with a flat counterpart. For such surfaces, the relation between the normal force and the indentation depth is known to be $F_N \propto \exp(-d/l)$ [11,22], where l is of the order of magnitude of the rms roughness. For the second derivative of the force, we have $\partial^2 F_N/\partial d^2 = F_N/l^2$. Thus, for rough surfaces, the damping is proportional to the normal force. Substitution into (12) gives:

$$W = \frac{8}{3}\frac{G^*}{E^*}\frac{F_N}{l^2}u_x^{(0)2}|u_z^{(0)}|\sin^2\varphi_0. \tag{18}$$

Physical interpretation. Finally, let us come back to the physical nature of the relaxation damping. Brillouin was probably the first to recognize that a non-vanishing dissipation at low velocity can only occur if there are some discontinuous jumps from one state to another in the system[26]. In other words, movement with finite velocity must occur in the system even if it is driven quasi-statically. Such rapid movements due to elastic instabilities are e.g. the reason for the appearance of finite dissipation in the celebrated Prandtl-Tomlinson-model[8]. At first glance, the oscillating contacts discussed in this Paper do not lead to any rapid movements. However, a singularity of stresses does exist at the border of the contact. This singularity leads to infinitely rapid movements even if the configuration of the contact changes quasi-statically. Let us illustrate this by the distribution of tangential stresses in the contact plane. The tangential stress distribution can be easily calculated from the linear force density $q(x)$ in the one-dimensional MDR-model by applying the integral transformation[11]

$$\tau(r) = -\frac{1}{\pi}\int_r^\infty \frac{q_x{}'(x)\,dx}{\sqrt{x^2 - r^2}}. \tag{19}$$

The tangential stress as a function of coordinate and time is shown in Fig. 4 as a color map. Of interest is the range of coordinates where the indenter is in contact only over some part of the oscillation period. In this range, one can see two maxima of the stress: the first one is located at the left boundary of the range. A detailed analysis shows that this is a logarithmic singularity, which is "pulsating" but not moving spatially. The second singularity is located at the right boundary of the contact; it develops and persists during the phase of the oscillation when the indenter is "pulled away". This is a "square root singularity", which is moving spatially. Movement of this singularity leads to infinitely rapid movements in the medium even if the indenter is moving quasi-statically. The existence of a singularity of tangential stress distribution is a general property of any contact configuration with infinite friction[27], which is also confirmed by our numerical analysis.

In the realistic case of finite coefficient of friction, there will be no singularity of tangential stress due to the appearance of a slip region at the boundary of the contact area. Let us discuss the process of energy dissipation in this case. Note that the method of dimensionality reduction is also applicable to the superimposed normal and tangential contact in the presence of a finite coefficient of friction[11]. The process of dissipation of the elastic energy of the "border springs" of the equivalent elastic foundation described at the beginning of the paper will now occur not instantly at the moment of loss of contact but continuously during a finite interval shortly before loss of contact, so that at the moment of final separation the springs will be completely un-stressed. However, if the interval of stress relaxation is small enough, the amount of energy loss will be practically independent of whether it was lost instantly or during a very short time (or displacement) interval. This amount is equal to the elastic energy stored in the border springs before the start of the relaxation process and does not depend on the details of the

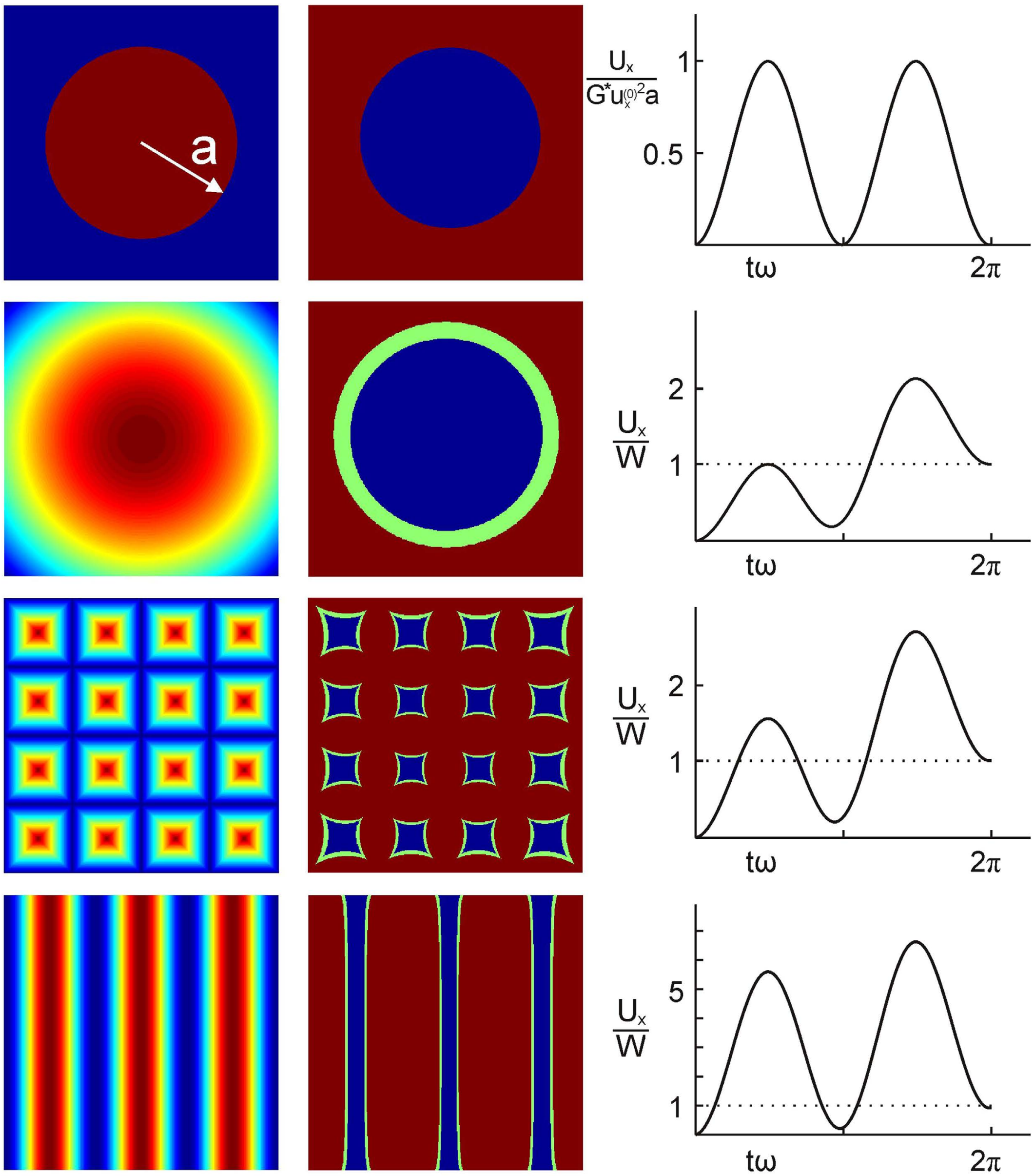

Figure 3. (**a**) Various surface profiles used to validate Eq. (12) by direct three-dimensional simulations of oscillating contact: a sharp-edged cylindrical profile; a parabolic surface; an arrangement of 16 pyramid indenters; a series of elongated sinusoidal profiles. (**b**) The contact configurations for the corresponding profiles. The minimum contact regions of a complete cycle are colored in blue and the additional regions at maximum contact in green. (**c**) Time plots of the work done by external forces in the x-direction on the system over one period of oscillation, normalized by the prediction W according to eq. (12). In the first example, the contact area is not changed in the cycle so no dissipation takes place. In the other cases, the curves reach unity after one cycle, thereby confirming the validity of eq. (12). In all studied cases, the direct simulations reproduce the analytical result with an error not exceeding 5%, which is primarily caused by the difficulty of determining $\partial^2 F_N / \partial d^2$ from discrete samples.

dissipation mechanism. The same amount of energy would be dissipated if the coefficient of friction were infinite but the material had viscoelastic properties. The application of the MDR in this case requires the replacement of the springs of the elastic foundation by corresponding rheological elements[11]. Let us discuss the simplest case of the Kelvin body. In this case, the elements of the linear viscoelastic foundation will consist of springs connected in parallel to linear dampers. During the superimposed normal and tangential oscillations, such an element will come into contact and will be dragged tangentially exactly as described in the case of purely elastic elements at the beginning of the paper. During this

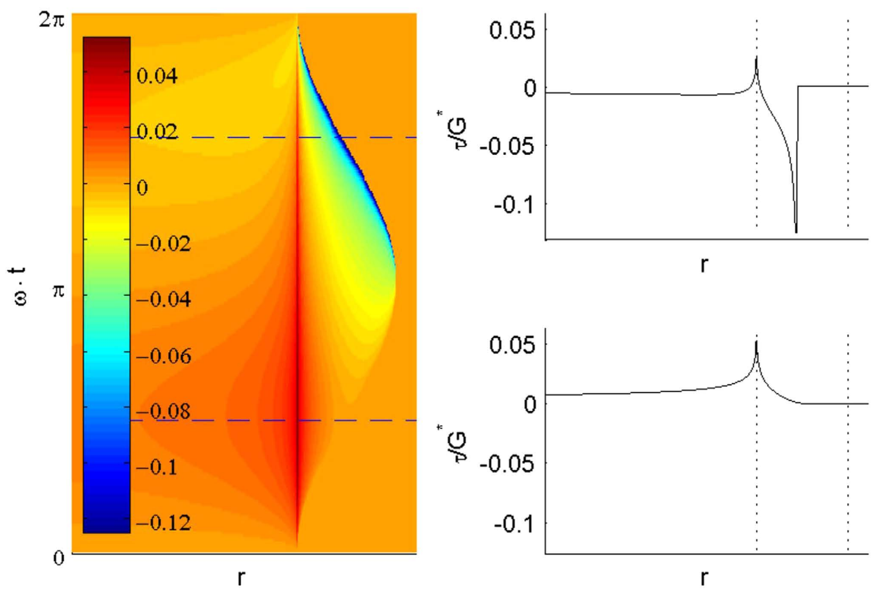

Figure 4. Color map of the distribution of tangential stress as function of radius *r* (horizontal axis) and time (vertical axis) over one period of the oscillation $z(t) = -z^{(0)} + u_z^{(0)} \cos\ \omega t$ and $x(t) = x^{(0)} + u_x^{(0)} \cos(\omega t + \varphi_0)$ with the phase shift $\varphi_0 = \pi/2$. At the beginning of the motion, a positive singularity appears at the initial boundary of the contact and remains at this point during the whole oscillation period (right lower subplot.) No energy dissipation is associated with this non-moving singularity. At the moment of reversal of the indentation movement (start of the "pulling" phase) a square-root-singularity appears at the right boundary of the contact and moves subsequently to the left, together with the shrinking contact region (right upper sub-plot.) At the same time, irreversible energy dissipation takes place. The right subplots correspond to the times shown in the color map with horizontal dashed lines. In the sub-plots, the maximum and the minimum extent of the contact region during an oscillation period are shown with dotted lines.

process, elastic energy will be stored in the spring. At the moment when the normal pressure becomes zero, the element starts relaxing. If the relaxation time of the viscoelastic material is much smaller than the period of oscillations, then practically the whole elastic energy will be dissipated. Its amount again, is given by Eq. (8) or for the whole contact by (12). Thus, the dissipative contribution described in the paper will be, in the case of a viscoelastic material, the same as in the elastic case provided the relaxation time of the viscoelastic materials is much smaller than the period of the oscillation (so that during the non-contact time the material can really almost completely relax). The most important feature of the considered dissipation mechanism is that the amount of the dissipated energy is completely independent of the particular dissipation mechanism, be it microslip or internal dissipation in the material. Its basic mechanism is that the pre-stressed spring becomes unstressed (relaxed) due to normal movement. The term "relaxation damping" reflects this physical mechanism of energy loss.

Discussion

In conclusion, the effect of relaxation damping was discussed using the example of axis-symmetric elastic bodies with infinite friction in the contact area. The discussion was generalized to bodies with arbitrary surface topography, in particular multi-contact systems and contact of bodies with rough surfaces. We have shown that a superposition of normal and tangential oscillation (both with equal and different frequencies) leads to a specific damping, which we call "relaxation damping". The damping is proportional to the amplitude of the normal oscillations and to the square of the amplitude of the tangential oscillations. For nominally flat rough surfaces, it is also proportional to the applied normal force. The assumption of the infinite coefficient of friction was made only to study the effect in the pure. However, all results are directly applicable to systems with a finite coefficient of friction provided that the changes in the radius of the stick region are much smaller than those due to changing indentation. To show this, let us compare the dissipated energy per cycle due to purely tangential vibration ("Mindlin contribution"[1]), $W_{Mindlin} = \frac{2}{3}\frac{G^{*2}}{E^*} R^{1/2} \mu^{-1} d^{-1/2} (u_x^{(0)})^3$ (which can also be written as $W_{Mindlin} = \frac{4}{3}\frac{G^{*2}}{E^*} c^{-1} \mu^{-1} (u_x^{(0)})^3$) with the energy lost (11) due to relaxation damping. The relaxation damping exceeds the Mindlin damping if $4\mu \frac{E^*}{G^*} \frac{|u_z^{(0)}|}{|u_x^{(0)}|} \sin^2 \varphi_0 > 1$. Note that the left-hand side of this inequality is proportional to the ratio of the changes in the contact radius due to purely normal and purely tangential oscillation.

The above comparison provides an impression of the relative importance of the Mindlin damping and the relaxation damping. As E^*/G^* and $\sin^2\varphi_0$ typically have the order of magnitude of unity, the relative importance of the "Mindlin damping" and the relaxation damping is given by the factor $4\mu|u_z^{(0)}|/|u_x^{(0)}|$. For example, for the coefficient of friction of $\mu=1/4$ the relative contribution will be given just by the ratio of the normal and tangential oscillation, $|u_z^{(0)}|/|u_x^{(0)}|$. For a typical contact in a system subjected to vibrations, it is common for normal and tangential oscillations to have the same order of magnitude. This means that the relaxation damping for a "typical system" has the same order of magnitude as frictional dissipation.

Let us stress that the present paper is based on the assumption that the amplitude of the tangential oscillation is much smaller than the radius of the contact. While this condition is met on the macroscopic scale (through the assumption of small oscillation amplitudes), it can be easily violated on the scale of microcontacts[28]. This may pose some restrictions to the applicability of the equations (12) and (18) to contacts of rough surfaces. Another restriction is due to the assumption of perfect elasticity. We neglected any kinetic processes, such as creep of micro-contacts[29], which lead to deviations from the theory already in the case of pure tangential loading and surely have to be considered in the general case as well.

Our analysis shows that application of normal oscillations will significantly change the damping behaviour of tangential movement in a system with friction. This may be used for designing and tuning structural damping of systems with frictional contacts. Further, the effect of the relaxation damping may account for the well-known effect of suppression of frictional instabilities by application of ultrasonic oscillations, which was studied both theoretically[30] and experimentally[31].

Methods

In the theoretical part, we use the Method of Dimensionality Reduction (MDR) in contact mechanics[11]. Within the usual assumptions of contact mechanics, the MDR has been proven rigorously for normal and tangential contacts of simple (axially symmetric) surfaces.

Additional verification and extension to non-axisymmetric indenters is done using the three-dimensional Boundary Element Method (BEM)[25]. We use an implementation of the BEM that is based on the Fast Fourier Transform, and was developed by one of the authors (R.P.)

*Let us briefly sketch the reasons for this supposed generality. Consider a contact of an *arbitrarily* shaped rigid indenter with an elastic half-space and assume the decoupling of the normal and tangential problems. The normal force F_N will then depend only on the indentation depth d, that is $F_N=F_N(d)$. Let us define the incremental normal contact stiffness $k_z(d)$ and the incremental tangential stiffness $k_x(d)$. Now we simultaneously change the indentation by $\mathrm{d}d$ and the tangential displacement by $\mathrm{d}x$ and calculate the incremental changes of the normal and tangential forces: $\mathrm{d}F_N=k_z(d)\mathrm{d}d$, $\mathrm{d}F_x=k_x(d)\mathrm{d}x$. The ratio of these increments is equal to $\mathrm{d}F_N/\mathrm{d}F_x=(k_z(d)/k_x(d))(\mathrm{d}d/\mathrm{d}x)$. For all axis-symmetric contacts, the ratio of the normal and tangential stiffness is constant and equal to $k_z(d)/k_x(d)=E^*/G^*$, see[15]. Indeed, the integral relations connecting the normal and tangential displacements in the origin of coordinates ($x=y=0$) with normal and tangential stresses read

$$u_z(0,0) = \frac{1}{\pi E^*}\iint_A \frac{\sigma_{zz}(\tilde{x},\tilde{y})}{R}\mathrm{d}\tilde{x}\mathrm{d}\tilde{y},$$

$$u_x(0,0) = \frac{1}{2\pi G}\iint_A \sigma_{zx}(\tilde{x},\tilde{y})\left[\frac{1-\nu}{R}+\frac{\nu\tilde{x}^2}{R^3}\right]\mathrm{d}\tilde{x}\mathrm{d}\tilde{y}$$

with $R=\sqrt{\tilde{x}^2+\tilde{y}^2}$. In the axis-symmetric case, the second term in the previous equation can be averaged over the polar angle in the contact area providing

$$u_x(0,0) = \frac{1}{2\pi G}\iint_A \sigma_{zx}(\tilde{x},\tilde{y})\left[\frac{1-\nu}{R}+\frac{\nu}{2R}\right]\mathrm{d}\tilde{x}\mathrm{d}\tilde{y} = \frac{2-\nu}{4\pi G}\iint_A \frac{\sigma_{zx}(\tilde{x},\tilde{y})}{R}\mathrm{d}\tilde{x}\mathrm{d}\tilde{y}.$$

The same stress distributions in normal and tangential direction will thus produce displacements whose ratio is $u_z(0,0)/u_x(0,0)=4\pi G/((2-\nu)E^*)=G^*/E^*$, which means that the stiffness ratio is E^*/G^*. This result happens to be extremely robust and is valid in good approximation not only for axis-symmetric contacts. For example, in[22], it was shown theoretically and numerically that the ratio of the normal and tangential stiffness remains the same for arbitrary randomly rough surfaces. If we assume that this is valid for any contact configuration, then for the ratio of forces we get $\mathrm{d}F_N/\mathrm{d}d=(E^*/G^*)\mathrm{d}F_x/\mathrm{d}x$ which means that the *tangential reaction of any contact is uniquely determined by its normal reaction*. In other words, if for two contact systems the normal reaction $F_N(d)$ is identical, then the tangential reaction will also be identical. In the papers[23,24] this has been confirmed by numerical simulation of contacts of rough surfaces with arbitrary coefficient of friction. This further means that any arbitrary contact satisfying the conditions of decoupling of the normal and tangential contact behaves in the same way in terms of displacement and forces as an equivalent single-contact axisymmetric system having the same normal reaction. From this it follows that all properties that depend solely on the force-displacement reactions of the system will be identical for all contacts having the same dependence of the normal force on indentation. This provides further support to the generality of the equations (12) and (17).

References

1. Mindlin, R. D., Mason, W. P., Osmer, J. F. & Deresiewicz, H. Effects of an oscillating tangential force on the contact surfaces of elastic spheres. *Proc. 1st US National Congress of Applied Mech.*, ASME, New York, 203–208 (1952).
2. Gaul, L. & Lenz, J. Nonlinear dynamics of structures assembled by bolted joints. *Acta Mechanica* **125(1–4)**, 169–181 (1997).
3. Akay, A. Acoustics of friction. *J. of Acoust. Soc. of America* **111(4),** 1525–1548 (2002).
4. Zhou, X., Shin, E., Wang, K. W. & Bakis, C. E., Interfacial damping characteristics of carbon nanotube-based composites. *Composites Sci. and Technology*. **64(15),** 2425–2437 (2004).
5. Davies, M., Barber, J. R. & Hills, D. A. Energy dissipation in a frictional incomplete contact with varying normal load. *Intl. J. of Mech. Sci.* **55,** 13–21 (2012).
6. Putignano, C., Ciavarella, M. & Barber, J. R. Frictional energy dissipation in contact of nominally flat rough surfaces under harmonically varying loads. *J. of the Mech. and Phys. of Solids* **59,** 2442–2454 (2011).
7. Landau, L. D. On the vibrations of the electronic plasma. *J. of Exp. and Theor. Phys.* **10,** 25 (1946).
8. Popov, V. L. & Gray, J. A. T. Prandtl-Tomlinson model: history and applications in friction, plasticity, and nanotechnologies. *ZAMM-J. of Applied Math. and Mech.* **92,** 683–708 (2012).
9. Meyer, E., Overney, R. M., Dransfeld, K. & Gyalog, T. *Nanoscience: friction and rheology on the nanometer scale*. World Scientific, Singapore (1998).
10. Müser, M. H., Urbakh, M. & Robbins, M. O. Statistical mechanics of static and low-velocity kinetic friction. *Advances in Chem. Phys.* **126,** 187–272 (2003).
11. Popov, V. L. & Heß, M. *Method of dimensionality reduction in contact mechanics and friction*. (Springer, 2014).
12. Galin, L. A. *Contact problems in the theory of elasticity*. (North Carolina State College, 1961). This book is an English translation of the Russian original of 1953: Галин Л. А. *Контактные задачи теории упругости*. (1953).
13. Sneddon, I. N. The relation between load and penetration in the axisymmetric Boussinesq problem for a punch of arbitrary profile. *Intl. J. of Eng. Sci.* **3(1),** 47–57 (1965).
14. Cattaneo, C. Sul contatto di due corpi elastici: distribuzione locale degli sforzi. *Rendiconti dell'Accademia Nazionale dei Lincei* **27,** 342–348, 434–436, 474–478 (1938).
15. Mindlin, R. D. Compliance of elastic bodies in contact. *J. of Applied Mech.* **16,** 259–268 (1949).
16. Jäger, J. Axi-symmetric bodies of equal material in contact under torsion or shift. *Archive of Applied Mech.* **65,** 478–487 (1995).
17. Ciavarella, M. The generalized Cattaneo partial slip plane contact problem. I: Theory. *Intl. J. of solids and structures* **35,** 2349–2362 (1998).
18. Heß, M. *Über die Abbildung ausgewählter dreidimensionaler Kontakte auf Systeme mit niedrigerer räumlicher Dimension*. (Göttingen: Cuvillier-Verlag, 2011).
19. Munisamy, R. L., Hills, D. A. & Nowell, D. Static axisymmetric Hertzian contacts subject to shearing forces. *J. of Applied Mech.* **61,** 278–283 (1994).
20. Popov, V. L. *Contact mechanics and friction*. (Springer, 2010).
21. Greenwood, J. A. & Williamson, J. B. P., Contact of nominally flat surfaces. *Proc. of Royal Soc.* A **295 No 1442**, 300–319 (1966).
22. Campana, C., Persson, B. N. J. & Müser, M. H. Transverse and normal interfacial stiffness of solids with randomly rough surfaces. *J. of Phys.: cond. mat.* **23(8),** 085001 (2011).
23. Paggi, M., Pohrt, R. & Popov, V. L. Partial-slip frictional response of rough surfaces. *Scientific Reports* **4,** 5178 (2014).
24. Grzemba, B., Pohrt, R., Teidelt, E. & Popov, V. L. Maximum micro-slip in tangential contact of randomly rough self-affine surfaces. *Wear* **309,** 256–258 (2014).
25. Pohrt, R. & Li, Q. Complete boundary element formulation for normal and tangential contact problems. *Phys. Mesomechanics* **17(4),** 334–340 (2014).
26. Brillouin, M. *Notice sur les travaux scientifiques*. (Gauthiers-Vilars, Paris, 1990).
27. Ciavarella, M., Hills, D. A. & Moobola, R. Analysis of plane and rough contacts, subject to a shearing force. *Intl. J. of Mech. Sci.* **41(1),** 107–120 (1999).
28. Prevost, A., Scheibert, J. & Debregas, G. Probing the micromechanics of a multi-contact interface at the onset of frictional sliding. *European Phys. J. E* **36(2),** 1–12 (2013).
29. Bureau, L., Caroli, C. & Baumberger, T. Elasticity and onset of frictional dissipation at a non-sliding multi-contact interface. *Proc. of Royal Soc.* A **459 No 2039**, 2787–2805 (2003).
30. Guerra, R., Vanossi, A. & Urbakh, M. Controlling microscopic friction through mechanical oscillations. *Phys. Rev. E* **78(3),** 036110 (2008).
31. Popov, V. L. & Starcevic, J. Effect of vibrations on the laboratory model "earthquake" statistics. *Techn. Phys. Lett.* **32,** 630–633 (2006).

Acknowledgements
We acknowledge useful discussions with N. Popov. This work was supported in part by the Ministry of Education of the Russian Federation, by COST Action MP1303 and by Deutsche Forschungsgemeinschaft.

Author Contributions
M.P. and V.L.P. conceived the research and performed the theoretical analysis. R.P. verified the results with 3D boundary element simulations. All authors discussed the results and contributed to the manuscript.

Additional Information
Competing financial interests: The authors declare no competing financial interests.

How to cite this article: Popov, M. *et al.* Relaxation damping in oscillating contacts. *Sci. Rep.* **5**, 16189; doi: 10.1038/srep16189 (2015).

2.2 Publication 2

This short note represents a direct application of the results from Publication 1 in the context of woven fabrics. A unit cell of the fabric, consisting of two crossed elastic beams, is considered, with three ends held fixed and one end subjected to normal and tangential oscillation (with equal frequencies and a phase shift). The geometric factor $\partial^2 F_z/\partial u_z^2$ is derived for the system by combining thin beam theory and Hertzian contact mechanics. With that, the energy dissipated per oscillation cycle is obtained directly by referencing Eq. (12) of the previous paper. The dependence on the oscillation parameters is unchanged from the indenter-on-plane configuration, however an inverse dependence on the fifth power of the fiber aspect ratio is found. This implies that relaxation damping is only likely to play a role in densely woven fabrics, a consideration that may be relevant in estimating internal damping in fiber composites. However, all such conclusions must be considered qualitative, due to the strongly simplified nature of the mesh cell model.

FACTA UNIVERSITATIS
Series: **Mechanical Engineering** Vol. 13, N° 1, 2015, pp. 21 - 25

NON-FRICTIONAL DAMPING IN THE CONTACT OF TWO FIBERS SUBJECT TO SMALL OSCILLATIONS

UDC 539.3

Mikhail Popov[1,2]

[1]Berlin University of Technology, Germany
[2]National Research Tomsk State University, Russia

Abstract *Structural damping is discussed for the contact of two fibers in a woven material. In the presence of both normal and tangential oscillations, structural (relaxation) damping takes place even with perfect sticking in the contact, where slip-related frictional damping disappears. For the case of an infinite coefficient of friction and small amplitudes a closed-form solution for energy lost during one oscillation cycle is obtained.*

Key Words: *Woven Composites, Structural Damping, Oscillating Contacts*

1. Introduction

The present paper is concerned with internal damping in woven materials. When fabrics are deformed, energy is dissipated in the contacts between fibers, and it is well known that at least part of this dissipation is due to friction in partial slip zones of the contact. Exact solutions for frictional damping in the contact of spheres due to tangential oscillations go back to Mindlin et. al. [1] and are also applicable to the contact of two crossed cylinders (such as the fibers in a woven material). Damping in the presence of both normal and tangential oscillations, however, has never been described exhaustively and it remains a current research topic [2],[3]. Recently it has been suggested [4] that the superposition of normal and tangential oscillations leads, in addition to slip-related frictional dissipation, to a new type of non-frictional damping that is caused by elastic relaxation due to variations in normal load and therefore contact area. It is found that in the absence of slip (an infinite coefficient of friction) and for small oscillation amplitudes, the energy dissipated during an oscillation cycle is described by

Received: January 05, 2015
Corresponding author: Popov Mikhail
Technische Universität Berlin, 10623 Berlin, Germany
E-mail: mikhail.popov@tu-berlin.de

$$Q = \frac{8}{3}\frac{G^*}{E^*}\frac{\partial^2 F_n}{\partial u_z^{\,2}} u_x^{(0)2}\left|u_z^{(0)}\right|\sin^2\phi_0 \tag{1}$$

where $u_x^{(0)}$ and $u_z^{(0)}$ are the tangential and normal oscillation amplitudes, ϕ_0 is the phase shift between the oscillations (the oscillation frequencies are identical), F_n is the normal contact force, u_z the indentation depth (relative approach of bodies). E^* and $G^*$are the reduced elastic and shear moduli and can be expressed through elastic modulus E and Poisson's ratio ν as follows, when both contact partners are made from the same linear, homogeneous, isotropic material.

$$E^* = \frac{E}{2(1-\nu^2)} \tag{2}$$

$$G^* = \frac{E}{(1+\nu)(2-\nu)} \tag{3}$$

In the present work we specialize the above result for a system of two fibers crossed at right angles, representing a single mesh cell of a woven material. Small oscillations that are applied to the end of one fiber produce oscillations in the contact, leading to structural damping (and frictional damping, if slip is permitted). All assumptions from [4] (linearly elastic materials without viscous effects, infinite coefficient of friction, small amplitudes) are used here as well, so as to isolate the contribution of structural damping to overall losses.

2. Analysis

We consider a very simple model representing a mesh cell of a woven material: two fibers with circular sections (with radius R) that are crossed at right angles, Fig.1. The fibers lie in x, y - plane, while the upward-facing axis is labeled z. Three of the four fiber ends are rigidly embedded in the plane at $z = 0$, while one end is connected to a parallel guide that permits motion in x, y - plane (horizontal and vertical). These boundary conditions are neither the only possible nor necessarily the most representative of real fabrics. The above model is chosen for its simplicity, while other possible configurations are left for future work. The movable end is pre-stressed by deflecting it downwards by $W_{z,0}$, which is of the order of $2R$ in woven materials, due to symmetrical boundary conditions. Through this initial displacement, contact between the fibers is established, and base loading $F^{(0)}$ is produced in the contact. In addition, the movable end of the fiber is forced to oscillate with amplitudes ΔW_x, ΔW_z, a common frequency and phase shift ϕ_0.

Our general approach is as follows: Firstly, the oscillation amplitudes of the movable fiber end are related to force oscillations, with certain amplitudes, in the contact. Linear beam theory is used for this, while the influence of indentation depth u_z is neglected (our general assumption is that $W_{z,0} >> u_z >> \Delta W$). The force oscillations in the contact are then related to geometrical oscillations through the contact stiffness, which is itself determined by the contact configuration, and therefore $W_{z,0}$.

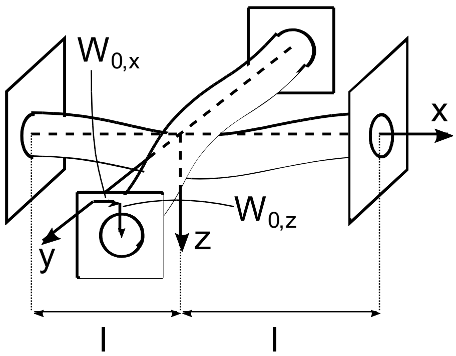

Fig. 1 Two crossed fibers are considered as elastic beams with circular cross-section

Consider a beam of length $2l$ that is stressed with a contact force F_z in the middle and deflected by $W_{0,z}$ at one end. The deflection of the central point (at $x = l$) of the beam with these boundary conditions is known to be [5]

$$W_{I,z}(l) = -\frac{F_z l^3}{24EI} + \frac{W_{0,z}}{2}, \tag{4}$$

where $I = \pi R^4/4$ is the area moment of inertia. For the beam with two fixed ends, only the first component, due to the contact force in the middle, is present:

$$W_{II,z}(l) = \frac{F_z l^3}{24EI}. \tag{5}$$

The difference between the two is equal to indentation depth u_z in the contact:

$$u_z = W_{I,z}(l) - W_{II,z}(l) = -\frac{F_z l^3}{12EI} + \frac{W_{0,z}}{2}. \tag{6}$$

As noted above, we assume that the indentation depth is small compared to the deflection of the beam, and apply non-penetration condition, $u_z = 0$, which leads to a linear relationship between contact force and deflection of the free end:

$$F_z = 6W_{0,z}\frac{EI}{l^3}. \tag{7}$$

For tangential loading, the lower beam is stressed length-wise; its deformation therefore can be neglected. The equations in this case become

$$W_{I,x}(l) = -\frac{F_x l^3}{24EI} + \frac{W_{0,x}}{2}, \tag{8}$$

$$W_{II,x} = 0. \tag{9}$$

Proceeding as above, we obtain

$$F_x = 12W_{0,x}\frac{EI}{l^3}. \tag{10}$$

The force is thus linearly proportional to the deflection of the end of the movable beam. If the latter is now oscillating according to $W_z = W_{z,0} + \Delta W_z \sin \omega t$ and $W_x = \Delta W_x \sin(\omega t + \phi_0)$, then the amplitudes of the force oscillations in the contact are

$$\Delta F_z = 6\Delta W_z \frac{EI}{l^3}, \tag{11}$$

$$\Delta F_x = 12\Delta W_x \frac{EI}{l^3}. \tag{12}$$

Now, when the oscillation of contact forces is known, the corresponding components of relative displacement of contacting bodies, u_x and u_z can be found by dividing the force increments by contact stiffness k_x in the tangential direction or k_z in normal direction. The latter are known to be

$$k_x = 2G^* a, \tag{13}$$

$$k_z = 2E^* a, \tag{14}$$

where a, the contact radius, is equal to $\sqrt{Ru_z}$ in the contact of a sphere with a plane or the contact of two crossed cylinders [6]. The derivative of the normal contact stiffness with respect to indentation depth u_z is given by

$$\frac{\partial^2 F_n}{\partial u_z^{\,2}} = \frac{\partial k_z}{\partial u_z} = E^* \sqrt{\frac{R}{u_z}}. \tag{15}$$

One last step is necessary to tie all equations together: indentation depth u_z, which, for a spherical contact, is given by [6]

$$u_z = \left(\frac{3F^{(0)}}{4E^* \sqrt{R}} \right)^{2/3}, \tag{16}$$

where $F^{(0)} = 6W_{z,0} \dfrac{EI}{l^3}$ is the initial loading determined with Eq. (7). Substituting all factors into the relaxation-damping Eq. (1) and simplifying, gives the following result:

$$Q = 4\left(\frac{2}{3}\right)^{2/3} \pi^{5/3} \frac{(1+\nu)(2-\nu)}{(1-\nu^2)^{1/3}} E \left(\frac{R}{l}\right)^5 \left(\frac{R}{W_{z,0}}\right)^{4/3} \Delta W_x^2 \left|\Delta W_z\right| \sin^2 \phi_0 . \tag{17}$$

By introducing fiber aspect ratio $\alpha = l/R$, the normalized initial displacement $\tilde{W}_0 = \Delta W_z / R$ and grouping some of the factors under

$$q = 4\left(\frac{2}{3}\right)^{2/3} \pi^{5/3} \frac{(1+\nu)(2-\nu)}{(1-\nu^2)^{1/3}}, \tag{18}$$

we can write the result more compactly as

$$Q = q\alpha^{-5} \tilde{W}_0^{-4/3} E \left(\Delta W_x\right)^2 \left|\Delta W_z\right| \sin^2 \phi_0 . \tag{19}$$

Note that q varies only slightly for typical values of ν. Its numerical value is approximately 45 for $\nu = 0.2$, 47 for $\nu = 0.3$ and 51 for $\nu = 0.5$).

3. Discussion

The obtained result for a system of two crossed fibers is similar to Eq. (1) that describes relaxation damping when oscillations are applied to the contact directly. In particular, the proportionality to the square of the tangential oscillation amplitude, and the modulus of the normal oscillation amplitude is preserved, which is, of course, not surprising, since linearity is assumed in the derivation. More interesting is the inverse proportionality to the fifth power of the aspect ratio of the fibers, which means that the effect will be much more pronounced in densely woven fabrics than in sparse ones.

The obtained result is only valid for an infinite coefficient of friction. An interesting avenue for future work would be to consider realistic coefficients of friction and to determine the relative importance of frictional and structural damping. Also, although a physical interpretation of relaxation damping in perfect stick conditions is given in [4], the underlying mechanism in the presence of sliding is yet to be determined. Other unexplored possibilities involve other boundary conditions for the mesh cell, embedding the cell in a viscous medium (which would extend the results to woven composites), as well as experimental verification.

Acknowledgements: *The author would like to thank Valentin L. Popov for many useful discussions. This work is supported in part by Tomsk State University Academic D.I. Mendeleev Fund Program.*

References

1. Mindlin R.D., Mason W.P., Osmer J.F., Deresiewicz H., 1952, *Effects of an oscillating tangential force on the contact surfaces of elastic spheres*, Pros. 1st US National Congress of Applied Mechanics, ASME, New York, pp. 203–208.
2. Davies M., Barber J.R., Hills D.A., 2012, *Energy dissipation in a frictional incomplete contact with varying normal load*, Int. J. Mech. Sci., 55, pp. 13–21.
3. Putignano C., Ciavarella M., Barber J.R., 2011, *Frictional energy dissipation in contact of nominally flat rough surfaces under harmonically varying loads*, J. of the Mechanics and Physics of Solids, 59, pp. 2442–2454.
4. Popov M., Popov V.L., Pohrt R., 2014, *Relaxation damping in oscillating contacts*, arXiv:1410.3238 [cond-mat.soft].
5. Landau L.D., Lifshitz E.M., 1970, *Theory of Elasticity*, 2nd English Edition, §2, Pergamon Press.
6. Popov V.L., 2010, *Contact mechanics: Physical principles and applications*, Springer-Verlag.

2.3 Publication 3

The following short note considers relaxation damping in a contact with superimposed torsional and normal oscillation. This work was prompted by a recent (at the time of publication) extension of the Method of Dimensionality Reduction, which allowed rigorous reduction of a torsionally loaded contact to a contact with a one-dimensional elastic foundation with transverse spring movement. Using this result, the present paper repeats the procedure laid out in Publication 1 to obtain the energy dissipation per cycle under phase-shifted torsional and normal oscillation. The result (Eqs. 14, 15) is nearly the same as in the tangential/normal case, except for a different reduced shear modulus and a non-linear term related to the non-constant contact radius (which disappears if the normal oscillation amplitude is small). The source of this similarity is immediately apparent when considered within the framework of the MDR, but would have taken some work to arrive at using more conventional methods of contact mechanics.

Finally, a system with three overlaid oscillations, where the tangential and torsional components have respective phase shifts φ_1 and φ_2 relative to the normal oscillation, is considered. The result (Eq. 20, 21) is very straight-forward due to additivity of the elastic energy components.

ISSN 1029-9599, Physical Mesomechanics, 2016, Vol. 19, No. 2, pp. 178–181. © Pleiades Publishing, Ltd., 2016.
Original Text © M. Popov, V.L. Popov, 2015, published in Fizicheskaya Mezomekhanika, 2015, Vol. 18, No. 4, pp. 57–60.

Relaxation Damping in Contacts under Superimposed Normal and Torsional Oscillation

M. Popov[1,2]* and V. L. Popov[1,2,3]

[1] *Berlin University of Technology, Berlin, 10623 Germany*
[2] *National Research Tomsk State University, Tomsk, 634050 Russia*
[3] *National Research Tomsk Polytechnic University, Tomsk, 634050 Russia*
** e-mail: mikhail.popov@tu-berlin.de*

Received June 19, 2015

Abstract—It was recently shown that if a contact of two purely elastic bodies with no sliding is subjected to oscillations in normal and tangential directions, a kind of damping occurs due to relaxation of tangential stress in areas of intermittent contact, despite the absence of sliding and corresponding frictional work. In the present paper we show that the same mechanism acts in contacts with superimposed normal and torsional oscillations. A closed-form solution for the torsional and combined (torsional/tangential) relaxation dissipation for a contact of arbitrary bodies of revolution is presented.

DOI: 10.1134/S1029959916020107

Keywords: structural damping, contact mechanics, torsional oscillations, method of dimensionality reduction

1. INTRODUCTION

Oscillating tangential contacts exhibit partial slip at the border of the contact area and energy dissipation related to this slip. Mindlin et al. studied this frictional damping both analytically and experimentally [1] in 1952. The contact damping plays an important role in numerous applications in structural mechanics [2], tribology [3], materials science [4] and technological processes related to the dynamics of granular media [5–8]. As partial slip is the main cause of this sort of damping, the damping disappears when the coefficient of friction increases and tends toward infinity [1]. However, when a contact oscillates in both normal and tangential directions, the situation changes. Such damping has been recently studied by Davies et al. [9] for smooth two-dimensional profiles and by Putignano et al. [10] for rough surfaces. However, the fact that dissipation exists even in the limiting case of an infinite coefficient of friction, when relative frictional movement of the contacting bodies does not occur, went unnoticed and was first pointed out in [11]. The effect of relaxation damping as proposed in [11] can be easily extended to a contact with torsional (instead of tangential) oscillation superimposed with normal oscillation, which is the purpose of the present paper. As in the original paper [11], we assume perfect stick throughout the contact.

2. ANALYSIS

Consider a contact between two axially-symmetric elastic bodies with moduli of elasticity of E_1 and E_2, Poison's ratios of ν_1 and ν_2, and shear moduli of G_1 and G_2, accordingly. We denote the difference between the profiles of bodies as $\tilde{z} = f(r)$, where $\tilde{z}$ is the coordinate normal to the contact plane, and r is in the in-plane polar radius. The profiles are brought into contact and are subjected to a superposition of normal, tangential, and torsional oscillations with small amplitudes. This contact problem can be reduced to the contact of a rigid profile $\tilde{z} = f(r)$ with an elastic half-space (Fig. 1a).

Derivations of the present paper are based on the method of dimensionality reduction in contact mechanics (MDR) [12, 13], which recently was extended to torsional contacts [14]. In the framework of the method of dimensionality reduction, two preliminary steps are performed [13]. First, the three-dimensional elastic bodies are replaced by a one-dimensional linearly elastic foundation consisting of an array of independent springs, with a sufficiently small separation Δx and normal and tangential stiffness Δk_z and Δk_x defined according to the rules

$$\Delta k_z = E^* \Delta x \quad \text{with} \quad \frac{1}{E^*} = \frac{1-\nu_1^2}{E_1} + \frac{1-\nu_2^2}{E_2}, \tag{1}$$

$$\Delta k_x = G^* \Delta x \quad \text{with} \quad \frac{1}{G^*} = \frac{2-\nu_1}{4G_1} + \frac{2-\nu_2}{4G_2}. \tag{2}$$

In the second step, the three-dimensional profile $z = f(r)$ is transformed into a one-dimensional profile according to

$$g(x) = |x| \int_0^{|x|} \frac{f'(r)}{\sqrt{x^2 - r^2}} \mathrm{d}r. \tag{3}$$

If now the MDR-transformed profile $g(x)$ is indented into the defined elastic foundation by the indentation depth d and is moved normally and tangentially according to arbitrary law, the force-displacement relations of the equivalent one-dimensional system will reproduce those of the original three-dimensional contact problem (proofs have been done in [12]).

In [14], it was shown that this procedure can be extended to torsional contacts by also allowing movement of the springs in the y-direction and by defining the corresponding stiffness according to the rule

$$\Delta k_y = \tilde{G} \Delta x \quad \text{with} \quad \frac{1}{\tilde{G}} = \frac{1}{8G_1} + \frac{1}{8G_2}. \tag{4}$$

This rule guarantees the correct description of the dependence of the torsional moment on the torsional angle, while the z-axis is considered as axis of rotation.

From the correctness of the force-displacement and torque-angle relations, it follows that the work and the dissipated energy will also be reproduced correctly. This is the reason for using the method of dimensionality reduction for calculation of energy dissipation.

In the following, we consider a rigid conical indenter

$$z = f(r) = r \tan\theta \tag{5}$$

in a contact with a half-space (Fig. 1a). This choice means no restriction as the results can be generalized very easily to an arbitrary axis-symmetrical shape (see discussion below). The one-dimensional MDR-image of the conical profile (5), according to (3), is

$$g(x) = |x| \frac{\pi}{2} \tan\theta = c|x|, \tag{6}$$

where $c = \pi/2 \tan\theta$ is the slope of the one-dimensional equivalent profile (Fig. 1b). The generalization for an arbitrary axis-symmetrical shape is possible due to the fact that the central area of permanent contact does not contribute to relaxation damping. Only the edge of the contact needs to be considered, and if the amplitude of normal oscillation is sufficiently small compared to the curvature of the indenter, the shape of the edge of the contact will always be approximately linear. In this case, all axially-symmetric indenters will behave like conical indenters and the slope c at the edge of the contact of the one-dimensional MDR-transformed profile becomes the only shape-related parameter. For example, for a parabolic indenter $\tilde{z} = r^2/(2R)$, the MDR-transformed profile is $\tilde{z} = g(x) = x^2/R$ and the edge slope is $c = 2a/R$ where a is the contact radius. As shown already in [11], the parameter c can be represented in a universal form which does not depend on the profile shape. The incremental contact stiffness is known to be equal to $\partial F_\mathrm{n}/\partial d = 2aE^*$ [15]. Deriving this equation once more gives $\partial^2 F_\mathrm{n}/\partial d^2 = 2E^* \partial a/\partial d = 2E^*/c$. Thus, the slope of the MDR-transformed profile can be calculated as

$$\frac{1}{c} = \frac{1}{2E^*} \frac{\partial^2 F_\mathrm{n}}{\partial d^2}. \tag{7}$$

Consider a point of the rigid indenter with initial distance $z^{(0)}$ from the plane and let us assume that the oscillations in the normal and tangential direction are given by

$$\begin{aligned} z(t) &= -z^{(0)} + u_z^{(0)} \cos(\omega t), \\ y(t) &= x\varphi^{(0)} \cos(\omega t + \varphi_0), \end{aligned} \tag{8}$$

where $\varphi^{(0)}$ is the amplitude of the angle of torsion. All points of the medium which are in contact with the indenter follow this motion. If $|u_z^{(0)}| > z^{(0)}$, the point of the rigid surface will come into contact with one of the springs of the elastic foundation when the coordinate of the indenter will be y_1 and the indenter will drag it along to point y_2, where contact is lost and the spring

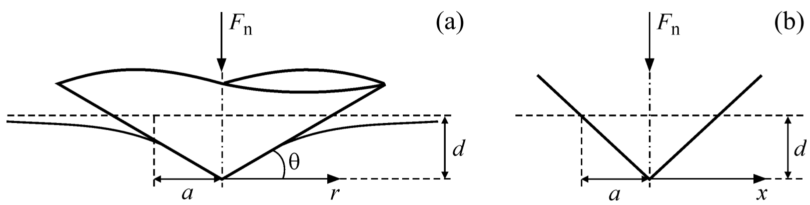

Fig. 1. Contact of a rigid cone with a half-space (a) and the corresponding MDR-transformed one-dimensional profile (b).

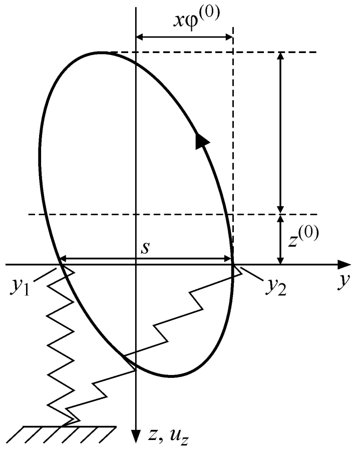

Fig. 2. A point of the rigid surface with the initial coordinate $z = -z^{(0)}$ oscillates around this position. It comes into contact with a spring in point y_1 and loses contact in point y_2.

relaxes over the distance $s = y_2 - y_1$. The coordinates y_1 and y_2 are determined by setting $z = 0$. After simple calculations we get

$$s = y_2 - y_1 = 2x\varphi^{(0)}\sqrt{1-\left(\frac{z^{(0)}}{u_z^{(0)}}\right)^2}\sin\varphi_0. \quad (9)$$

The energy lost in one oscillation cycle (in the entire contact) by a conical indenter is

$$W = \tilde{G}\int_{a_{\min}}^{a_{\max}} s^2 \mathrm{d}x, \quad (10)$$

where

$$z_0 = g(x) - d = cx - d \quad (11)$$

and the minimal and maximal contact radii are

$$a_{\min} = \frac{d - u_z^{(0)}}{c}, \; a_{\max} = \frac{d + u_z^{(0)}}{c}. \quad (12)$$

The integral (10) evaluates to

$$W = \frac{16}{3}\tilde{G}\varphi^{(0)2}\sin^2\varphi_0\left(\frac{d^2 u_z^{(0)}}{c^3} + \frac{u_z^{(0)3}}{5c^3}\right). \quad (13)$$

Introducing the "average contact radius", $a = d/c$, we can rewrite this as

$$W = \frac{16}{3}\frac{\tilde{G}}{c}(a\varphi^{(0)})^2\left|u_z^{(0)}\right|\sin^2\varphi_0\left(1 + \frac{u_z^{(0)2}}{5d^2}\right). \quad (14)$$

Using equation (7), the dissipated energy during one cycle in a contact under action of normal and torsional oscillations will therefore be given by:

$$W = \frac{8}{3}\frac{\tilde{G}}{E^*}\frac{\partial^2 F_{\mathrm{n}}}{\partial d^2}a^2\varphi^{(0)2}\left|u_z^{(0)}\right|\sin^2\varphi_0\left(1 + \frac{u_z^{(0)2}}{5d^2}\right). \quad (15)$$

For the example case of a contact of a rigid indenter with an elastic half-space having the Young modulus E and Poisson ratio ν, we have

$$\frac{\tilde{G}}{E^*} = \frac{8G}{2G(1+\nu)} = \frac{4}{1+\nu}$$

and the dissipation equation takes the form

$$W = \frac{32}{3(1+\nu)}\frac{\partial^2 F_{\mathrm{n}}}{\partial d^2}a^2\varphi^{(0)2}\left|u_z^{(0)}\right| \times \sin^2\varphi_0\left(1 + \frac{u_z^{(0)2}}{5d^2}\right). \quad (16)$$

Note that this result can be further generalized to superimposed oscillations in the normal and tangential direction as well as torsion. As the tangential force does not influence the torsional moment, the force-displacement and the moment-angle relations will be independent, which means that the corresponding relaxation contributions can be just added. For oscillations described by

$$z(t) = -z^{(0)} + u_z^{(0)}\cos(\omega t), \quad (17)$$

$$x(t) = u_x^{(0)}\cos(\omega t + \varphi_1), \quad (18)$$

$$\varphi(t) = \varphi^{(0)}\cos(\omega t + \varphi_2) \quad (19)$$

the energy dissipation per cycle will be

$$W = \frac{8}{3}\frac{1}{E^*}\frac{\partial^2 F_{\mathrm{n}}}{\partial d^2}\left|u_z^{(0)}\right| \times\left(G^* u_x^{(0)2}\sin^2\varphi_1 + \tilde{G}a^2\varphi^{(0)2}\sin^2\varphi_2\left(1 + \frac{u_z^{(0)2}}{5d^2}\right)\right). \quad (20)$$

If the oscillation amplitude is small $u_z^{(0)} \ll d$, then the second term in the last brackets can be dropped, therefore

$$W = \frac{8}{3}\frac{1}{E^*}\frac{\partial^2 F_{\mathrm{n}}}{\partial d^2}\left|u_z^{(0)}\right| \times(G^* u_x^{(0)2}\sin^2\varphi_1 + \tilde{G}a^2\varphi^{(0)2}\sin^2\varphi_2). \quad (21)$$

3. CONCLUSION

In the present paper, the effect of relaxation damping described in [11] was extended for the superimposed normal, tangential and torsional contact of arbitrary axis-symmetric elastic bodies with infinite friction in the contact area. The assumption of the infinite coefficient of friction was made only to study the effect in the pure. However, all results are also applicable to systems with a finite coefficient of friction provided that the changes in the radius of the stick region are much smaller than those due to changing indentation. The dissipated energy is proportional to the amplitude of the normal oscillation and to square of the amplitude of torsional oscillations and to second derivative of the normal force with respect to the indentation depth.

ACKNOLEDGMENTS

This work was supported in part by Tomsk State University Academic D.I. Mendeleev Fund Program, project No. 8.2.19.2015.

REFERENCES

1. Mindlin, R.D., Mason, W.P., Osmer, J.F., and Deresiewicz, H., Effects of an Oscillating Tangential Force on the Contact Surfaces of Elastic Spheres, in *Pros. 1st US National Congress of Applied Mechanics*, ASME, New York, 1952, pp. 203–208.
2. Gaul, L. and Lenz, J., Nonlinear Dynamics of Structures Assembled by Bolted Joints, *Acta Mech*., 1997, vol. 125(4), pp. 169–181.
3. Akay, A., Acoustics of Friction, *J. Acoust. Soc. Am*., 2002, vol. 111(4), pp. 1525–1548.
4. Zhou, X., Shin, E., Wang, K.W., and Bakis, C.E., Interfacial Damping Characteristics of Carbon Nanotube-Based Composites, *Compos. Sci. Technol*., 2004, vol. 64(15), pp. 2425–2437.
5. Thornton, C. and Yin, K.K., Impact of Elastic Spheres with and without Adhesion, *Powder Technol*., 1991, vol. 65, pp. 153–166.
6. Ciamarra, M.P., Lara, A.H., Lee, A.T., Goldman, D.I., Vishik, I., and Swinney, H.L., Dynamics of Drag and Force Distributions for Projectile Impact in a Granular Medium, *Phys. Rev. Lett*., 2004, vol. 92, p. 194301.
7. Jop, P., Forterre, Y., and Pouliquen, O., A Constitutive Law for Dense Granular Glows, *Nature*, 2006, vol. 441, pp. 727–730.
8. Brilliantov, N.V., Spahn, F., Hertzsch, J.-M., and Pöschel, T., Model for Collisions in Granular Gases, *Phys. Rev. E*, 1996, vol. 53, pp. 5382–5392.
9. Davies, M., Barber, J.R., and Hills, D.A., Energy Dissipation in a Frictional Incomplete Contact with Varying Normal Load, *Int. J. Mech. Sci*., 2012, vol. 55, pp. 13–21.
10. Putignano, C., Ciavarella, M., and Barber, J.R., Frictional Energy Dissipation in Contact of Nominally Flat Rough Surfaces under Harmonically Varying Loads, *J. Mech. Phys. Solids*, 2011, vol. 59, pp. 2442–2454.
11. Popov, M., Popov, V.L., and Pohrt, R., Relaxation Damping in Oscillating Contacts, *arXiv:1410.3238 [cond-mat.soft]*, 2014.
12. Popov, V.L. and Heß, M., *Method of Dimensionality Reduction in Contact Mechanics and Friction*, Berlin: Springer, 2014.
13. Popov, V.L. and Hess, M., Method of Dimensionality Reduction in Contact Mechanics and Friction: a Users Handbook. I. Axially-Symmetric Contacts, *Facta Univ. Mech. Eng*., 2014, vol. 12, pp. 1–14.
14. Willert, E., Heß, M., and Popov, V.L., Application of the Method of Dimensionality Reduction to Contacts under Normal and Torsional Loading, *Facta Univ. Mech. Eng*., 2015, vol. 13, no. 2, pp. 81–90.
15. Popov, V.L., *Contact Mechanics and Friction. Physical Principles and Applications*, Berlin: Springer-Verlag, 2010.

Chapter 3

Publications: Active Control of Friction

This chapter presents seven publications on the topic of active control of friction by externally applied oscillation:

P4: M. Popov, V. L. Popov, and N. V. Popov. "Reduction of friction by normal oscillations. I. Influence of contact stiffness". *Friction* 5.1 (2017), pp. 45–55

P5: X. Mao, V. L. Popov, J. Starcevic, and M. Popov. "Reduction of friction by normal oscillations. II. In-plane system dynamics". *Friction* 5.2 (2017), pp. 194–206

P6: M. Popov. "Critical velocity of controllability of sliding friction by normal oscillations in viscoelastic contacts". *Facta Universitatis, Series: Mechanical Engineering* 14.3 (2016), pp. 335–341

P7: M. Popov and Q. Li. "Multimode Active Control of Friction, Dynamic Ratchets and Actuators". *Physical Mesomechanics* 21.1 (2018), pp. 24–31

P8: J. Benad, K. Nakano, V. L. Popov, and M. Popov. "Active control of friction by transverse oscillations". *Friction* 7.1 (2018), pp. 1–12

P9: M. Popov. "The influence of vibration on friction: a contact-mechanical perspective". *Frontiers in Mechanical Engineering* 6.10.3389 (2020), p. 69

P10: M. Popov. "Friction under large-amplitude normal oscillations". *Facta Universitatis, Series: Mechanical Engineering* 19.1 (2021), pp. 105–113

Two publications are of particular note: P4, which introduces the theoretical framework that is used in subsequent publications and considers the canonical case of friction control by normal oscillations—and P9, which provides a more general formulation of the problem and provides a high-level overview of new results obtained since the publication of P4.

The other publications extend the original model in various directions and consider a number of applications: In the companion paper P5 inertial effects are explored (as opposed to the rest of the papers, where quasi-staticity is generally assumed). P6 and P8 consider different directions of oscillation: longitudinal (in the direction of motion), combined normal and longitudinal, as well as transverse. P7 contains a short note on reduction of friction in contacts with viscoelastic media, while P10 revisits the case of "jumping" contacts (i.e., where the amplitude is greater than mean indentation).

The publications are presented in the original layout and in chronological order (minus publication delays). Each publication is preceded with a brief commentary that summarizes the contents and provides some additional perspective.

3.1 Publication 4

This publication proposes a new model for explaining and describing the phenomenon of friction reduction by normal (out-of-plane) vibration. Unlike previous works in the field, the presented model is entirely macroscopic and is based on classical, quasi-static contact mechanics. The system in question is a body that is sliding on a plane with constant velocity, while being subjected to a harmonic, displacement-controlled oscillation in the normal direction. The novelty of the approach presented here, is that the finite stiffness of the contact in both normal and lateral directions is taken into account. To simplify the analysis, it is initially assumed that the stiffness of the contact is load-independent, so that the body can be modeled as a single linear spring element.

While the body is sliding, the instantaneous force of friction is exactly balanced by the lateral spring force (since we are working in the quasi-static limit). But the force of friction is proportional to the instantaneous normal force, which implies that the lateral deflection is proportional to the normal load as well, and further that the relative velocity of the contact point is proportional to the *rate of normal loading* (with a negative sign). With a sufficiently quick increase of normal load, the velocity of the contact point can compensate the sliding velocity and thereby transition from slip to stick (Eq. 2).

During the stick phase, the body continues to move with constant velocity, which leads to a linear increase of tangential force, until it can no longer be sustained by static friction (Eq. 7), at which point the contact starts sliding again (usually during the unloading part of the normal oscillation). The described process repeats periodically. This stick-slip motion is responsible for the reduction of the macroscopic coefficient of friction, since the lateral spring force during stick is, by definition, lower than the maximum sustainable friction force $\mu_0 F_z$, as illustrated in Fig. 2.

Another noteworthy point is that stick-slip—and therefore reduction of friction—is not always possible. There is a maximum sliding velocity (Eq. 26), beyond which the oscillation fails to precipitate stick-slip and therefore has no effect on the coefficient of friction (within the approximations employed in the model). Later publications refer to this important quantity as the *critical velocity of controllability*.

The rest of the paper concerns itself with a quantitative exploration of the phenomenon. A compact empirical approximation of the macroscopic coefficient of friction is given in Eq. (11), in terms of the dimensionless variable $\bar{v}$, which is the sliding velocity v_0 as a fraction of the aforementioned critical velocity. An exact low-velocity asymptote is derived as well (Eq. 12), but it should be kept in mind that both results are only valid for a displacement-controlled harmonic oscillation. The same analysis is then performed for the case where the amplitude is larger than the mean indentation, so that the body is "hopping" over the plane (Eq. 21).

The assumption of constant contact stiffness is lifted in Section 3, where the full Hertzian contact is considered. The use of the Method of Dimensionality Reduction (MDR) makes the generalization from single spring to proper 3D contact very straightforward. It is also noted that the MDR is not even necessary if the amplitude of oscillation is small, since the contact stiffness becomes approximately constant, and the results obtained with the single-spring model apply. While technically true, this fact no longer seems important to the author, since the magnitude of the reduction effect is always bounded by the amplitude. E.g., if the amplitude is 5% of the mean indentation, then the COF cannot be reduced by more than that amount at any sliding velocity. Numerical calculation is ultimately required for practical surface topographies and amplitudes, but this is very simple thanks to the MDR-based formulation.

Friction ISSN 2223-7690
DOI 10.1007/s40544-016-0136-4 CN 10-1237/TH
RESEARCH ARTICLE

Reduction of friction by normal oscillations. I. Influence of contact stiffness

M. POPOV[1,2,3,*], **V. L. POPOV**[1,2,3], **N. V. POPOV**[1]
[1] *Berlin University of Technology, Berlin 10623, Germany*
[2] *Tomsk Polytechnic University, Tomsk 634050, Russia*
[3] *Tomsk State University, Tomsk 634050, Russia*

Received: 04 June 2016 / Revised: 25 September 2016 / Accepted: 29 November 2016

Abstract: The present paper is devoted to a theoretical analysis of sliding friction under the influence of oscillations perpendicular to the sliding plane. In contrast to previous works we analyze the influence of the stiffness of the tribological contact in detail and also consider the case of large oscillation amplitudes at which the contact is lost during a part of the oscillation period, so that the sample starts to "jump". It is shown that the macroscopic coefficient of friction is a function of only two dimensionless parameters—a dimensionless sliding velocity and dimensionless oscillation amplitude. This function in turn depends on the shape of the contacting bodies. In the present paper, analysis is carried out for two shapes: a flat cylindrical punch and a parabolic shape. Here we consider "stiff systems", where the contact stiffness is small compared with the stiffness of the system. The role of the system stiffness will be studied in more detail in a separate paper.

Keywords: sliding friction; out-of-plane oscillation; contact stiffness; coefficient of friction; active control of friction

1 Introduction

The influence of vibration on friction is of profound practical importance [1]. This phenomenon is used in wire drawing [2, 3], press forming [4] and many other technological applications. Experimental studies of the influence of ultrasonic oscillations on friction started in the late 1950s [5]. In the subsequent years several illuminating works were performed using various techniques, e.g., measurement of electrical conductivity of the contact [6, 7]. Reduced friction has been observed both with oscillations in the contact plane (in-plane) [8] and perpendicular to it (out-of-plane) [9]. In the 2000s, interest in the interaction of friction and oscillations was promoted by applications such as traveling wave motors [10, 11] and the rapidly developing field of nanotribology [12, 13]. In recent years, detailed studies of the influence of ultrasonic oscillations and comparisons with various theoretical models have been performed by Chowdhury et al. [14] and Popov et al. for in-plane oscillations [15], and by Teidelt et al. for out-of-plane oscillations [16]. The latter paper also includes a comprehensive overview of previous works in the field up to 2012.

The above works provided an empirical basis for a qualitative understanding of the influence of oscillations on friction. However, good quantitative correspondence between experimental results and theoretical models could never be achieved (see, e.g., a detailed discussion in Ref. [17]), so it is not clear whether we adequately understand the physics of this phenomenon. Even the question of which oscillation properties determine the reduction of friction force is still under discussion: While in the case of static friction it seems to be the amplitude of displacement oscillation [15], for sliding friction it is believed to be the amplitude of velocity oscillation [11]. In the following, we will show that, in general, friction under oscillation is determined by both of these parameters.

The main novelty of the present paper compared to

* Corresponding author: M. POPOV, E-mail: m@popov.name

earlier work on the influence of oscillation on friction is explicit consideration of the *contact stiffness*. The influence of the contact stiffness is closely related to a fundamental and still unresolved question about the physical nature of the characteristic length determining the crossover from static friction to sliding. In earlier works on this topic, it was assumed that this characteristic length is an intrinsic property of a frictional couple and that its physical nature is rooted in microscopic interactions between the surfaces [15]. However, later investigations suggested another interpretation. Studies of friction in stick-slip microdrives [17, 18] have shown that the static and dynamic behavior of drives can be completely understood and precisely described without any fitting parameters just by assuming that the characteristic length responsible for the "pre-slip" during tangential (in-plane) loading of a contact is equivalent to partial slip in a tangential contact of bodies with curved surfaces. This contact-mechanical approach was substantiated in Ref. [19] by a theoretical study of the influence of in-plane oscillations on the static force of friction. It was shown that the characteristic length is simply the indentation depth multiplied by the coefficient of friction. Later, it was found that this is valid independently of the shape of the contact and also holds true for rough surfaces [20]. This hypothesis of the purely contact mechanical nature of the pre-slip and of the characteristic amplitude was verified experimentally for a wide range of radii of curvature and applied forces in Refs. [21, 22]. It was thus confirmed that describing friction under oscillation, including pre-slip, is basically a matter of correct contact mechanics and that the main governing parameter for both normal and tangential oscillation is the indentation depth. This realization also led to new generalizations in the physics of friction [23, 24], which, however, still need experimental verification.

In the present paper we utilize this new understanding of the importance of the precise contact mechanics and the key property of contact stiffness when considering the details of frictional processes. We focus our attention on the influence of normal (out-of-plane) oscillations on the macroscopic frictional force. We begin by looking at a simple system consisting of a single spring and a frictional point, then extend our analysis to the Hertzian (parabolic) contact using the Method of Dimensionality Reduction [25]. For simplicity we do not deal with system dynamics, and instead impose a forced oscillation of the indentation depth. This restricts our analysis to systems where the contact stiffness is small compared with the stiffness of the system as a whole and the inertia of the contact region thus does not play any role. An analysis involving system dynamics is published in the second part of this two-part paper.

Another contribution of this paper is the consideration of large oscillation amplitudes, when the indenter starts jumping. To our knowledge this case has not previously been considered in theoretical models.

2 Simplified one-spring model

Let us consider an elastic body that is brought into contact with a flat substrate and then subjected to a superposition of an oscillation in the direction normal to the substrate and movement with a constant velocity in the tangential direction. We will assume that Coulomb's law of friction with a constant coefficient of friction μ_0 is valid in the contact. We first consider a very simple model consisting of a single spring with normal stiffness k_z and tangential stiffness k_x. As the reference state, the unstressed state in the moment of first contact with the substrate is chosen. Let us denote the horizontal and vertical displacements of the upper point of the spring from the reference state by u_x and u_z and the horizontal displacement of the lower (contact) point by $u_{x,c}$. The upper point is forced to move according to

$$u_z = u_{z,0} - \Delta u_z \cos\omega t \text{ and } \dot{u}_{\dot{x}} = v_x \tag{1}$$

(see Fig. 1).

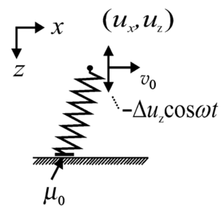

Fig. 1 The simplest model of a tribological contact with a constant contact stiffness represented as a single spring, which has a normal stiffness k_z and a tangential stiffness k_x. The upper end of the spring is forced to move according to Eq. (1). At the lower end (immediate contact spot), Coulomb's law of friction with a constant coefficient of friction μ_0 is assumed.

2.1 Small oscillation amplitudes (no "jumping")

Let us start our consideration with the case of sufficiently small oscillation amplitudes, $\Delta u_z < u_{z,0}$, so that the indenter remains in contact with the substrate at all times. As for the horizontal movement, the lower point of the spring can be either in stick or slip states. During the slip phase the tangential force $f_x = k_x(u_x - u_{x,c})$ is equal to the normal force $f_z = k_z(u_{z,0} - \Delta u_z \cos\omega t)$ multiplied with the coefficient of friction: $k_x(u_x - u_{x,c}) = \mu_0 k_z(u_{z,0} - \Delta u_z \cos\omega t)$. Differentiating this equation with respect to time gives $k_x(v_0 - \dot{u}_{x,c}) = \mu_0 k_z \omega \Delta u_z \sin\omega t$. For the tangential velocity of the lower contact point, it follows that $\dot{u}_{x,c} = v_0 - \mu_0(k_z/k_x)\omega\Delta u_z \sin\omega t$. This equation is only valid when $\dot{u}_{x,c} > 0$, and the foot point of the spring will transition from the sliding state to the sticking state when the condition $\dot{u}_{x,c} = 0$ is fulfilled. This occurs at the time t_1 which satisfies the following equation:

$$\dot{u}_{x,c} = v_0 - \mu_0(k_z/k_x)\omega\Delta u_z \sin\omega t_1 = 0 \tag{2}$$

Introducing a dimensionless velocity

$$\bar{v} = \frac{k_x}{k_z}\frac{v_0}{\mu_0 \omega \Delta u_z} \tag{3}$$

we can rewrite Eq. (2) in the form

$$\sin\omega t_1 = \bar{v} \tag{4}$$

For $\bar{v} > 1$, this equation has no solutions, and the spring continues sliding at all times. Since, in this case, the tangential force remains proportional to the product of the normal force and the macroscopic coefficient of friction μ_0 at all times, there is no reduction of the macroscopic force of friction.

For dimensionless velocities smaller than one, $\bar{v} < 1$, Eq. (4) has solutions and the movement of the contact point will consist of a sequence of sliding and sticking phases, where the sliding phase ends at time t_1 given by Eq. (4). The tangential force at this point is equal to $f_x = \mu_0 k_z(u_{z,0} - \Delta u_z \cos\omega t_1)$ or taking Eq. (4) into account:

$$f_x(t_1) = \left(\mu_0 k_z u_{z,0} - \sqrt{\left(\mu_0 k_z \Delta u_{z,0}\right)^2 - \left(\frac{v_x k_x}{\omega}\right)^2}\right) \tag{5}$$

During the sticking stage the tangential force increases linearly according to

$$f_x^{(\text{stick})}(t) = f_x(t_1) + k_x v_x(t - t_1) \tag{6}$$

The next phase of slip starts at time t_2 when the tangential force becomes equal to the normal force multiplied by the coefficient of friction (see Fig. 2):

$$f_x(t_1) + k_x v_x(t_2 - t_1) = \mu_0 k_z(u_{z,0} - \Delta u_z \cos\omega t_2) \tag{7}$$

Or taking Eqs. (5) and (4) into account and using the dimensionless variable Eq. (3),

$$\cos\omega t_2 = \bar{v}\left(\omega t_2 - \arcsin\bar{v}\right) + \sqrt{1 - \bar{v}^2} \tag{8}$$

The average value of the frictional force during the whole oscillation period can be calculated as follows:

$$\langle f_x \rangle = \frac{\omega}{2\pi}\left[\int_{t_1}^{t_2} f_x^{(\text{stick})}(t)\mathrm{d}t + \int_{t_2}^{2\pi/\omega + t_1} f_x(t)\mathrm{d}t\right] \tag{9}$$

Divided by the average normal force, this gives the macroscopic coefficient of friction

$$\mu_{\text{macro}} = \langle f_x \rangle / \langle f_z \rangle \tag{10}$$

where $\langle f_z \rangle = k_z u_{z,0}$ in the non-jumping case, which is considered here. The result of numerical evaluation of the macroscopic coefficient of friction, normalized by the local coefficient of friction μ_0 is presented in Fig. 3. It was found that the numerically obtained dependences of the coefficient of friction on dimensionless velocity and amplitude can be approximated very accurately with the following equation:

$$\frac{\mu_{\text{macro}}}{\mu_0} \approx 1 - \frac{\Delta u_z}{u_{z,0}}\left[\frac{3}{4}(\bar{v}-1)^2 + \frac{1}{4}(\bar{v}-1)^4\right] \tag{11}$$

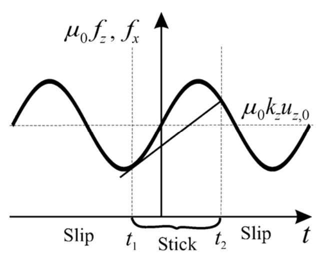

Fig. 2 Schematic presentation of the normal force multiplied with the coefficient of friction (sinusoidal curve) and tangential force (straight line). During the slip phase (before t_1 and after t_2), the tangential force is equal to the normal force times the coefficient of friction, thus both curves coincide. During the stick phase (between t_1 and t_2), the tangential force is smaller than the normal force multiplied by the coefficient of friction. Both forces become equal again at time t_2, where the stick phase ends.

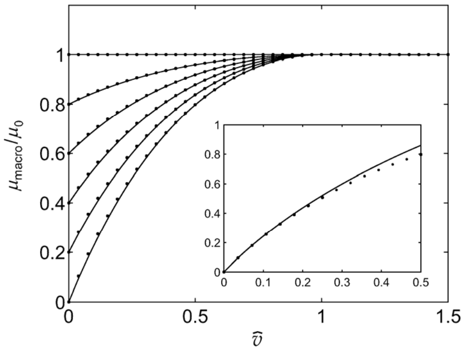

Fig. 3 Dependence of the normalized coefficient of friction on the normalized velocity for $\Delta u_z / u_{z,0} = 0$, 0.2, 0.4, 0.6, 0.8, 1.0 (from top to bottom). Points represent the results of numerical evaluation of the Integral (9). Solid lines represent the empirical Approximation (11). The inset shows the low-velocity asymptotic Solution (12) (solid line) compared to the numerical Solution (9) (points).

A comparison of this approximation with numerical results provided by Eqs. (9) and (10) is shown in Fig. 3. The low-velocity limit of the coefficient of friction can be derived analytically by replacing the time-dependence of the normal force with its Taylor series around the points $\omega t = 0$ and $\omega t = 3\pi/2$ and repeating the above calculations including integration of (9), which provides the result

$$\frac{\mu_{\text{macro}}}{\mu_0} = 1 + \frac{\Delta u_z}{u_{z,0}}\left(-1 + \pi\bar{v} - \frac{4}{3}\sqrt{\pi}\bar{v}^{3/2} + \frac{1}{2}\bar{v}^2\right) \tag{12}$$

This dependence is asymptotically exact in the limit of small sliding velocities. Like the empirical Approximation (11) it contains only two dimensionless variables: the dimensionless amplitude of oscillation $\Delta u_z / u_{z,0}$ and the dimensionless sliding velocity (3). A comparison with the numerical results is shown for the case of the critical oscillation amplitude, $\Delta u_z / u_{z,0} = 1$, in the inset of Fig. 3.

Equation (11) can be rewritten in a form explicitly giving the average tangential force (force of friction):

$$\langle f_x \rangle = \mu_0 k_z u_{z,0}\left(1 - \frac{\Delta u_z}{u_{z,0}}\left[\frac{3}{4}(\bar{v}-1)^2 + \frac{1}{4}(\bar{v}-1)^4\right]\right) \tag{13}$$

Note that the *change* of the friction force due to oscillation, as compared with sliding without oscillation, does depend on the amplitude of oscillation, but does *not* depend on the average normal force:

$$\Delta\langle f_x \rangle = -\mu_0 k_z \Delta u_z \left[\frac{3}{4}(\bar{v}-1)^2 + \frac{1}{4}(\bar{v}-1)^4\right] \tag{14}$$

As will be shown later, this property implies that Eq. (14) is valid for *arbitrarily-shaped* contacts if the oscillation amplitude is small, and k_x and k_z are understood as the incremental tangential and normal stiffness of the contact.

Equation (11) provides a compact representation of the law of friction. However, it is not always convenient for interpretation of experimental results, as the dimensionless velocity (3) is normalized by the amplitude of velocity oscillation and thus the scaling of the velocity depends on the oscillation amplitude. To facilitate the physical interpretation of experimental results it may be more convenient to normalize the velocity using a value that does not depend on the oscillation amplitude. Introducing a new normalized velocity $\hat{v}$ according to the definition

$$\hat{v} = \frac{k_x}{k_z}\frac{v_x}{\mu_0 \omega u_{z,0}} \tag{15}$$

we can rewrite Eq. (11) in the form

$$\frac{\mu_{\text{macro}}}{\mu_0} \approx 1 - \frac{\Delta u_z}{u_{z,0}}\left[\frac{3}{4}\left(\hat{v}\frac{u_{z,0}}{\Delta u_z} - 1\right)^2 + \frac{1}{4}\left(\hat{v}\frac{u_{z,0}}{\Delta u_z} - 1\right)^4\right] \tag{16}$$

This dependence is presented in Fig. 4.

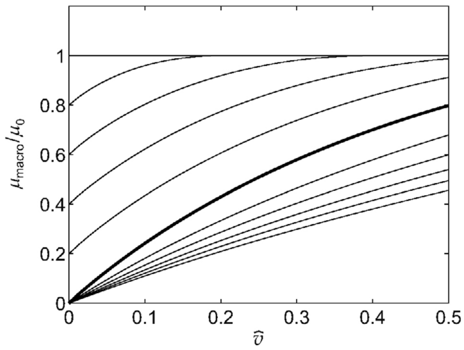

Fig. 4 Dependence of the normalized coefficient of friction on the dimensionless velocity (15): The horizontal line at the constant value 1 corresponds to sliding friction without oscillation. When the oscillation amplitude increases, the static force of friction (at zero velocity) decreases until it vanishes (bold line). This trend is shown in the upper part of the plot for amplitudes $\Delta u_z / u_{z,0} = 0.2$, 0.4, 0.6, 0.8, 1.0 (from top to bottom). Further increase of the oscillation amplitude leads to loss of contact during a part of the oscillation period. In this range of oscillation amplitudes, the static friction force remains zero, and the slope of the dependency decreases with increasing oscillation amplitude. This is shown in the lower part of the plot for amplitudes $\Delta u_z / u_{z,0} =$ 1.2, 1.4, 1.6, 1.8, 2.0 (from top to bottom).

2.2 Large oscillation amplitudes ("jumping")

If the amplitude of normal oscillations exceeds the average indentation depth, the indenter starts to "jump": In this case it will be in contact with the substrate only during part of the oscillation period and in the no-contact-state for the rest of the time. For a jumping contact, analytical considerations become too cumbersome, and we will only present the results of numerical modeling of the behavior of the system. In our model, the movement of the contact point is determined by local stick and slip conditions: As long as the tangential spring force is smaller than the normal force multiplied by the coefficient of friction, the contact point is considered to be stuck to the substrate. If in any particular time step the tangential force exceeds the maximum friction force, it is brought into equilibrium by appropriately changing the contact coordinate. Overall, the system undergoes alternating contact and non-contact phases, while each contact phase may be divided into stick and slip phases. The average force during one complete period of oscillation, divided by the average normal force, results in the macroscopic coefficient of friction, μ_{macro}. It can be shown that, as in the non-jumping case, the dimensionless coefficient of friction μ_{macro}/μ_0 is a function of only the dimensionless velocity $\bar{v}$ given by Eq. (3) and the dimensionless oscillation amplitude. This property was checked by varying (dimensional) system parameters while preserving the values of the two dimensionless parameters. The numerical results for the jumping case are shown in Fig. 5. One can see that the dependence of the reduced coefficient of friction on the reduced velocity does not change significantly after the reduced oscillation amplitude exceeds the critical value 1, where static friction first disappears. Thus, as a very rough approximation, one can use the relation (11) with the critical oscillation amplitude for the whole range of jumping contacts:

$$\frac{\mu_{\text{macro}}}{\mu_0} \approx 1 - \left[\frac{3}{4}(\bar{v}-1)^2 + \frac{1}{4}(\bar{v}-1)^4\right] \text{(for the jumping case)} \tag{17}$$

It is interesting to note that the critical value of the dimensionless velocity $\bar{v}$, after which there is continuous sliding and the macroscopic coefficient of friction coincides with the microscopic one, is equal to 1 both in the non-jumping and jumping regimes.

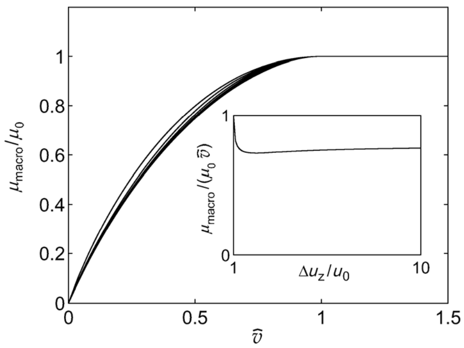

Fig. 5 Dependence of the normalized coefficient of friction on the dimensionless velocity $\bar{v}$ (3) for the "jumping" case, i.e., when the oscillation amplitude exceeds the average indentation depth. Curves are shown for 11 oscillation amplitudes from $\Delta u_z/u_{z,0} = 1$ to $\Delta u_z/u_{z,0} = 2$ with a step of 0.1. The curves for higher oscillation amplitudes "pile up" towards a limiting curve. The inset shows the dependence of the slope of the low-velocity asymptote (21) on $\Delta u_z/u_{z,0}$. One can see that it depends only weakly on the oscillation amplitude: Once the sample starts jumping the slope drops rapidly by about 20% and then remains practically constant with a limiting value of $\pi/4$.

The low-velocity asymptote of the dependence of the coefficient of friction can be easily found analytically. It is instructive to do this for a better understanding of the details of the dependence and of possible deviations from the rough estimate (17). At sufficiently low velocities, the spring will stick as soon as it comes into contact with the substrate. From Eq. (1), we can see that the times when contact is lost or regained are determined by the equation

$$\omega t_{1,2} = \pm \arccos(u_0/\Delta u_z), \text{ for } |\Delta u_z| > u_0 \tag{18}$$

The spring comes into contact in fully relaxed state and is then moved with the constant velocity v_0 during the contact time $t_{\text{contact}} = 2\pi/\omega - 2t_2$. At low velocities the spring will remain in stick for almost the entire contact time, so that the average tangential force during the contact time can be estimated as $\langle F_x \rangle_{\text{contact}} = k_x v_0 t_{\text{contact}}/2$ and the average tangential force during the whole oscillation period as

$$\langle F_x \rangle = \frac{k_x v_0 \omega t_{\text{contact}}^2}{2 \cdot 2\pi} = \frac{k_x v_0}{\pi\omega}\left(\pi - \arccos\left(\frac{u_0}{\Delta u_z}\right)\right)^2 \tag{19}$$

The average normal force is given by:

$$\langle F_z \rangle = k_z u_0 \left(1 - \frac{1}{\pi}\arccos\left(\frac{u_0}{\Delta u}\right) + \frac{1}{\pi}\frac{\Delta u}{u_0}\sqrt{1-\left(\frac{u_0}{\Delta u}\right)^2}\right) \quad (20)$$

with which we finally find the normalized coefficient of friction:

$$\frac{\mu_{\text{macro}}}{\mu_0} = \bar{v}\frac{\left(1-\frac{1}{\pi}\arccos\left(\frac{u_0}{\Delta u_z}\right)\right)^2}{\frac{u_0}{\Delta u_z}\left(1-\frac{1}{\pi}\arccos\left(\frac{u_0}{\Delta u_z}\right)+\frac{1}{\pi}\frac{\Delta u}{u_0}\sqrt{1-\left(\frac{u_0}{\Delta u_z}\right)^2}\right)} \quad (21)$$

This result illustrates once more that the reduced coefficient of friction is a function of only the dimensionless velocity $\bar{v}$ and the dimensionless oscillation amplitude $\Delta u_z / u_{z,0}$. The dependence of the slope of the low-velocity asymptote on the dimensionless oscillation amplitude $\Delta u_z / u_{z,0}$ is shown in the inset of Fig. 5. One can see that when the sample starts jumping the slope drops rapidly by about 20% and then it remains nearly constant at the limiting value of $\pi/4$, thus an explicit expression for the low-velocity asymptote in the jumping regime can be written (in the original dimensional variables) as:

$$\mu_{\text{macro}} \approx \frac{\pi}{4}\frac{k_x}{k_z}\frac{v_0}{\omega \Delta u_z} \text{ (low velocity asymptote; } \Delta u_z > u_{z,0}) \quad (22)$$

As mentioned above, for comparison with experiments it may be preferable to use the dimensionless velocity $\hat{v}$ (15), which does not depend on the oscillation amplitude. In terms of this velocity, the coefficient of friction is shown in Fig. 4 for both jumping and non-jumping regimes, separated by a bold solid line corresponding to the critical amplitude $\Delta u_z / u_{z,0} = 1$. Overall, one can see that an increase of the oscillation amplitude first leads to a decrease of the static coefficient of friction at low sliding velocities. At the critical amplitude, the static coefficient of friction vanishes and remains zero during further increases of the oscillation amplitude, while the overall dependence on velocity starts to "tilt" (the slope of the dependence decreases with increasing oscillation amplitude).

3 Reduction of friction in a Hertzian contact

In Section 2, we considered a simplified model in which it was assumed that the contacting bodies have a constant contact stiffness that does not depend on the indentation depth. This model can be realized experimentally by using a flat-ended cylindrical pin or a curved body with a flat end (e.g., due to wear). However, in the general case the body in contact will have curved or rough surfaces so that the contact stiffness will depend on the indentation depth. In this section we generalize the results obtained in the previous section for more general contact configurations.

In our analysis of the contact of a curved body with the substrate we will use the so-called Method of Dimensionality Reduction (MDR). As shown in Ref. [26], the contact of arbitrarily shaped bodies can be described (in the usual half-space approximation) by replacing it with a contact of an elastic foundation with a properly defined planar shape $g(x)$, as shown in Fig. 6. The elastic foundation consists of a linear arrangement of independent springs with normal stiffness Δk_z and tangential stiffness Δk_x and with sufficiently small spacing Δx. For an exact mapping, the stiffness of the springs has to be chosen according to Refs. [25, 27]:

$$\Delta k_z = E^* \Delta x \text{ with } \frac{1}{E^*} = \frac{1-\nu_1^2}{E_1} + \frac{1-\nu_2^2}{E_2} \quad (23)$$

$$\Delta k_x = G^* \Delta x \text{ with } \frac{1}{G^*} = \frac{2-\nu_1}{4G_1} + \frac{2-\nu_2}{4G_2} \quad (24)$$

where E_1 and E_2 are the moduli of elasticity, ν_1 and ν_2 the Poisson numbers, and G_1 and G_2 the shear moduli of the bodies. The "equivalent shape" $g(x)$ providing the exact mapping can be determined either

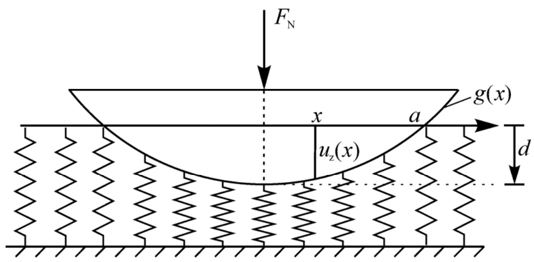

Fig. 6 Schematic presentation of the contact of a transformed planar profile with an effective elastic foundation as prescribed by the rules of the Method of Dimensionality Reduction (MDR).

analytically (e.g., for axis-symmetric profiles [25, 27]), or by asymptotic [26], numerical [26, 28] or experimental methods. It is important to note that an equivalent profile does exist for arbitrary topographies of contacting bodies. Once determined, this equivalent profile can be used to analyze arbitrary dynamic normal and tangential loading histories. If the body is moved tangentially, the same law of friction that is valid for the three-dimensional bodies is applied for each individual spring, using the same coefficient of friction μ_0. If the above rules are observed, the relations between macroscopic properties of the contact (in particular the normal and tangential force-displacement-relationships) will identically coincide with those of the initial three-dimensional problem [26].

3.1 Arbitrary surface topography and small amplitude of oscillations

Let us start by deriving the reduction of friction force for the case of arbitrary contact geometry and *small* oscillation amplitudes. Consider the MDR-representation of the problem in Fig. 6. If the oscillation amplitude is small, then most springs which came into contact with the elastic foundation during the initial indentation by $u_{z,0}$ will remain in contact at all times. Thus, the result (14), which is valid in the non-jumping case, is applicable for most of the springs in the contact; we only have to replace the normal contact stiffness by the stiffness of a single spring:

$$\Delta\langle f_x\rangle_{\text{one spring}} = -\mu_0 \Delta k_z \Delta u_z \left[\frac{3}{4}(\bar{v}-1)^2 + \frac{1}{4}(\bar{v}-1)^4\right] \quad (25)$$

The oscillation amplitude and the expression in the brackets are the same for all springs. Summing over all springs therefore just means replacing the stiffness of one spring by the total stiffness of all springs in contact, k_z, which leads us back to Eq. (14), which is thus generally valid for arbitrary contact shapes.

3.2 Parabolic surface profile and arbitrary amplitude of oscillations

For a parabolic profile $z = r^2/(2R)$ the equivalent plane profil $g(x)$ is given by Ref. [25]: $g(x) = x^2/R$. In our numerical simulations, this profile was first indented by $u_{z,0}$. Subsequently, the indenter was subjected to superimposed normal oscillation and tangential movement with constant velocity according to Eq. (1). Since the springs of the MDR model are independent, the simulation procedure for each spring is exactly as described in Section 2: The movement of the contact point of each spring of the elastic foundation was determined by the stick and slip conditions: as long as the tangential spring force remained smaller than the normal force multiplied by the coefficient of friction, the contact point remained stuck to the substrate. If in a particular time step the tangential force exceeded the critical value, it was reset to the critical value by appropriately changing the contact coordinate. This procedure unambiguously determines the normal and tangential force in each spring of the elastic foundation at each time step. By summing the forces of all springs the total normal and tangential force are determined. After averaging over one period of oscillation, the macroscopic coefficient of friction was found by dividing the mean tangential force by the mean normal force. This coefficient of friction, normalized by the local coefficient of friction μ_0, once again appears to be a function of only two parameters: the dimensionless velocity (either $\bar{v}$ (3), see Fig. 7, or $\hat{v}$ (15), see Fig. 8) and the dimensionless oscillation amplitude $\Delta u_z/u_{z,0}$.

For a parabolic profile, the dependences look qualitatively very similar to those for a single spring (compare with Fig. 3 and Fig. 4). The dependences have two characteristic features: (a) the static force of friction—the starting point of the curve at zero velocity and (b) the critical velocity $\bar{v} = 1$ after which there is no further influence of oscillations on the macroscopic coefficient of friction.

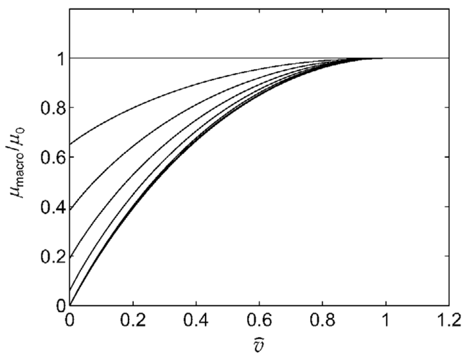

Fig. 7 Dependence of the normalized coefficient of friction on the normalized velocity $\bar{v}$ defined by Eq. (3) for the oscillation amplitudes $\Delta u_z/u_{z,0} = 0,\ 0.2,\ 0.4,\ 0.6,\ 0.8,\ 1.0$ (top to bottom).

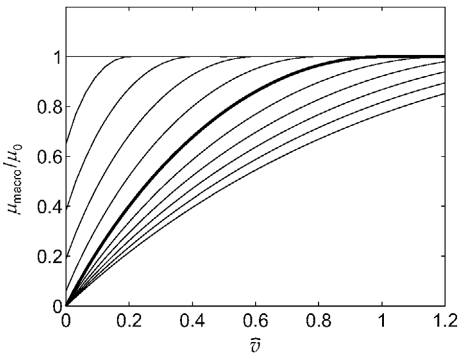

Fig. 8 Dependence of the normalized coefficient of friction on the normalized velocity $\overline{v}$ defined by Eq. (15) for the oscillation amplitudes $\Delta u_z/u_{z,0}=0$, 0.2, 0.4, 0.6, 0.8, 1.0 (the bold line and all curves in the upper-left part) and for $\Delta u_z/u_{z,0}=1.2$, 1.4, 1.6, 1.8, 2.0 (bottom-right part).

4 Discussion

Let us summarize and discuss the main findings of the present study and provide a comparison with experimental results. The structure of the obtained dependences of the macroscopic coefficient of friction on the velocity in the presence of oscillations is simple and contains only two main reference points: the static friction force and the critical velocity. The dependence of the static friction force is extremely simple: it is determined just by the minimum of the normal force during the oscillation cycle. The differences of the static friction force for indenters of different shape will therefore be completely determined by the solution of the corresponding normal contact problem. The second reference point is the critical velocity, which separates the velocity interval where the coefficient of friction does depend on the velocity from the interval where there is no further dependence. This critical point is given by the condition $\overline{v}=1$ or explicitly, in dimensional variables:

$$v_0 = \frac{E^*}{G^*}\mu_0\omega\Delta u_z \tag{26}$$

Since Mindlin's ratio E^*/G^* is on the order of unity and $\omega\Delta u_z$ is the amplitude of *velocity oscillation*, this means that the critical velocity is roughly speaking the amplitude of the velocity oscillation multiplied with the coefficient of friction. It is astonishing that this simple result is absolutely universal and is valid for both the non-jumping and jumping regimes and for indenters of arbitrary shape.

Thus, one of the reference points is determined solely by the amplitude of displacement oscillation and the other solely by the amplitude of the velocity oscillation. Between these points, the dependence of the coefficient of friction on sliding velocity is accurately approximated by Eq. (11), which can be rewritten in a universal form that does not depend on the indenter shape:

$$\frac{\mu_{\mathrm{macro}}}{\mu_0} \approx 1-\left(1-\frac{\mu_{\mathrm{static}}}{\mu_0}\right)\left[\frac{3}{4}(\overline{v}-1)^2+\frac{1}{4}(\overline{v}-1)^4\right] \tag{27}$$

The indenter shapes will only influence the static coefficient of friction in the above equation.

For practical applications one can use an even simpler approximation differing from Eq. (27) by 1% or less:

$$\frac{\mu_{\mathrm{macro}}}{\mu_0} \approx 1-\left(1-\frac{\mu_{\mathrm{static}}}{\mu_0}\right)(1-\overline{v})^{2.4} \tag{28}$$

Substituting the definition of $\overline{v}$, we can write this dependence in the initial dimensional variables:

$$\mu_{\mathrm{macro}} \approx \mu_0-(\mu_0-\mu_{\mathrm{static}})\left(1-\frac{G^*}{E^*}\frac{v_0}{\mu_0\omega\Delta u_z}\right)^{2.4} \tag{29}$$

This equation contains in a condensed form all essential results of the present study. Most interestingly, it is approximately valid in both non-jumping and jumping regimes and for all indenter shapes. As long as the amplitude of oscillation is smaller than the average indentation (no jumping), the static friction force decreases monotonously with increasing oscillation amplitude. After reaching the critical oscillation amplitude, the static friction force vanishes and remains zero at larger oscillation amplitudes, but Eq. (27) still remains valid in a good approximation. From the critical amplitude onwards, the force-velocity dependencies start to "tilt".

The described features can be readily recognized in the experimental data shown in Fig. 9.

Comparison of the experimental results with the theoretical predictions in Fig. 4 shows both similarities and differences. For example, we also observe the

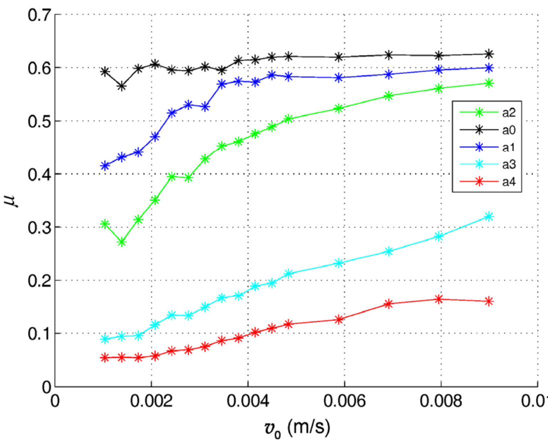

Fig. 9 Experimentally determined dependences of the coefficient of friction on sliding velocity between a steel sphere and a steel disc for increasing amplitudes of out-of-plane oscillation obtained by Milahin (Source: [29], reproduced with permission of the author). The upper-most curve corresponds to sliding in the absence of oscillation. The second, third and fourth curves correspond to amplitudes of $\Delta u_z = 0.06$ μm, $\Delta u_z = 0.10$ μm, $\Delta u_z = 0.16$ μm and $\Delta u_z = 0.27$ μm.

decrease of static friction and subsequent "tilting" of the dependences in the experimental data. Similar behavior was also observed in Ref. [30]. A difference between our theory and experiment is that the static coefficient of friction does not vanish entirely even at large oscillation amplitudes. This effect is known also for other modes of oscillation and is related to the microscopic heterogeneity of the frictional system, which means that Coulomb's law of friction is not applicable at very small space scales [31].

As we noted in the introduction, we considered a case of a soft contact and a rigid measuring system. In the opposite case of a very stiff contact and soft surrounding system, the dependences of the coefficient of friction on the oscillation amplitude appear to be essentially influenced by the inertial properties of the system [16]. An analysis carried out by Teidelt in Ref. [30] has shown that for the measuring system described in Ref. [16] a reasonable agreement between experiment and theory can only be achieved if the contact stiffness is taken into account. However, under other conditions—and in particular depending on the frequency of oscillations—the assumption of soft contact can fail. For such cases, a more general analysis has to be carried out, which is provided in the second part of this series [32].

Acknowledgements

This work was supported in part by the Ministry of Education of the Russian Federation, by COST Action MP1303 and the Deutsche Forschungsgemeinschaft.

References

[1] Eaves A, Smith A, Waterhouse W, Sansome D. Review of the application of ultrasonic vibrations to deforming metals. *Ultrasonics* **13**(4): 162–170 (1975)

[2] Siegert K, Ulmer J. Superimposing ultrasonic waves on the dies in tube and wire drawing. *J Eng Mater Technol* **123**(4): 517 (2001)

[3] Murakawa M. The utility of radially and ultrasonically vibrated dies in the wire drawing process. *J Mater Process Technol* **113**(1–3): 81–86 (2001)

[4] Ashida Y, Aoyama H. Press forming using ultrasonic vibration. *J Mater Process Technol* **187–188**: 118–122 (2007)

[5] Fridman H D, Levesque P. Reduction of static friction by sonic vibrations. *J Appl Phys* **30**(10): 1572 (1959)

[6] Pohlman R. Influence of ultrasonic vibration on metallic friction. *Ultrasonics* **4**: 178–185 (1966)

[7] Godfrey D. Vibration reduces metal to metal contact and causes an apparent reduction in friction. *Tribol Trans* **10**(2): 183–192 (1967)

[8] Lenkiewicz W. The sliding friction process—Effect of external vibrations. *Wear* **13**(2): 99–108 (1969)

[9] Tolstoi D M. Significance of the normal degree of freedom and natural normal vibrations in contact friction *Wear* **10**(3): 199–213 (1967)

[10] Schmidt J. A note on the contact problem in an ultrasonic travelling wave motor. *Int J Non-Linear Mech* **31**(6): 915–924 (1996)

[11] Storck H, Littmann W, Wallaschek J, Mracek M. The effect of friction reduction in presence of ultrasonic vibrations and its relevance to travelling wave ultrasonic motors. *Ultrasonics* **40**(1–8): 379–383 (2002)

[12] Socoliuc A, Gnecco E, Maier S, Pfeiffer O, Baratoff A, Bennewitz R, Meyer E. Atomic-scale control of friction by actuation of nanometer-sized contacts. *Science* **313**(5784): 207–210 (2006)

[13] Guo W, Yin J, Qiu H, Guo Y, Wu H, Xue M. Friction of low-dimensional nanomaterial systems. *Friction* **2**(3): 209–225 (2014)

[14] Chowdhury M, Helali M. The effect of amplitude of vibration on the coefficient of friction for different materials. *Tribol Int* **41** (4): 307–314 (2008)

[15] Popov V L, Starcevic J, Filippov A E. Influence of ultrasonic in-plane oscillations on static and sliding friction and intrinsic length scale of dry friction processes. *Tribol Lett* **39**: 25–30 (2010)

[16] Teidelt E, Starcevic J, Popov V L. Influence of ultrasonic oscillation on static and sliding friction. *Tribol Lett* **48**: 51–62 (2012)

[17] Teidelt E, Willert E, Filippov A E, Popov V L. Modeling of the dynamic contact in stick-slip microdrives using the method of reduction of dimensionality. *Phys Mesomech* **15**(5–6): 287–292 (2012)

[18] Nguyen H X, Teidelt E, Popov V L, Fatikow S. Dynamical tangential contact of rough surfaces in stick-slip microdrives: modeling and validation using the method of dimensionality reduction. *Phys Mesomech* **17**(4): 304–310 (2014)

[19] Starcevic J, Filippov A E. Simulation of the influence of ultrasonic in-plane oscillations on dry friction accounting for stick and creep. *Phys Mesomech* **15**(5–6): 330–332 (2012)

[20] Grzemba B, Pohrt R, Teidelt E, Popov V L. Maximum micro-slip in tangential contact of randomly rough self-affine surfaces. *Wear* **309**(1): 256–258 (2014)

[21] Milahin N, Starcevic J. Influence of the normal force and contact geometry on the static force of friction of an oscillating sample. *Phys Mesomech* **17**(3): 228–231 (2014)

[22] Milahin N, Li Q, Starčević J. Influence of the normal force on the sliding friction under ultrasonic oscillations. *Facta Universitatis. Series: Mechanical Engineering* **13**(1): 27–32 (2015)

[23] Popov V L, Dimaki A, Psakhie S, Popov M. On the role of scales in contact mechanics and friction between elastomers and randomly rough self-affine surfaces. *Sci Rep* **5**: 11139 (2015)

[24] Popov V L. What does friction really depend on? Robust governing parameters in contact mechanics and friction. *Phys Mesomech* **19** (2): 115–122 (2016)

[25] Popov V L, Heß M. *Method of Dimensionality Reduction in Contact Mechanics and Friction*. Berlin-Heidelberg (Germany): Springer, 2015.

[26] Argatov I, Heß M, Pohrt R, Popov V L. The extension of the method of dimensionality reduction to non-compact and non-axisymmetric contacts. *ZAMM-J Appl Math Mech* 96(10): 1144–1155 (2016)

[27] Popov V L. *Kontaktmechanik und Reibung. Von der Nanotribologie bis zur Erdbebendynamik.* 3. überarbeitete Auflage. Berlin-Heidelberg (Germany): Springer Vieweg, 2015.

[28] Popov V L, Pohrt R, Heß M. General procedure for solution of contact problems under dynamic normal and tangential loading based on the known solution of normal contact problem. *J Strain Analysis* **51**(4): 247–255 (2016)

[29] Milahin N. Robuste Einflussparameter für Reibung und Oberflächenmodifizierung unter Einfluss von Ultraschall. PhD thesis. Technische Universität Berlin, 2016.

[30] Teidelt E. Oscillating contacts: Friction induced motion and control of friction. PhD thesis. Technische Universität Berlin, 2015.

[31] Dudko O K, Popov V L, Putzar G. Tribospectroscopy of randomly rough surfaces. *Tribol Int* **39**(5): 456–460 (2006)

[32] Mao X, Popov V L, Starcevic J, Popov M. Reduction of friction by normal oscillations. II. In-plane system dynamics. *Friction*, accepted (2017)

Mikhail POPOV. He obtained a bachelor degree in computer science from the Freie Universität Berlin in 2011 and a master degree in engineering science from the Tomsk Polytechnic University and Berlin Technical University in 2016. Currently he is a research assistant at the Tomsk Polytechnic University and a PhD student at the Berlin University of Technology. His research interests include efficient numerical methods in tribology, rubber friction, as well as friction and damping under the influence of oscillations.

Valentin L. POPOV. He is full professor at the Berlin University of Technology, studied physics (1976—1982) and obtained his doctorate in 1985 from the Moscow State Lomonosov University. He worked at the Institute of Strength Physics of the Russian Academy of Sciences. After a guest professorship in the field of theoretical physics at the University of Paderborn (Germany) from 1999 to 2002, he has headed the Department of System Dynamics and the Physics of Friction of the Institute of Mechanics at the Berlin University of Technology. His areas of interest include tribology, nanotribology, tribology at low temperatures, biotribology, the influence of friction through ultrasound, numerical simulation of frictional processes, research regarding earthquakes, as well as topics related to materials science such as the mechanics of elastoplastic media with microstructures, strength of metals and alloys, and shape memory alloys. He has published over 100 papers in leading international journals during the past 5 years. He is the author of the book "*Contact Mechanics and Friction: Physical Principles and Applications*" which appeared in three German, two English, Chinese, and Russian editions and co-author of the book on "*Method of dimensionality Reduction in Contact Mechanics and Friction*" which appeared in German, English and Chinese editions. He is the joint editor of international journals and regularly organizes international conferences and workshops on diverse tribological themes. He is a member of the Scientific Council of the German Tribological Society. He has intensively collaborated with many industrial corporations and possesses experience in implementing the results of scientific research in industrial applications.

Nikita POPOV. Master student in two majors: (a) physics and (b) computer science at the Berlin University of Technology.

3.2 Publication 5

The publications in this thesis are based on the assumption of quasi-staticity. This is a convenient approximation for elucidating basic mechanisms, but is often insufficient for describing practical systems. Since the highly deformed contact region is usually very small (both in size and mass) compared to the entire system, its inertia can almost always be safely neglected, and propagation of elastic disturbances across the contact region can be considered instantaneous. However, the same cannot always be said of the *surrounding system*, and its dynamics in interaction with the contact forces should be described explicitly for realistic modeling. Due to the great diversity of possible systems this is ultimately the realm of numerical simulation and applied engineering. However, the present paper provides a very simple example of this hybrid approach, which nonetheless uncovers some qualitatively new behaviors.

The modeled scenario roughly corresponds to a pin-on-disc tribometer with an externally applied out-of-plane harmonic oscillation. The pin is considered to be rigid in the normal direction, but having a finite bending stiffness and mass. In the model these are represented with the system spring k_x and system mass m (Fig. 1b). All other aspects of the model are the same as in the first part of the study, including the displacement-controlled oscillation (only *in-plane* dynamics is considered here).

Since the oscillation is still displacement-controlled, the static COF is the same as in the previous publication. However, the *critical velocity* (above which stick-slip is eliminated and reduction of friction becomes impossible), is changed substantially:

$$v_0^* = \mu_0 \omega \Delta u_z \frac{k_{z,c}}{k_{x,c}} \frac{|k_{x,c} + k_x - m\omega^2|}{|k_x - m\omega^2|}$$

Note that if the system spring is sufficiently soft ($k_x \ll m\omega^2 \ll k_{x,c}$), the critical velocity reduces to $\mu_0 \Delta F_N / m\omega$, which matches the result obtained by Teidelt et al. [78]. In case of a very stiff system ($k_x \to \infty$), the critical velocity reduces to $\mu_0 \omega \Delta u_z k_{z,c}/k_{x,c}$, which reproduces the result obtained for the non-inertial system in P4.

More interesting are the two resonant cases, which only arise in the inertial model: If $k_{x,c} + k_x - m\omega^2 \approx 0$, the critical velocity tends to zero, meaning that reduction of friction is prevented even at very low sliding velocity. On the other hand, if $k_x - m\omega^2 \approx 0$, the critical velocity tends to infinity and the system consequently never achieves the state of continuous sliding. At large v_0 the coefficient of friction still reaches a plateau value, but this plateau can be significantly lower than μ_0, so this case is of considerable practical interest.

The two resonances inform the choice of two dimensionless parameters α and β (Eq. 20) that are of key importance in describing the system. A large part of the paper is devoted to a numerical exploration of the (α, β) parameter plane, which uncovers some unusual velocity-dependencies of the COF, with multiple intermediate plateaus (see e.g. Fig. 5b).

The second resonant case is then analyzed in some detail and an asymptotic expression for the plateau value of the COF at large velocities is derived (Eq. 37). This plateau lies at the "halfway point" between the static coefficient of friction and μ_0. The paper is rounded out by consideration of the "jumping" case and a limited comparison with experimental data. The main results are summarized graphically in Fig. 10.

Friction **5**(2): 194–206 (2017) ISSN 2223-7690
DOI 10.1007/s40544-017-0146-x CN 10-1237/TH
RESEARCH ARTICLE

Reduction of friction by normal oscillations. II. In-plane system dynamics

Xinyu MAO[1,2], **Valentin L. POPOV**[1,3,4,*], **Jasminka STARCEVIC**[1,4], **Mikhail POPOV**[1,3,4]

[1] *Technische Universität Berlin, Berlin 10623, Germany*

[2] *Tsinghua University, Beijing 100084, China*

[3] *Tomsk Polytechnic University, Tomsk 634050, Russia*

[4] *Tomsk State University, Tomsk 634050, Russia*

Received: 31 August 2016 / Revised: 24 December 2016 / Accepted: 11 January 2017

Abstract: The influence of out-of-plane oscillations on friction is a well-known phenomenon that has been studied extensively with various experimental methods, e.g., pin-on-disk tribometers. However, existing theoretical models have yet achieved only qualitative correspondence with experiment. Here we argue that this may be due to the system dynamics (mass and tangential stiffness) of the pin or other system components being neglected. This paper builds on the results of a previous study [19] by taking the stiffness and resulting dynamics of the system into account. The main governing parameters determining macroscopic friction, including a dimensionless oscillation amplitude, a dimensionless sliding velocity and the relation between three characteristic frequencies (that of externally excited oscillation and two natural oscillation frequencies associated with the contact stiffness and the system stiffness) are identified. In the limiting cases of a very soft system and a very stiff system, our results reproduce the results of previous studies. In between these two limiting cases there is also a resonant case, which is studied here for the first time. The resonant case is notable in that it lacks a critical sliding velocity, above which oscillations no longer reduce friction. Results obtained for the resonant case are qualitatively supported by experiments.

Keywords: sliding friction; out-of-plane oscillation; stiffness; system dynamics; macroscopic friction coefficient

1 Introduction

Vibrations can be applied to reduce and control friction, which is widely used in many industrial branches, such as metal forming, wire drawing and drilling [1, 2]. One of the earliest studies of friction reduction due to oscillations was carried out by Godfrey in 1967 [3]. He conducted experiments, in which a rider slid along a steel plate and was vibrated in the direction perpendicular to the plane. Afterwards numerous studies were carried out, which can be roughly classified by whether the static or sliding friction is considered and by the direction of the oscillations, see, e.g., Refs. [4–6]. The three possible directions of oscillation are: (1) in the sliding direction; (2) perpendicular to the sliding direction in the contact plane; (3) perpendicular to the contact plane (out-of-plane oscillations). Arbitrary combinations of these three modes are also possible, some of which can produce directed motion even in the absence of a directed mean force, thus producing a frictional drive. In this regard, active control of friction through oscillations is closely related to oscillation-based frictional drives [7, 8]. However, in the present paper we consider only sliding friction under the influence of out-of-plane oscillations.

Friction under the action of out-of-plane oscillations has been studied experimentally in the past in a number of works [9–12]. The first theoretical description

* Corresponding author: Valentin L. POPOV, E-mail: v.popov@tu-berlin.de

was proposed in Refs. [13, 14], where the movement of a rigid body under constant tangential force and oscillating normal force was considered. Unfortunately this model achieved only qualitative correspondence with experimental results. In Ref. [7], it was shown that the macroscopic behavior of a frictional contact is strongly influenced by the contact stiffness. Related studies of the dependence of friction on tangential oscillations [15, 16] and a study of frictional drives [17] came to the same conclusion. In a recent experimental study [18] the contact stiffness was also confirmed as one of the main parameters governing the response of a tribological contact to high frequency oscillations.

Based on these indications of the importance of contact stiffness, Popov et al. [19] carried out a theoretical study of friction under the action of out-of-plane oscillations with explicit account of finite contact stiffness. In this paper it was assumed that the stiffness of the system is much larger than that of the contact, which allowed avoiding consideration of system dynamics. In real systems, depending on their particular mechanical design, the stiffness of the system may be comparable with the contact stiffness, thus bringing the whole system dynamics into play. In the present paper, we extend the previous study [19] by considering the complete dynamics of a system with a tribological contact.

2 Simplified model of the experimental set-up

The model studied in the present paper is motivated by experimental studies of active control of friction by out-of-plane oscillations in a pin-on-disk tribometer (e.g., Refs. [7, 14–16]). The design of the pin is shown in Fig. 1(a). Assuming that the vertical stiffness of the set-up is much larger than the normal contact stiffness, the vertical macroscopic motion of the pin can be considered to be displacement controlled. The tangential stiffness of the pin assembly is much smaller than its vertical stiffness, so that it is no longer guaranteed that the tangential stiffness of the pin is larger than the tangential contact stiffness. Therefore, the tangential stiffness of the pin is explicitly taken into account in our model. Assuming that the transversal dynamics of the pin is controlled by only one bending normal mode of the pin, we arrive at the simplified model of the system, which is sketched in Fig. 1(b): a one-degree-of-freedom model taking into account the normal and tangential contact stiffness, the inertia of the pin and its tangential stiffness. Modal analysis of the pin could be used for estimation of a more accurate modal mass, but we do not do this here, as our aim is to present a high-level analysis without considering particular geometrical realizations. We will show that the frequency of free oscillations of the pin, $\omega_0 = \sqrt{k_x / m}$, is the most important system parameter; when describing a real experiment, it has to be adjusted to the ground frequency of the free oscillations of the pin. Naturally, our model abstracts away many (possibly important) aspects of real frictional systems, in particular the differential contact stiffness of curved bodies (we model the contact as a single spring with constant stiffness). However, in the first part of this series [19] we found that the detailed contact mechanics had surprisingly little influence on the results, relative to a one-spring model. In particular, abstracting the exact geometry of the contact does not change the relevant dimensionless variables. Due to this, and in view of the already large number of system parameters, we restrict ourselves to the simple model described above.

The model, as shown in Fig. 1(b), consists of a rigid body with mass m that is connected to an external actuator, which imposes the body's z-coordinate. The body is pulled by a spring with a tangential stiffness k_x and interacts with the substrate through a "contact spring" that has the normal stiffness $k_{z,\mathrm{c}}$ and tangential stiffness $k_{x,\mathrm{c}}$. The vertical movement of the mass is determined explicitly by the external oscillation:

$$u_z = u_{z,0} + \Delta u_z \cos \omega t \tag{1}$$

where $u_{z,0}$ is a constant initial indentation, Δu_z is the amplitude of normal oscillations, and ω is the angular frequency of the oscillation. The attached "system spring" is pulled tangentially with a constant velocity v_0. The motion of the body in the x-direction under the influence of the attached springs is described by Newton's Second Law for the tangential displacement u_x. The tangential displacement of the immediate contact point is denoted with $u_{x,\mathrm{c}}$. For simplicity, we assume Coulomb's law of friction with a constant

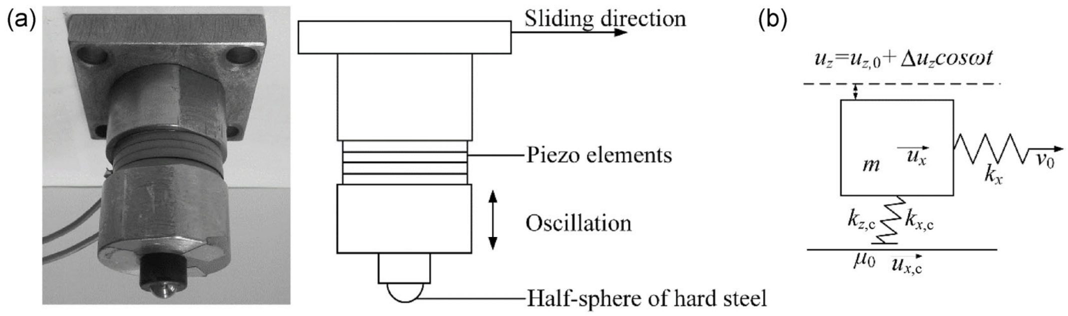

Fig. 1 (a) Photograph and diagram of the pin assembly of a pin-on-disk tribometer used in Refs. [7, 16] and in the experimental part of the present study; (b) a simplified model of the pin in contact with the disk, which is studied in the present paper.

coefficient of friction μ_0 in the immediate contact point between the substrate and the contact spring. Although this may be an unrealistic assumption in general, the aim of this study is to understand how changes in the *macroscopic* coefficient of friction can arise from pure system dynamics even with *constant microscopic* friction. Experimental results might be best approximated by a combined theory, including system dynamics, contact mechanics and changes of the local coefficient of friction, but this is left for later studies.

Note that the amplitude of oscillation can be either smaller than the mean indentation (non-jumping), in which case the body is always in contact with the substrate, or larger (jumping case), where contact with the substrate is intermittent. Initially we will focus on the permanent contact case. Jumping will be introduced later in the paper.

3 Qualitative analysis

All previous studies of the influence of normal oscillations on friction, including the first part of the present work [19], have shown qualitatively the same dependence of the macroscopic coefficient of friction (COF) on velocity: At zero velocity the friction force is at its static value, which is determined solely by the minimum value of normal force during one oscillation cycle:

$$\mu(v_0 = 0) = \begin{cases} \mu_0(1 - \Delta u_z / u_{z,0}), & \text{for } \Delta u_z < u_{z,0} \\ & \text{(non-jumping case)} \\ 0, & \text{for } \Delta u_z > u_{z,0} \\ & \text{(jumping case)} \end{cases} \quad (2)$$

At higher velocities the COF increases until it reaches μ_0 at some critical velocity v_0^* ("point of insensitivity"), and remains constant thereafter. The static COF and the critical velocity v_0^* are the two main reference points of the velocity dependence of the COF. While the first reference point is universal (Eq. (2)), the second one is determined by the dynamics of the tribological system.

We begin our analysis with the case of small oscillation amplitudes, $\Delta u_z < u_{z,0}$, so that the lower point of the indenter remains in contact with the substrate at all times. In this case, the normal component of the contact force F_N is non-vanishing and is determined by the product of the current indentation depth (Eq. (1)) with the normal contact stiffness $k_{z,c}$:

$$F_N = k_{z,c}(u_{z,0} + \Delta u_z \cos \omega t) \quad (3)$$

At sufficiently large pulling velocities v_0, the contact point will be sliding all the time (without stick) in one direction (except for the resonant case that will be described later). Under these conditions, the average tangential force is equal to the average normal force times μ_0, and the macroscopically observed COF, which we define as the ratio of the mean values of tangential and normal forces over one period of oscillation, will be constant and equal to μ_0. When the above conditions are satisfied the tangential force of the contact spring is in equilibrium with the friction force (normal force times μ_0), since the contact stiffness is not associated with any mass:

$$k_{x,c}(u_x - u_{x,c}) = \mu_0 k_{z,c}(u_{z,0} + \Delta u_z \cos \omega t) \quad (4)$$

The equation of motion of the body m along the

x-axis is

$$m\ddot{u}_x = k_x(v_0 t - u_x) - k_{x,c}(u_x - u_{x,c}) \quad (5)$$

Taking Eq. (4) into account, the equation of motion reads

$$m\ddot{u}_x + k_x u_x = k_x v_0 t - \mu_0 k_{z,c}\Delta u_z \cos\omega t - \mu_0 k_{z,c} u_{z,0} \quad (6)$$

The particular solution of this equation is

$$u_x = v_0 t - \mu_0 \frac{k_{z,c}}{k_x} u_{z,0} + \frac{\mu_0 k_{z,c}\Delta u_z}{m\omega^2 - k_x}\cos\omega t \quad (7)$$

Differentiating this solution with respect to time gives

$$\dot{u}_x = v_0 - \frac{\mu_0 k_{z,c}\Delta u_z}{m\omega^2 - k_x}\omega \sin\omega t \quad (8)$$

Differentiating the equilibrium condition (Eq. (4)),

$$k_{x,c}(\dot{u}_x - \dot{u}_{x,c}) = -\mu_0 k_{z,c}\Delta u_z \omega \sin\omega t \quad (9)$$

Substituting Eq. (8) into Eq. (9) and resolving the resulting equation with respect to $\dot{u}_{x,c}$, we obtain the following expression for the sliding velocity of the immediate contact point (lower point of the contact spring)

$$\dot{u}_{x,c} = v_0 - \frac{k_{z,c}}{k_{x,c}} \frac{k_{x,c} + k_x - m\omega^2}{(m\omega^2 - k_x)} \mu_0 \omega \Delta u_z \sin\omega t \quad (10)$$

Due to our previous assumption of continuous sliding this velocity must remain positive at all times. This is the case if

$$v_0 > v_0^* \quad (11)$$

where

$$v_0^* = \mu_0 \omega \Delta u_z \frac{k_{z,c}}{k_{x,c}} \frac{\left|k_{x,c} + k_x - m\omega^2\right|}{\left|k_x - m\omega^2\right|} \quad (12)$$

This relatively simple equation is one of the central results of the present paper and it is instructive to discuss it in some detail. First, let us consider limiting cases that have already been studied in the literature:

I. In the case of a very soft system ($k_x << m\omega^2$) with very large contact stiffness ($k_{x,c} >> m\omega^2$) we effectively have a rigid body under the action of constant tangential force. In this case, which was considered in Ref. [14] (see esp. Fig. 20 and discussion) the critical velocity reduces to

$$v_{0,\text{soft}}^* = \mu_0 \omega \frac{\Delta u_z k_{z,c}}{\left|m\omega^2\right|} = \mu_0 \frac{\Delta F_N}{m\omega} \quad (13)$$

II. The limiting case of a very stiff system ($k_{x,c} << \left|k_x - m\omega^2\right|$) was considered in the first part of the present work [19]. In this case Eq. (12) simplifies to

$$v_{0,\text{stiff}}^* = \mu_0 \omega \Delta u_z \frac{k_{z,c}}{k_{x,c}} \quad (14)$$

There are two other limiting cases which involve resonances and have not yet been considered in the literature:

III. If $k_{x,c} + k_x - m\omega^2 \approx 0$, the critical velocity is very small: $v_0^* \approx 0$. The body is in permanent sliding state even at very low velocities and the COF is constant and equal to μ_0 at all sliding velocities.

IV. If $k_x - m\omega^2 \approx 0$, the critical velocity is infinitely large and the system never achieves the state of continuous sliding. It will be shown that in this case the macroscopic coefficient of friction reaches a plateau at large velocities, with a value lower than μ_0. This case is of a special interest and it will be considered below in detail and was also studied experimentally.

Let us now consider the movement of the body in the general case, when the contact point slides during some part of the oscillation cycle and sticks at other times. The movement of the slider is still governed by the Eq. (5), however, Eq. (4), which describes the tangential force in the contact spring, is only valid during the sliding part of the period, while during the sticking phase the following is true for the immediate contact point:

$$\dot{u}_{x,c} = 0, \quad k_{x,c}(u_x - u_{x,c}) < \mu_0 k_{z,c}(u_{z,0} + \Delta u_z \cos\omega t) \quad (15)$$

To study the dynamics of the system in detail, the equation of motion (Eq. (5)) was integrated numerically with account of Eqs. (4) and (15). The nontrivial behavior that can result when both stick and slip occur is illustrated in Fig. 2, which presents the time dependencies of the normal and tangential force (the

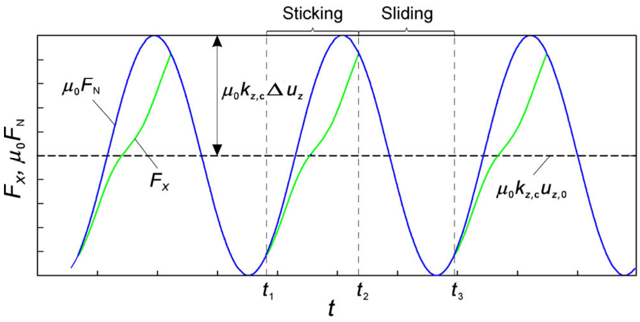

Fig. 2 An example of the dynamics of normal and tangential contact forces showing the phases of slip, where the tangential force (green line) coincides with the normal force multiplied with μ_0 (blue line), and the sticking phase, where the tangential force is smaller than the normal force multiplied with μ_0.

former multiplied with μ_0). During the sliding phase (e.g., before t_1 and between t_2 and t_3), these two quantities are equal, while during the sticking phase the tangential force (green line) is less than the normal force times μ_0 (blue line). The beginning of stick (t_1) is determined by the condition that the velocity of the immediate contact point (lower end of the contact spring) becomes zero, while the end of the sticking phase (t_2) is determined by the condition that the tangential force becomes equal to the normal force times μ_0.

4 Dimensionless formulation of the problem

Introducing the dimensionless variables

$$\bar{v} = \frac{v_0}{v_0^*} \tag{16}$$

$$\tau = \omega t \tag{17}$$

$$\xi = u_x \frac{\omega}{v_0^*} \tag{18}$$

$$\xi_c = u_{x,c} \frac{\omega}{v_0^*} \tag{19}$$

where v_0^* is defined by Eq. (12), with two additional dimensionless parameters

$$\alpha = \frac{k_x}{m\omega^2}, \quad \beta = \frac{k_x + k_{x,c}}{m\omega^2} \tag{20}$$

We can rewrite the Eqs. (4), (5) and (15) in the following form:

$$(\xi - \xi_c) = \left(\frac{u_{z,0}}{\Delta u_z} + \cos\tau\right)\frac{\alpha - 1}{\beta - 1} \tag{21}$$

$$\xi'' = \alpha(\bar{v}\tau - \xi) - (\beta - \alpha)(\xi - \xi_c) \tag{22}$$

$$\xi_c' = 0, \quad \xi - \xi_c < \left(\frac{u_{z,0}}{\Delta u_z} + \cos\tau\right)\frac{\alpha - 1}{\beta - 1} \tag{23}$$

where $\xi' = \mathrm{d}\xi/\mathrm{d}\tau$, $\xi'' = \mathrm{d}^2\xi/\mathrm{d}\tau^2$.

One can see that the behavior of the above system is unambiguously determined by the following set of variables:

$$\bar{v}, \ \Delta u_z / u_{z,0}, \ \alpha, \text{ and } \beta \tag{24}$$

After solving the Eqs. (21)–(23), one can go back to the initial dimensional variables and calculate the average normal force $\langle F_N \rangle$ and the average tangential force $\langle F_x \rangle = \langle k_x (v_0 t - u_x) \rangle$. The macroscopic coefficient of friction is then defined as

$$\mu_{\text{macro}} = \frac{\langle F_x \rangle}{\langle F_N \rangle} \tag{25}$$

It is easy to see that with the given dimensionless variables (24) the macroscopic coefficient of friction will be proportional to μ_0. Thus, it is more convenient to define the reduced coefficient of friction, $\mu_{\text{macro}} / \mu_0$, which is a function solely of the variables (24). In the following, we will explore the dependence of the reduced COF on the dimensionless velocity (16) on the parameter plane (α, β).

5 Numerical results and analysis

We begin with a general classification of the numerical results (Fig. 3). According to the definition (20), β is always larger than α, therefore we only consider the upper half of the parameter space above the line $\alpha = \beta$. In the figure, it is easy to identify the previously described special cases: the limiting case of a very soft system with a stiff contact (case I, according to the above classification) corresponds to small values of $\alpha \ll 1$ and large values of $\beta \gg 1$, and is thus to be found in the upper left corner of the diagrams. The limiting case of very stiff system with low contact stiffness (case II), corresponds to $\alpha \approx \beta$ and is found along the diagonal of the diagram. The resonant

Friction **5**(2): 194–206 (2017) 199

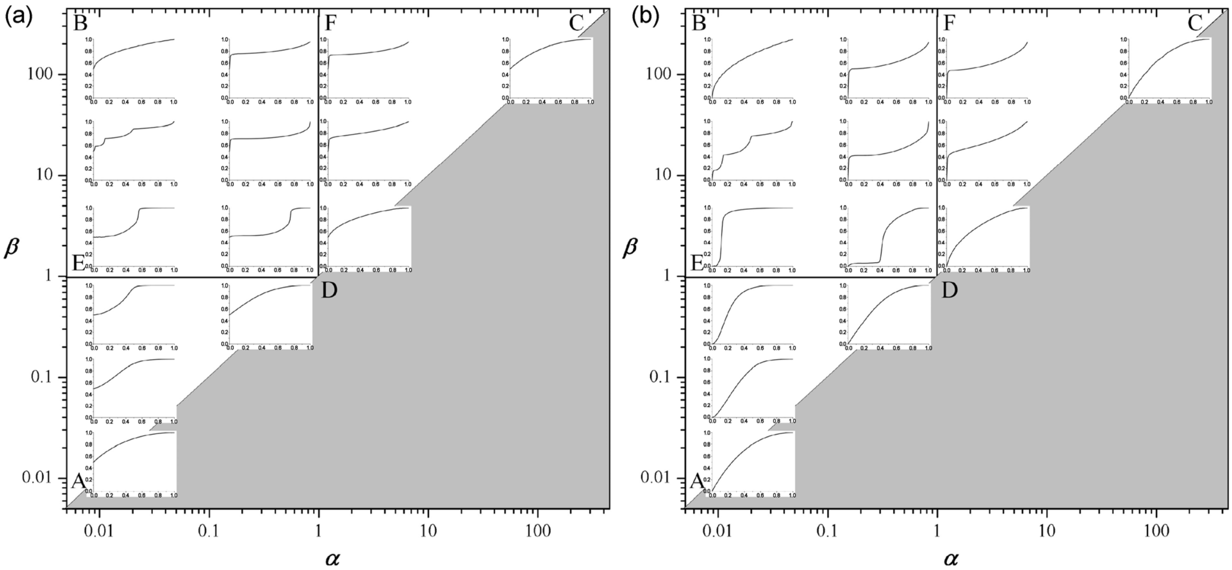

Fig. 3 Typical dependencies of $\mu_{\rm macro}/\mu_0$ on $\overline{v}$ for the oscillation amplitude $\Delta u_z/u_{z,0}=0.5$ (a) and for the maximal non-jumping oscillation amplitude $\Delta u_z/u_{z,0}=1.0$ (b) arranged in a matrix of the dimensionless parameters α and β. The individual curves start at the static COF value at $\overline{v}=0$, which only depends on the oscillation amplitude and is equal to $\mu_0/2$ in (a) and zero in the diagrams in (b). With increasing velocity, the reduced COF monotonically increases and reaches the value "1" at the velocity $\overline{v}=1$. In between, however, the velocity-dependence of the COF is determined by the particular system dynamics.

case III corresponds to the line $\beta=1$ and the resonant case IV to $\alpha=1$.

Since case II occupies the diagonal of the diagram, there are infinitely many possible transitions from II to I. We will consider two such transitions: between A and B in Fig. 3, which passes over the resonant case III and from C to B, which passes over the resonant case IV.

5.1 Limiting cases of soft (case I) and stiff (case II) system and transition over resonant case III

Let us consider the transition from the stiff to the soft system over the resonant case III in more detail. We start with the separate consideration of the limiting cases of the very stiff and the very soft system. The diagram in Fig. 4(a) shows results of numerical simulation for the parameter set $(\alpha,\beta)=(0.01,0.02)$, which corresponds to the limiting case I according to the classification of Section 3. This case was considered in detail in the publication [19]. In Fig. 4, results of numerical simulations are compared with the semi-empirical equation

$$\frac{\mu_{\rm macro}}{\mu_0}\approx 1-\frac{\Delta u_z}{u_{z,0}}\left[\frac{3}{4}(\overline{v}-1)^2+\frac{1}{4}(\overline{v}-1)^4\right] \tag{26}$$

derived in Ref. [19] with $\overline{v}$ given by Eq. (16) and v_0^* by Eq. (14). The numerical data practically ideally coincide with the result (Eq. (26)).

The right-hand-side diagram Fig. 4(b) presents a comparison for the opposite case of very soft system. Again, numerical data are compared with the analytical expression

$$\frac{\mu_{\rm macro}}{\mu_0}=\left(1-\frac{\Delta F_{\rm N}}{F_{\rm N,0}}\right)+\frac{\Delta F_{\rm N}}{F_{\rm N,0}}\left[\sqrt{\frac{4\pi}{9}\overline{v}}+\left(1-\sqrt{\frac{4\pi}{9}}\right)\overline{v}^{1.2}\right] \tag{27}$$

obtained in Ref. [14], with v_0^* given by Eq. (13). In this case too we see a very good agreement. However, numerical data have a noticeable fine structure which the limiting-case curves do not have (a sort of small-amplitude oscillations).

With these two limiting cases, we establish the connection to previous studies and at the same time pose the more general problem of investigating the dependencies of the coefficient of friction on velocity in between these two poles.

As the character of the transformation of the law of friction is very similar for various oscillation amplitudes, in the following we illustrate this transformation only

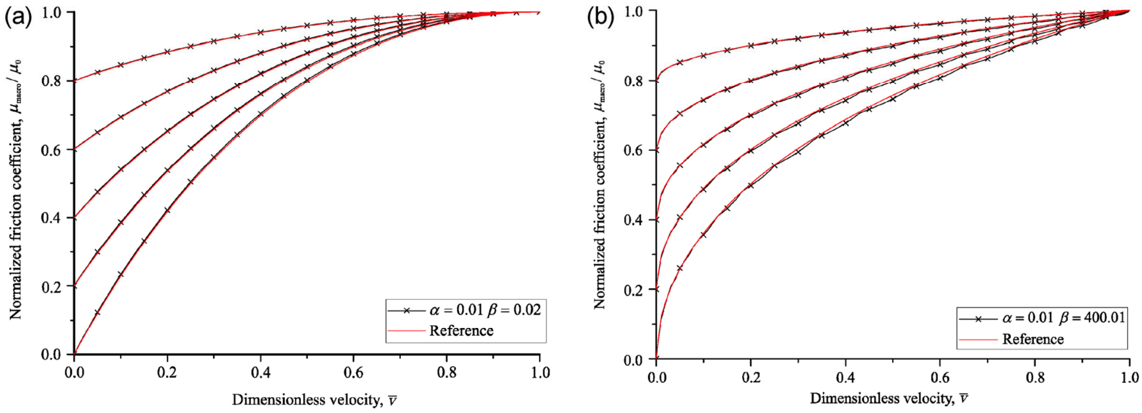

Fig. 4 The dependence of $\mu_{\text{macro}} / \mu_0$ on $\bar{v}$ for $(\alpha,\beta) = (0.01, 0.02)$ and $(\alpha,\beta) = (0.01, 400.01)$ for the oscillation amplitudes $\Delta u_z / u_{z,0} = 0.2,\ 0.4,\ 0.6,\ 0.8,\ 1.0$ (from top to bottom). The crosses and black lines represent results of numerical simulation and the red lines the analytical results (26) and (27).

for the case of the critical amplitude $\Delta u_z / u_{z,0} = 1$. The transition from the lower left corner of the diagram in Fig. 3 to the upper left corner means that the value of the parameter α remains small, while parameter β is changing from very small to very large values. The corresponding transformation of the dependencies of the reduced coefficient of friction on the dimensionless velocity is shown in Fig. 5(a) for the values of β in the lower left quarter of the parameter space and in Fig. 5(b) for the values of β in the upper left quarter of the diagram. In the lower quarter, the changes of the form are relatively slow until parameter β becomes very close to the value of "1". In the vicinity of this "resonant value" the upper point of the curve starts to slide to the left forming a plateau (as is clearly seen in Fig. 5(a) for $\beta = 0.91$). In the exact resonant case, the whole "dependence" consists only of this single plateau, that means that the coefficient of friction is constant and equal to μ_0. Much more dramatic changes occur after passing the resonant value $\beta = 1$. The resonant plateau then sharply decreases and a second plateau appears at the same time. This process repeats many times producing an oscillating curve whose "upper envelope" tends toward the limiting solution for the soft system, as already shown in Fig. 4(b).

5.2 Resonant case IV

We now turn our attention to the resonant case IV, where the frequency of oscillation is equal to the natural

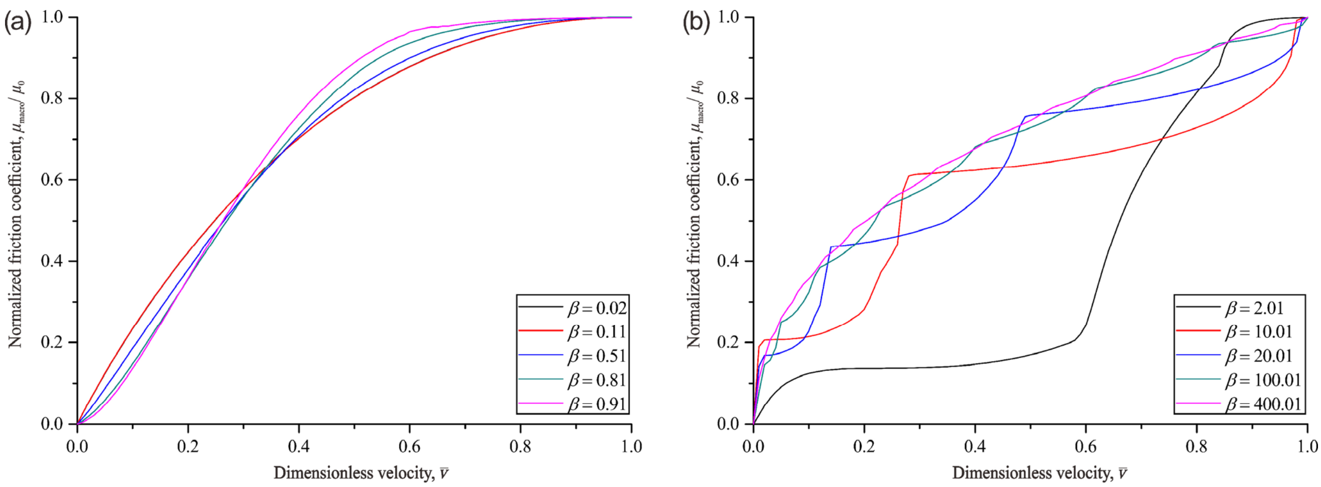

Fig. 5 The dependence of μ_{macro}/μ_0 on $\bar{v}$ for $\Delta u_z/u_{z,0}=1$, $\alpha = 0.01$ and a series of β: (a) lower left quarter of the diagram in Fig. 3 (note that the curves for β = 0.02 and 0.11 practically coincide and cannot be resolved in the figure), (b) upper left quarter of the diagram.

frequency of the slider $\omega = \sqrt{k_x / m}$ and the system's behavior is qualitatively different from previously considered cases. For convenience we consider an equivalent system, where the right end of the system spring k_x in Fig. 1 is fixed and the substrate is instead moving with velocity v_0. Note also that the velocity dependence of the COF cannot be displayed as a function of $\overline{v}$ in the resonant case, because v_0^* tends to infinity and $\overline{v}$ becomes zero. We therefore return to the ordinary dimensional variables in this section. Since we are here concerned with very large values of β, we can consider the contact stiffness to be infinitely large for the purposes of this analysis. We chose the direction of the x-axis as the direction of movement of the substrate. The equation of motion then reads

$$m\ddot{x} + k_x x = \mu_0 F_{\mathrm{N}} \mathrm{sign}(v_0 - \dot{x}) \tag{27}$$

In our model the normal force oscillates according to

$$F_{\mathrm{N}} = F_{\mathrm{N},0} + \Delta F \cdot \cos \omega t \tag{28}$$

Thus, the complete equation of motion is

$$m\ddot{x} + k_x x = \mu_0 (F_{\mathrm{N},0} + \Delta F \cdot \cos \omega t) \mathrm{sign}(v_0 - \dot{x}) \tag{29}$$

For an approximate analysis, let us assume that the body begins with a small-amplitude oscillation

$$\dot{x} = \Delta v \cos \omega t \tag{30}$$

Then the amplitude will be increasing over time until Δv becomes larger than v_0. Indeed, multiplying Eq. (29) with Eq. (30) and noting that the left-hand side of the resulting equation is the time derivative of the energy of the system, we arrive at the energy equation

$$\frac{\mathrm{d}}{\mathrm{d}t}\left(\frac{m\dot{x}^2}{2} + \frac{k_x x^2}{2} \right) = \mu_0 (F_{\mathrm{N},0} + \Delta F \cdot \cos \omega t) \Delta v \cos \omega t \cdot \mathrm{sign}(v_0 - \Delta v \cos \omega t) \tag{31}$$

If $\Delta v < v_0$, then the average value of the right-hand side is positive, and the energy of the system is monotonously increasing from one period to the next. However, if $\Delta v > v_0$ then the amplitude of oscillation stabilizes at the value for which the average change in energy during one period vanishes

$$\langle (F_{\mathrm{N},0} + \Delta F \cdot \cos \omega t) \Delta v \cos \omega t \cdot \mathrm{sign}(v_0 - \Delta v \cos \omega t) \rangle = 0 \tag{32}$$

where $\langle \ldots \rangle$ means averaging over one period of oscillation. During one oscillation period, there is a time interval $\tau_1 < \tau < \tau_2$ where $v_0 - \Delta v \cos \tau < 0$:

$$\tau_{1,2} = \pm \tau^* = \pm \arccos(v_0 / \Delta v) \tag{33}$$

Assuming that the oscillation amplitude Δv exceeds the mean sliding velocity v_0 only slightly, τ^* can be approximated by

$$\tau^* \approx \sqrt{2(1 - v_0 / \Delta v)} \tag{34}$$

In this approximation, the condition (32) can be written, after some simple transformations, as $-4(F_{\mathrm{N},0} + \Delta F)\sqrt{2(1 - v_0 / \Delta v)} + \pi \Delta F = 0$. For the ratio of sliding velocity and oscillation velocity amplitude we finally find

$$\frac{v_0}{\Delta v} = 1 - \frac{1}{2}\left(\frac{\pi \Delta F}{4\left(F_{\mathrm{N},0} + \Delta F\right)} \right)^2 \tag{35}$$

Let us now calculate the macroscopic coefficient of friction. It is given by the equation

$$\begin{aligned} \mu &= \mu_0 \frac{\langle (F_{\mathrm{N},0} + \Delta F \cdot \cos \tau) \mathrm{sign}(v_0 - \dot{x}) \rangle}{F_{\mathrm{N},0}} \\ &= \frac{\mu_0}{2\pi}\left[-4\int_0^{\tau^*}\left(1 + \frac{\Delta F}{F_{\mathrm{N},0}} \cdot \cos \tau \right) \mathrm{d}\tau + 2\pi \right] \end{aligned} \tag{36}$$

which, assuming sufficiently small τ^* and considering Eqs. (34) and (35), leads to the equation

$$\frac{\mu_{\mathrm{macro}}}{\mu_0} \approx 1 - \frac{\Delta F}{2F_{\mathrm{N},0}} \tag{37}$$

Comparing this with numerical results (Fig. 6) shows that the obtained approximation describes the plateau value of the COF in the resonant case very well.

6 Large oscillation amplitudes ("jumping")

If the amplitude of normal oscillation Δu_z exceeds the average indentation depth $u_{z,0}$, the body starts to "jump": For part of the oscillation period, it will be in contact with the substrate and out of contact the rest of the time. In previous studies this case has not usually been studied in detail. In the first part of this

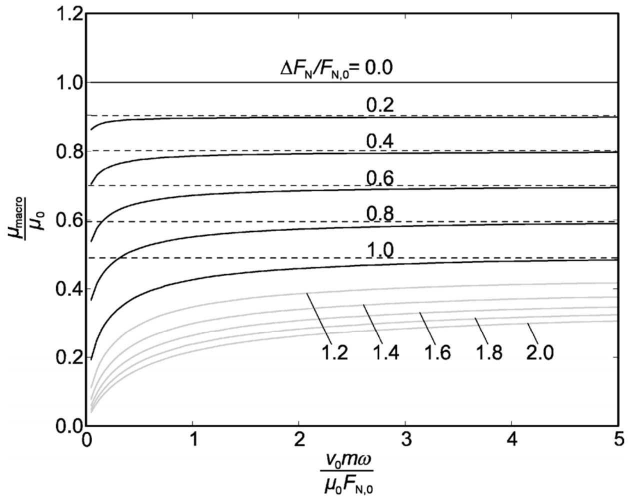

Fig. 6 The dependence of $\mu_{\text{macro}} / \mu_0$ on the dimensionless velocity $v_0 m\omega / (\mu_0 F_{\text{N},0})$ for the resonant case. The curves start at zero velocity at the static value $\mu / \mu_0 = 1 - \Delta F_{\text{N}} / F_{\text{N},0}$ and tend to the limiting value $\mu / \mu_0 = 1 - \Delta F_{\text{N}} / (2F_{\text{N},0})$ given by Eq. (37) at large velocities. The black curves correspond to the non-jumping case $\Delta F_{\text{N}} / F_{\text{N},0} \leqslant 1$, and the gray curves to jumping conditions ($\Delta F_{\text{N}} / F_{\text{N},0} > 1$).

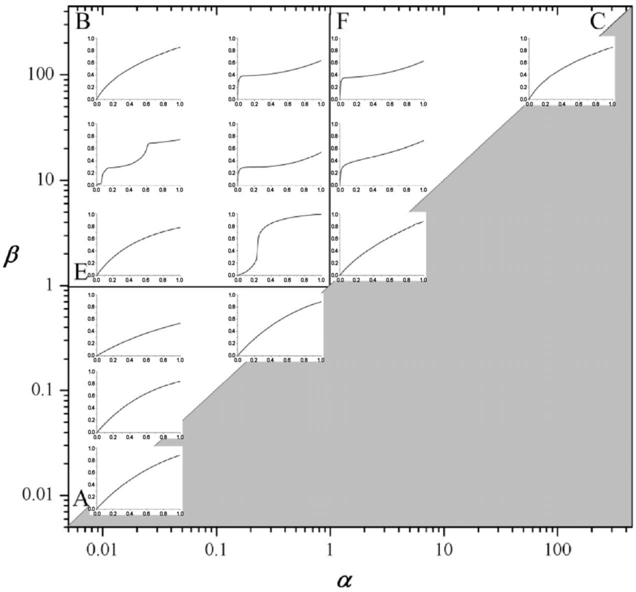

Fig. 7 Typical dependencies of the reduced coefficient of friction $\mu_{\text{macro}} / \mu_0$ on the dimensionless velocity $\bar{v}$ for the relative oscillation amplitude $\Delta u_z / u_{z,0} = 1.5$ (jumping case).

publication [19] the jumping case was also considered (in the context of a stiff system) and it was found that the general character of the dependence of the coefficient of friction on dimensionless sliding velocity is very similar between the jumping and non-jumping cases: In both cases there is a critical velocity above which the COF no longer depends on velocity. Also, the shape of the velocity-dependences changes little after exceeding the critical oscillation amplitude ($\Delta u_z = u_{z,0}$). In analogy to Fig. 3 we present the different dependences for the jumping case in Fig. 7. Comparison with the corresponding graph at the critical amplitude $\Delta u_z = u_{z,0}$ presented in Fig. 3(b) shows that the general character of the dependences remains roughly the same. In particular, in the resonant case IV considered above (corresponding to $\alpha = 1$) there is still a plateau. However, the level of the plateau decreases with increasing oscillation amplitude.

7 Comparison with experiment in the resonant case

Of the various cases considered in the above discussion, several were studied experimentally in the past. The case I of a stiff system (or high-frequency oscillation) was studied experimentally, e.g., in Ref. [16]. On the other hand, we are not aware of previous experiments for the resonant case IV. We therefore conducted experiments using a pin-on-disc tribometer (Fig. 8(a)). The natural frequency of the pin was determined by impacting the pin and measuring its damped oscillation with a laser vibrometer (Fig. 8(b)).

As the determined natural frequency was around 800 Hz, the usual method of exciting oscillations with built-in piezo-elements could not be used, and the tribometer was extended with an electromagnetic shaker as shown in Fig. 8(a). The frequency of the shaker was tuned to the natural frequency of the pin, thus creating the conditions of the resonant case IV. The results are presented in Fig. 9. In contrast with non-resonant cases, where the COF increases monotonically with increasing velocity, in the resonant case it was approximately constant (within the relatively large stochastic error).

8 Summary

We presented a general theoretical analysis of the influence of out-of-plane oscillations on the macroscopically observed coefficient of friction. Unlike previous works, we explicitly took into account both the contact stiffness and the stiffness of the measuring system.

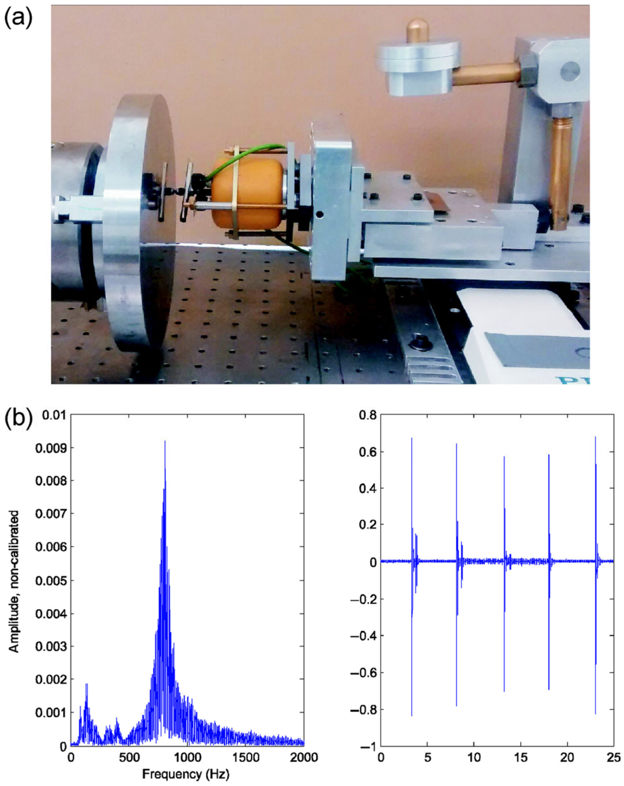

Fig. 8 (a) A photograph of the experimental set-up: a pin-on-disc tribometer is equiped with an electromagnetic shaker producing out-of-plane oscillations at the resonant frequancy of the pin. (b) The resonant frequency was determined by impacting the pin in the tangential direction and determining the Fourier spectrum of the response. The measured natural frequency of the pin was about 800 Hz.

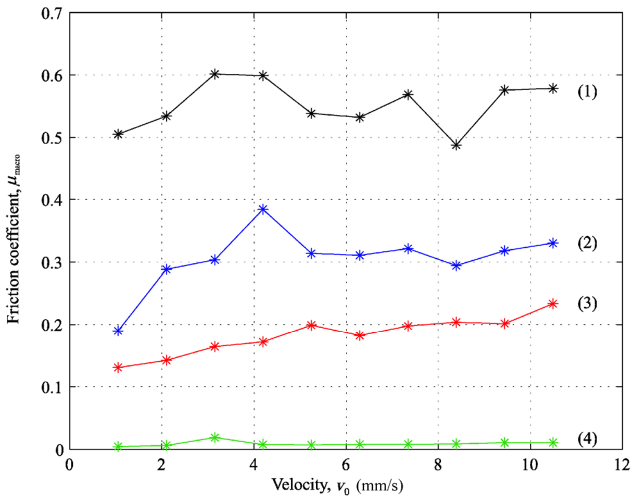

Fig. 9 Dependence of the coefficient of friction on velocity for the resonant case. The oscillation amplitudes were: (1) 1.3 μm; (2) 5.4 μm; (3) 8.2 μm; (4) 60 μm.

The main governing parameters of the resulting system appear to be the ratios of two natural frequencies of the system (one related to the contact stiffness of the system and the other to combined stiffness of the system and contact) to the frequency of the normal oscillation. As observed in previous works, the velocity-dependence of the COF was found to have two main reference points:

(1) The value at vanishing sliding velocity (static coefficient of friction), which naturally does not depend on the dynamic properties and is solely determined by the smallest normal force during the oscillation cycle.

(2) The characteristic velocity above which the COF no longer depends on the sliding velocity and is equal to its microscopic value μ_0.

The only exceptions from this rule are the two resonant cases: One where the COF is constant and equal to μ_0 at all velocities (III) and a second case where the oscillation frequency is equal to the natural frequency of the pin. In this latter case the COF tends to a plateau value below μ_0 and does not have a maximum velocity above which the reduction of the COF disappears. To the best of our knowledge, this resonance case was not studied yet and is described here for the first time.

Figure 10 summarizes schematically the main findings of the present paper. Contrary to the previous figures, we use the non-normalized coefficient of friction and the non-normalized sliding velocity v_0,

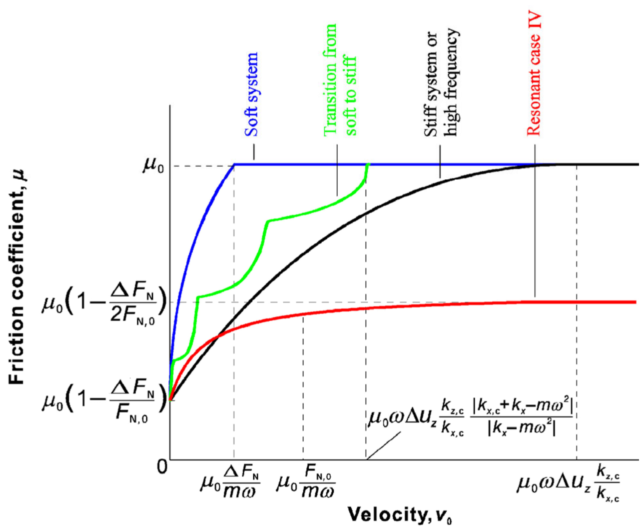

Fig. 10 Schematic representation of the law of frition (dependence of the friction coefficient on the macroscopic sliding velocity) for different relations between the contact and system stiffness as well as eigenfrequencies and the oscillation frequency.

as this better highlights the main tendencies and is easier to compare with experiment.

All dependencies of the macroscopically observed coefficient of friction start at the same static value $\mu_0(1-\Delta F_N / F_{N,0})$, which is determined by the smallest normal force during the oscillating cycle. The further shape of the law of friction depends strongly on the dynamical properties of the system.

The case of the very soft system (and stiff contact), which was studied theoretically in Refs. [7] and [14], is shown in Fig. 10 with a blue line. In this case, the coefficient of friction first increases very rapidly from the static value, reaches the macroscopic value μ_0 at the critical velocity $\mu_0 \Delta F_N / m\omega$ and does not further change with increasing velocity. The critical velocity, in this case, depends solely on the inertial properties of the system, but not on its stiffness. However, in this approximation the theoretical predictions showed poor fit with experimental data [7]. According to Ref. [7] a much better fit to experimental data is achieved if the contact stiffness is taken into account.

The case of finite contact stiffness and very rigid measuring system was considered in detail in the first part of this series [19] and is represented in Fig. 10 with a black curve. The curve starts at the same static value $\mu_0(1-\Delta F_N / F_{N,0})$ of the COF and increases with increasing velocity, however not as rapidly as in the case of the soft system. After reaching the value μ_0 at the critical velocity $\mu_0 \omega \Delta u_z k_{z,c} / k_{x,c}$, it remains constant. In this case the critical velocity does not depend on inertial properties of the system. However, the contact stiffness also does not enter explicitly into the critical velocity; only the ratio of the normal and tangential stiffness (the Mindlin ratio) appears in the equation. This ratio only depends on the Poisson ratio of the contacting partners and is equal to 1.25 for the typical case of $\nu = 1/3$. As shown in this paper, this case is also applicable at very high oscillation frequencies independently of contact and system stiffness.

The law of friction in the transition region between soft and stiff system is schematically represented by the green curve in Fig. 10. In the transition region the dependencies of the coefficient of friction on the sliding velocities can have a complicated shape and are sensitive to the parameters of the system and the frequency of oscillations (see Figs. 5 and 6). Regardless of this complexity, all curves start at the same static friction value $\mu_0(1-\Delta F_N / F_{N,0})$ and reach μ_0 at the critical velocity given by Eq. (12). Depending on parameters, this velocity can range from zero to infinity.

When approaching the resonant case IV where the frequency of the external oscillation is equal to the natural frequency of the system, the critical velocity tends to infinity and the COF reaches a plateau value less than μ_0. For the exactly resonant case, the COF does not exceed the value $\mu_0(1-\Delta F_N / (2F_{N,0}))$, which is larger than the static value $\mu_0(1-\Delta F_N / F_{N,0})$, but smaller than μ_0 even at very high sliding velocities.

In conclusion, we would like to stress once again that the entire analysis of this paper is based on the assumption that Coulomb's law of friction with a constant coefficient of friction is valid locally, in the immediate contact point. We have shown that the macroscopic behavior can be very non-trivial despite the simplicity of the underlying local law of friction. However, a more general analysis taking into account system dynamics, contact stiffness and changes of local friction may eventually achieve the best fit with experimental data. Nonetheless, we believe that changes in the local COF will not impact the overall classification of the discussed dynamic cases. One of the most robust predictions of the present analysis is the existence of the characteristic velocity above which the coefficient of friction does not depend any more on the presence of oscillations. The existence of such velocity was already confirmed for a more general case of a contact with a viscoelastic material [20].

Acknowledgements

The authors would like to thank Juliane Wallendorf and Qiang Li for their help with preparing figures for the paper. This work was supported in part by Tomsk State University Academic D.I. Mendeleev Fund Program (No. 8.2.19.2015).

References

[1] Siegert K, Ulmer J. Superimposing ultrasonic waves on tube and wire drawing. *J Eng Mater Technol* **123**(724): 517–523 (2000)

[2] Egashira K, Mizutani K, Nagao T. Ultrasonic vibration drilling of microholes in glass. *CIRP Ann Technol* **51**(1): 339–342 (2002)

[3] Godfrey D. Vibration reduces metal to metal contact and causes an apparent reduction in friction. *ASLE Trans* **10**(2): 183–192 (1967)

[4] Fridman H D, Levesque P. Reduction of static friction by sonic vibrations. *J Appl Phys* **30**(10): 1572–1575 (1959)

[5] Broniec Z, Lenkiewicz W. Static friction processes under dynamic loads and vibration. *Wear* **80**(3): 261–271 (1982)

[6] Littmann W, Storck H, Wallaschek J. Sliding friction in the presence of ultrasonic oscillations: superposition of longitudinal oscillations. *Arch Appl Mech* **71**(8): 549–554 (2001)

[7] Teidelt E. Oscillating contacts: Friction induced motion and control of friction. Ph.D. Thesis. Berlin (Germany): Technische Universität Berlin, 2015.

[8] Popov V L, Wetter R. Symmetry breaking as a general design principle of oscillation-based methods for fixation and manipulation of nano-objects. *Advanced Biomaterials and Devices in Medicine* **3**(1): 10–18 (2016)

[9] Weishaupt W. Reibungsverminderung durch mechanische Schwingungen. *Tech Mess* **11**: 345–348 (1976)

[10] Goto H, Ashida M, Terauchi Y. Effects of ultrasonic vibration on the wear characteristics of a carbon steel: Analysis of the wear mechanism. *Wear* **94**(1): 13–27 (1984)

[11] Chowdhury M A, Helali M M. The effect of frequency of vibration and humidity on the coefficient of friction. *Tribol Int* **39**(9): 958–962 (2006)

[12] Chowdhury M A, Helali M M. The effect of amplitude of vibration on the coefficient of friction for different materials. *Tribol Int* **41**(4): 307–314 (2008)

[13] Popov V L, Starcevic J, Filippov A E. Influence of ultrasonic in-plane oscillations on static and sliding friction and intrinsic length scale of dry friction processes. *Tribol Lett*: **39**(1): 25–30 (2010)

[14] Teidelt E, Starcevic J, Popov V L. Influence of ultrasonic oscillation on static and sliding friction. *Tribol Lett* **48**(1): 51–62 (2012)

[15] Milahin N, Li Q, Starcevic J. Influence of the normal force on the sliding friction under ultrasonic oscillations. *Facta Univ Ser Mech Eng* **13**(1): 27–32 (2015)

[16] Milahin N. Robuste Einflussparameter für Reibung und Oberflä-chenmodifizierung unter Einfluss von Ultraschall. Ph.D. Thesis. Berlin (Germany): Technische Universität Berlin, 2016.

[17] Nguyen H X, Teidelt E, Popov V L, Fatikow S. Dynamical tangential contact of rough surfaces in stick-slip microdrives: modeling and validation using the method of dimensionality reduction. *Physical Mesomechanics* **17**(4): 304–310 (2014)

[18] Cabboi A, Putelat T, Woodhouse J. The frequency response of dynamic friction: enhanced rate-and-state models. *Journal of the Mechanics and Physics of Solids* **92**: 210–236 (2016)

[19] Popov M, Popov V L, Popov N V. Reduction of friction by normal oscillations. I. Influence of contact stiffness. *Friction* **5**(1): 45–55 (2017)

[20] Popov M. Critical velocity of controllability of sliding friction by normal oscillations in viscoelastic contacts. *Facta Universitatis, Series: Mechanical Engineering* **14**(3): 335–341 (2016)

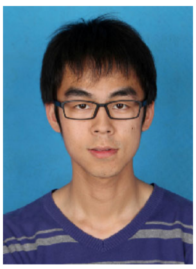

Xinyu MAO. Double master degree candidate in the majors of Mechanical Engineering at the Tsinghua University and Engineering Science at the Berlin University of Technology. He obtained his bachelor degree in mechanical engineering at Tsinghua University in 2014. His research interests include tribological simulations, especially friction and wear (fretting) under the action of vibration.

Valentin L. POPOV. Full professor at the Berlin University of Technology, studied physics (1976–1982) and obtained his doctorate in 1985 from the Moscow State Lomonosov University. He worked at the Institute of Strength Physics of the Russian Academy of Sciences. After a guest professorship in the field of theoretical physics at the University of Paderborn (Germany) from 1999 to 2002, he has headed the Department of System Dynamics and the Physics of Friction of the Institute of Mechanics at the Berlin University of Technology. His areas of interest include tribology, nanotribology, tribology at low temperatures, biotribology, the influence of friction through ultrasound, numerical simulation of frictional processes, research regarding earthquakes, as well as topics related to materials science such as the mechanics of elastoplastic media with microstructures, strength of metals and alloys, and shape memory alloys. He has published over 100 papers in leading international journals during the past 5 years. He is the author of the book "*Contact Mechanics and Friction: Physical Principles and Applications*" which appeared in three German, two English, Chinese, and Russian editions and co-author of the book on "*Method of Dimensionality Reduction in Contact Mechanics and Friction*" which appeared in German, English and Chinese editions. He is the joint editor of international journals and regularly organizes international conferences and workshops on diverse tribological themes. He is a member of the Scientific Council of the German Tribological Society. He has intensively collaborated with many industrial corporations and possesses experience in implementing the results of scientific research in industrial applications.

Jasminka STARCEVIC. She is the head of experimental laboratories at the Institute of Mechanics at the Berlin University of Technology. She studied mechanical engineering at the Berlin University of Technology and obtained the degree of Diplom-Ingeneiur in 1997 and the doctorate in 2008. She is a co-author of 25 papers in international journals. Her research interests include physics of friction, active control of friction by ultrasonic oscillations, tribospectroscopy, as well as development of methods for earthquake prediction. She has intensively collaborated with many industrial corporations and possesses experience in implementing the results of scientific research in industrial applications.

Mikhail POPOV. He obtained the bachelor degree in computer science from the Freie Universität Berlin in 2011 and the master degree in engineering science from the Tomsk Polytechnic University and Berlin Technical University in 2016. Currently he is a research assistant at the Tomsk Polytechnic University and Berlin University of Technology. His research interests include efficient numerical methods in tribology, rubber friction, as well as friction and damping under the influence of oscillations.

3.3 Publication 6

In this short note the inertial model from P5 is combined with viscoelasticity. The system model and oscillation parameters remain the same, but the contact is changed from purely elastic to viscoelastic by addition of a parallel velocity-proportional damper (Fig. 2). However, a full numerical analysis is not undertaken, since it would likely end up even more extensive than in P5, due to the additional parameters. Instead, the publication only endeavors to find the critical velocity of controllability for this system, which already allows to get some qualitative impression of the system's behavior, and can inform the choice of dimensionless variables for an actual parameter study.

After establishing the model, the static coefficient of friction is calculated (Eq. 7), which is once again independent of the mass, due to displacement-controlled oscillation, but dependent on frequency, due to the viscoelastic response. To determine the critical velocity, the equation of motion is set up and solved for the lateral displacement of the contact point (Eq. 13). Differentiation produces the velocity of the contact point (Eq. 14), from which the critical velocity is extracted by determining the amplitude of the time-dependent part (Eq. 15).

FACTA UNIVERSITATIS
Series: **Mechanical Engineering** Vol. 14, N° 3, 2016, pp. 335 - 341
DOI: 10.22190/FUME1603335P

CRITICAL VELOCITY OF CONTROLLABILITY OF SLIDING FRICTION BY NORMAL OSCILLATIONS IN VISCOELASTIC CONTACTS

UDC 539.3

Mikhail Popov[1,2,3]

[1]Tomsk Polytechnic University, Tomsk, Russia
[2]Technische Universität Berlin, Berlin, Germany
[3]Tomsk State University, Tomsk, Russia

Abstract. *Sliding friction can be reduced substantially by applying ultrasonic vibration in the sliding plane or in the normal direction. This effect is well known and used in many applications ranging from press forming to ultrasonic actuators. One of the characteristics of the phenomenon is that, at a given frequency and amplitude of oscillation, the observed friction reduction diminishes with increasing sliding velocity. Beyond a certain critical sliding velocity, there is no longer any difference between the coefficients of friction with or without vibration. This critical velocity depends on material and kinematic parameters and is a key characteristic that must be accounted for by any theory of influence of vibration on friction. Recently, the critical sliding velocity has been interpreted as the transition point from periodic stick-slip to pure sliding and was calculated for purely elastic contacts under uniform sliding with periodic normal loading. Here we perform a similar analysis of the critical velocity in viscoelastic contacts using a Kelvin material to describe viscoelasticity. A closed-form solution is presented, which contains previously reported results as special cases. This paves the way for more detailed studies of active control of friction in viscoelastic systems, a previously neglected topic with possible applications in elastomer technology and in medicine.*

Key Words: *Active Control of Friction, Ultrasonic Vibration, Viscoelastic Contact, Critical Velocity*

Received October 22, 2016 / Accepted November 30, 2016
Corresponding author: Mikhail Popov
Technische Universität Berlin, Str. des 17. Juni 135, 10623 Berlin
E-mail:m@popov.name

1. Introduction

The reduction of static and sliding friction by ultrasonic oscillation in various directions is a well-known phenomenon with many applications ranging from wire drawing and press forming, stabilization of system dynamics, as in brake squeal suppression, and production of directed motion, as in ultrasonic motors and linear actuators. The effect has been studied for several decades, both experimentally and theoretically. Among the proposed explanations, microscopic theories have historically been prevalent. E.g. Zaloj et al. [1] suggest that the effect may be due to the dilatation caused by sliding. V. Popov et al. point to the possible importance of the microscopic interaction potential [2]. Although plausible, microscopic models could never achieve good, quantitative correspondence between theoretical predictions and experimental results, e.g. [3]. Opposite to that stand purely macroscopic models, which explain the phenomenon using macroscopic contact mechanics or system dynamics. Several system configurations have been considered from that perspective [3, 4, 5] and it was found that the macroscopic models can describe the observed behavior of the systems without fitting parameters. This result is in fact somewhat surprising, considering that these macroscopic theories assume a constant microscopic coefficient of friction and a friction law of the form $F_f = \mu_0 F_n$. When the average force of friction is determined by integrating the force of friction over time (or integrating stress over time and contact area) and dividing by the integral of the normal force, the direct proportionality of the assumed law of friction will insure that the integrals of normal force will cancel out, with the end result that the average coefficient of friction $\bar{\mu}$ must *always* be equal to μ_0. This reasoning, however, is subtly flawed, in that it assumes sliding in one direction with a nonzero velocity. It is also possible for the body to temporarily cease motion (e.g. due to increasing normal force or more complicated reasons relating to system dynamics). During such stick phases, the law of friction needs to be written in its static form: $F_f \leq \mu_0 F_n$. Note the *less than or equal* in this formula, which breaks the proportionality and allows $\bar{\mu}$ to be less than μ_0. To the author's knowledge, the possibility that the influence of normal oscillations on sliding friction may be explained entirely by the presence of intermittent stick phases has not been made explicit before the publication of the two part-study [6, 7]. In these papers, the stick-induced reduction of friction force was studied in a displacement-controlled setting with and without in-plane system dynamics. Although a closed-form solution for the actual force of friction under the action of normal vibrations does not exist in either case, it has turned out to be possible to calculate the critical velocity v_c for a broad class of problems. This critical velocity refers to the maximum sliding velocity, above which vibration no longer has any influence on friction (at a given frequency and amplitude). This is illustrated in Fig. 1, which qualitatively describes the behavior of the average coefficient of friction, as it increases from its static value to μ_0 with increasing sliding velocity. In the theory presented in [6] it was argued that this critical velocity is related to the disappearance of stick in the contact. Also in [6], the following expression was obtained for the critical velocity in an entirely displacement-controlled system:

$$v_c = \mu_0 \omega \Delta u_z \frac{E^*}{G^*} \,, \tag{1}$$

where $\omega\Delta u_z$ is the amplitude of velocity oscillation and E^*/G^* is the ratio of the normal and tangential stiffness of the contact (the so-called Mindlin-ratio). Since this ratio is generally of the order of unity, one can roughly say that the critical sliding velocity is equal to the maximum velocity in the normal direction (due to the oscillation) times the microscopic coefficient of friction. This critical velocity also enters into the primary dimensionless parameter characterizing the behavior of the system, which makes accurate analysis of this quantity doubly important.

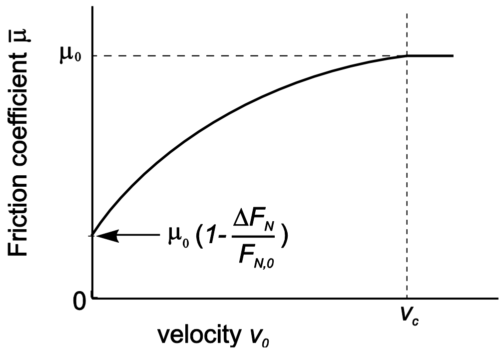

Fig. 1 Qualitative dependence of the average coefficient of friction (COF) on sliding velocity under action of normal oscillations. Of particular interest are the "static COF" at zero velocity, the monotonous increase of the COF with increasing sliding velocity and the critical velocity of controllability, above which the average COF is equal to the microscopic COF, μ_0, with or without oscillations.

If the model is augmented with a system spring and a contact mass, thus enabling in-plane system dynamics, the expression for the critical velocity becomes [7]:

$$v_c = \mu_0 \omega \Delta u_z \frac{k_{z,c}}{k_{x,c}} \frac{|k_{x,c} + k_x - m\omega^2|}{|k_x - m\omega^2|} , \tag{2}$$

where $k_{x,c}$ and $k_{z,c}$ are the tangential and normal stiffness of the contact (in this model, the contact stiffness is assumed to be constant), k_x is the tangential stiffness of the surrounding system and m is the mass of the sliding body. The only difference compared to Eq. (1) is the additional dependence on the two natural frequencies of the system. Indeed, if k_x tends to infinity, Eq. (2) reduces to the previous result. Another notable feature is the presence of two resonant frequencies, in particular $\omega = \sqrt{k_x/m}$ where v_c becomes infinite. Numerical experiments show that in this case, the coefficient of friction reaches a plateau (which is less than μ_0) at fairly low sliding velocities and does not change thereafter. For the full analysis, the reader is referred to [6, 7].

In the present paper these previous results are extended to also include *viscoelastic* contacts. Active control of friction and system stability seems to be an underexplored topic when viscoelastic contacts are concerned, despite many possible applications in conjunction with the ubiquitous use of elastomers and the rising demands placed on devices in contact with biological tissues in medical technology. With this paper we would like to begin establishing a quantitative framework for the analysis of viscoelastic friction under oscillation, by proposing that the same methods used in [6, 7] can be applied in viscoelastic contacts in order to calculate the critical velocity in closed form.

2. Model and Analysis

2.1. Formulation of the model

The model that will be analyzed in this paper is very similar to the one presented in [7]. It consists of a mass m that is pulled with a constant velocity v_0 through a system spring with a constant stiffness k_x (see Fig. 2). In addition, a displacement-controlled harmonic oscillation is imposed in the direction normal to the plane. The oscillation is defined by:

$$u_z = u_{z,0} + \Delta u_z \cos \omega t , \tag{3}$$

where u_z is the coordinate of the body in the normal direction, $u_{z,0}$ the mean indentation depth, Δu_z the oscillation amplitude and ω the frequency. The body is connected to the substrate through a contact point, in which Amontons' law of friction with a constant coefficient of friction μ_0 is assumed. The main difference is that the contact is not elastic but viscoelastic and characterized not only by the constant tangential and normal spring stiffness $k_{x,c}$ and $k_{z,c}$, but also by the dynamic viscosities $\gamma_{x,c}$ and $\gamma_{z,c}$. This corresponds to the Kelvin material, the simplest model of viscoelasticity. The relevant dynamics of the resulting system is confined to the sliding plane and is characterized by u_x, the position of the body and $u_{x,c}$, the position of the contact point.

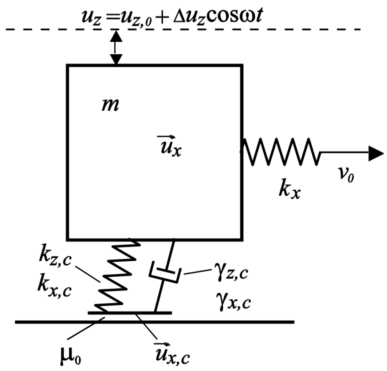

Fig. 2 Schematic representation of the considered system, consisting of a mass, a system spring and a viscoelastic contact with the sliding plane.

2.2. Analysis of the model

2.2.1. Normal force

The normal force in the spring-damper combination is given by:

$$F_N = k_{z,c} u_z + \gamma_{z,c} \dot{u}_z = k_{z,c}(u_{z,0} + \Delta u_z \cos \omega t) - \gamma_{z,c} \omega \Delta u_z \sin \omega t . \tag{4}$$

To ensure that the body is always in contact with the plane, the normal force must always remain positive. This is the case if:

$$k_{z,c}u_{z,0} > \Delta u_z \sqrt{k_{z,c}{}^2 + \gamma_{z,c}{}^2\omega^2} \ . \tag{5}$$

Only this “non-jumping” case is considered in the following.

The static force of friction (the force at zero sliding velocity) can be calculated easily by noting that, according to Eq. (4), the amplitude of the oscillation of the normal force is equal to:

$$\Delta F_N = \Delta u_z \sqrt{k_{z,c}{}^2 + \gamma_{z,c}{}^2\omega^2} \ . \tag{6}$$

The static force of friction is equal to the minimal normal force during an oscillation cycle, multiplied with the coefficient of friction:

$$F_s = \mu_0(F_{N,0} - \Delta F_N) = \mu_0(k_{z,c}u_{z,0} - \Delta u_z \sqrt{k_{z,c}{}^2 + \gamma_{z,c}{}^2\omega^2}) \ . \tag{7}$$

2.2.2 Tangential movement

Under the assumption that the immediate contact point is always in the sliding state, the equation of motion of mass *m* reads:

$$m\ddot{u}_x = k_x(v_0 t - u_x) - \mu_0 F_N \ . \tag{8}$$

The equilibrium condition for the “foot point” of the spring-damper combination reads:

$$k_{x,c}(u_x - u_{x,c}) + \gamma_{x,c}(\dot{u}_x - \dot{u}_{x,c}) = \mu_0 F_N \ , \tag{9}$$

where F_N is given by Eq. (4).

Equation (8), after inserting Eq. (4) on the right hand side, can be easily solved with respect to u_x:

$$u_x = v_0 t - \mu_0 \frac{k_{z,c}}{k_x} u_{z,0} + \frac{\mu_0 \Delta u_z}{m\omega^2 - k_x}(k_{z,c} \cos\omega t - \gamma_{z,c}\omega \sin\omega t) \ . \tag{10}$$

In our analysis we assume that the material of the contacting elastomer body is isotropic, with a constant (frequency-independent) Poisson number. Under these conditions, we have:

$$\frac{\gamma_{x,c}}{\gamma_{z,c}} = \frac{k_{x,c}}{k_{z,c}} \ . \tag{11}$$

Equation (9) can also be solved with respect to $(u_x - u_{x,c})$:

$$u_x - u_{x,c} = \mu_0 \frac{k_{z,c}}{k_{x,c}}(u_{z,0} + \Delta u_z \cos\omega t) \ . \tag{12}$$

From Eqs. (10) and (12) we can first determine $u_{x,c}$:

$$u_{x,c} = v_0 t - \mu_0 k_{z,c} u_{z,0}\left(\frac{1}{k_x}+\frac{1}{k_{x,c}}\right) + \frac{\mu_0 \Delta u_z}{m\omega^2 - k_x}(k_{z,c}\cos\omega t - \gamma_{z,c}\omega \sin\omega t) - \mu_0 \frac{k_{z,c}}{k_{x,c}}\Delta u_z \cos\omega t \quad (13)$$

and finally $\dot{u}_{x,c}$:

$$\begin{aligned}\dot{u}_{x,c} &= v_0 + \frac{\mu_0 \Delta u_z}{m\omega^2 - k_x}(-k_{z,c}\omega \sin\omega t - \gamma_{z,c}\omega^2 \cos\omega t) + \mu_0 \frac{k_{z,c}}{k_{x,c}}\Delta u_z \omega \sin\omega t \\ &= v_0 - \frac{\mu_0 \Delta u_z}{m\omega^2 - k_x}\gamma_{z,c}\omega^2 \cos\omega t + \mu_0 \Delta u_z \omega \frac{k_{z,c}}{k_{x,c}} \frac{-k_{x,c} - k_x + m\omega^2}{(m\omega^2 - k_x)}\sin\omega t\end{aligned} \quad (14)$$

The critical velocity of controllability is given by the condition that the amplitude of the oscillating part of this solution becomes equal to constant sliding velocity v_c:

$$v_c = \frac{\mu_0 \Delta u_z \omega}{|m\omega^2 - k_x|}\sqrt{(\gamma_{z,c}\omega)^2 + \left(\frac{k_{z,c}}{k_{x,c}}\cdot(m\omega^2 - k_{x,c} - k_x)\right)^2}\;. \quad (15)$$

Note that the critical velocity depends on the oscillation amplitude but *not on the average indentation*.

In the limit of a very stiff system spring, $k_x \to \infty$, the critical velocity, Eq. (15), is reduced to Eq. (1), which thus appears to be valid independently of the viscoelastic properties of the medium. According to the Method of Dimensionality Reduction (MDR) [8], any rotationally symmetric contact can be equivalently represented by a model consisting of a series of independent springs (note that an equivalent one-dimensional model can in fact be constructed for almost arbitrary, e.g. rough, contacts, although there may be no closed-form mapping rule in the general case). As has been argued in [6], the existence an equivalent model with *uncoupled* spring elements, together with the indentation-independence of Eq. (15), implies that the obtained result in Eq. (15) is valid not only for the simple considered model with a single spring-damper combination, but also for quite general contacts (so long as the amplitude of oscillation remains small).

3. Conclusion

While the details of the influence of oscillation on friction may be very complicated at intermediate sliding velocities [7], there are still two simple and nearly universal (except in resonant cases) characteristic points: First, the velocity-dependences all start from the static value at vanishing velocity. Second, the coefficient of friction increases monotonically (again, barring exceptional system-dynamical circumstances) until it reaches the microscopic value at some critical velocity. These two points, the static coefficient of friction, and the critical velocity of controllability of friction, are the most important characteristics of any oscillating frictional system. It so happens that both of these points can be determined analytically for very general classes of contacts with and without system dynamics.

In the present paper, the critical velocity of controllability was determined for the simplest possible viscoelastic rheology (Kelvin body) and the simplest possible contact geometry (contact with constant contact stiffness, e.g. cylindrical punch). Eq. (15) provides an explicit analytical solution. Even under these simple assumptions, the critical velocity depends on almost all system and loading parameters: the local coefficient of friction μ_0, mass *m* of the system, the stiffness of the contact and of the system, the frequency of oscillations, the damping coefficient of the contact, and on the amplitude of oscillations. However, it does not depend on absolute indentation, which permits easy generalization to more realistic contact geometry.

Further, in the case of displacement-controlled horizontal movement (corresponding to an infinitely stiff surrounding system, which eliminates system dynamics in the contact) it was found that the critical velocity is given by Eq. (1), without dependence on the rheological properties of the contact: only the ratio of the contact stiffness (Mindlin ratio) appears in the expression for this critical velocity.

In the future, the critical velocity could also be considered for materials with more general rheology. The Method of Dimensionality Reduction [8] provides a natural theoretical framework for this and for further generalizations to arbitrary contact geometries and loading histories.

Acknowledgements: *The author would like to thank V. L. Popov and A. E. Filippov for inspiring discussions concerning the present work.*

References

1. Zaloj, V, Urbakh, M, Klafter, J., 1999, *Modifying friction by manipulating normal response to lateral motion.* Physical review letters 82(24), pp. 4823, 1999.
2. Popov, VL, Starcevic, J, Filippov, AE., 2010, *Influence of ultrasonic in-plane oscillations on static and sliding friction and intrinsic length scale of dry friction processes.* Tribology Letters, 39 (1), 25-30, 2010.
3. Teidelt, E, 2015, *Oscillating contacts: friction induced motion and control of friction*, Dissertation, TU Berlin, Germany, 151 p.
4. Milahin, N., Starcevic, J., 2014, *Influence of the normal force and contact geometry on the static force of friction of an oscillating sample*. Physical Mesomechanics, 17(3), pp. 84-8.
5. Milahin, N., Li, Q., 2016, *Friction and wear of a spherical indenter under influence of out-of-plane ultrasonic oscillations*. Physical Mesomechanics, 19(2), pp. 149-153.
6. Popov, M., Popov, VL, Popov, NV, 2016, *Reduction of friction by normal oscillations. I. Influence of contact stiffness*, arXiv:1611.07017.
7. Mao, X, Popov, VL, Starcevic, J., Popov, M, 2016, *Reduction of friction by nor-mal oscillations. II. In-plane system dynamics*, arXiv:1611.07018.
8. Popov, VL., Heß, M. 2015, *Method of dimensionality reduction in contact mechanics and friction*, Springer, Berlin, Heidelberg, 265 p.

3.4 Publication 7

While the preceding publications were focused on friction control by normal oscillations, Publication 7 considers tangential (aligned with the direction of sliding) and combined tangential and normal oscillations. The model is carried over from P4, except for an additional phase-shifted oscillation in the x-direction.

The analysis mirrors that performed in P4, and the first notable result is the critical velocity given in Eq. (8). The critical velocity is asymmetric with respect to the direction of motion, which is unsurprising, since the combined normal and tangential oscillations describe the path of an inclined ellipse. Although this is not mentioned in the paper, the critical velocity can also be written as $(v_x^2 + 2v_x v_z \cos\varphi + v_z^2)^{1/2}$, where v_x and v_z are the separate critical velocities associated with the tangential and normal oscillations and φ is the phase shift.

The static COF is derived next. Some approximations have to be made to keep the analysis simple. In particular, the case where a large tangential amplitude causes the contact point to reverse the direction of sliding, with two intervening stick phases per cycle, is neglected. The result is given in Eqs. (18, 19) and is likewise asymmetric.

This is as far as analytical estimations can go, and further results are numerical. The normalized velocity-dependence of the COF for a purely tangential oscillation is shown in Fig. 3. At low amplitudes the dependencies are very similar to the ones for normal oscillation (given in Fig 2. for comparison), but at higher amplitudes the dependence splits into a low-velocity and a high-velocity part. This qualitative transition is explained by the appearance of the already mentioned direction-reversal mode when the velocity amplitude of the oscillation exceeds the sliding velocity. Note also that the "negative coefficient of friction" in these figures has no physical significance and simply carries over the sign of the friction force. This makes some of the latter figures with pronounced directional asymmetry easier to interpret.

Under purely normal or tangential oscillation friction is "ordinary", in that the friction vector is directed opposite to the direction of sliding and has the same magnitude in both directions. Combining both oscillations is symmetry-breaking, however, and creates a continuum of systems that range from 1) ordinary friction, over 2) "dynamic ratchets" in which friction is still opposed to the direction of motion, but no longer symmetric, and finally 3) "active frictional drives", in which the asymmetry progresses to the point that the time-averaged lateral force acts in the direction of motion. These additional modes are described in the rest of the paper. The active drive mode in particular is of interest for practical applications, due to the current proliferation of ultrasonic motors and positioning systems in both consumer and industrial applications.

ISSN 1029-9599, Physical Mesomechanics, 2018, Vol. 21, No. 1, pp. 24–31. © Pleiades Publishing, Ltd., 2018.
Original Text © M. Popov, Q. Li, 2017, published in Fizicheskaya Mezomekhanika, 2017, Vol. 20, No. 5, pp. 26–32.

Multimode Active Control of Friction, Dynamic Ratchets and Actuators

M. Popov[1,2,3]* and Q. Li[4]

[1] *Department of Continuum Mechanics and Theory of Materials, Technische Universität Berlin, Berlin, 10587 Germany*
[2] *National Research Tomsk Polytechnic University, Tomsk, 634050 Russia*
[3] *National Research Tomsk State University, Tomsk, 634050 Russia*
[4] *Department of System Dynamics and the Physics of Friction, Technische Universität Berlin, Berlin, 10623 Germany*
** e-mail: m@popov.name*

Received April 12, 2017

Abstract—Active control of friction by ultrasonic vibration is a well-known effect with numerous technical applications ranging from press forming to micromechanical actuators. Reduction of friction is observed with vibration applied in any of the three possible directions (normal to the contact plane, in the direction of motion and in-plane transverse). In this work, we consider the multi-mode active control of sliding friction, where phase-shifted oscillations in two or more directions act at the same time. Our analysis is based on a macroscopic contact-mechanical model that was recently shown to be well-suited for describing dynamic frictional processes. For simplicity, we limit our analysis to a constant, load-independent normal and tangential stiffness and two superimposed phase-shifted harmonic oscillations, one of them being normal to the plane and the other in the direction of motion. As in previous works utilizing the present model, we assume a constant local coefficient of friction, with reduction of the observed force of friction arising entirely from the macroscopic dynamics of the system. Our numerical simulations show that the resulting law of friction is determined by just three dimensionless parameters. Depending on the values of these parameters, three qualitatively different types of behavior are observed: (a) symmetric velocity-dependence of the coefficient of friction (same for positive and negative velocities), (b) asymmetric dependence with respect to the sign of the velocity, but with zero force at zero velocity, and (c) asymmetric dependence with nonzero force at zero velocity. The latter two cases can be interpreted as a "dynamic ratchet" (b) and an actuator (c).

DOI: 10.1134/S1029959918010046

Keywords: vibration, dual-mode, active control of friction, ratchet, actuator

1. INTRODUCTION

Both static and sliding friction can be significantly reduced by vibration. This is a well-known phenomenon with numerous technical applications, e.g. in metal forming [1] or ultrasonic machining [2], as well as in stabilization of system dynamics, e.g. suppression of brake squeal. Since the 1950s the influence of vibration on friction has been studied experimentally [3] and various theoretical models have been proposed [4]. Reduction of friction has been observed both under the influence of oscillations in the contact plane and perpendicular to the plane [5]. Tolstoi [6] was one of the first to emphasize the importance of normal oscillations for the correct understanding of friction. Extensive studies have been carried out in [4, 7] and in a series of dissertations [8–10]. Various configurations (oscillations in the sliding direction and perpendicular to the sliding direction in the contact plane; oscillations perpendicular to the contact plane (out-of-plane oscillations)) as well as a microscopic interpretation of the phenomenon are discussed in [11]. In a series of recent papers, it was shown experimentally that an important parameter in the problem of active control of friction is the contact stiffness [12, 13]. This influence was analyzed in detail in [14] and [15] for the case of normal oscillations. In the present paper we consider the more general case of superimposed oscillations in normal and tangential directions ("dual-mode" active control of friction). We will show that this significantly changes the situation compared with "single-mode" control. In the case of dual-mode control a qualitatively different behavior can be observed, which we call "dynamic ratcheting".

2. SPRING MODEL AND THEORETICAL ANALYSIS

We consider an elastic body sliding on a flat plane with a constant velocity v_0, which is subjected to a superposition of external normal and tangential oscillations. It is assumed that Coulomb's law of friction with a constant local coefficient of friction μ_0 is valid within the contact. Similarly to [14], we model the contact as a single linear spring with constant normal and tangential stiffness k_z and k_x. This model corresponds to the contact of a flat-ended cylinder with a plane. The unstressed state in contact with the plane is chosen as the reference state. The vertical and horizontal displacements of the upper point of the spring are denoted as u_z and u_x, and the horizontal displacement of the lower point as $u_{x,\mathrm{c}}$. The upper point experiences a forced oscillation according to

$$u_z = u_{z,0} - \Delta u_z \cos(\omega t) \quad (1)$$

in the vertical direction, and a composition of translation with constant velocity and a harmonic oscillation with the same frequency ω and a phase difference φ

$$u_x = v_0 t + \Delta u_x \cos(\omega t + \varphi) \quad (2)$$

in the horizontal direction (Fig. 1), where $u_{z,0}$ corresponds to the average indentation depth and Δu_z and Δu_x are the amplitudes of oscillation. We assume that the spring is always in contact with the plane, i.e. $\Delta u_z < u_{z,0}$. The main difference compared to [14] is the presence of the tangential oscillation $\Delta u_x \times \cos(\omega t + \varphi)$ in Eq. (2). This change results in qualitatively changed, ratchet-like or actuator-like behavior.

2.1. Critical Velocity

One of the characteristics of reduction of friction by vibration is the existence of a critical sliding velocity, above which the reduction is no longer possible and the average coefficient of friction is equal to its local value μ_0. In [14] and [15], it was shown that this critical velocity can be calculated from the contact-mechanical model for fairly general system configurations. These calculations were based on the observation that reduction of friction must be due to intermittent stick states during sliding, since the tangential force is less than the ordinary sliding friction force only during stick. The critical sliding velocity is thus determined by considering the point where stick becomes impossible and the system transitions into continuous sliding. In [16] this analysis was further generalized for the case of simple viscoelastic contacts. In the following we will calculate the critical velocity of controllability for dual mode control of friction.

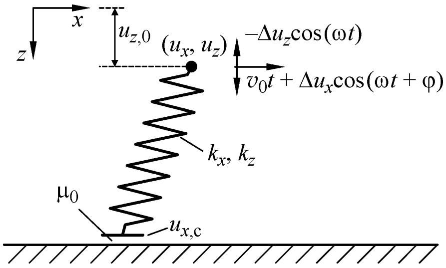

Fig. 1. A single-spring model of frictional contact under superimposed oscillation in normal and tangential directions.

As described above, the upper point of spring is forced to move according to Eqs. (1) and (2). However, the movement of lower point is unknown and can be either in stick or slip state. The normal and tangential force of the spring are given by

$$f_z = k_z u_z = k_z(u_{z,0} - \Delta u_z \cos(\omega t)), \quad (3)$$

$$f_x = k_x(u_x - u_{x,\mathrm{c}}) = k_x(v_0 t + \Delta u_x \cos(\omega t + \varphi) - u_{x,\mathrm{c}}). \quad (4)$$

If the tangential force of the spring is smaller than the normal force multiplied by the coefficient of friction, $f_x < \mu_0 f_z$, the lower point will be in a stick state. Otherwise, it will slip relative to the plane and in this case $f_x = \mu_0 f_z$:

$$k_x(v_0 t + \Delta u_x \cos(\omega t + \varphi) - u_{x,\mathrm{c}}) = \mu_0 k_z (u_{z,0} - \Delta u_z \cos(\omega t)). \quad (5)$$

To find the critical velocity for continuous sliding, we assume that Eq. (5) is fulfilled at all times. Derivation of (5) with respect to time gives

$$\dot{u}_{x,\mathrm{c}} = v_0 - \omega \Delta u_x \sin(\omega t + \varphi) - \operatorname{sgn} v_0 \times \mu_0 (k_z/k_x) \omega \Delta u_z \sin(\omega t) \quad (6)$$

or

$$\dot{u}_{x,\mathrm{c}} = v_0 - \omega\big[(\Delta u_x \cos\varphi + \operatorname{sgn} v_0 \times \mu_0 (k_z/k_x)\Delta u_z)\sin(\omega t) + (\Delta u_x \sin\varphi)\cos(\omega t)\big]. \quad (7)$$

The lower point will slide continuously in one direction if its velocity does not change sign or turn to zero at any point. By looking at Eq. (7), we see that this is the case if the constant part of the velocity is larger than the amplitude of the oscillating part. The latter will also be equal to the sought critical velocity:

$$v_0 > v_c = \omega\Big[(\Delta u_x \cos\varphi + \operatorname{sgn} v_0 \times \mu_0 (k_z/k_x)\Delta u_z)^2 + (\Delta u_x \sin\varphi)^2\Big]^{1/2}$$
$$= \omega\Big[(\Delta u_x)^2 + 2\mu_0 (k_z/k_x)\Delta u_x \Delta u_z \operatorname{sgn} v_0 \times \cos\varphi + (\mu_0 (k_z/k_x)\Delta u_z)^2\Big]^{1/2}. \quad (8)$$

For $v_0 > 0$, the critical velocity is maximal

$$v_{c\max} = \omega(\Delta u_x + \mu_0 (k_z/k_x)\Delta u_z), \quad (9)$$

when the phase difference is zero, and reaches its minimal value

$$v_{c\min} = \omega\,|\Delta u_x - \mu_0 (k_z/k_x)\Delta u_z| \quad (10)$$

at $\varphi = \pi$. For $v_0 < 0$, the corresponding phases are swapped.

It is interesting to note that for positive v_0, if $\varphi = \pi$ and $\Delta u_x = \mu_0 (k_z/k_x)\Delta u_z$, the critical velocity is equal to zero, which means that the coefficient of friction remains unchanged at any velocity v_0. Since only the ratio of the stiffness appears here, this result should be independent of the indenter shape at least for small oscillation amplitudes.

2.2. Static Friction

Another distinctive feature of the influence of vibration on friction is the static force of friction at zero sliding velocity. This can also be calculated analytically in many cases. The static force of friction is the largest force that does not result in slip. For this to be true, the lower point of the spring must not move from its initial position: $u_{x,c} = 0$ and the tangential force on the spring must remain less than the force of friction at all times:

$$|f_x| < \mu_0\, |f_z| \quad (11)$$

or

$$|k_x (u_{x,0} + \Delta u_x \cos(\omega t + \varphi))| < \mu_0\, |k_z (u_{z,0} - \Delta u_z \cos(\omega t))|. \quad (12)$$

Here $u_{x,0}$ is the equilibrium tangential displacement of the spring, around which $u_x(t)$ oscillates. Remember that we assumed that the spring is always in contact with the substrate and the normal force thus always nonnegative. For this reason we can drop the modulus on the right hand side of Eq. (12). For the following analysis we will also drop the modulus on the left hand side. This makes our calculations less than perfectly rigorous and numerical simulations confirm that this results in incorrect static force for some values of φ. Nonetheless, this assumption seems to be valid in most cases, which is why we present the following, admittedly incomplete, analysis.

With the above assumption, we solve for $u_{x,0}$ and obtain:

$$u_{x,0} < \mu_0 \frac{k_z}{k_x} u_{z,0} - \mu_0 \frac{k_z}{k_x} \Delta u_z \cos(\omega t) - \Delta u_x \cos(\omega t + \varphi) = \mu_0 \frac{k_z}{k_x} u_{z,0} - \cos(\omega t)\left(\mu_0 \frac{k_z}{k_x}\Delta u_z + \Delta u_x \cos\varphi\right) + \Delta u_x \sin(\omega t)\sin\varphi. \quad (13)$$

Thus, the stick condition is satisfied if

$$u_{x,0} < \mu_0 \frac{k_z}{k_x} u_{z,0} - \left[\left(\mu_0 \frac{k_z}{k_x}\Delta u_z + \Delta u_x \cos\varphi\right)^2 + \Delta u_x^2 \sin^2\varphi\right]^{1/2} = \mu_0 \frac{k_z}{k_x} u_{z,0} - \left[\left(\mu_0 \frac{k_z}{k_x}\Delta u_z\right)^2 + 2\mu_0 \frac{k_z}{k_x}\Delta u_z \Delta u_x \cos\varphi + \Delta u_x^2\right]^{1/2}. \quad (14)$$

The maximum equilibrium displacement is maximized when $\varphi = \pi$:

$$u_{x,0} < \mu_0 \frac{k_z}{k_x} u_{z,0} - \left|\mu_0 \frac{k_z}{k_x}\Delta u_z - \Delta u_x\right| \quad (15)$$

and is minimized at $\varphi = 0$

$$u_{x,0} < \mu_0 \frac{k_z}{k_x} u_{z,0} - \left|\mu_0 \frac{k_z}{k_x}\Delta u_z + \Delta u_x\right|. \quad (16)$$

The static friction force is obtained by multiplying $u_{x,0}$ with the tangential stiffness:

$$F_s = k_x\left(\mu_0 \frac{k_z}{k_x} u_{z,0} - \left[\left(\mu_0 \frac{k_z}{k_x}\Delta u_z\right)^2 + 2\mu_0 \frac{k_z}{k_x}\Delta u_z \Delta u_x \cos\varphi + \Delta u_x^2\right]^{1/2}\right). \quad (17)$$

Dividing by the average normal force finally gives us the static coefficient of friction:

$$\frac{\mu_s}{\mu_0} = \frac{F_s}{k_z u_{z,0}} = 1 - \left[\left(\frac{\Delta u_z}{u_{z,0}}\right)^2 + \frac{2}{\mu_0}\frac{k_x}{k_z}\frac{\Delta u_z \Delta u_x}{u_{z,0}^2}\cos\varphi + \left(\frac{k_x \Delta u_x}{\mu_0 k_z u_{z,0}}\right)^2\right]^{1/2}. \quad (18)$$

Once again, for $v_0 > 0$, if $\varphi = \pi$ and $\Delta u_z / u_{z,0} = k_x \Delta u_x \times (\mu_0 k_z u_{z,0})^{-1}$ or $k_x \Delta u_x / (\mu_0 k_z \Delta u_z) = 1$, then $\mu_s = \mu_0$.

Note that the above is valid if the force is applied in the positive *x* direction. If the force acts in the opposite direction without changing the polarity of oscillation, then Eq. (14) becomes

$$|u_{x,0}| < \mu_0 \frac{k_z}{k_x} u_{z,0} - \left[\left(\mu_0 \frac{k_z}{k_x} \Delta u_z\right)^2 - 2\mu_0 \frac{k_z}{k_x} \Delta u_z \Delta u_x \cos\varphi + \Delta u_x^2\right]^{1/2}, \qquad (19)$$

with equivalent changes to Eqs. (17) and (18). The maximum displacement (15) is reached at $\varphi = 0$ and the minimum displacement at $\varphi = \pi$.

3. NUMERICAL SIMULATION

While the critical velocity and the static coefficient of friction can be calculated in closed form in our model, the overall dependence of the coefficient of friction on sliding velocity cannot. The detailed dependences were therefore obtained numerically (by explicit integration). The macroscopic coefficient of friction was determined as the average value of tangential force divided by the average normal force in one oscillation period:

$$\mu = \langle f_x \rangle / \langle f_z \rangle, \qquad (20)$$

where the normal and tangential force are calculated according to Eqs. (3) and (4) in every time step. It should be pointed out that by this definition μ has the same sign as the sliding velocity, since we do not take the modulus. Also, as will be shown in a moment, in some cases μ can have a sign opposite to that of the velocity, which allows the system to function as a vibrational motor or actuator.

During integration, the coordinate of the contact point is updated whenever the tangential force exceeds the current maximum frictional force. In such a case the contact point is moved such that the spring is shortened and the two forces match. It should also be noted that results are only presented for the steady state. It may take several cycles of oscillation for the tangential force or stress to reach its equilibrium value. Especially at low velocities this may take a relatively long time. Any such kinetic effects are not subject of this study.

3.1. Single-Mode Oscillation

We first present results for single-mode control with either purely normal or purely tangential oscillation.

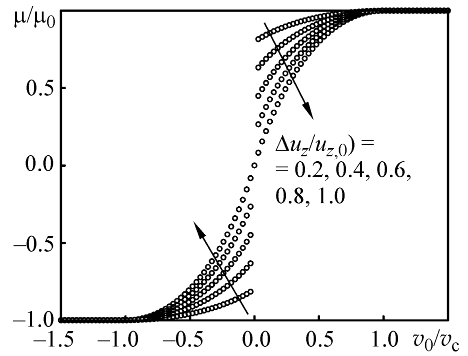

Fig. 2. Dependence of the macroscopic coefficient of friction on sliding velocity for the case of purely normal oscillation ($\Delta u_x = 0$), for details see [14].

Figures 2 and 3 show the dependences of the macroscopic coefficient of friction on sliding velocity for these two special cases. In Fig. 2, only normal oscillation is applied ($\Delta u_x = 0$). This case was already discussed in detail in paper [14], where the following numerical approximation (accurate to within 1%) for

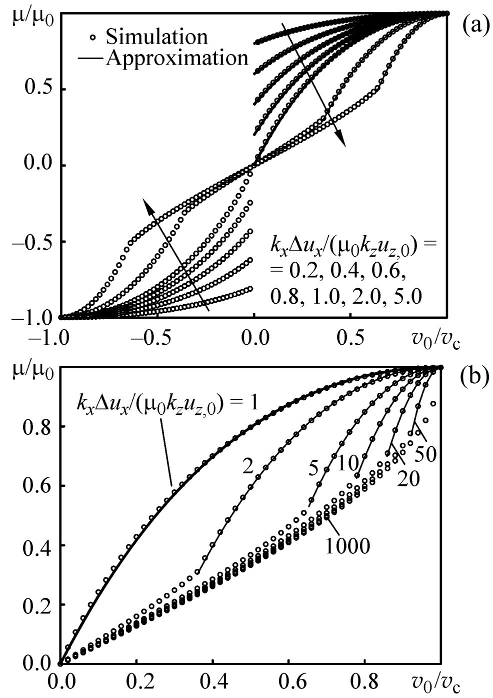

Fig. 3. Dependence of macroscopic coefficient of friction on sliding velocity for the case of purely tangential oscillation ($\Delta u_z = 0$): for small values of $k_x \Delta u_x / (\mu_0 k_z u_{z,0})$ (*a*); for large values of $k_x \Delta u_x / (\mu_0 k_z u_{z,0})$ (*b*). The solid lines correspond to the approximation (24) and the dots represent numerical results.

the velocity dependence of the coefficient of friction was obtained:

$$\frac{\mu}{\mu_0} \approx 1 - \frac{\Delta u_z}{u_{z,0}}\left[\frac{3}{4}\left(\frac{v_0}{v_c}-1\right)^2 + \frac{1}{4}\left(\frac{v_0}{v_c}-1\right)^4\right]. \quad (21)$$

Let us now turn to purely tangential oscillation. This case has been considered in the literature for very small system stiffness [5], but it has never been completely analyzed for a stiff system and a soft contact. Results for this case (with $\Delta u_z = 0$) are presented in Fig. 3. In this case, the critical value of sliding velocity, according to Eq. (8), reduces to

$$v_c = \omega \Delta u_x, \quad (22)$$

which is simply the velocity amplitude of tangential oscillation. Numerical simulations show that the coefficient of friction in this case is a function of only two dimensionless parameters v_0/v_c and $(\mu_0 k_x u_{z,0})^{-1} \times (k_x \Delta u_x)$:

$$\frac{\mu}{\mu_0} = f\left(\frac{v_0}{v_c}, \frac{k_x \Delta u_x}{\mu_0 k_z u_{z,0}}\right) \text{ for } \Delta u_z = 0. \quad (23)$$

Furthermore, for small values of the parameter $k_x \Delta u_x \times (\mu_0 k_x u_{z,0})^{-1} \le 1$, the curves are exactly the same as in the case of purely normal oscillation (Fig. 2), and can therefore be described with a very similar approximation:

$$\frac{\mu}{\mu_0} \approx 1 - \frac{k_x \Delta u_x}{\mu_0 k_z u_{z,0}}\left[\frac{3}{4}\left(\frac{v_0}{\omega \Delta u_x}-1\right)^2 + \frac{1}{4}\left(\frac{v_0}{\omega \Delta u_x}-1\right)^4\right] \text{ for } k_x \Delta u_x/(\mu_0 k_z u_{z,0}) \le 1. \quad (24)$$

The results of numerical simulation and the approximation (24) are compared in Fig. 3a. For values of $k_x \Delta u_x/(\mu_0 k_x u_{z,0}) > 1$, the dependence still coincides with Eq. (24) at large velocities, but at low velocities or very large values of $k_x \Delta u_x/(\mu_0 k_x u_{z,0})$, there are significant deviations. This is shown in more detail in Fig. 3b. For very large values of the dimensionless parameter it can be seen that the dependence becomes roughly linear.

3.2. General Case: Bimodal Oscillation

In the two cases considered above, the dependences are symmetric for positive and negative sliding velocity. In the following we will consider more general cases, which produce some interesting phenomena. First, both dimensional analysis and numerical results show that the coefficient of friction can be presented in the most general case as a function of four dimensionless parameters:

$$\frac{\mu}{\mu_0} = f\left(\frac{v_0}{v_c}, \frac{\Delta u_z}{u_{z,0}}, \frac{k_x \Delta u_x}{\mu_0 k_z u_{z,0}}, \varphi\right) \quad (25)$$

or

$$\frac{\mu}{\mu_0} = f\left(\frac{v_0}{v_c}, \frac{\Delta u_z}{u_{z,0}}, \frac{k_x \Delta u_x}{\mu_0 k_z \Delta u_z}, \varphi\right) \quad (26)$$

if this choice is more convenient. It is clear that Eq. (23) is just the limiting case of (25) for $\Delta u_z = 0$.

Qualitatively different behaviors for the case of zero phase shift are shown in Fig. 4, where the normalized coordinates μ/μ_0 and v_0/v_c are used. The dependence of the coefficient of friction on sliding velocity becomes asymmetric and sometimes qualitatively different for the positive and negative sliding directions. At small positive velocities (still with $\varphi = 0$), a negative coefficient of friction (opposite frictional force) is observed, especially if the amplitude of normal oscillation is large.

Note that the critical velocity v_c is different for positive and negative sliding velocities (see Eq. (8)).

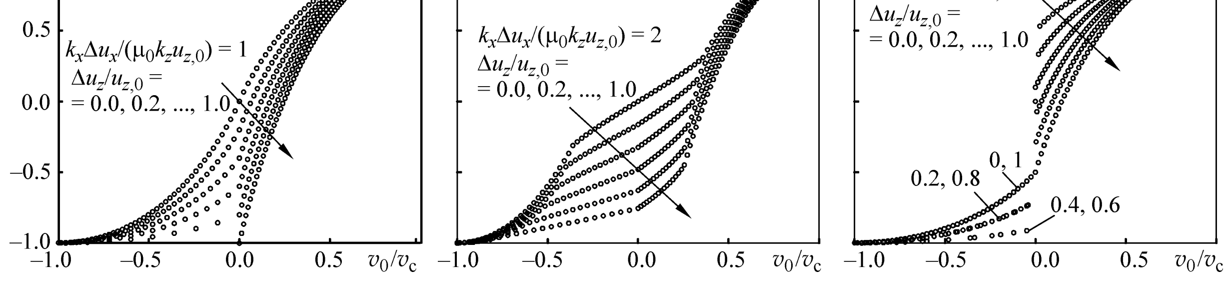

Fig. 4. A few examples of dependences of the coefficient of friction on velocity with phase difference $\varphi = 0$, $\Delta u_z/\Delta u_{z,0} = 0, ..., 1$ and $k_x \Delta u_x/(\mu_0 k_z u_{z,0}) = 1$ (a), 2 (b), 0.5 (c)

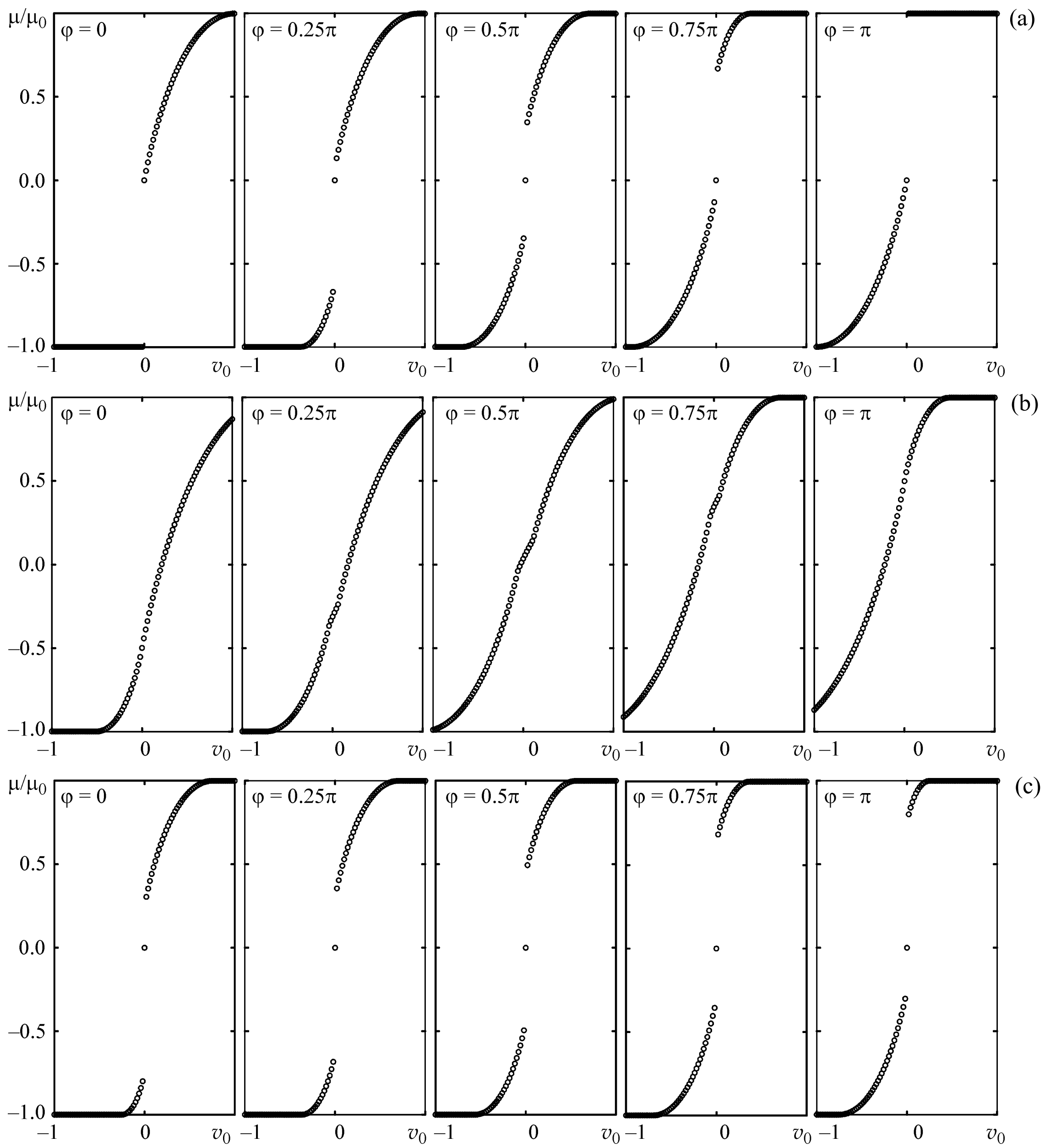

Fig. 5. Velocity dependences of the coefficient of friction for different phase shifts φ for the case $k_x\Delta u_x/(\mu_0 k_z u_{z,0})$ = 1 (a), 2 (b), 0.5 (c); $\Delta u_z/u_{z,0} = 0.5$.

The two sides of Fig. 4 are normalized to these two different critical velocities, resulting in a visible "kink" at $v_0/v_c = 0$ in many of the curves.

In Fig. 5, on the other hand, we use dimensional (non-normalized) velocity to get a clearer physical picture. These figures show the dependence of the coefficient of friction on the sliding velocity for different values of $k_x\Delta u_x/(\mu_0 k_z \Delta u_z)$ and different phase shifts while $\Delta u_z/u_{z,0}$ is fixed.

In Fig. 5a corresponding to $k_x\Delta u_x/(\mu_0 k_z \Delta u_z) = 1$, for $\varphi = \pi/2$ the dependence is symmetrical with respect of change of the sign of the velocity. For other phase shifts the dependencies are asymmetrical and become extremely asymmetrical at φ = 0 and φ = π. The first and the last subplots correspond to the particular cases $v_c = 0$ for $k_x\Delta u_x/(\mu_0 k_z \Delta u_z) = 1$, and φ = π at positive velocity and φ = 0 at negative velocity (see Eqs. (10) and (18)).

The dependences of the coefficient of friction on the sliding velocity presented in Figs. 2 to 5 can be classified in three qualitatively different categories:

I. Active control of friction. If the dependence is symmetrical with respect to reversing the sign of velocity, we have a classical "law of friction". The external oscillation influences the static force of friction and the velocity-dependence but does not change the basic character of the force as a dissipative force which is always directed opposite to the velocity. This case is found (always) with single-mode oscillations (Figs. 2 and 3) as well as with dual-mode oscillations when $\varphi = 0.5\pi$ (Fig. 5).

II. Dynamic ratchet. Into the second class fall dependences that are asymmetrical with respect to change of the sign of velocity but remain "dissipative" (thus, the force of friction is still directed opposite to the velocity). The most extreme case in this category is represented by the first and the last subplots in Fig. 5a. In these extreme cases, the static coefficient of friction for backward movement is μ_0 and zero for forward movement at $\varphi = 0$ and vice versa at $\varphi = \pi$. This means that if the substrate is subjected to a low-frequency tangential force, it will move forth in the positive half-period and will stick in the negative half-period, thus resembling the action of a mechanical ratchet. We therefore call this class a "dynamic ratchet".

III. Drive or actuator. Finally, we have the cases where the "law of friction" is not only asymmetric but "active", in that the direction of the average tangential force is the same as the direction of movement at small velocities. This is functionally equivalent to a vibrational drive or actuator. This case is represented by all curves in Figs. 4a and 4b with the exception of the upper-most curve, which corresponds to a purely horizontal oscillation. The same situation can be found in Fig. 5b for $\varphi \neq \pi/2$.

4. CONCLUSION

We considered bimodal control of friction by a superposition of normal and tangential (in the direction of motion) oscillations. In the presence of oscillations in both directions, the dependence of the macroscopic coefficient of friction (which is here formally defined as the normalized tangential force and can assume both positive and negative values) on the macroscopic sliding velocity becomes asymmetric in the general case. While the asymmetry as such is understandable from general considerations (see e.g. [17]), the detailed form of the laws of friction and their classification seems to be nontrivial and has not been described earlier. In particular, apart from known effects of active control of friction on one hand and oscillation induced actuation on the other hand, we predict a third, intermediate type of behavior which we call "dynamic ratchet". Dynamic ratchets are realized for values of the governing parameter $k_x \Delta u_x / (\mu_0 k_z u_z)$ smaller than 1 while drives result with $k_x \Delta u_x / (\mu_0 k_z u_z) > 1$.

Finally, let us note that the one-spring model is not an essential assumption for the described qualitative behavior. As any contact can be mapped to a contact with a one-dimensional elastic foundation [18, 19], this analysis can be easily generalized.

ACKNOWLEDGMENTS

The authors thank V.L. Popov for valuable discussions. This work was partially supported by the German Academic Exchange Service (DAAD).

REFERENCES

1. Siegert, K. and Ulmer, J., Influencing the Friction in Metal Forming Processes by Superimposing Ultrasonic Waves, *CIRP Ann. Manufact. Technol.*, 2001, vol. 50, no. 1, pp. 195–200.
2. Onikura, H., Ohnishi, O., Feng, J., et al., Effects of Ultrasonic Vibration on Machining Accuracy in Microdrilling, *J. Japan Soc. Proc. Eng.*, 1996, vol. 62, no. 5, pp. 676–680.
3. Fridman, H.D. and Levesque, P., Reduction of Static Friction by Sonic Vibrations, *J. Appl. Phys.*, 1959, vol. 30, pp. 1572–1575.
4. Chowdhury, M. and Helali, M., The Effect of Amplitude of Vibration on the Coefficient of Friction for Different Materials, *Tribology Int.*, 2008, vol. 41, no. 4, pp. 307–314.
5. Teidelt, E., Starcevic, J., and Popov, V.L., Influence of Ultrasonic Oscillation on Static and Sliding Friction, *Tribol. Lett.*, 2012, vol. 48, no. 1, pp. 51–62.
6. Tolstoi, D.M., Significance of the Normal Degree of Freedom and Natural Normal Vibrations in Contact Friction, *Wear*, 1967, vol. 10, no. 3, pp. 199–213.
7. Storck, H., Littmann, W., Wallaschek, J., and Mracek, M., The Effect of Friction Reduction in Presence of Ultrasonic Vibrations and Its Relevance to Travelling Wave Ultrasonic Motors, *Ultrasonics*, 2002, vol. 40, no. 1–8, pp. 379–383.
8. Starcevic, J., Tribospektroskopie als neue Methode zur Untersuchung von Reibungsmechanismen: Theoretische Grundlagen und Experiment: PhD Thesis, *Technische Universitat Berlin*, 2008.

9. Teidelt, E., *Oscillating Contacts: Friction Induced Motion and Control of Friction*: PhD Thesis, Technische Universitat Berlin, 2015.
10. Milahin, N., *Robuste Einflussparameter fur Reibung und Oberflachenmodifizierung unter Einfluss von Ultraschall*: PhD Thesis, Technische Universitat Berlin, 2016.
11. Popov, V.L., *Contact Mechanics and Friction: Physical Principles and Applications*, Berlin: Springer, 2017.
12. Teidelt, E., Willert, E., Filippov, A.E., and Popov, V.L., Modeling of the Dynamic Contact in Stick-Slip Microdrives Using the Method of Reduction of Dimensionality, *Phys. Mesomech.*, 2012, vol. 15, no. 5–6, pp. 287–292.
13. Milahin, N., Li, Q., and Starcevic, J., Influence of the Normal Force on the Sliding Friction under Ultrasonic Oscillations, *Facta Univer. Mech. Eng.*, 2015, vol. 13, no. 1, pp. 27–32.
14. Popov, M., Popov, V.L., and Popov, N.V., Reduction of Friction by Normal Oscillations. I. Influence of Contact Stiffness, *Friction*, 2017, vol. 5, no. 1, pp. 45–55.
15. Mao, X., Popov, V.L., Starcevic, J., and Popov, M., Reduction of Friction by Normal Oscillations: II. In-Plane System Dynamics, *Friction*, 2017, vol. 5, no. 2, pp. 194–206.
16. Popov, M., Critical Velocity of Controllability of Sliding Friction by Normal Oscillations in Viscoelastic Contacts, *Facta Univer. Mech. Eng.*, 2016, vol. 14, no. 3, pp. 335–341.
17. Popov, V.L. and Wetter, R., Symmetry Breaking as a General Design Principle of Oscillation-Based Methods for Fixation and Manipulation of Nano-Objects, *Adv. Biomater. Devices Med.*, 2016, vol. 3, no. 1, pp. 10–18.
18. Popov, V.L. and Heβ, M., *Method of Dimensionality Reduction in Contact Mechanics and Friction*, Berlin–Heidelberg: Springer, 2015.
19. Popov, V.L. and Heβ, M., Method of Dimensionality Reduction in Contact Mechanics and Friction: A User's Handbook. I. Axially-Symmetric Contacts, *Facta Univer. Mech. Eng.*, 2014, vol. 12, no. 1, pp. 1–14.

3.5 Publication 8

While the control of friction by oscillations normal to the plane or in the direction of motion are well known, the possibility of doing the same with *transverse* in-plane oscillations has received relatively little attention. This is the focus of the present publication.

The model used here follows the same general pattern as in the other publications: the contact is modeled as a massless linear-elastic spring, which can be deflected in both of the in-plane directions (x and y). The spring is under constant normal load and slides in the x-direction with constant velocity. The oscillation is harmonic and applied transversely (in the y-direction).

Despite the model being quite similar, the actual mechanism of friction reduction turns out to be different from the normal and tangential oscillation cases. Stick-slip can also occur in this system, but it no longer takes center stage. Instead, the reduction of friction is achieved by "redistributing" some of the magnitude of the friction vector away from the bulk sliding direction: The transverse oscillation causes the contact point to slide on a sinusoidal path, with the friction vector constantly realigning itself with this path as well. Due to this, some part of the friction force is always pointing orthogonally to the direction of bulk motion. And since the *magnitude* of the friction vector remains constant, this means that less of this magnitude is projected onto the direction of macroscopic sliding, creating the impression of a lowered coefficient of friction.

This difference in mechanism brings with it qualitatively different behavior of the coefficient of friction as well. For example, the static COF (Eq. 16) never formally reaches zero even at large amplitudes, although it can be made arbitrarily small. Also, the transition from pure slip to stick-slip does not produce a qualitative change in the velocity dependence (Figs. 7, 8). This also implies that there is also no real "critical velocity" (although something resembling it can still be defined), and that reduction of friction is possible to some degree at all sliding velocities.

The paper presents a fairly detailed numerical and semi-analytical study of the described model, with some of the main results being summarized visually in Fig. 11.

Friction
https://doi.org/10.1007/s40544-018-0202-1
ISSN 2223-7690
CN 10-1237/TH
RESEARCH ARTICLE

Active control of friction by transverse oscillations

J. BENAD[1], **K. NAKANO**[2,*], **V. L. POPOV**[1,3,*], **M. POPOV**[1,3,4]

[1] *Technische Universität Berlin, Berlin 10623, Germany*

[2] *Yokohama National University, Yokohama 240-8501, Japan*

[3] *National Research Tomsk Polytechnic University, Tomsk 634050, Russia*

[4] *National Research Tomsk State University, Tomsk 634050, Russia*

Received: 06 September 2017 / Accepted: 24 November 2017

Abstract: The present paper is devoted to a theoretical analysis of sliding friction under the influence of in-plane oscillations perpendicular to the sliding direction. Contrary to previous studies of this mode of active control of friction, we consider the influence of the stiffness of the tribological contact in detail and show that the contact stiffness plays a central role for small oscillation amplitudes. In the present paper we consider the case of a displacement-controlled system, where the contact stiffness is small compared to the stiffness of the measuring system. It is shown that in this case the macroscopic coefficient of friction is a function of two dimensionless parameters—a dimensionless sliding velocity and dimensionless oscillation amplitude. In the limit of very large oscillation amplitudes, known solutions previously reported in the literature are reproduced. The region of small amplitudes is described for the first time in this paper.

Keywords: sliding friction; in-plane oscillation; contact stiffness; coefficient of friction; active control of friction

1 Introduction

The interrelation of oscillations and friction is an old problem with fundamental importance for the understanding of friction and for countless practical applications. From the physical point of view, friction is fundamentally a non-stationary process. Brillouin [1] pointed out as early as 1899 that dry friction can occur at low velocities only due to elastic instabilities on the microscale. Vibrations can strongly influence friction [2] and friction often leads to vibrational instabilities [3]. Thus, friction should always be understood as the interplay of dynamics and friction on different spatial and temporal scales. This interplay has many particular aspects which have been studied intensively in the past decades: (I) Influence of vibrations on friction was studied, e.g., in Refs. [4–6]. (II) Frictionally induced oscillations have been studied, e.g., in Refs. [3, 7–9]. (III) The interaction of self-excited vibrations and friction was subject of studies [10–12]. (IV) The interplay of vibrations and oscillations is a central principle of oscillation-based actuation [13–17]. (V) Finally, oscillations may lead to energy dissipation, which of course is intimately connected with all other above mentioned points in Refs. [18–20].

The present paper is devoted exclusively to the aspect (I) of the above list—the direct influence of oscillations on friction. Studies of this influence started in the late 50s and 60s of the 20th century [21–25]. Most models used for the analysis of the active control of friction were based on the study of dynamics of rigid bodies. Only recently it was recognized that the deformability of the bodies and especially the contact stiffness plays a central role in determining the frictional behavior at small oscillation amplitudes and small sliding velocities [26, 27, 6]. However, of the three possible oscillation directions: (a) out-of-plane, (b) in-plane perpendicular to sliding, (c) in-plane

* Corresponding authors: K. NAKANO, nakano@ynu.ac.jp; V. L. POPOV, v.popov@tu-berlin.de

in sliding direction—only the influence of out-of-plane oscillations has been studied in detail so far [28, 29]. Complete studies of friction under in-plane oscillations – both in the sliding direction and perpendicular to the sliding direction—are yet to be performed.

The present paper partially closes this gap and provides an analysis of friction under transverse oscillations—in-plane oscillations perpendicular to the sliding direction. The particular interest in this mode of active control of friction is partly due to the recently demonstrated importance of transverse oscillations both for the stability of macroscopic sliding and the design of robust tribological measurement techniques [30–33].

To achieve qualitative understanding of the corresponding phenomena, we follow the strategy already used in a recent analysis of out-of-plane oscillations [28, 37]: we start with a very simple model, where the contact is modeled as a single spring with constant normal and tangential stiffness in a displacement-controlled setting (i.e., with a very stiff surrounding system). System-dynamical "feedback" from the contact to the surrounding system is thereby neglected.

2 Simplified one-spring model

Let us consider an elastic body that is brought into contact with a flat elastic substrate and then subjected to a superposition of horizontal movement with a constant velocity and sideways oscillations. In the contact of elastic bodies, both normal and tangential contact problems can be reduced to a contact of an elastic body and a rigid substrate with renormalized elastic coefficients [34]. In this paper we further reduce the elastic body to a single spring with some normal stiffness (the magnitude of which does not play any role in the present study) and tangential stiffness k. We assume that between the spring and the plane, there is a friction force described by the simplest form of Coulomb's law of friction [35, 36] with a constant coefficient of friction μ_0. A schematic drawing of the model is shown in Fig. 1: the "body" (the upper point P of the spring) is forced to move with a constant velocity v_0 in the x-direction, and also to perform a harmonic oscillation in the y-direction according to $y_P = y_0 \sin\omega t$.

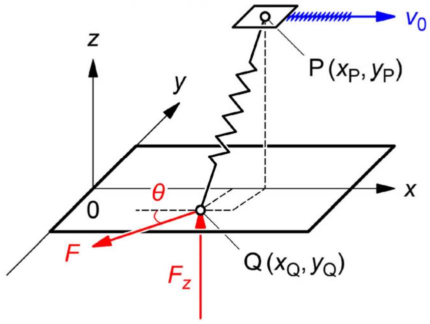

Fig. 1 Schematic representation of the considered system: An elastic body modeled as a spring is forced into a controlled movement at the upper point P, while the immediate contact point Q follows according to the equilibrium conditions. It is assumed that between the contact point and the horizontal plane there is a force of friction described by the classical Coulomb law.

While the time-resolved reaction of the instantaneous friction force on the loading history is also of interest, in this paper we consider exclusively the forces in the steady state, averaged over one period of oscillation. In this connection it is important to lay down the terminology used in the paper: all processes referring to the time scale much smaller than the period of one oscillation are considered here as "microscopic" while the processes and quantities running or defined on the time scale much larger than the period of one oscillation are called "macroscopic". Our goal is to determine the macroscopic values of normal and tangential forces (meaning their average values over one oscillation period) and the corresponding macroscopic coefficient of friction. The above-mentioned time-resolved reaction, on the contrary, refers to the microscopic scale; it will be considered in a separate paper.

Figure 2 shows the system projected onto the contact plane (x, y) for the cases when the immediate contact point sticks (Fig. 2(a)) and for the sliding state (Fig. 2(b)). In the sticking state, the velocity of the "foot point" Q is zero.

As the vector of the spring force is determined uniquely by two quantities: the elongation l and the inclination angle θ to the direction of the macroscopic movement, it is convenient to write equations in terms of these two quantities.

The coordinates of the upper end of the spring can be written as

$$x_P = v_0 t, \quad y_P = y_0 \sin\omega t \tag{1}$$

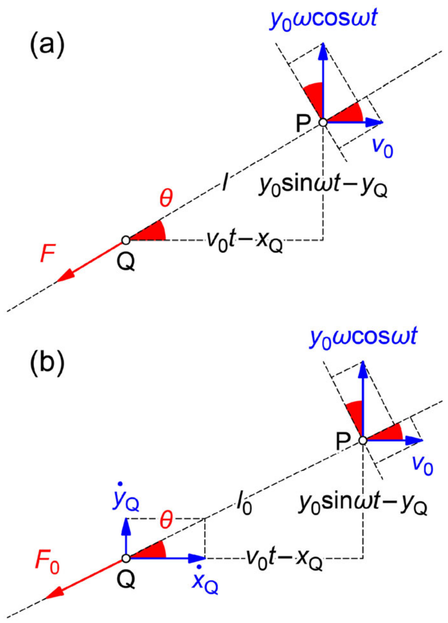

Fig. 2 Projection of the considered system onto the (x-y)-plane. (a) stick phase; (b) sliding phase.

and the corresponding velocities

$$\dot{x}_P = v_0, \quad \dot{y}_P = y_0\omega\cos\omega t \tag{2}$$

Sticking phase: if the immediate contact point is sticking then the equations for the angle θ and the length l are

$$\dot{\theta} = \frac{y_0\omega\cos\omega t\cos\theta - v_0\sin\theta}{l} \tag{3}$$

$$\dot{l} = y_0\omega\cos\omega t\sin\theta + v_0\cos\theta \tag{4}$$

where $y_0\omega\cos\omega t\cos\theta - v_0\sin\theta$ is the component of the velocity of the point P in the direction perpendicular to the elongation l and $y_0\omega\cos\omega t\sin\theta + v_0\cos\theta$ is the velocity component of the same point in the direction of the elongation (see Fig. 2(a) for illustration).

These equations remain valid as long as the elongation l remains smaller than the critical value

$$l < l_0 = \frac{\mu_0 F_z}{k} \tag{5}$$

Slipping phase: after the elongation l reaches the critical value l_0, it does not increase further, but remains equal to l_0. Note that due to the equilibrium conditions in the immediate contact point Q, its movement occurs always in the direction of the elongation. Thus it has no velocity component perpendicular to the direction of l. The angular velocity of the direction of the elongation l is given by the ratio of the difference of the transversal velocity components of points P and Q to the (constant) length l_0. However, as the transversal component of velocity of point Q is zero, Eq. (3) remains valid, except that l has to be replaced by l_0:

$$\dot{\theta} = \frac{y_0\omega\cos\omega t\cos\theta - v_0\sin\theta}{l_0} \tag{6}$$

This equation remains valid as long as the projection of the velocity of point P on the direction of l remains positive:

$$y_0\omega\cos\omega t\sin\theta + v_0\cos\theta > 0 \tag{7}$$

This condition guarantees that the point Q is following P in the direction of the elongation. Otherwise it stops until the condition Eq. (5) is fulfilled again.

Introducing dimensionless variables and operators

$$\tau = \omega t, \quad (\,)' = \frac{\mathrm{d}}{\mathrm{d}\tau}, \quad \tilde{y}_0 = \frac{y_0}{l_0}, \quad \tilde{l} = \frac{l}{l_0}, \quad \tilde{v}_0 = \frac{v_0}{l_0\omega} \tag{8}$$

one can rewrite Eqs. (3) and (4) as

$$\theta' = \frac{1}{\tilde{l}}\left(-\tilde{v}_0\sin\theta + \tilde{y}_0\cos\theta\cos\tau\right), \quad \text{for stick phase} \tag{9}$$

$$\tilde{l}' = \tilde{y}_0\sin\theta\cos\tau + \tilde{v}_0\cos\theta, \quad \text{for stick phase} \tag{10}$$

and Eqs. (6) and (7) as

$$\theta' = -\tilde{v}_0\sin\theta + \tilde{y}_0\cos\theta\cos\tau, \quad \text{for slip phase} \tag{11}$$

$$\tilde{y}_0\sin\theta\cos\tau + \tilde{v}_0\cos\theta > 0. \quad \text{for slip phase} \tag{12}$$

The goal of our study is to determine the average force component in the sliding direction

$$\langle F_x\rangle = \langle k\cdot l\cdot\cos\theta\rangle = \mu_0 F_z\langle\tilde{l}\cdot\cos\theta\rangle \tag{13}$$

(where $\langle\ldots\rangle$ denotes averaging over one period of oscillation in the steady state) and the corresponding macroscopic coefficient of friction defined as

$$\mu_{\text{macro}} = \frac{\langle F_x\rangle}{F_z} = \mu_0\langle\tilde{l}\cdot\cos\theta\rangle \tag{14}$$

or the normalized coefficient of friction

$$\tilde{\mu}_{\text{macro}} = \frac{\mu_{\text{macro}}}{\mu_0} = \left\langle \tilde{l} \cdot \cos\theta \right\rangle \tag{15}$$

Note that all the Eqs. (9)–(12) as well as definition, Eq. (15), depend only on two dimensionless parameters $\tilde{y}_0$ and $\tilde{v}_0$. We therefore present all the results of this paper as function of these parameters.

3 Static coefficient of friction

If the system starts from the neutral state with zero tangential force and moves slowly in the x-direction, while at the same time oscillating in the y-direction with amplitude y_0 (see Fig. 3), then the macroscopically seen (average) spring force will be increasing until the critical state shown in Fig. 3 is reached. In this state, the component of the spring force in the x-direction is equal to $F_x = \mu_0 F_z \sqrt{1 - y_0^{\,2}/l_0^{\,2}}$ and remains unchanged during the entire oscillation cycle.

Thus, the average coefficient of friction in this state, which we can interpret as the static coefficient of friction is given by

$$\tilde{\mu}_{\text{macro,static}} = \sqrt{1 - y_0^2 / l_0^2} = \sqrt{1 - \tilde{y}_0^2} \tag{16}$$

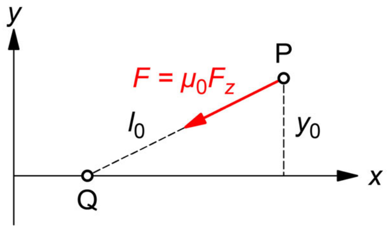

Fig. 3 Critical state of a system with oscillation amplitude y_0 and very slow motion in the x-direction.

4 Continuous sliding and stick-slip motion

It is intuitively clear that at sufficiently high sliding velocities v_0, the contact point will be in the sliding state all the time, while at smaller sliding velocities the motion will consist of a sequence of stick and slip phases. On the parameter plane ($\tilde{v}_0$, $\tilde{y}_0$), the region of continuous sliding is separated from the stick-slip region by a boundary that can be found numerically by solving Eq. (11), which is valid in the region of continuous sliding, and checking the fulfillment of the condition (12). Figure 4 shows the areas of the continuous and intermittent sliding and the boundary line between them.

4.1 Small oscillation amplitudes $\tilde{y}_0 << 1$

As can be seen from Eq. (11), in this case the angle also remains small, so that we can set in Eq. (11) $\sin\theta \approx \theta$ and $\cos\theta \approx 1$:

$$\theta' + \tilde{v}_0 \theta = \tilde{y}_0 \cos\tau \tag{17}$$

The steady-state solution of this equation is given by

$$\theta = \frac{\tilde{y}_0}{\sqrt{1 + \tilde{v}_0^{\,2}}} \cos(\tau + \varphi) \tag{18}$$

with

$$\tan\varphi = -1/\tilde{v}_0 \tag{19}$$

This equation is valid for small angles, i.e.

$$\frac{\tilde{y}_0}{\sqrt{1 + \tilde{v}_0^{\,2}}} << 1 \tag{20}$$

The borderline between small and large angles is shown in Fig. 4 by a dashed line. Substituting Eq. (18) into the condition for continuous sliding, Eq. (12), we can rewrite this condition as

$$\frac{\tilde{y}_0^{\,2}}{\sqrt{1 + \tilde{v}_0^{\,2}}} \cos(\tau + \varphi) \cos\tau + \tilde{v}_0 > 0 \tag{21}$$

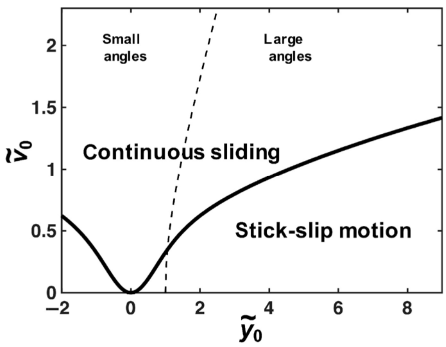

Fig. 4 Area of continuous sliding and area of stick-slip motion (separated by the bold line) over the two system parameters. Also shown are the regions of small and large angles according to Eq. (20) (dashed line).

or

$$\frac{\tilde{y}_0^{\ 2}}{2\sqrt{1+\tilde{v}_0^{\ 2}}}\cos\left(2\tau+\varphi\right)+\tilde{v}_0+\frac{\tilde{y}_0^{\ 2}\tilde{v}_0}{2\left(1+\tilde{v}_0^{\ 2}\right)}>0 \tag{22}$$

It is fulfilled for any τ if

$$\tilde{y}_0^{\ 2}<2\tilde{v}_0\left(1+\tilde{v}_0^{\ 2}\right)\left[\sqrt{1+\tilde{v}_0^{\ 2}}+\tilde{v}_0\right] \tag{23}$$

Expanding the right-hand-side of Eq. (23) up to the terms of second order in $\tilde{v}_0$, we obtain the condition $\tilde{y}_0^{\ 2}=2\tilde{v}_0\left(1+\tilde{v}_0\right)$ for the border line. Solving it with respect to $\tilde{v}_0$ gives

$$\tilde{v}_{0,\text{crit}}=\sqrt{\frac{1}{4}+\frac{1}{2}\tilde{y}_0^2}-\frac{1}{2} \tag{24}$$

This limiting case is displayed in Fig. 5.

4.2 Large oscillation amplitudes $\tilde{y}_0>>1$

In this case the motion occurs almost perpendicular to the direction of the average velocity and during most of the oscillation period the contact is sliding. Only in the vicinity of the "turning points" there arises the possibility of stick, because both components of the driving velocity become small. The first turning point corresponds to $\tau=\pi/2$. Introducing a new variable $\xi=\tilde{v}_0(\tau-\pi/2)$, we can rewrite Eq. (11) as

$$\frac{\mathrm{d}\theta}{\mathrm{d}\xi}=-\sin\theta-\frac{\tilde{y}_0}{\tilde{v}_0^{\ 2}}\xi\cos\theta \tag{25}$$

The behavior described by this equation depends on the single parameter $\tilde{y}_0/\tilde{v}_0^2$. Its numerically

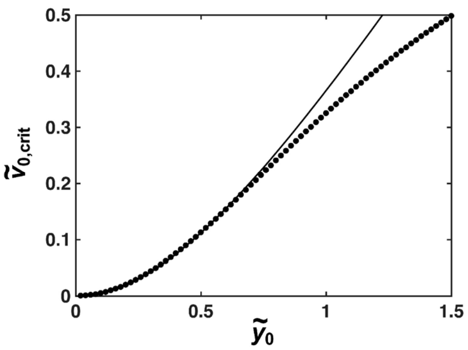

Fig. 5 Approximation of the numerical results for the border line (dots) with Eq. (24) (solid line) for small oscillation amplitudes.

determined critical value is $\tilde{y}_0/\tilde{v}_0^2\approx 4.5$. Thus for the critical velocity we get

$$\tilde{v}_{0,\text{crit}}\approx\frac{1}{\sqrt{4.5}}\tilde{y}_0^{1/2}\approx 0.47\cdot\tilde{y}_0^{1/2} \tag{26}$$

While this equation describes the asymptotic behavior very well, a slightly more complex equation can be constructed to approximate the complete dependence, both for small and large oscillation amplitudes:

$$\tilde{v}_{0,\text{crit}}=\frac{0.47\tilde{y}_0^{\ 5/2}}{\tilde{y}_0^{\ 2}+\dfrac{0.94\tilde{y}_0^{\ 1/2}}{1+\tilde{y}_0^{\ 2}}} \tag{27}$$

This approximation is shown in Fig. 6 together with Eq. (26) and the numerical results.

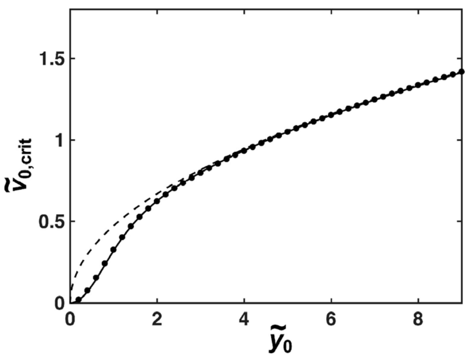

Fig. 6 Approximation of the numerical results for the border line (dots) with relation Eq. (26) (dashed line) and relation Eq. (27) (solid line).

5 The macroscopic coefficient of friction over the entire parameter space

For each point $(\tilde{v}_0,\tilde{y}_0)$ in the parameter plane, there is a macroscopic coefficient of friction $\tilde{\mu}_{\text{macro}}$. It is displayed over the entire parameter space in Fig. 7.

In the Fig. 8 the same dependence is shown by cuts of the plot in Fig. 7 along the $\tilde{v}_0$-axis.

While the exact quantitative description of the coefficient of friction on the entire parameter plane is complicated, the general structure of the dependence is relatively simple and is determined by a small number of "cornerstone" features. The general classification of various behaviors is very similar to that

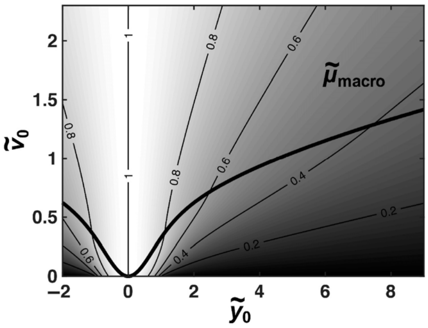

Fig. 7 The macroscopic coefficient of friction displayed over the two system parameters. The region of continuous sliding is above the bold line.

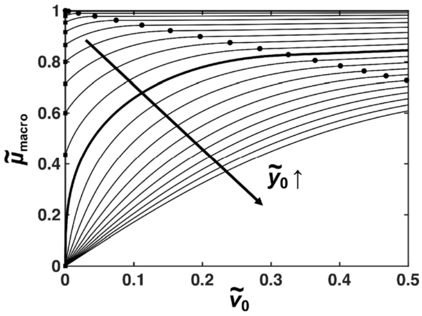

Fig. 8 The lines show the macroscopic coefficient of friction over the dimensionless velocity. They represent vertical cuts through the surface shown in Fig. 7. The graphs are shown for $\tilde{y}_0 = 0,\ 0.1,\ 0.2,\ 0.3,\ 0.4,\ ...,\ 2$. The amplitude $\tilde{y}_0 = 1$ is highlighted with the bold solid line. The round dots represent the border line, here indicating the critical macroscopic coefficient of friction over the critical velocity. The squares mark the static coefficient of friction as given by Eq. (16).

given in Ref. [37] for the case of normal oscillations:

– Without oscillations, the macroscopic coefficient of friction is constant and equal to its microscopic value μ_0, thus $\tilde{\mu}_{\text{macro}} = 1$.

– With increasing oscillation amplitude, the static coefficient of friction decreases according to Eq. (16) and vanishes at $\tilde{y}_0 = 1$ (bold line in Fig. 8).

– Further increase of the oscillation amplitude leads to further decrease of the macroscopic coefficient of friction at finite sliding velocities while the static coefficient of friction remains zero.

– The qualitative behavior of the coefficient of friction as a function of velocity is different for the cases of small ($\tilde{y}_0 << 1$) and large ($\tilde{y}_0 >> 1$) oscillation amplitudes:

(1) In the region of small oscillation amplitudes, the coefficient of friction is roughly speaking increasing monotonically from its static value to the value corresponding to the point of continuous sliding. After this point, the coefficient of friction increases very slowly and can be approximately assumed to be constant. The critical velocity of continuous sliding thus retains at least approximately the meaning of the "critical velocity of controllability" of friction introduced in Ref. [37]. A more detailed analysis of this range of oscillation amplitudes, which is of most interest to applications, is provided in the next section.

(2) In the region of large oscillation amplitudes, the differentiation between the cases of continuous sliding and intermittent sliding loses its importance, so that one can define a law of friction that is valid with good accuracy in the whole range of sliding velocities. A detailed analysis is given in the next Section. Note that this case was the only one considered in the earlier studies of the influence of sideways oscillations on friction Refs. [4, 5, 2].

6 Coefficient of friction at low and high oscillation amplitudes

6.1 Coefficient of friction at low oscillation amplitudes

The simple structure of the frictional law in the region of small oscillation amplitudes, $\tilde{y}_0 << 1$, is illustrated in Fig. 9, where the dependencies of the coefficient of friction on the velocity are shown in normalized variables: the deviation of the macroscopic coefficient

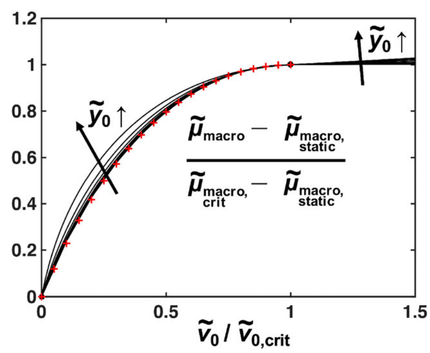

Fig. 9 Displayed are transformed lines from Fig. 8 so that the square markers of the static friction coefficient and the round markers of the critical friction coefficient lie on top of each other. Displayed in this figure are only lines that lie above the bold line in Fig. 8: $\tilde{y}_0 = 0.1,\ 0.2,\ 0.3,\ ...,\ 0.9$, the bold line itself is not displayed here. The approximation Eq. (28) of this "master curve" is shown with red crosses.

of friction from its static value normalized by the difference between the value of the border line between stick-slip and continuous sliding vs. velocity normalized by the critical velocity of continuous sliding.

One can see that at small oscillation amplitudes these dependences collapse with acceptable accuracy to a single "master curve", which can be approximated with

$$\frac{\tilde{\mu}_{\text{macro}}-\tilde{\mu}_{\text{macro,static}}}{\tilde{\mu}_{\text{macro,crit}}-\tilde{\mu}_{\text{macro,static}}}=1-\left[\frac{3}{4}\left(\frac{\tilde{v}_0}{\tilde{v}_{0,\text{crit}}}-1\right)^2+\frac{1}{4}\left(\frac{\tilde{v}_0}{\tilde{v}_{0,\text{crit}}}-1\right)^4\right] \tag{28}$$

which coincides with the velocity dependence in the case of out-of-plane oscillations considered in Ref. [28] (shown with red crosses in Fig. 9). After passing the critical value of velocity the coefficient of friction changes only very slowly.

Thus, for small oscillation amplitudes the "law of friction" is completely determined by the value of the static coefficient of friction, Eq. (16), the value of the coefficient of friction in the critical state and the more or less universal transition between both points, Eq. (28).

From the above-mentioned three determining parameters of the law of friction at low oscillation amplitudes, static coefficient of friction, critical velocity of continuous sliding and coefficient of friction at the critical velocity, two are already known and given by Eq. (16) and Eq. (27), respectively. We now consider the macroscopic coefficient of friction $\tilde{\mu}_{\text{macro,crit}}$ directly on the border line. For very low values of $\tilde{y}_0$, the coefficient of friction in the area of continuous sliding (including the border line) can be calculated by substituting Eq. (18) into Eq. (15):

$$\tilde{\mu}_{\text{macro}}=\left\langle\cos\left(\kappa\cos\left(\tau+\varphi\right)\right)\right\rangle \tag{29}$$

with

$$\kappa=\frac{\tilde{y}_0}{\sqrt{1+\tilde{v}_0^{\,2}}} \tag{30}$$

Expanding Eq. (29) up to the second power of κ gives

$$\tilde{\mu}_{\text{macro}}=1-\frac{\kappa^2}{2}\left\langle\cos^2\left(\tau+\varphi\right)\right\rangle=1-\frac{1}{4}\frac{\tilde{y}_0^{\,2}}{\left(1+\tilde{v}_0^{\,2}\right)} \tag{31}$$

For large velocities, the coefficient of friction tends to the limiting value $\tilde{\mu}_{\text{macro}}=1$, as it should. At the borderline defined by $\tilde{v}_0\approx\tilde{y}_0^{\,2}/2$ in the first approximation we get

$$\tilde{\mu}_{\text{macro,crit}}=1-\frac{\tilde{y}_0^{\,2}}{4} \tag{32}$$

6.2 Coefficient of friction at high oscillation amplitudes

In the case $\tilde{y}_0>>1$, for most of the oscillation cycle the contact point Q is in the sliding state with the possible exception of "turning points" which, however, do not substantially influence the average coefficient of friction. In this case, in Eq. (11), the derivative on the left-hand-side can be neglected compared with the terms on the right-hand side and this equation can be written as

$$0=-\tilde{v}_0\sin\theta+\tilde{y}_0\cos\theta\cos\tau \tag{33}$$

Hence,

$$\tan\theta=\frac{\tilde{y}_0}{\tilde{v}_0}\cos\tau \tag{34}$$

For the macroscopic coefficient of friction, we obtain, using Eq. (15):

$$\tilde{\mu}_{\text{macro}}=\left\langle\cos\theta\right\rangle=\left\langle\frac{1}{\sqrt{1+\tan^2\theta}}\right\rangle=\frac{1}{2\pi}\int_0^{2\pi}\frac{\mathrm{d}\tau}{\sqrt{1+\left(\frac{\tilde{y}_0}{\tilde{v}_0}\right)^2\cos^2\tau}}=\frac{2}{\pi}K\left(i\frac{\tilde{y}_0}{\tilde{v}_0}\right) \tag{35}$$

where

$$K(\xi)=\int_0^{\pi/2}\frac{\mathrm{d}\tau}{\sqrt{1-\xi^2\sin^2\tau}} \tag{36}$$

is the complete elliptic integral of the first kind. The dependence Eq. (35) is shown in Fig. 10. This dependence reproduces the results of earlier studies of this mode of active control of friction in Refs. [4, 5, 2]. Equation (35) shows that the coefficient of friction at large oscillation amplitudes is a function of a single

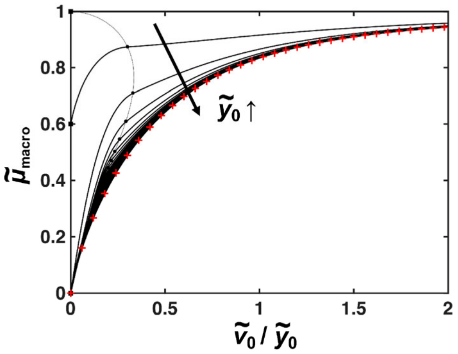

Fig. 10 Dependence of the coefficient of friction on the $\tilde{v}_0 / \tilde{y}_0$ -ratio shown for oscillation amplitudes $\tilde{y}_0 = 0$, 0.8, 1.6, 2.4, ... all the way up to very high values of $\tilde{y}_0 = 80$. The results converge to relation Eq. (35), which is shown with red crosses. Also displayed is the border line (thin solid line with black dots).

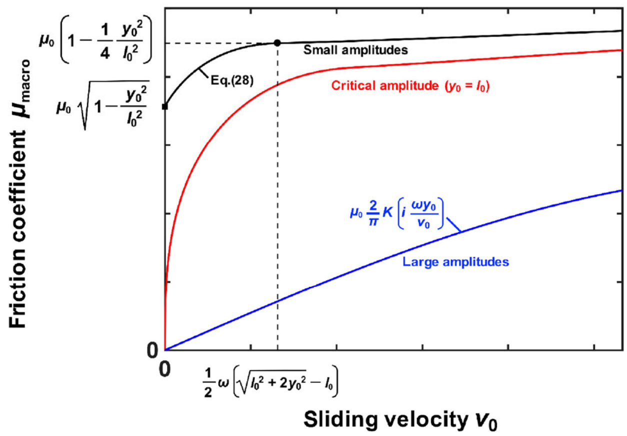

Fig. 11 Schematic representation of the law of friction (dependence of the friction coefficient on the macroscopic sliding velocity).

parameter combination $\frac{\omega y_0}{v_0} \frac{\tilde{y}_0}{\tilde{v}_0} = \frac{\omega y_0}{v_0}$. Figure 10 shows that the dependences of the normalized coefficient of friction on the parameter $\tilde{y}_0 / \tilde{v}_0$ really do tend towards the "master curve" given by Eq. (35) (red crosses in Fig. 10).

7 Summary

We presented a general theoretical analysis of the influence of transverse oscillations on the macroscopically observed coefficient of friction. Unlike previous works, we explicitly took into account the contact stiffness. The natural length scale of the system is the elongation l_0 at which sliding starts, which depends on the normal force, the contact stiffness and the coefficient of friction according to Eq. (5). The natural scale of velocity is given by the sliding velocity v_0 . Oscillation introduces an additional variable having the dimension of length—the oscillation amplitude, y_0, and an additional quantity having the dimension of velocity, $l_0\omega$. We have found that the dependence of the coefficient of friction on velocity is completely determined by two dimensionless parameters: the dimensionless amplitude of oscillation $\tilde{y}_0 = y_0 / l_0$ given by the ratio of the above two characteristic lengths; and dimensionless velocity, $\tilde{v}_0 = v_0 / l_0\omega$.

Figure 11 summarizes schematically the main findings of the present paper. Contrary to the previous figures, we use the non-normalized coefficient of friction and the non-normalized sliding velocity v_0, as this better highlights the main tendencies and is easier to compare with experiment.

As in the case of out-of-plane oscillations discussed in Ref. [33], there is qualitatively different behavior in the case of oscillation amplitudes smaller than some critical value (which in the present case is given by $y_0 = l_0$) and in the case of large oscillation amplitudes.

In the case of large amplitudes, the behavior is relatively simple and coincides with the well-known solution obtained in Ref. [4] and later in Ref. [5] which, however, never could be fitted to experimental results Ref. [15]. In this case the static friction force is identically zero and the coefficient of friction is increasing monotonically according to the more or less universal law given by Eq. (35) tending to the microscopic value in the limit of very high velocities. In dimensional variables it reads:

$$\mu_{\text{macro}} = \mu_0 \frac{2}{\pi} K\left(i \frac{\omega y_0}{v_0}\right) \tag{37}$$

In the case of small oscillation amplitudes, there is a final static friction coefficient. In this region, the law of friction is roughly determined by three parameters: the static coefficient of friction, Eq. (16) or in non-normalized form:

$$\mu_{\text{macro,static}} = \mu_0 \sqrt{1 - y_0^2 / l_0^2} \tag{38}$$

the critical velocity of continuous sliding, Eq. (24) which in dimensional variables reads

$$v_{0,\mathrm{crit}} = \frac{1}{2}\omega\left[\sqrt{l_0^{\,2} + 2y_0^{\,2}} - l_0\right] \tag{39}$$

and the coefficient of friction at this velocity, Eq. (32):

$$\mu_{\mathrm{macro,crit}} = \mu_0\left(1 - \frac{1}{4}\frac{y_0^{\,2}}{l_0^{\,2}}\right) \tag{40}$$

At larger velocities, the coefficient of friction has a very slowly changing plateau.

Let us briefly discuss the physical mechanism of the reduction of friction by transverse oscillations. In the case of out-of-plane oscillations, this reduction is exclusively due to the stick-slip motion: during the stick-phase the force of friction is smaller than the sliding frictional force; therefore, the average frictional force is smaller than the force at stationary sliding [28]. In the case of transverse oscillations, there are two main causes of friction reduction: (a) the occurrence of phases of stick and (b) the deflection of the local force of friction in the contact point from the direction of the macroscopic sliding. The first of these mechanisms is common for all kinds of active control of friction by oscillations. The second one is characteristic only for the case of transverse oscillations considered in the present paper. While the absolute value of the sliding force remains constant, the macroscopic coefficient of friction is determined by the projection of the force on the direction of the macroscopic sliding which in the case of transverse oscillations does not coincide with the direction of macroscopic sliding. Thus, it is always reduced compared to the absolute value of the sliding friction by the average value of $\cos\theta$, where θ is the angle between the sliding direction and the direction of the instant force of friction. This mechanism manifests itself in Eq. (15). Due to this second mechanism, the reduction of friction occurs even in the cases of continuous sliding.

8 Outlook

In the future, several problems have to be considered that have not been studied yet. From the three basic oscillation directions till now only two have been studied in detail, with account of the contact stiffness—the out-of-plane oscillations [28], and the in-plane sideways oscillations (present paper). The complete study of the active control of friction by the in-plane oscillations in the sliding direction is still open.

Further generalization of the present work could lead to consideration of contacts under simultaneous oscillations in many directions. An example of such a study carried out in Ref. [14] shows that multi-mode "active control of friction" leads to some qualitatively new effects such as actuation due to symmetry breaking.

Finally, let us mention that the present study can be extended by consideration of the contact dynamics on the time scale that was classified as "microscopic" in the present study. This would lead to non-local (temporal) dependences of the frictional force on the loading, or in other words the kinetics of the coefficient of friction. The basics for such a consideration are already given by Eqs. (9)–(12) but have not been an explicit subject of study in the present paper.

Acknowledgements

This work was supported in part by the program ACCEL of Japan Science and Technology Agency, the Deutsche Forschungsgemeinschaft and the Ministry of Education of the Russian Federation.

References

[1] Brillouin M, *Théorie moléculaire du frottement des solides polis*, Paris (France): V. Masson, 1899.

[2] Popov V L. *Contact Mechanics and Friction. Physical Principles and Applications*. 2nd ed. Berlin (Germany): Springer, 2017.

[3] Bowden F P, Tabor D. *The Friction and Lubrication of Solids*. New York (USA): Oxford University Press, 1950.

[4] Storck H, Littmann W, Wallaschek J, Mracek M. The effect of friction reduction in presence of ultrasonic vibrations and its relevance to travelling wave ultrasonic motors. *Ultrasonics* **40**(1–8): 379–383 (2002)

[5] Teidelt E, Starcevic J, Popov V L. Influence of ultrasonic oscillation on static and sliding friction. *Tribol Lett* **48**(1): 51–62 (2012)

[6] Milahin N, Li Q, Starčević J. Influence of the normal force on the sliding friction under ultrasonic oscillations. *Facta Univ Ser Mech Eng* **13**(1): 27–32 (2015)

[7] Hoffmann N, Fischer M, Allgaier R, Gaul L. A minimal model for studying properties of the mode-coupling type instability in friction induced oscillations. *Mech Res Commun* **29**(4): 197–205 (2002)

[8] von Wagner U, Hochlenert D, Hagedorn P. Minimal models for disk brake squeal. *J Sound Vib* **302**(3): 527–539 (2007)

[9] Adams G G. Self-excited oscillations of two elastic half-spaces sliding with a constant coefficient of friction. *J Appl Mech* **62**(4): 867–872 (1995)

[10] Comninou M, Dundurs J. Can two solids slide without slipping? *Int J Solids Struct* **14**(4): 251–260 (1978)

[11] Adams G G. Steady sliding of two elastic half-spaces with friction reduction due to interface stick-slip. *J Appl Mech* **65**(2): 470–475 (1998)

[12] Wetter R, Popov V L. The influence of system dynamics on the frictional resistance: insights from a discrete model. *Tribol Lett* **61**(2): 15 (2016)

[13] Popov V L. Oscillation-based methods for actuation and manipulation of nano-objects. AIP Conference Proceedings 1882, 020056 (2017); https://doi.org/10.1063/1.5001635

[14] Popov M, Li Q. Multi-mode active control of friction, dynamic ratchets and actuators. *Phys Mesomechan* **21**(1): (2018)

[15] Teidelt E. Oscillating contacts: friction induced motion and control of friction. Ph.D. Thesis. Berlin (Germany): Technische Universität, 2015.

[16] Wallaschek J. Contact mechanics of piezoelectric ultrasonic motors. *Smart Mater Struct* **7**(3): 369–381 (1998)

[17] Edeler C, Meyer I, Fatikow S. Modeling of stick-slip micro-drives. *J Micro-Nano Mechatron* **6**(3–4): 65–87 (2011)

[18] Mindlin R D, Mason W P, Osmer J F, Deresiewicz H. Effects of an oscillating tangential force on the contact surfaces of elastic spheres. In *Proceedings of the 1st US National Congress of Applied Mech.*, New York, 1952: 203–208.

[19] Gaul L, Lenz J. Nonlinear dynamics of structures assembled by bolted joints. *Acta Mech* **125**(1–4): 169–181 (1997)

[20] Popov M, Popov V L, Pohrt R. Relaxation damping in oscillating contacts. *Sci Rep* **5**: 16189 (2015)

[21] Fridman H D, Levesque P. Reduction of static friction by sonic vibrations. *J Appl Phys* **30**(10): 1572–1575 (1959)

[22] Pohlman R, Lehfeldt E. Influence of ultrasonic vibration on metallic friction. *Ultrasonics* **4**(4): 178–185 (1966)

[23] Godfrey D. Vibration reduces metal to metal contact and causes an apparent reduction in friction. *ASLE Trans* **10**(2): 183–192 (1967)

[24] Lenkiewicz W. The sliding friction process—effect of external vibrations. *Wear* **13**(2): 99–108 (1969)

[25] Tolstoi D M. Significance of the normal degree of freedom and natural normal vibrations in contact friction *Wear* **10**(3): 199–213 (1967)

[26] Starcevic J, Filippov A E. Simulation of the influence of ultrasonic in-plane oscillations on dry friction accounting for stick and creep. *Phys Mesomech* **15**(5–6): 330–332 (2012)

[27] Teidelt E, Willert E, Filippov A E, Popov V L. Modeling of the dynamic contact in stick-slip microdrives using the method of reduction of dimensionality. *Phys Mesomech* **15**(5–6): 287–292 (2012)

[28] Popov M, Popov V L, Popov N V. Reduction of friction by normal oscillations. I. Influence of contact stiffness. *Friction* **5**(1): 45–55 (2017)

[29] Mao X Y, Popov V L, Starcevic J, Popov M. Reduction of friction by normal oscillations. II. In-plane system dynamics. *Friction* **5**(2): 194–206 (2017)

[30] Kado N, Tadokoro C, Nakano K. Measurement error of kinetic friction coefficient generated by frictional vibration. *Trans Jpn Soc Mech Eng Ser C* **79**(803): 2635–2643 (2013)

[31] Kado N, Tadokoro C, Nakano K. Kinetic friction coefficient measured in tribotesting: influence of frictional vibration. *Tribol Online* **9**(2): 63–70 (2014)

[32] Kado N, Sato N, Tadokoro C, Skarolek A, Nakano K. Effect of yaw angle misalignment on brake noise and brake time in a pad-on-disc-type apparatus with unidirectional compliance for pad support. *Tribol Int* **78**: 41–46 (2014)

[33] Kado N, Nakano K. Stabilizing effect of in-plane angular misalignment in 2DOF sliding system with in-plane anisotropic stiffness. *Mech Res Commun* **84**: 14–19 (2017)

[34] Johnson KL. *Contact Mechanics*. Cambridge (UK): Cambridge University Press, 1985.

[35] Coulomb C A. *Theorie des Machines Simple* (*Theory of Simple Machines*). Paris (France): Bachelier, 1821.

[36] Popova E, Popov V L. The research works of Coulomb and Amontons and generalized laws of friction. *Friction* **3**(2): 183–190 (2015)

[37] Popov M. Critical velocity of controllability of sliding friction by normal oscillations in viscoelastic contacts. *Facta Univ Ser Mech Eng* **14**(3): 335–341 (2016)

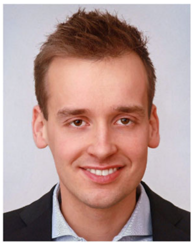

Justus BENAD. He is a research assistant at the Berlin University of Technology where he obtained a Bachelor degree in Aerospace Engineering in 2015 and a Master degree in Engineering Science in 2017. He has work experience in the aerospace industry and in academic research and teaching. He is interested in a wide range of engineering disciplines, among them are numerical simulation methods, software development, tribology, fluid and solid mechanics, materials, gas turbines, aircraft design, and areodynamics. Recent projects he has worked on include the simulation of stresses in turbine blades, the preliminary design of a flying-wing aircraft, the development of a hydrofoil control system for racing sailboats, and the simulation of rolling noise of train wheels. He is a scholar of the German National Academic Foundation and has received awards from the Royal Aeronautical Society and the German Aerospace Center.

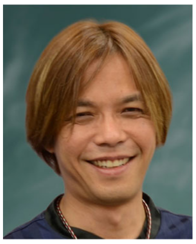

Ken NAKANO. He is a full professor at Faculty of Environment and Information Sciences of Yokohama National University. He studied aeronautics and astronautics at University of Tokyo (1988-1997), and obtained his doctorate from University of Tokyo (1997). He worked at Department of Mechanical Engineering of Saitama University as an assistant professor (1997-2000). After working at Department of Mechanical Engineering of Yokohama National University as an associate professor (2000–2015), he obtained a full professorship at Yokohama National University (2015). His areas of interest include tribo-physics (e.g., multiscale and multiphysics of solid friction), tribo-dynamics (e.g., stabilization mechanisms of tribosystems by breaking structural symmetry), and tribo-informatics (e.g., objective evaluation of tactile sensations). In 2015, from Japan Society of Mechanical Engineers (JSME), he was awarded with the JSME Medal for Outstanding Paper on the measurement error of friction coefficient generated by friction-induced vibration. He is the chair of the technical committee on tribo-dynamics of Japanese Society of Tribologists (JAST). He is also a board member of JAST.

Valentin L. POPOV. He is a full professor at the Berlin University of Technology, studied physics (1976–1982) and obtained his doctorate in 1985 from the Moscow State Lomonosov University. He worked at the Institute of Strength Physics of the Russian Academy of Sciences. After a guest professorship in the field of theoretical physics at the University of Paderborn (Germany) from 1999 to 2002, he has headed the department of System Dynamics and the Physics of Friction of the Institute of Mechanics at the Berlin University of Technology. His areas of interest include tribology, nanotribology, tribology at low temperatures, biotribology, the influence of friction through ultrasound, numerical simulation of frictional processes, research regarding earthquakes, as well as topics related to materials science such as the mechanics of elastoplastic media with microstructures, strength of metals and alloys, and shape memory alloys. He has published over 100 papers in leading international journals during the past 5 years. He is the author of the book "Contact Mechanics and Friction: Physical principles and applications" which appeared in three German, two English, Chinese, and Russian editions and co-author of the book on "Method of Dimensionality Reduction in Contact Mechanics and Friction" which appeared in German, English and Chinese editions. He is the joint editor of international journals and regularly organizes international conferences and workshops over diverse tribological themes. He is a member of the Scientific Council of the German Tribological Society. He has intensively collaborated with many industrial corporations and possesses experience in implementing the results of scientific research in industrial applications.

Mikhail POPOV. He received a Bachelor degree in Computer Science from the Freie Universität Berlin in 2011 and a Master degree in Engineering Science from the Tomsk Polytechnic University and the Berlin University of Technology in 2016. Currently he is a doctoral student at the Berlin University of Technology and a research assistant at the Tomsk Polytechnic University. His research interests include efficient numerical methods in tribology, rubber friction, as well as friction and damping under the influence of oscillations.

3.6 Publication 9

This paper is partly an overview and integration of the studies published since the appearance of P4. It presents many of the old ideas and results in a new light, with the exposition being more representative of the author's current understanding of the material. Other aspects of previous publications are generalized and extended, with several new results being presented.

The first topic to be revisited is static friction under oscillation in various directions, which is put on a common basis and developed systematically. The main analysis is then devoted to sliding friction under normal oscillation. Unlike previous publications, which always dealt with harmonic oscillations, the analysis in this paper is kept as general as possible and is developed for an arbitrary waveform. The transition from slip to stick and back is derived in the usual fashion. The concept of critical velocity is abandoned and instead replaced with a fully dimensionless treatment.

The macroscopic coefficient of friction is written in general form, and the wavefom-specific "reduction function" Ψ_w is introduced, which contains in itself all nonlinear behavior of the dependence. The reduction function is then calculated in closed form for a number of simple oscillation waveforms, which allows to compare the efficacy of these waveforms for the reduction of friction. Some additional discussion of the properties of Ψ_w can be found in appendix **A**. This material was omitted from the original publication due to scope limitations.

The main properties and differences of the tangential and transverse modes of oscillation are then reviewed, and their energy efficiency is compared.

frontiers in Mechanical Engineering

HYPOTHESIS AND THEORY
published: 20 August 2020
doi: 10.3389/fmech.2020.00069

The Influence of Vibration on Friction: A Contact-Mechanical Perspective

Mikhail Popov[1,2*]

[1] Department of Continuum Mechanics and Constitutive Theory, Technische Universität Berlin, Berlin, Germany, [2] Tomsk State University, Tomsk, Russia

A unified model for active control of static and sliding friction by normal, tangential, and transverse oscillations is discussed, building on a series of past publications. The model in question is quasi-static, uses Amontons friction and takes into account *contact stiffness* in both normal and tangential directions. This makes the model fully macroscopic, which stands in contrast to Prandtl-Tomlinson-derived microscopic models that seem to be the currently preferred explanation for the influence of vibration on friction. While many technical details and numerical simulations based on our model have already appeared in a series of publications, here we attempt to give a high-level overview and discuss the main properties of friction under oscillation as generally as possible, while making a minimum of assumptions.

Keywords: vibration, friction, contact mechanics, active control, stick-slip actuation

OPEN ACCESS

Edited by:
Marco Paggi,
IMT School for Advanced Studies Lucca, Italy

Reviewed by:
Shingo Ozaki,
Yokohama National University, Japan
Varvara Romanova,
Institute of Strength Physics and Materials Science (ISPMS SB RAS), Russia
Vladislav Aleshin,
UMR8520 Institut d'électronique, de Microélectronique et de Nanotechnologie (IEMN), France

Correspondence:
Mikhail Popov
mpopov@fastmail.fm

Specialty section:
This article was submitted to Tribology, a section of the journal Frontiers in Mechanical Engineering

Received: *29 May 2020*
Accepted: *14 July 2020*
Published: *20 August 2020*

Citation:
Popov M (2020) The Influence of Vibration on Friction: A Contact-Mechanical Perspective. Front. Mech. Eng. 6:69. doi: 10.3389/fmech.2020.00069

1. INTRODUCTION

The fact that vibration can be used to significantly reduce the force of friction has been known since at least the 1950s (Fridman and Levesque, 1959). Since then, the effect has been studied extensively and exploited in many practical applications. Classical examples are to be found in wire drawing (Murakawa and Jin, 2001; Siegert and Ulmer, 2001), press forming (Eaves et al., 1975; Ashida and Aoyama, 2007), cutting (Thoe et al., 1998; Eggers et al., 2004), and other machining processes. Also well-known is the use of vibration for stabilization of system dynamics, e.g., suppression of brake squeal (Müller and Ostermeyer, 2007) and cornering noise (Heckl and Huang, 2000).

There are also a number of advanced applications that move beyond simple reduction of sliding or static friction, and involve vibration-driven directed transport or exact positioning (Popov, 2017). The most famous example of this are traveling wave motors (Schmidt et al., 1996; Storck et al., 2002), which are used to adjust focus in camera lenses, among many other applications. Similar principles are employed in high-precision linear actuators and positioning systems (Socoliuc et al., 2006), vibrational conveyors (Gaberson, 1971, 1972), and other types stick-slip drives.

The above examples are only a small sample of technical applications at the intersection of friction and vibration. Correspondingly, there is a large body of existing research in this field (see e.g., Pohlman and Lehfeldt, 1966; Godfrey, 1967; Storck et al., 2002; Chowdhury and Helali, 2008). Most of it is practical in nature, even though several well-known theoretical models have been proposed as well (De Wit et al., 1995). However, it is the contention of the author that an important factor is missing from currently popular models: the compliance of the contact and its interaction with the applied oscillation. The currently prevailing tendency is to ascribe the reduction of friction by vibration mostly to processes at the micro-scale (Popov et al., 2010). However, here we will argue that the *primary* (but not necessarily exclusive) mechanism is to be found on the macro-scale, in ordinary contact mechanics. It should be noted that this does not automatically invalidate previous work. In fact, it seems likely that a truly accurate model will be multiscale, combining both macroscopic dynamics and microscopic processes.

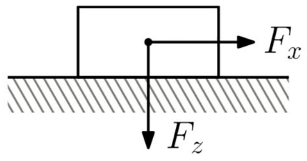

FIGURE 1 | Static friction model. The intrinsic coefficient of friction in the contact is μ_0. The y-axis points out of the plane.

The primary advantage of our model is its simplicity. It relies only on macroscopic contact mechanics and introduces no new physics. In fact, it is likely to be the *simplest possible* model that is rich enough to describe almost the full range of behaviors exhibited by friction under the influence of external vibration. For this reason, the present paper can be seen as an exercise in minimalism, attempting to cover as much phenomenological ground as possible with a minimum of assumptions and variables.

1.1. Contributions

This work draws heavily on results recently published in a series of papers with participation of the present author (Mao et al., 2017; Popov et al., 2017; Benad et al., 2018a,b; Popov and Li, 2018). While there is substantial overlap with these papers, the present work is organized differently, seeking to present a "big picture" view without getting bogged down in details. Several results have been generalized from previous publications, while the discussion of the influence of oscillation waveforms has, to the best knowledge of the author, not previously appeared in the literature.

2. STATIC FRICTION

To warm up, we consider static friction. This case is much simpler than the sliding case and leads to some satisfyingly general results. The system under consideration consists of a body resting on a plane (**Figure 1**). The body is pressed into the plane with a force F_z and pulled sideways with a force F_x. The coefficient of friction between the body and the plane is assumed to be constant and equal to μ_0. The body remains at rest while

$$|F_x| < \mu_0 F_z \tag{1}$$

where $\mu_0 F_z$ is the critical force at which the body just begins to slide. The static coefficient of friction is defined as the ratio of this critical force to the normal load. In the absence of oscillation, it is equal to μ_0:

$$\mu_s = \mu_0 \tag{2}$$

Things get slightly more interesting when we add an oscillatory force component. If the force oscillation acts normal to the plane, we denote it by $A_z g(t)$, where A_z is the amplitude. The stick condition in that case needs to be amended to:

$$|F_x| < \mu_0 \left(F_z + A_z g(t)\right)^+ \tag{3}$$

The $(..)^+$ notation denotes the ramp function, which clips negative values to zero. It is necessary because the normal force does not turn negative when contact is lost.

It is easy to see that the critical force is reduced relative to the non-oscillatory case, since the above inequality must hold at all times, including the times when the normal force drops below its mean value F_z. In other words, static friction is limited by the *minimum* of normal force encountered during the oscillation. For the coefficient of static friction under normal oscillation we thus obtain:

$$\mu_{s,z} = \mu_0 \left(1 - A_z/F_z\right)^+ \tag{4}$$

In a similar fashion, we can add an oscillatory component $A_x g(t)$ that is aligned with the tangential force F_x. This results in the stick condition

$$|F_x + A_x g(t)| < \mu_0 F_z \tag{5}$$

Note that this inequality is only satisfiable when $A_x < \mu_0 F_z$. Otherwise the body starts to slide in place and the contact loses its ability to statically sustain a lateral force. Thus, μ_s can be expressed as:

$$\mu_{s,x} = \left(\mu_0 - A_x/F_z\right)^+ \tag{6}$$

Notice the slight difference between this result and Equation (4). In particular, note that a tangential oscillation will reduce μ_s by a larger amount than a normal oscillation of the same amplitude if $\mu_0 < 1$, and by a smaller amount otherwise.

Transverse oscillations are also able to reduce static friction. This case is qualitatively similar to that of tangential oscillation, with the difference that we need to use the vector norm of the in-plane forces instead of adding them directly:

$$F_x^2 + \left(A_y g(t)\right)^2 < \left(\mu_0 F_z\right)^2 \tag{7}$$

Once again, stick is impossible if $A_y \geq \mu_0 F_z$, and for the static coefficient of friction we obtain:

$$\mu_{s,y} = \sqrt{\left(\mu_0^2 - A_y^2/F_z^2\right)^+} \tag{8}$$

One particularly useful thing about these results is that they are quite general, and in particular independent of contact geometry, frequency of oscillation, and the shape of the oscillation waveform.

2.1. Static Friction Under Superimposed Oscillation

Things become considerably less transparent when we consider simultaneous oscillation in multiple directions. The stick condition itself does not change much, and in the most general case can be expressed as:

$$\left(F_x + A_x g_x(t)\right)^2 + \left(A_y g_y(t)\right)^2 < \mu_0^2 \left(F_z + A_z g_z(t)\right)^2 \tag{9}$$

Unfortunately, actually finding the maximal F_x that still satisfies this inequality at all times quickly becomes unwieldy, leading to

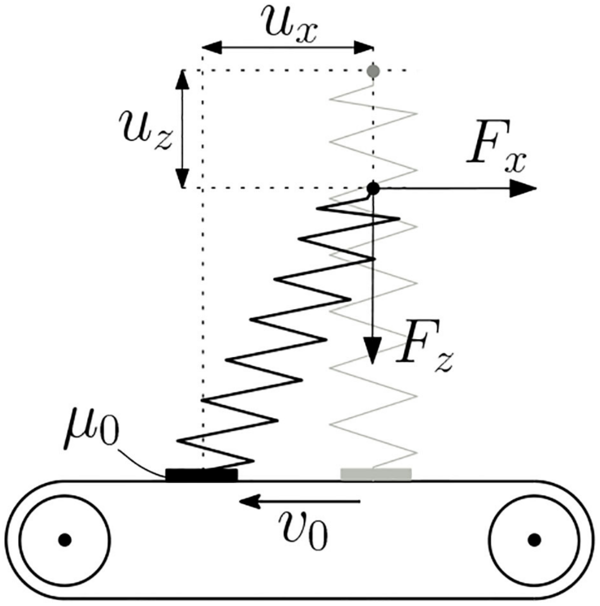

FIGURE 2 | A single massless spring, which serves as a minimal model of a sliding frictional contact. The sliding velocity is constant, while the vertical coordinate oscillates. Amontons friction with the constant coefficient of friction μ_0 is assumed in the contact point.

a large number of case distinctions—if a closed-form solution is possible at all. In addition, when the compliance of the contact is taken into account, the static coefficient of friction may become *negative*, in the sense that a constant force needs to be applied to *prevent* the contact from sliding. This effect is what frictional drives and actuators are based on. For an analysis of this case the reader is referred to Popov and Li (2018). In this paper, however, we ignore superimposed oscillation.

3. SLIDING FRICTION UNDER NORMAL OSCILLATION

The key feature of the model that we use to describe dynamic friction is that the *compliance* of the contact is taken into account. In the initial formulation, the contact is modeled as a single Hookean spring that has an associated normal stiffness k_z and a lateral stiffness k_x (**Figure 2**). This is a reasonable approximation of a flat-ended cylinder in contact with a plane. The model can also be extended to cover arbitrary curved contacts with the help of the Method of Dimensionality Reduction (Popov and Heß, 2016). However, for a general analysis, a single spring is quite sufficient.

The model considered here is displacement-controlled and quasi-static. A force-controlled and/or inertial model can be formulated within the same framework, which, however, leads to certain complications (e.g., resonances) that are outside the focus of the present paper. For an analysis of such a model, the reader is referred to Mao et al. (2017).

The kinematics of the model is as follows: The contact spring is pulled over a flat plane with a constant velocity v_0, although for convenience we consider the spring to be stationary, while the substrate slides underneath it. The normal displacement u_z of the spring is measured relative to the state of unstressed first contact with the substrate. $u_z(t)$ represents the externally applied oscillation and is thus given explicitly. The lateral displacement u_x, on the other hand, depends on the current state of the system and is the only unknown variable.

We assume that Amontons' law of friction (with a constant coefficient of friction μ_0 that is the same for both static and sliding friction) holds in the contact point. In general, this may be an unrealistic assumption. However, the use of a constant coefficient of friction not only simplifies calculations, but also eliminates all possible micro-scale influences from the model. Since one of the primary aims of this paper is to advertise the feasibility of a purely macroscopic theory of friction under oscillation, making μ_0 constant is actually a prerequisite.

The *effective* coefficient of friction $\bar{\mu}$, which is to be determined in the sequel, is defined as the average tangential force exerted by the spring divided by the average normal force:

$$\bar{\mu} = \frac{\langle F_x(t) \rangle}{\langle F_z(t) \rangle} \tag{10}$$

where $\langle .. \rangle$ denotes averaging over one period of oscillation.

Previous publications on the topic assumed that the imposed normal oscillation is harmonic, so as to simplify analysis. However, this turned out to be an unnecessary restriction, so here we will work with a general periodic function that is parameterized as follows:

$$u_z(t) = \bar{u}_z + A_z w(ft) \tag{11}$$

Here $\bar{u}_z$ is the mean indentation, A_z is the amplitude and f the frequency of the oscillation. $w(\varphi)$ is a dimensionless function describing the "shape" of the oscillation, with $\varphi = ft$. The waveform w is normalized such that it is zero-mean, with a period of 1 and a minimum value of -1. Note however, that the *maximum* of w is left unconstrained.

3.1. Pure Sliding

While the behavior of a frictional couple under oscillation has its complexities in general, there are two extreme cases that lend themselves to easy and precise analysis: One of them, static friction, was already discussed above. The second, pure sliding, is briefly discussed here. The most important thing about pure sliding is that oscillations do not influence the coefficient of friction in that mode. This can be easily seen from the fact that the instantaneous tangential force is uniquely defined during slip ($F_x = \mu_0 F_z$), from which the effective coefficient of friction is immediately obtained:

$$\bar{\mu}_{\text{slip}} = \frac{\langle F_x(t) \rangle}{\langle F_z(t) \rangle} = \frac{\langle \mu_0 F_z(t) \rangle}{\langle F_z(t) \rangle} = \mu_0 \tag{12}$$

Irrespective of how complex the dependence $F_z(t)$ may be, it always cancels out—by linearity of sliding friction. While this result may seem unimpressive by itself, it establishes an important "boundary condition" for the more general case of friction with stick-slip. Also, as in the static case, the coefficient of friction in pure slip has the important property of not being dependent on contact geometry and oscillation parameters. The result $\bar{\mu}_{\text{slip}} = \mu_0$ is also valid for tangential and combined normal/tangential oscillations. It can also be shown to be valid in the inertial case (Mao et al., 2017). However, *transverse* oscillations do not, strictly speaking, have this limiting case, although the deviation becomes negligible at high velocities. This will be discussed in more detail later.

3.2. Stick-Slip

Two extreme points have now been established: pure stick (static friction) and pure slip (plateau). Reason suggests that there is also something in between. It would be physically implausible for the coefficient of friction under oscillation to "snap" from near zero back to μ_0 due to arbitrarily slow sliding. And this is in fact not observed experimentally: At a given amplitude and frequency, the static coefficient of friction is lowest, and then smoothly increases with the sliding velocity until reaching a plateau of sorts. Fortunately, the transition region can also be described in our model. Unsurprisingly, it is dominated by stick-slip.

Let us now consider this phenomenon in more detail. During sliding, we have $F_x = \mu_0 F_z$, which can also be written as $k_x u_x(t) = \mu_0 k_z u_z(t)$. Substituting u_z from Equation (11) and rearranging gives us the lateral displacement and velocity of the contact point:

$$u_x(t) = \mu_0 \frac{k_z}{k_x} \left(\bar{u}_z + A_z w(ft)\right) \tag{13}$$

$$\dot{u}_x(t) = \mu_0 \frac{k_z}{k_x} A_z f w'(ft) \tag{14}$$

A transition from slip to stick happens when the relative motion between the substrate and the contact point vanishes, i.e., when $\dot{u}_x(t) = v_0$. From this condition, the point of stick onset can be determined:

$$\varphi_1 = ft_1 = \left(w'\right)^{-1} \left(\frac{k_x v_0}{\mu_0 k_z A_z f}\right) \tag{15}$$

It becomes obvious that φ_1 is a function of a single compound variable, which combines all parameters of the system, *except* $\bar{u}_z$. To simplify further calculations, we introduce some dimensionless variables, α (corresponding to amplitude), β (corresponding to velocity), and φ (phase):

$$\alpha = \frac{A_z}{\bar{u}_z} \tag{16}$$

$$\beta = \frac{k_x v_0}{\mu_0 k_z A_z f} \tag{17}$$

$$\varphi = ft \tag{18}$$

Using these variables, the static coefficient of friction (Equation 4) can be expressed as $\mu_{s,x} = \mu_0(1-\alpha)^+$, while Equation (15) can be written as

$$\varphi_1 = \left(w'\right)^{-1}(\beta) \tag{19}$$

Noting that β is a positive quantity and assuming that w is differentiable (but not necessarily invertible—there can be multiple stick events), it can be seen that the above equation has solutions if

$$\beta < \max_{\varphi} w'(\varphi) = \beta_c \tag{20}$$

where β_c denotes the critical value that separates the stick-slip region from the continuous sliding region. A harmonic oscillation, for example, has $\beta_c = 2\pi$, while a right-leaning sawtooth function has $\beta_c = 2$, which is in fact the smallest possible value. The larger β_c, the more effective the waveform is at reducing friction at high velocities, but more on that later.

Once stick is initiated, the contact point is dragged along by the substrate with velocity v_0, so that the tangential displacement and force increase linearly with time:

$$F_{\text{stick}}(t) = \mu_0 F_z(t_1) + k_x v_0 (t - t_1) \tag{21}$$

This continues while the condition for static friction holds:

$$F_{\text{stick}}(t) < \mu_0 F_z(t) \tag{22}$$

Trivial as it is, this inequality lies at the core of reduction of friction in our model. It serves as the sole source of nonlinearity that allows the system to break free of the trivial solution exemplified by Equation (12). With pure slip, the spring force is always equal to $\mu_0 F_z(t)$, while in stick-slip it is sometimes lower, which leads to lower average force and coefficient of friction (see also **Figure 3**). Another way of looking at it is that the contact point stands still when the normal force is highest, and covers more distance when the normal load diminishes. This leads to lower energy dissipation over the same distance. The whole process is somewhat similar to walking, where one leg carries the load without dissipation, while the other is lifted and advanced to the next position. Something analogous happens in our model, only there is just one "leg" and it is not necessarily lifted all the way.

The stick phase ends at time t_2 when the condition $F_{\text{stick}}(t_2) = \mu_0 F_z(t_2)$ is met. Expanding this condition yields

$$\mu_0 k_z u_z(t_1) + k_x v_0 (t_2 - t_1) = \mu_0 k_z u_z(t_2) \tag{23}$$

or, more conveniently,

$$\frac{v_0 k_x}{\mu_0 k_z} (t_2 - t_1) = u_z(t_2) - u_z(t_1) \tag{24}$$

Substituting u_z and $t = \varphi / f$, this can be rewritten as:

$$\beta (\varphi_2 - \varphi_1) = w(\varphi_2) - w(\varphi_1) \tag{25}$$

Once again $\bar{u}_z$ cancels out, leaving us with a function of only β. Unfortunately, the equation is implicit and cannot be solved symbolically for φ_2 except in the simplest cases (sawtooth, square wave, etc). In the case of a harmonic oscillation, for example, Equation (25) takes the form ($\cos x = a + bx$), which does not have a closed-form solution in terms of standard functions. Numerical solution is required in most cases.

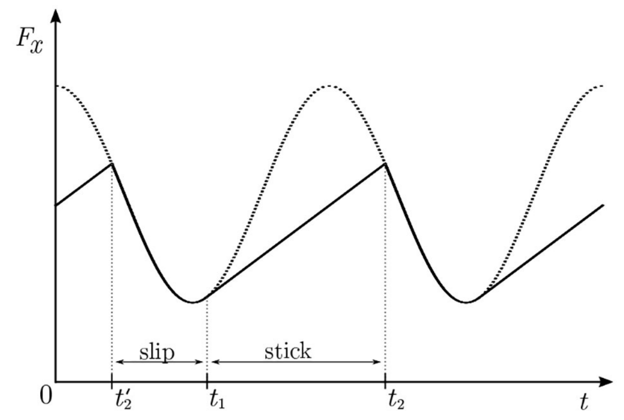

FIGURE 3 | Stick and slip under the influence of a harmonic oscillation. The dotted line represents the tangential force as it would be in pure slip [$F_{\text{slip}} = \mu_0 F_z(t)$]. The solid line is the actual tangential force in the presence of stick-slip. The stick phases are the straight segments, e.g., between t_1 and t_2, while slip phases are the sinusoidal segments, e.g., between t_2' and t_1, repeating periodically. Note that $F_x \leq F_{\text{slip}}$ everywhere, which is the origin of friction reduction in our model.

3.3. Effective Coefficient of Friction

We define the "macroscopic" or "effective" force of friction simply as the tangential force averaged over one period $T = 1/f$:

$$\langle F_x \rangle = \frac{1}{T} \int_0^T F_x(t) \mathrm{d}t \tag{26}$$

However, it will become clear in a moment that it is more convenient to consider the difference or *reduction* of the force of friction relative to the state of continuous sliding:

$$\Delta F_x = \langle F_{\text{slip}} \rangle - \langle F_x \rangle = \frac{1}{T} \int_0^T \left(F_{\text{slip}}(t) - F_x(t) \right) \mathrm{d}t \tag{27}$$

Since F_x only differs from F_{slip} during the stick phase, we can tighten the integration bounds:

$$\Delta F_x = \frac{1}{T} \int_{t_1}^{t_2} \left(\mu_0 F_z(t) - F_{\text{stick}}(t) \right) \mathrm{d}t \tag{28}$$

This form is convenient for numerical solution. However, some additional properties can gleaned by expanding F_{stick} and $u_z(t)$ and making the substitution $\mathrm{d}t = T \mathrm{d}\varphi$:

$$\begin{aligned} \Delta F_x &= \frac{1}{T} \int_{t_1}^{t_2} \left(\mu_0 F_z(t) - \mu_0 F_z(t_1) - k_x v_0 \, (t - t_1) \right) \mathrm{d}t \\ &= \frac{1}{T} \int_{t_1}^{t_2} \mu_0 k_z \big(\bar{u}_z + A_z w(ft) - \bar{u}_z - A_z w(ft_1) \\ &\quad - \frac{k_x v_0}{\mu_0 k_z} \, (t - t_1) \big) \mathrm{d}t \\ &= \mu_0 k_z A_z \int_{\varphi_1}^{\varphi_2} \left(w(\varphi) - w(\varphi_1) - \beta \, (\varphi - \varphi_1) \right) \mathrm{d}\varphi \end{aligned} \tag{29}$$

It becomes apparent that the expression for ΔF_x can be split into the dimensional factor $\mu_0 k_z A_z$ and a dimensionless function Ψ_w of a single variable:

$$\Delta F_x = \mu_0 k_z A_z \Psi_w(\beta) \tag{30}$$

where

$$\Psi_w(\beta) = \int_{\varphi_1}^{\varphi_2} \left(w(\varphi) - w(\varphi_1) - \beta \, (\varphi - \varphi_1) \right) \mathrm{d}\varphi \tag{31}$$

We refrain from integrating this expression, since a closed-form solution is precluded by the lack of an explicit formula for φ_2. We merely draw attention to the fact that ΔF_x is invariant with respect to mean indentation. The same is not true for the *coefficient of friction*:

$$\bar{\mu} = \frac{\langle \mu_0 F_z \rangle - \Delta F_x}{\langle F_z \rangle} = \mu_0 - \frac{\Delta F_x}{k_z \bar{u}_z} \tag{32}$$

However, the dependence on $\bar{u}_z$ is incidental, merely reflecting the fact that ΔF_x is subtracted from different baselines of friction force. Using our dimensionless variables, the above can also be written in the following compact form:

$$\bar{\mu} = \mu_0 \left(1 - \alpha \Psi_w(\beta) \right) \tag{33}$$

Further, it can be shown that Ψ_w is a fairly well-behaved function that has unit range and is monotonously decreasing and convex for all waveforms and any number of stick events per cycle of oscillation. However, space considerations prevent us from including a formal proof of these properties.

3.4. Oscillation Waveforms

The functional dependence (33) presented in the previous section permits an interesting observation: the overall strength of the friction reduction effect is primarily governed by the *amplitude* of the oscillation and not by the frequency. In principle, the effective coefficient of friction can be reduced to very low values, but that requires a force amplitude that is comparable to the mean normal force. Thus, the technique is not very useful for reducing friction in highly loaded contacts, e.g., rail-car or truck wheels.

Furthermore, a higher frequency cannot be used to compensate for small amplitude. However, frequency is still an important parameter, since it determines the "velocity-resistance" of the effect: As has been pointed out before, the largest reduction is always seen in the static case, and becomes lower with increasing sliding velocity. The frequency determines the scaling of this decline, and a strong reduction can be achieved even at high sliding velocities if the frequency of the applied oscillation is high enough. However, frequency is not the only factor that determines this "velocity-resistance." The waveform of the oscillation is also quite important, which is why we briefly discuss it here.

By far the most important property of a waveform w is the maximal positive value of its first derivative, or β_c. A *right-leaning* sawtooth function, for example, has $\beta_c = 2$; a harmonic oscillation has $\beta_c = 2\pi$, which is slightly better; however, a *left-leaning* sawtooth function has $\beta_c = \infty$, which is ideal. An infinite value of β_c implies that the oscillation will provide some measure of friction reduction at arbitrarily high velocities. While this is not really possible in practice, the general rule for waveform selection is nevertheless that the load should increase as fast as possible and then relax slowly. Thus, approximations of left-leaning sawtooth or the square wave are preferable to smooth and symmetric functions like the harmonic oscillation. Naturally, this recommendation is subordinate to practical technological constraints. For example, a high-amplitude harmonic oscillation could be generated by exciting a natural vibrational mode of the system, while a square wave would likely require more sophisticated equipment.

We conclude this section by giving Ψ_w for a few common waveforms explicitly. For both sawtooth variants and the square wave Ψ_w can be calculated in closed form. However, for most oscillations, including sinusoidal ones, this is not possible. Nonetheless, the function can easily be computed numerically for arbitrary waveforms, and so we include two empirical approximations for the harmonic oscillation, which were first obtained in Popov et al. (2017). The first approximation is slightly more accurate.

$$\Psi_{\mathrm{str}}(\beta) = 1 - \frac{\beta}{2} \tag{34}$$

$$\Psi_{\mathrm{stl}}(\beta) = \frac{2}{2+\beta} \tag{35}$$

$$\Psi_{\mathrm{sqr}}(\beta) = \begin{cases} 1 - \beta/8\,, & \text{for } \beta < 4 \\ 2/\beta\,, & \text{for } \beta > 4 \end{cases} \tag{36}$$

$$\Psi_{\sin}(\beta) \approx \frac{3}{4}\,(1 - \beta/\beta_c)^2 + \frac{1}{4}\,(1 - \beta/\beta_c)^4 \tag{37}$$

$$\approx (1 - \beta/\beta_c)^{2.4} \tag{38}$$

For a visual comparison, the dependence of the coefficient of friction on β is plotted in **Figure 4** for all four of the above waveforms. To keep things simple, only the case of *maximal* friction reduction is shown $\alpha = 1$, in which case Equation (33) reduces to $\bar{\mu} = \mu_0[1 - \Psi_w(\beta)]$. This is why all curves show zero static friction. For other values of α the shapes of the curves would remain the same, but they would start at nonzero values of μ_s and would be scaled accordingly.

As a final remark, we note that there is a unique optimal waveform with regards to reduction of friction. It is given by the periodic extension of $\delta(\varphi) - 1$, where δ is the Dirac delta function. This "impulse wave" is -1 everywhere, except for very short positive spikes (impulses) that occur with a period of 1 and each integrate to 1, so that the average of the function is zero. With this degenerate waveform, the system slides most of the time, with only an infinitesimal stick phase at each spike, which implies that Ψ is very close to 1 for all β:

$$\Psi_{\mathrm{imp}}(\beta) \to 1 \tag{39}$$

Thus, we conclude that friction can be reduced, in principle, to an arbitrary degree even at high sliding velocities, by effectively hopping over the surface. In practice, this approach will be limited by plastic deformation, radiation of elastic waves and the sheer difficulty of generating such an oscillation.

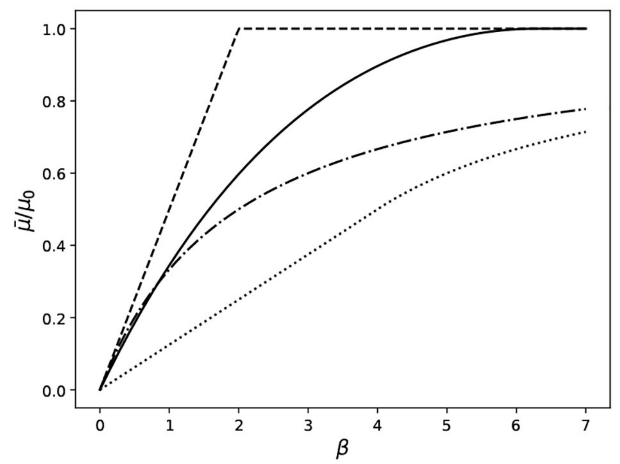

FIGURE 4 | Coefficient of friction under normal vibration with different waveforms, computed using Equation (33) and the individual influence factors Equations (34)–(37). Note that for all curves $\alpha = 1$, which corresponds to *maximal* friction reduction. Legend: dashed line—right-leaning sawtooth function (Equation 34); solid line—harmonic oscillation (Equation 37); dash-dotted line—left-leaning sawtooth function (Equation 35); dotted line—square wave (Equation 36).

4. TANGENTIAL AND TRANSVERSE OSCILLATIONS

Most of this paper was devoted to reduction of friction by normal oscillations. This focus is explained partly by the fact that the normal case is easiest to analyze, and partly because normal oscillations are generally the most efficient way to reduce friction, out of the three possible directions. Nevertheless, both tangential (in the direction of sliding) and transverse (in-plane, but orthogonal to sliding) vibration can reduce friction. For detailed analysis of the tangential case the reader is referred to Popov and Li (2018) and for the transverse case to Benad et al. (2018a). Here we only present some highlights and point out the major differences between normal oscillations and the other two modes.

In the tangential oscillation case the normal indentation is kept constant while an oscillatory component is added to the base of the spring. Sliding friction under such conditions can proceed in three modes: (I) pure sliding, in which the effective coefficient of friction is equal to μ_0, as argued previously. (II) simple stick-slip, which occurs for obvious reasons when the velocity amplitude is greater than the mean sliding velocity ($A_x f w'(ft) > v_0$). (III) multiple stick-slip, which occurs when the velocity amplitude is much larger than v_0, so that the contact point slides back-and-forth in each cycle, going through two stick and slip phases each.

The most important difference between friction reduction by normal and tangential oscillations is that normal oscillations actually reduce the total dissipated energy through a walking-like mechanism, while tangential oscillations do not. The author is not aware of a good analogy to visualize the mechanism in the tangential case. But it is clear that, since the normal load (and therefore the force of sliding friction) is constant, the dissipated energy is simply friction force times distance (in mode II). Although the effective coefficient of friction (i.e., average spring force) may be lowered, the missing energy must be supplied by the oscillator. In mode III, when the amplitude is large enough to cause in-place sliding, the total sliding distance actually increases, and the total energy expenditure becomes *larger* than without oscillations, even though the effective coefficient of friction will still appear lower than μ_0.

Friction reduction by transverse oscillation always operates in something like mode III of tangential oscillation: it causes additional sliding in the direction orthogonal to the main sliding motion, thereby increasing the total path and therefore energy expenditure. However, the apparent coefficient of friction is reduced, because the magnitude of the local friction force is still limited to $\mu_0 F_z$, but now shared between the force components parallel and orthogonal to the main sliding direction. Thus, transverse oscillations are effectively "stealing" the friction vector from the slider, but at considerable expense of energy by the oscillator. This also accounts for the fact, mentioned previously, that the system never formally reaches the "invariant plateau" ($\bar{\mu}_{\text{slip}} = \mu_0$) even at high sliding velocities, because the projection of the local friction force onto the sliding direction is always less than its total magnitude, so long as the transverse amplitude is non-zero. However, for sufficiently large sliding velocities this difference becomes very small, so for all practical purposes the plateau exists in the transverse case as well.

To summarize, normal oscillations are most effective at reducing dynamic friction and should be used in preference to the other directions. Not only do they actually reduce the total dissipated energy, but normal oscillations also act at right angles (by definition) to the sliding motion. Thus, they technically do not require energy to keep going. Of course, this is never quite the case in practice, but by exciting a resonant frequency the power needed to drive the oscillator can usually be made quite small. Compared to that, tangential oscillation requires a powerful oscillator (except in the static case), while transverse oscillation is even more energetically expensive, and also less effective overall. There are cases, however, where energy expenditure is not a primary concern (e.g., stabilization of system dynamics) and normal oscillations cannot be easily applied due to technological constraints. In such cases, tangential and even transverse oscillations are viable alternatives.

5. CONCLUSION

The present paper summarizes and generalizes a series of recent works that aim to establish a simple macroscopic contact model as a viable explanation for active control of friction by externally applied vibration. Despite its apparent simplicity, the model not only captures the full range of experimentally observed effects, but is also very flexible, being able to adapt to static and dynamic friction, oscillations in normal, tangential and transverse directions, contacts of curved bodies, etc. Apart from straight-forward reduction-of-friction settings, the model can also be applied to the study of frictional drives and actuators under complicated loading scenarios. A similar approach was also highly successful in modeling positioning systems without using any modified friction laws such as the elastoplastic model (see e.g., Teidelt et al., 2012; Grzemba et al., 2014; Teidelt, 2015).

DATA AVAILABILITY STATEMENT

All datasets generated for this study are included in the article/supplementary material.

AUTHOR CONTRIBUTIONS

MP conceived and conducted the research and prepared the manuscript.

ACKNOWLEDGMENTS

This work was supported in part by the *Tomsk State University competitiveness improvement programme*, which the author gratefully acknowledges.

REFERENCES

Ashida, Y., and Aoyama, H. (2007). Press forming using ultrasonic vibration. *J. Mater. Process. Technol.* 187, 118–122. doi: 10.1016/j.jmatprotec.2006.11.174

Benad, J., Nakano, K., Popov, V. L., and Popov, M. (2018a). Active control of friction by transverse oscillations. *Friction* 7, 1–12. doi: 10.1007/s40544-018-0202-1

Benad, J., Popov, M., Nakano, K., and Popov, V. L. (2018b). Stiff and soft active control of friction by vibrations and their energy efficiency. *Forsch. Ingenieurw.* 82, 331–339. doi: 10.1007/s10010-018-0281-1

Chowdhury, M. A., and Helali, M. (2008). The effect of amplitude of vibration on the coefficient of friction for different materials. *Tribol. Int.* 41, 307–314. doi: 10.1016/j.triboint.2007.08.005

De Wit, C. C., Olsson, H., Astrom, K. J., and Lischinsky, P. (1995). A new model for control of systems with friction. *IEEE Trans. Autom. Control* 40, 419–425. doi: 10.1109/9.376053

Eaves, A., Smith, A., Waterhouse, W., and Sansome, D. (1975). Review of the application of ultrasonic vibrations to deforming metals. *Ultrasonics* 13, 162–170. doi: 10.1016/0041-624X(75)90085-2

Eggers, G., Klein, J., Blank, J., and Hassfeld, S. (2004). Piezosurgery®: an ultrasound device for cutting bone and its use and limitations in maxillofacial surgery. *Br. J. Oral Maxillof. Surg.* 42, 451–453. doi: 10.1016/j.bjoms.2004.04.006

Fridman, H. D., and Levesque, P. (1959). Reduction of static friction by sonic vibrations. *J. Appl. Phys.* 30, 1572–1575. doi: 10.1063/1.1735002

Gaberson, H. A. (1971). Particle motion on oscillating conveyors: the equations of motion and the rules for predicting motion form transitions. *J. Eng. Ind.*. 94, 50–56. doi: 10.1115/1.3428154

Gaberson, H. A. (1972). Particle motion on oscillating conveyors-part 2. practical solutions to the equations of motion and the extension of the theory to beds of granular material. *J. Eng. Ind*. 94, 57–63. doi: 10.1115/1.3428155

Godfrey, D. (1967). Vibration reduces metal to metal contact and causes an apparent reduction in friction. *ASLE Trans*. 10, 183–192. doi: 10.1080/05698196708972178

Grzemba, B., Pohrt, R., Teidelt, E., and Popov, V. L. (2014). Maximum micro-slip in tangential contact of randomly rough self-affine surfaces. *Wear* 309, 256–258. doi: 10.1016/j.wear.2013.11.050

Heckl, M. A., and Huang, X. (2000). Curve squeal of train wheels, part 3: active control. *J. Sound Vibrat*. 229, 709–735. doi: 10.1006/jsvi.1999.2512

Mao, X., Popov, V. L., Starcevic, J., and Popov, M. (2017). Reduction of friction by normal oscillations. ii. in-plane system dynamics. *Friction* 5, 194–206. doi: 10.1007/s40544-017-0146-x

Müller, M., and Ostermeyer, G. (2007). Cellular automata method for macroscopic surface and friction dynamics in brake systems. *Tribol. Int*. 40, 942–952. doi: 10.1016/j.triboint.2006.02.045

Murakawa, M., and Jin, M. (2001). The utility of radially and ultrasonically vibrated dies in the wire drawing process. *J. Mater. Process. Technol.* 113, 81–86. doi: 10.1016/S0924-0136(01)00635-5

Pohlman, R., and Lehfeldt, E. (1966). Influence of ultrasonic vibration on metallic friction. *Ultrasonics* 4, 178–185. doi: 10.1016/0041-624X(66)90244-7

Popov, M., and Li, Q. (2018). Multimode active control of friction, dynamic ratchets and actuators. *Phys. Mesomech*. 21, 24–31. doi: 10.1134/S1029959918010046

Popov, M., Popov, V. L., and Popov, N. V. (2017). Reduction of friction by normal oscillations. I. influence of contact stiffness. *Friction* 5, 45–55. doi: 10.1007/s40544-016-0136-4

Popov, V. L. (2017). Oscillation-based methods for actuation and manipulation of nano-objects. *AIP Conf. Proc*. 1882:020056. doi: 10.1063/1.5001635

Popov, V. L., and Heß, M. (2016). *Method of Dimensionality Reduction in Contact Mechanics and Friction.* Berlin: Springer. doi: 10.1007/978-3-642-53876-6

Popov, V. L., Starcevic, J., and Filippov, A. (2010). Influence of ultrasonic in-plane oscillations on static and sliding friction and intrinsic length scale of dry friction processes. *Tribol. Lett*. 39, 25–30. doi: 10.1007/s11249-009-9531-6

Schmidt, J. P., Hagedorn, P., and Bingqi, M. (1996). A note on the contact problem in an ultrasonic travelling wave motor. *Int. J. Nonlin. Mech*. 31, 915–924. doi: 10.1016/S0020-7462(96)00112-6

Siegert, K., and Ulmer, J. (2001). Superimposing ultrasonic waves on the dies in tube and wire drawing. *J. Eng. Mater. Technol*. 123, 517–523. doi: 10.1115/1.1397779

Socoliuc, A., Gnecco, E., Maier, S., Pfeiffer, O., Baratoff, A., Bennewitz, R., and Meyer, E. (2006). Atomic-scale control of friction by actuation of nanometer-sized contacts. *Science* 313, 207–210. doi: 10.1126/science.1125874

Storck, H., Littmann, W., Wallaschek, J., and Mracek, M. (2002). The effect of friction reduction in presence of ultrasonic vibrations and its relevance to travelling wave ultrasonic motors. *Ultrasonics* 40, 379–383. doi: 10.1016/S0041-624X(02)00126-9

Teidelt, E. (2015). *Oscillating contacts: friction induced motion and control of friction* (Ph.D. thesis). TU Berlin, Berlin, Germany.

Teidelt, E., Willert, E., Filippov, A., and Popov, V. L. (2012). Modeling of the dynamic contact in stick-slip microdrives using the method of reduction of dimensionality. *Phys. Mesomech*. 15, 287–292. doi: 10.1134/S1029959912030071

Thoe, T., Aspinwall, D., and Wise, M. (1998). Review on ultrasonic machining. *Int. J. Mach. Tools Manuf.* 38, 239–255. doi: 10.1016/S0890-6955(97)00036-9

Conflict of Interest: The author declares that the research was conducted in the absence of any commercial or financial relationships that could be construed as a potential conflict of interest.

3.7 Publication 10

This short note revisits the case of high-amplitude or "jumping" normal oscillation that was already treated in the original Publication 4. However, the derivation presented in this paper is no longer limited to the harmonic oscillation and presents some new results. The general approach is borrowed from the more recent Publication 9. The first new result is the general shape of the COF under an arbitrary normal oscillation (Eq. 15). Under jumping conditions, the COF is no longer independent of mean indentation depth and the dependence thus gains a second dimensionless parameter. In the general case, this dependence can only be determined numerically, but for triangle waves it can be calculated in closed form (Eqs. 17, 19). It is also possible to describe the asymptotic behavior of the COF if the waveform is shape-invariant under re-scaling (i.e. self-affine). The square wave is such a waveform, and is treated next. However, even not strictly self-affine waveforms can exhibit this behavior at larger amplitudes, which is demonstrated on the example of the harmonic oscillation (Fig. 4).

FACTA UNIVERSITATIS
Series: **Mechanical Engineering** Vol. 19, Nº 1, 2021, pp. 105 - 113
https://doi.org/10.22190/FUME201226017P

Original scientific paper

FRICTION UNDER LARGE-AMPLITUDE NORMAL OSCILLATIONS

Mikhail Popov[1,2]

[1]Technische Universität Berlin, Germany
[2]National Research Tomsk State University, Russia

Abstract. *Building on a recently proposed contact-mechanical theory of friction control by external vibration, the case of large-amplitude normal oscillation is revisited. It is shown that the coefficient of friction can be expressed in particularly simple form if the waveform of the displacement oscillation is triangular or rectangular, and the contact stiffness is constant. The latter requirement limits the scope of the exact solutions to contacts between a plane and a flat-ended cylinder or a curved shape with a wear flat, but the adopted methodology also enables efficient numerical solution in more general cases.*

Key words: *Contact Mechanics, Vibration, Control of Friction, Large Amplitudes, Sliding Friction*

1. INTRODUCTION

The ability of externally applied vibration to substantially reduce both static and sliding friction is well known and enjoys many practical applications. The classical examples of wire drawing [1,2] and metal forming [3,4] deserve mention, but a thorough review is outside the scope of this paper. While the effect has attracted a fair amount of research, most of the works are of an experimental, application-oriented nature [5-7], and proposed models are at best semi-empirical [8]. For this reason, no consensus has been established concerning the theoretical underpinnings of the phenomenon. A possible physical model based on macroscopic contact mechanics was recently proposed by the author and colleagues [9]. The mechanism of force reduction in this model is based on the observation that stick-slip can arise in an oscillating contact under suitable conditions, if the compliance of the contact is taken into account. During the stick phases the lateral force is by definition subcritical (i.e. less than what is required to sustain sliding), and therefore lowers the average friction force. Multiple extensions of this model have since

Received December 26, 2020 / Accepted February 08, 2021
Corresponding author: Mikhail Popov
Technische Universität Berlin, Institut für Mechanik, Fachgebiet Kontinuumsmechanik und Materialtheorie, Sekr. MS2, Einsteinufer 5, D-10587 Berlin
E-mail: mpopov@fastmail.fm

been published and were reviewed in a recent paper [10]. Here, the same approach is used to analyze the case of large-amplitude normal oscillation, when the amplitude is larger than the mean indentation and the body starts to "jump" over the plane.

2. MODEL

For a complete description of the model the reader is referred to previous publications [9,10], but a short overview is provided here for convenience. First and foremost, it is assumed that the contact is quasistatic and that the contact stiffness is independent of indentation depth. Both assumptions are nonessential for the model as such, but are required for analytical calculations. Together, they allow us to treat the contact as a single linearly elastic massless spring (Fig. 1) with normal and lateral stiffness k_z and k_x, respectively. If the modeled contact is a flat-ended cylinder with radius a, the stiffness values are given by:

$$\begin{aligned} k_z &= 2E^* a \quad \text{where} \quad \frac{1}{E^*} = \frac{1-\nu_1^2}{E_1} + \frac{1-\nu_2^2}{E_2} \\ k_x &= 2G^* a \quad \text{where} \quad \frac{1}{G^*} = \frac{2-\nu_1}{4G_1} + \frac{2-\nu_2}{4G_2} \end{aligned} \tag{1}$$

with E_i, G_i being the elastic and shear moduli of the contacting bodies and ν_i their Poisson numbers.

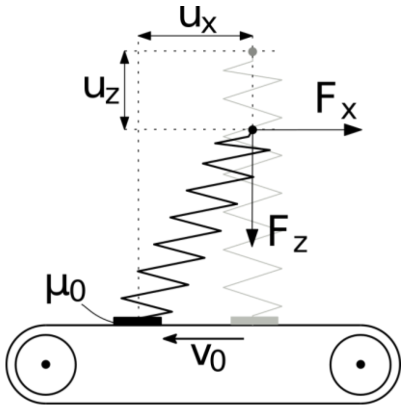

Fig. 1 A single massless spring, which serves as a minimal model of a sliding frictional contact. The sliding velocity is constant, while the vertical coordinate oscillates. Amontons friction with the constant coefficient of friction μ_0 is assumed in the contact.

The spring is pulled with a constant velocity v_0 while also being subjected to a normal oscillation that is parametrized as

$$u_z(t) = \bar{u}_z + A_z w(ft) \tag{2}$$

where $\bar{u}_z$ is the mean indentation, A_z the amplitude, f the frequency and w a zero-mean, unit-amplitude waveform. The lateral displacement u_x is the primary unknown of the system.

When the contact point is in a sliding state, its velocity can be shown to be

$$\dot{u}_x(t) = \mu_0 \frac{k_z}{k_x} A_z f w'(ft) \tag{3}$$

The contact transitions from slip to stick when this velocity vanishes. The point of stick onset $\varphi_1 = ft_1$ can therefore be written as:

$$\varphi_1 = (w')^{-1}(\beta) \tag{4}$$

where β is one of the dimensionless variables that parametrize the behavior of the system:

$$\alpha = \frac{A_z}{\bar{u}_z}, \quad \beta = \frac{k_x v_0}{\mu_0 k_z A_z f}, \quad \varphi = ft \tag{5}$$

The Eq. (4) does not necessarily have solutions. For stick-slip to be present, it is necessary that

$$\beta < \max_{\varphi} w'(\varphi) = \beta_c \tag{6}$$

where β_c is the maximum positive gradient of the oscillation waveform. If the dimensionless velocity β exceeds this threshold value, stick-slip becomes impossible and the macroscopic coefficient of friction $\bar{\mu}$ is the same as the intrinsic coefficient of friction μ_0. Otherwise it is reduced by some amount that depends on α, β and the shape of w.

If condition (6) is satisfied and stick is initiated, the spring continues stretching with the constant velocity v_0 and the lateral spring force therefore increases linearly with time:

$$F_{\text{stick}}(t) = \mu_0 F_z(t_1) + k_x v_0 (t - t_1) \tag{7}$$

This continues while the stick condition $F_{\text{stick}} < \mu_0 F_z(t)$ holds. Substituting $F_z = k_z u_z$ and rearranging gives the end of the stick phase φ_2 in implicit form:

$$\beta(\varphi_2 - \varphi_1) = w(\varphi_2) - w(\varphi_1) \tag{8}$$

The stick-slip process is visualized in Fig. 2.

The macroscopic friction force $\langle F_x \rangle$ is computed by integrating $F_x(t)$ over both the slip and stick periods:

$$\langle F_x \rangle = \frac{1}{T} \int_0^T F_x(t) \mathrm{d}t \tag{9}$$

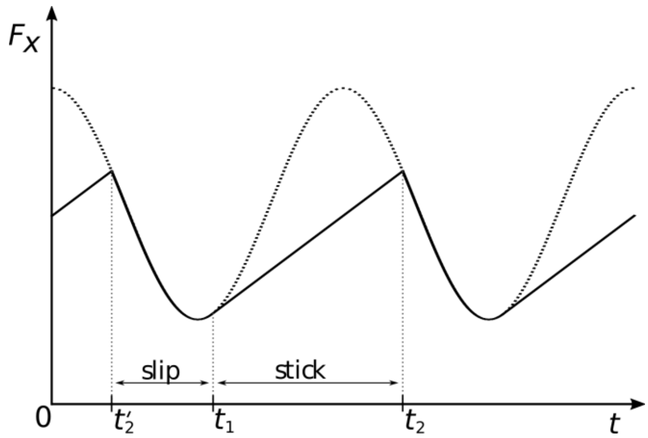

Fig. 2 Stick and slip under the influence of a harmonic oscillation. The dotted line represents the tangential force as it would be in pure slip, $F_{\text{slip}} = \mu_0 F_z(t)$. The solid line is the actual tangential force in the presence of stick-slip. The stick phases are the straight segments, e.g. between t_1 and t_2, while slip phases are the sinusoidal segments, e.g. between t_2' and t_1, repeating periodically. Note that $F_x \leq F_{\text{slip}}$ everywhere, which is the origin of friction reduction in our model.

Since F_x only differs from $\mu_0 F_z$ during the stick phase, it is actually more convenient to determine the absolute force reduction $\Delta F_x = \langle \mu_0 F_z \rangle - \langle F_x \rangle$:

$$\Delta F_x = \frac{1}{T}\int_{t_1}^{t_2} (\mu_0 F_z(t) - F_{\text{stick}}(t))\mathrm{d}t \tag{10}$$

After expanding and rearranging, it is found that ΔF_x can be expressed as

$$\Delta F_x = \mu_0 k_z A_z \Psi_w(\beta) \tag{11}$$

where Ψ_w is a dimensionless "reduction function" that is specific to the waveform w:

$$\Psi_w(\beta) = \int_{\varphi_1}^{\varphi_2} (w(\varphi) - w(\varphi_1) - \beta(\varphi - \varphi_1))\mathrm{d}\varphi \tag{12}$$

The macroscopic coefficient of friction $\bar{\mu}$ can then be recovered through

$$\bar{\mu} = \frac{\langle \mu_0 F_z \rangle - \Delta F_x}{\langle F_z \rangle} = \mu_0 - \frac{\Delta F_x}{k_z \bar{u}_z} = \mu_0 (1 - \alpha \Psi_w(\beta)) \tag{13}$$

This puts the dependence into a very simple form, with most of the complexity contained in a function of one argument, $\Psi_w(\beta)$. This function, however, needs to be determined numerically in most cases.

This concludes our whirlwind tour of the model framework that will be used in the sequel. A less hurried presentation can be found in [10].

3. Large Amplitudes

In the preceding discussion it was implicitly assumed that the amplitude A_z is smaller than the mean indentation $\bar{u}_z$, so that the bodies are permanently in contact and the normal force is non-negative. The purpose of this paper is to extend the analysis to $A_z > |\bar{u}_z|$, that is, cases where the bodies lose contact periodically. Equivalently, $-A_z < \bar{u}_z < A_z$, where we have excluded the trivial no-contact case. This form also makes evident the need for a small re-parametrization:

$$\gamma = \frac{1}{\alpha} = \frac{\bar{u}_z}{A_z} \tag{14}$$

which avoids the singularity at $\bar{u}_z = 0$.

The first thing to note about the jumping case is that the static coefficient of friction is always zero, because the contact obviously cannot sustain a lateral force while it is "in the air", and slow creep will therefore be present at arbitrarily small pulling forces. If measurements of the static coefficient of friction under normal oscillation do not go to zero at suitably large amplitudes, this probably indicates a misalignment in the measurement apparatus.

The second thing to note is that, in general, the simplicity of Eq. (13) can no longer be maintained. The clean separation between α and β is only possible because the stick-slip process is completely independent of mean indentation, so long as the normal force F_z is positive throughout. However, when $u_z(t)$ becomes negative in the jumping case, this causes F_z to become "clipped" at zero (assuming no adhesion). This destroys the invariance w.r.t. $\bar{u}_z$, because the waveform w effectively becomes "cut off", and has to be renormalized to maintain the properties of zero mean and unit amplitude. Thus, $w(\varphi)$ should properly be $w(\gamma,\varphi)$ in the jumping case. Overall, this leads us to expect the coefficient of friction to be a nonlinear function of two parameters (in addition to the waveform dependence):

$$\bar{\mu}_{\text{jmp}} = \mu_0 g_w(\beta, \gamma) \tag{15}$$

In general, the function g needs to be computed numerically. There are, however, a few cases of some practical importance that can be treated analytically. These include square and triangle waves, for which solutions can be obtained in closed form due to their simplicity; and certain self-similar oscillations, for which asymptotic behavior can be deduced. These cases are considered next.

3.1. Special case 1: Sawtooth and triangle wave

Of the possible waveforms with triangular shape, here we consider the left-leaning sawtooth function (stl), the right-leaning sawtooth function (str) and the symmetric triangle wave (tri). The normalized functions w for these waveforms can be defined on the unit interval (with periodic extension understood) as:

$$\begin{aligned} w_{\text{stl}} &= 1 - 2\varphi \\ w_{\text{str}} &= 2\varphi - 1 \\ w_{\text{tri}} &= \begin{cases} 4\varphi - 1, & \varphi < 1/2 \\ 3 - 4\varphi, & \varphi > 1/2 \end{cases} \end{aligned} \tag{16}$$

From geometrical considerations (which come down to determining the area between the waveform and a straight line with the slope β as in Fig. 2), it is easy to show that the corresponding reduction functions $\Psi_w(\beta)$ in the simple non-jumping case are given by:

$$\Psi_{\mathrm{str}}(\beta) = 1 - \frac{\beta}{2}, \quad \Psi_{\mathrm{stl}}(\beta) = \frac{2}{2+\beta}, \quad \Psi_{tri}(\beta) = \frac{4-\beta}{4+\beta} \tag{17}$$

The triangular waves have the unique property that clipping the waveform does not affect the coefficient of friction. To appreciate this, refer once again to Fig. 2. The coefficient of friction is given by the ratio of the area under F_x to the area under $\mu_0 F_z$. This ratio changes continuously as the waveform is clipped from below by increasingly large amplitudes. If the waveform is triangular, however, then the only effect from the cutoff is that the ramp of the stick phase starts later and later (in the point of first contact). The area ratio is not affected, which means that the coefficient of friction remains constant, despite the fact that Ψ_w formally depends on γ. This means that, for triangular waves,

$$\bar{\mu}(\beta, \gamma < 1) = \bar{\mu}(\beta, \gamma = 1) = \mu_0 (1 - \Psi_w(\beta)) \tag{18}$$

Using the reduction functions given in Eq. (17), this provides the following simple results for the coefficient of friction under large-amplitude oscillation:

$$\bar{\mu}_{\mathrm{str}}(\beta) = \mu_0 \frac{\beta}{2}, \quad \bar{\mu}_{\mathrm{stl}}(\beta) = \mu_0 \frac{\beta}{2+\beta}, \quad \bar{\mu}_{tri}(\beta) = \mu_0 \frac{2\beta}{4+\beta} \tag{19}$$

3.2. Special case 2: Self-similar waveforms, Square wave

The triangular waves are a special case of what could be termed *self-similar* waveforms. By this we mean that a cut-off waveform can be rescaled in such a fashion as to be identical to the original waveform. Assuming that the waveform is also *convex* ensures that stick is precipitated in the point of first contact, as in the case of the triangular wave. This means that the stick-slip graph of a cut-off waveform can be rescaled (together with the stick ramp) to have the same area ratio – and therefore the same coefficient of friction – as the same waveform at another cutoff. Of course, this rescaling also changes the slope β, which must be adjusted accordingly. Usually, it is convenient to choose the coefficient of friction at $\gamma = 1$ as a reference point, so that the large-amplitude coefficient of friction of a self-similar waveform can be expressed as:

$$\bar{\mu}(\beta, \gamma) = \mu_0 (1 - \Psi_w(\xi(\beta, \gamma))) \tag{20}$$

The function ξ which provides the remapping of β is specific to the waveform.

After the triangle, the next-simplest example of a self-similar waveform is the square wave, which alternates between 1 and -1 in equal intervals. It is easy to show that the remapping function for such an oscillation is given by:

$$\xi_{\mathrm{sqr}}(\beta, \gamma) = \frac{2\beta}{1+\gamma} \tag{21}$$

Using this mapping and the reduction function Ψ_{sqr} of the square wave (see Eq. (36) in [10]), the coefficient of friction under large-amplitude square wave oscillations can be written as:

$$\frac{\bar{\mu}_{\mathrm{sqr}}}{\mu_0} = \begin{cases} \dfrac{\beta}{4(1+\gamma)}, & \beta < 2(1+\gamma) \\ 1 - \dfrac{1+\gamma}{\beta}, & \beta > 2(1+\gamma) \end{cases} \tag{22}$$

This result is shown in Fig. 3 for the entire range of γ from 1 (starting to separate) to -1 (barely touching).

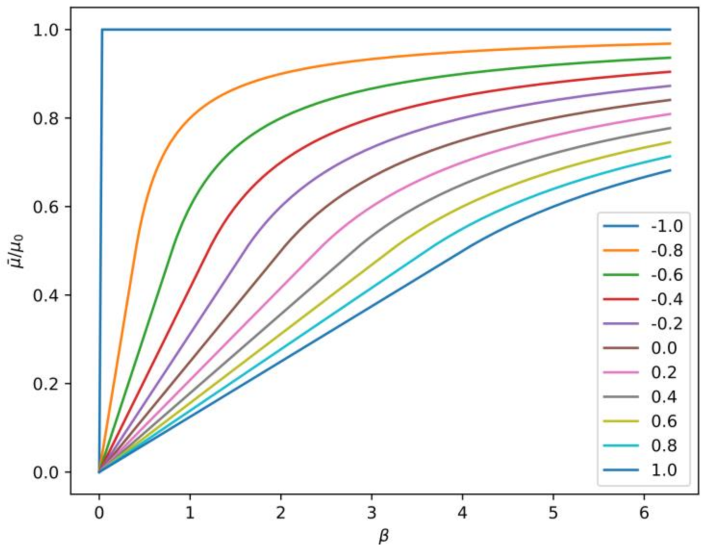

Fig. 3 Coefficient of friction under large-amplitude square wave oscillations with 11 different normalized indentations γ covering the entire jumping range from -1 to 1.

The concept of self-similar waveforms also applies to the harmonic oscillation, to a limited extent. While the entire sine wave is not self-affine according to our definition, it can be approximated piecewise by a parabola over some of its domain. Since the parabola is indeed a self-affine function, we can expect the coefficient of friction under harmonic oscillation to have the described behavior *asymptotically*, although it will not be valid for values of γ close to 1. The remapping function in this case can be shown to be

$$\xi_2(\beta,\gamma) = \beta\sqrt{\frac{1+\gamma_0}{1+\gamma}} \tag{23}$$

where γ_0 is the value of γ at the point where the self-affine scaling behavior started. More generally, for a waveform that can be asymptotically approximated by a power law φ^n, the corresponding remapping can be shown to be

$$\xi_n(\beta,\gamma) = \beta\left(\frac{1+\gamma_0}{1+\gamma}\right)^{1/n} \tag{24}$$

3.3. Numerical example: Harmonic oscillation

As an example of asymptotic scaling, Fig. 4 shows numerically determined coefficients of friction under large-amplitude harmonic oscillation. One thing to note is that for γ in the range of approximately -0.2 to 1, the coefficient of friction depends only weakly on γ, with all curves bunching fairly closely together. The dependence on γ is also non-monotonous in this range, leading to lower coefficients of friction at first (from $\gamma = 1$ to approx. 0.6), and then increasing again (from $\gamma = 0.6$ to -1). The value around $\gamma = -0.3$ is the point from which the remaining part of the cropped waveform can be regarded as roughly parabolical, and the subsequent behavior of the coefficient of friction can be described by the scaling given in Eq. (23). This is also shown in Fig. 4 with black dots.

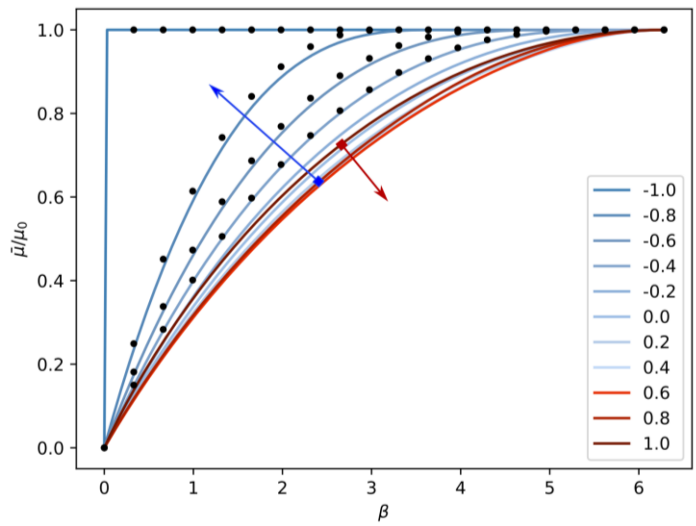

Fig. 4 Numerically computed coefficient of friction under large-amplitude harmonic oscillations with 11 different normalized indentations γ covering the entire jumping range from -1 to 1. Note the non-monotonous dependence on γ: The dark red line corresponds to the critical value $\gamma = 1$, which separates the jumping and non-jumping regions. From there, the coefficient of friction is first reduced with diminishing γ (red lines and arrow) and then increases again (blue lines and arrow) starting somewhere around $\gamma = 0.6$. Black dots indicate the expected scaling behavior according to Eq. (23) relative to $\gamma_0 = -0.3$.

4. Conclusions

The influence of large-amplitude normal oscillation on sliding friction, which has not previously received much attention in the literature, was analyzed in this work, based on a model proposed by the authors in a previous publication. It was shown that the coefficient of friction in the jumping case depends on the same dimensionless variables as in the low-amplitude case, but in a more complicated fashion. At low amplitudes, the influence of the two main variables, α and β is cleanly separated, while at large amplitudes they become entangled and influence the coefficient of friction in a nontrivial manner. This was demonstrated on the example of the harmonic oscillation, where the amplitude-dependence is non-monotonic and can only be determined numerically. However, some simple cases such as triangular, rectangular and more general self-similar waveforms yield relatively simple results, which allow the coefficient of friction to be expressed either in closed form or as an asymptotic scaling relation.

Acknowledgement: *This work was supported in part by the Tomsk State University competitiveness improvement programme, which the author gratefully acknowledges.*

REFERENCES

1. Siegert, K., Ulmer, J., 2001, *Superimposing ultrasonic waves on the dies in tube and wire drawing*, Journal of Engineering Materials and Technology, 123(4), pp. 517–523.
2. Murakawa, M., Jin, M., 2001, *The utility of radially and ultrasonically vibrated dies in the wire drawing process*, Journal of Materials Processing Technology, 113(1-3), pp. 81-86.
3. Eaves, A., Smith, A., Waterhouse, W., Sansome, D., 1975, *Review of the application of ultrasonic vibrations to deforming metals*, Ultrasonics, 13(4), pp. 162-170.
4. Ashida, Y., Aoyama, H., 2007, *Press forming using ultrasonic vibration*, Journal of Materials Processing Technology, 187, pp. 118-122.
5. Pohlman, R., Lehfeldt, E., 1966, *Influence of ultrasonic vibration on metallic friction*, Ultrasonics, 4(4), pp. 178-185.
6. Godfrey, D., 1967, *Vibration reduces metal to metal contact and causes an apparent reduction in friction*, ASLE transactions, 10(2), pp. 183-192.
7. Chowdhury, M.A., Helali, M., 2008, *The effect of amplitude of vibration on the coefficient of friction for different materials*, Tribology International, 41(4), pp. 307-314.
8. De Wit, C.C., Olsson, H., Satrom, K.J., Lischinsky, P., 1995, *A new model for control of systems with friction*, IEEE Transactions on automatic control, 40(3), pp. 419-425.
9. Popov, M., Popov, V.L., Popov, N.V., 2017, *Reduction of friction by normal oscillations. I. Influence of contact stiffness*, Friction, 5(1), pp. 45-55.
10. Popov, M., 2020, *The influence of vibration on friction: a contact-mechanical perspective*, Frontiers in Mechanical Engineering, 6, pp. 69.

Chapter 4

Discussion and Conclusions

This chapter serves as a summary and discussion of the results from the preceding publications. The first section provides a brief overview, discussion and integration of the obtained results, and how they relate to the current state of knowledge in the fields of damping, control of friction, and tribology in general. This is followed by a more philosophical digression about the role that macroscopic effects play in tribology, with some speculation about the possible misattribution of frictional phenomena to the micro-scale. Finally, the limits of the current model and some possible future research directions are discussed.

Note on notation: The presented papers were published over several years, and there were some concomitant changes in notation and terminology. Due to the need for a consistent presentation, the Discussion uses notation from the later publications (esp. P9), and some results from earlier papers were converted to this notation and rearranged in minor ways. However, the differences are mostly superficial and it is hoped that this will not cause too much confusion.

References to equations and figures in the original publications are prefixed with the publication number (such as Eq. P3-15).

4.1 Summary and Discussion of Main Results

4.1.1 Relaxation Damping

The overarching theme of the Publications 1–3 is the impact of the normal degree of freedom on energy dissipation in frictional couples, with a particular focus on an effect called relaxation damping. This effect is introduced in Publication 1, and is so named to contrast it with the ordinary frictional damping of oscillations confined to the contact plane.

When a non-conformal (curved) contact is subjected to periodic loading in the tangential direction *only*, it develops a zone of partial slip at the edge of the contact, where energy is dissipated in every cycle (and which also leads to the well-known fretting wear pattern). The corresponding contact problem was first studied in detail in the early 1950s by Mindlin et al. [42]. For a spherical indenter of radius R indented to a depth d into an elastic plane and subjected to tangential oscillations with an amplitude A_x, the energy lost per cycle due to microslip can be shown to be [63]:

$$W_{\text{Mindlin}} = \frac{2}{3}\frac{{G^*}^2}{E^*}\sqrt{\frac{R}{d}}\frac{A_x^3}{\mu} \tag{4.1}$$

where G^* and E^* are the reduced moduli of shear and elasticity (see Eqs. P1-1 and P1-2). The dissipation is inversely proportional to the coefficient of friction μ and therefore tends to zero in the limit of very high friction. This becomes especially obvious in the case of perfect stick, where there is no relative sliding at all, and therefore no dissipation.

However, when a contact is periodically loaded in both tangential *and normal* directions, qualitatively new behavior appears. Most distinctively, dissipation does *not* tend to zero when the condition of perfect stick is approached. Instead, it reaches a finite value that is determined by the stiffness ratio of the medium (G^*/E^*), the oscillation parameters and a geometry factor. This happens because the normal oscillation causes a periodic change of the contact area, and specifically because contact is lost in areas of nonzero shear stress. This stress is released abruptly and the stored energy is radiated away in the form of elastic waves, which are later thermalized by conventional means. The process can be likened to energy dissipation in a plucked string: elastic potential energy is first converted to vibrational energy—still mechanical, but less available—and is then gradually converted to sound and ultimately to thermal motion.

The mechanism is therefore qualitatively very simple, but it is less obvious how exactly this sort of elastic instability can materialize during *quasi-static motion*. In Publication 1, this is explained by the presence of a moving singularity at the edge of the contact, which is also confirmed by Boundary Element simulations. This kind of "elastic dissipation" has not been previously noted in the context of damping, to the knowledge of the author, but similar effects are occasionally found in other areas of contact mechanics, as pointed out by Ahn [1]. For example, in an elastic wheel rolling with traction on an elastic plane, dissipation is also present in the infinite-friction limit [9]. This happens due to loss of contact in a region of nonzero tangential stress at the trailing edge of the contact, and is therefore quite similar to relaxation damping. Another example is a system transmitting torque between two unequal pulleys via an elastic belt [32].

It should also be stressed that relaxation damping remains a meaningful concept when the coefficient of friction is finite. The physical mechanism described above is then no longer directly applicable, but the overall dynamics is relatively insensitive to the actual value of the COF, so long as a certain operating regime is present. This regime depends on the normal amplitude times μ being large compared to the tangential amplitude (in P1, the criterion $4\mu A_z > A_x$ is suggested). This causes areas in the intermittent contact regions to come into contact relatively abruptly and with immediate sticking. Disengagement during the upward half of the oscillation is likewise fairly abrupt, with actual sliding beginning only very shortly before the final loss of contact. The higher the ratio of normal to tangential amplitude and the higher μ, the shorter this final relaxation period becomes, and the closer does the system approximate the behavior of relaxation damping.

In short, the essential feature of relaxation damping is energy loss by unloading of tangentially stressed regions due to periodic changes of normal force, with the exact dissipation mechanism being less important. Depending on the specifics of the problem, it may take the form of ordinary friction, viscoelastic losses or radiation of elastic waves. The results derived in Publications 1–3 under the assumption of infinite friction are therefore valid in a much broader context. A quantitative study of the finite-friction case and the cross-over to relaxation damping can be found in a recent publication by Hanisch et al. [30].

Let us now turn to some specific results derived in Publication 1. For harmonic oscillations with small amplitudes A_x and A_z and a phase difference φ_0, the energy loss per cycle due to relaxation damping is given by (Eq. P1-12):

$$W = \frac{8G^*}{3E^*}\frac{\partial^2 F_N}{\partial d^2} A_x^2\, A_z \sin^2 \varphi_0 \tag{4.2}$$

A similar result was found for low-frequency tangential oscillations superimposed with high-frequency normal ones. Under the assumption of $\omega_z \gg \omega_x$, the energy dissipated per cycle of the low-frequency oscillation is given by (Eq. P1-17):

$$W = \left(\pi^2 - 4\right) \frac{G^*}{E^*}\frac{\partial^2 F_N}{\partial d^2} A_x^2\, A_z \frac{\omega_x}{\omega_z} \tag{4.3}$$

Notably, both results are valid for any reasonable contact geometry, so long as the second derivative of the normal contact force with respect to indentation, $\partial^2 F_N \,/\, \partial d^2$, can be determined. Eq. (4.2) was derived in Publication 1 analytically for bodies of revolution, and also verified numerically for some decidedly non-axis-symmetric contacts (Fig. P1-3). It was also applied to the contact of rough surfaces (Eq. P1-18). However, it should be kept in mind that this particular result is valid for normal amplitudes that are significantly smaller than l_0, the RMS-roughness of the surface.

An important difference between the classical Mindlin damping (Eq. 4.1) and relaxation damping (Eq. 4.2, 4.3), is that the energy loss in the former is proportional to the *cube* of the tangential amplitude A_x, while in the latter it is proportional to the *square* (and also proportional to the normal amplitude A_z). This difference is significant insofar as the dependence on A_x^3 leads to attenuation of free oscillations according to $A(t) = A_0 \,/ (1 - ct)$, with c being a system-dependent constant [63]. The dependence on A_x^2, on the other hand, leads to exponential attenuation of the in-plane component in contacts with relaxation damping. (Note that normal oscillations are not affected at all, to a first approximation).

This property of relaxation damping has a number of potential applications, for example in the active control and rapid suppression of oscillations in high-precision frictional positioning systems. Enhancement of damping in frictional joints in metallic structures [26] by deliberate introduction of high-frequency normal oscillations is also a possibility. This could be especially useful in the case of stiff and lightweight structures that are prone to vibration and difficult to effectively dampen otherwise, e.g., in aerospace applications. It also seems possible that the well-known ability of externally applied ultrasonic normal oscillations to suppress lower-frequency frictional instabilities is related to relaxation damping and the attendant exponential attenuation. At the time of writing, no concrete data is available to the author in this regard, but this does present a promising avenue for future research.

Another area where relaxation damping can play a role is internal damping in bulk materials. For example, relaxation-damping-like losses in breathing cracks were studied by Argatov et al. [4]. Losses from fiber-fiber contacts in woven fabrics and composite materials [86] are another possibility. These are considered in Publication 2.

The model used in P2 consists of a single contact between two crossed fibers with round cross section. The boundary conditions are chosen such that three ends are held fixed, with the remaining end being subjected to a combined normal and tangential oscillation with a phase shift φ_0. This is only one among many possibilities for modeling a mesh cell in a fabric, and the analysis presented in P1 should be understood as a proof of concept rather than a quantitative study of damping in real fabrics. Linear beam theory and Hertzian contact mechanics are combined to obtain the energy loss per cycle of oscillation (Eq. P2-17):

$$W_{\text{Fiber}} = 2\left(\frac{2}{3}\right)^{2/3} \pi^{5/3} \frac{(1+\nu)(2-\nu)}{(1-\nu^2)^{2/3}} E \left(\frac{R}{d_0}\right)^{4/3} \rho^{-5} A_x^2 A_z \sin^2\varphi_0 \tag{4.4}$$

where E and ν are the elastic modulus and Poisson ratio, R and d_0 are the radius and mean deflection of the fiber, and ρ is the aspect ratio of the fiber segment in a single mesh cell. This result has many similarities with Eq. (4.2), especially the dependence on $A_x^2 A_z \sin^2\varphi_0$. The most significant difference is the inverse-fifth-power dependence on the aspect ratio, which suggests that relaxation damping will be much stronger in densely woven fabrics. However, even if the magnitude of the resulting damping coefficient in a particular fabric or composite is small, the exponential decay of free oscillations may change the overall dynamics of internal damping.

In P3, the final publication of the series, it is shown that relaxation damping is also present in contacts with combined normal and torsional oscillation. Following a derivation similar to P1 and using the extension of the Method of Dimensionality Reduction for torsional contacts, the following result is obtained for phase-shifted harmonic oscillations with small amplitudes A_z and A_φ (Eq. P3-15):

$$W_{\text{Tors}} = \frac{8}{3}\frac{\tilde{G}}{E^*}\frac{\partial^2 F_N}{\partial d^2}(aA_\varphi)^2 A_z \sin^2\varphi_0 \left(1 - \frac{A_z^2}{5d^2}\right) \tag{4.5}$$

where $\tilde{G}$ is the reduced shear modulus for the torsional contact problem (Eq. P3-4) and a is the mean contact radius. aA_φ is the amplitude of in-plane displacements near the edge of the contact (in the region of intermittent contact significant for relaxation damping), and therefore plays the same role as A_x in Eq. (4.2). It should also be noted that for oscillations with $A_z \ll d$, the last term, $1 - A_z^2/5d^2$, will be very close to one, in which case the similarity with Eq. (4.2) becomes even more pronounced.

It is also possible to combine the solutions for relaxation damping with tangential and torsional components (Eq. P3-20). Because the tangential and torsional contact problems are assumed to be uncoupled, the stored elastic energies due to linear (in-plane) and torsional displacements are additive, and are also released at the same time by unloading in the normal direction. Thus, the energy dissipated per cycle in a system with superimposed normal, tangential and torsional oscillations reduces to a sum of the results (4.2) and (4.5).

This concludes our discussion of relaxation damping, which represents a qualitative change in the dynamics of periodically loaded frictional contacts due to the introduction of the normal degree of freedom. The model established here is further developed in the next section by introduction of bulk sliding, which transforms the problem from one of damping in stationary contacts to the reduction and active control of friction. As a parting note, we'd like to point out that, while the derivations presented Publications 1-3 are all based on Method of Dimensionality Reduction, this is not essential. Derivations using the classical methods of contact mechanics have been given by Ahn [1] and Barber [6].

4.1.2 Active Control of Friction

The series of publications 4–10 is devoted to the reduction and active control of friction by externally applied vibration. The contact-mechanical approach is inherited from the earlier publications on relaxation damping, except that the coefficient of friction is now finite and bulk sliding is permitted. Friction under the influence of normal, tangential and transverse oscillations is studied within this framework. The overall result of these studies is that more or less the entire known phenomenology of friction under the influence of vibration can be reproduced by a simple macroscopic model without recourse to specialized laws of friction. This represents a major departure from the established models of friction under transient loading in general, and vibration in particular.

In the context of damping, i.e., *nominally static* frictional contacts under the influence of vibration, the use of macroscopic contact mechanics is well-established at least since the work of Mindlin [42]. But in the case of *nominally sliding* frictional contacts under the influence of vibration, an entirely different paradigm has taken hold—with a strong focus on microscopic mechanisms and empirical friction laws. However, it has to be asked whether such a split is defensible on physical grounds. After all, the two problems can be essentially seen as one, differing only in whether the average lateral loading is zero or not. How can it be that completely different physical mechanisms are postulated in such closely related cases?

Thus, the publications 4–10 are based on the assumption that a Mindlin-style contact mechanical analysis is also applicable to frictional problems. This requires that the contact point be regarded as a proper contact, with compliance in both the normal and lateral directions. In exchange, no special microscopic friction laws are needed, with a constant microscopic coefficient of friction μ_0 being assumed throughout.

Normal Oscillation

The first paper in the series, P4, introduces the model and provides an analysis of the simplest case: static and sliding friction under the influence of a harmonic, displacement-controlled, out-of-plane oscillation. The model initially consists of a single spring (equivalent to a contact of a flat cylindrical punch on a plane) and is later extended to a parabolic surface using the Method of Dimensionality Reduction [63].

The force of static friction follows immediately from the assumptions of the model, and is simply the lowest normal force during an oscillation cycle times the coefficient of friction (if the lateral force is greater than this value, the contact will slide in at least one point of the cycle). Given A_z, the amplitude of the normal oscillation, and $\bar{u}_z$, the mean indentation, the static COF for a flat punch can be written as:

$$\mu_s = \mu_0 \left(1 - \frac{A_z}{\bar{u}_z} \right) \tag{4.6}$$

This reflects the known empirical result that the *static* force of friction depends on the *displacement* or force amplitude. The above equation is valid while $A_z < \bar{u}_z$. Once the amplitude exceeds the mean indentation, μ_s turns to zero, because the contact is unable to statically sustain a lateral load if it is periodically separated from the surface.

However, the core of Publication 4 deals with sliding friction. First, the relative velocity of the contact point and the substrate is determined from the force balance between the lateral contact force and the instantaneous force of friction (Eq. P4-2). The fact that this velocity may turn to zero leads to the conclusion that under certain conditions the contact can transition from slip to stick. This transition can only happen during the phase of increasing normal load and is referred to as *contact pinning* in later publications. For the harmonic oscillation, the condition for the presence of stick-slip is easily shown to be (adapted from Eq. P4-3):

$$v_c = \frac{G^*}{E^*} \frac{v_0}{\mu_0 \omega A_z} < 1 \tag{4.7}$$

The dimensionless quantity v_c is referred to as the *critical velocity of controllability*, and is noteworthy for two reasons. Firstly, the presence of stick-slip determines whether the macroscopic coefficient of friction is affected at all by the applied vibration. If $v_c > 1$, then $\bar{\mu} = \mu_0$ by linearity of Amontons' friction. Together with the static coefficient of friction, the critical velocity therefore sets the boundaries of the detailed dependence of the COF on the system parameters. Secondly, it is found that said dependence is a function of only two dimensionless parameters: the static COF (or equivalently $A_z/\bar{u}_z$), and v_c. Actually, in the non-jumping case ($A_z < \bar{u}_z$), the nontrivial part of the dependence is a function of v_c alone. In P4, this is only verified empirically. A rigorous proof is presented in a later publication (P9). Note also that the known empirical fact that the coefficient of *sliding friction* depends on the *velocity amplitude* is reflected in the term ωA_z being a part of v_c. This difference between the static and sliding cases follows naturally from our model, but is more difficult to accommodate in microscopic and empirical theories.

During the stick phase tangential load increases linearly in proportion to the continued lateral displacement of the upper part of the spring / sliding body. When the lateral load exceeds the instantaneous force of static friction, the transition back to sliding takes place (Eq. P4-7). Note that the lateral force F_x is, by definition, less than $\mu_0 F_z$ during the stick phase. This is ultimately the reason for the reduction of the apparent force of friction in our model: The contact is pinned at higher normal loads and "catches up" when the normal load is reduced again. This process is somewhat analogous to walking.

With the kinematics of the system established, determining the macroscopic coefficient of friction $\bar{\mu}$ is simply a matter of averaging F_x over both the stick and slip phases and dividing by the average normal load. Unfortunately, $\bar{\mu}$ cannot be expressed in terms of standard functions for the harmonic, and most other, oscillations. Publication 4 instead gives a fairly accurate numerical approximation (Eq. P4-11):

$$\frac{\bar{\mu}}{\mu_0} \approx 1 - \frac{A_z}{\bar{u}_z} \left(\frac{3}{4}(1 - v_c)^2 + \frac{1}{4}(1 - v_c)^4 \right) \tag{4.8}$$

An asymptotic expression for low sliding velocities is also provided (Eq. P4-12):

$$\frac{\bar{\mu}}{\mu_0} \approx 1 - \frac{A_z}{\bar{u}_z} \left(\frac{1}{2} v_c^2 - \frac{4\sqrt{\pi}}{3} v_c^{3/2} + \pi v_c - 1 \right) \tag{4.9}$$

In the case where the amplitude exceeds mean indentation, the separation between the two dimensionless variables is no longer given, and a fully nonlinear dependence on both is to be expected. However, in the case of the harmonic oscillation and moderate $A_z/\bar{u}_z$ ratios the shape of the dependence only depends very weakly on this parameter. Thus, as a first approximation, the following expression can be used for the jumping contact (Eq. P4-17):

$$\frac{\bar{\mu}_{\mathrm{jmp}}}{\mu_0} \approx 1 - \left(\frac{3}{4}(1 - v_c)^2 + \frac{1}{4}(1 - v_c)^4 \right) \tag{4.10}$$

Note that the factor $A_z/\bar{u}_z$ is entirely missing from this dependence, since the static COF is always zero in the jumping case, as noted previously. A low-velocity asymptote is also given (Eq. P4-21).

The fact that the same numerical approximation is useful both for a proper harmonic oscillation and for a cut off sinusoid may at first appear surprising. An explanation for this is provided in a later publication (P10), which considers the jumping case in greater detail. It is shown that, for a certain class of waveforms, the effect of an increasing jumping amplitude on the COF is equivalent to a nonlinear rescaling of the critical velocity. For this to be true, the waveform must be piecewise self-similar under rescaling of the axes. This applies to oscillations that are periodic extensions of a power-law (x^k) segment. The degenerate cases of the square ($k = \infty$) and triangle ($k = 0$) waves also meet this definition, and their shapes are simple enough that the coefficient of friction in the jumping case can be given in closed form. For the triangle wave, we get the particularly simple expression

$$\bar{\mu}_{\text{tri}} = \mu_0 \frac{v_c}{1 + v_c} \tag{4.11}$$

(adapted from Eq. P10-19 to match the definition of v_c used here, which would imply a triangle waveform with a period of 4). Similar results for the square wave and the sawtooth in both orientations are given in Eqs. (P10-16,19) and Fig. P10-3.

Returning to the case considered in P4, the harmonic waveform can be regarded as approximately parabolic in a fairly wide interval around the maximum. Thus, a change of amplitude is equivalent to a square-root rescaling of the critical velocity (Eq. P10-23) in a suitable range of amplitudes. But since the results of Publication 4 are generally *normalized* by the critical velocity, this rescaling is essentially eliminated and the dependencies all appear to collapse onto a single curve, which is fairly close to the non-cut-off waveform and can therefore be numerically approximated with the same expression. Later publications (P9 and P10) use a slightly different normalization that exposes the structure of the underlying dependencies more clearly. For example, Fig. P10-4 shows both the complex behavior of the COF under slightly jumping amplitudes—where the parabola is a poor fit for the sinusoid—as well as the predicted scaling behavior for larger amplitudes.

After the basic theory is established using a single-spring system, the contact of curved bodies is also considered in Publication 4. A useful approximation in the case of amplitudes that are much smaller than the mean indentation is to simply use the result (4.8) derived for a single spring. This is possible because the *absolute reduction* of the force of friction turns out to be independent of the average normal load in the non-jumping case (Eq. P4-14). Combining this fact with an MDR-based model, which rigorously maps a 3D contact to an elastic foundation consisting of independent springs, it becomes apparent that the force reduction in the individual springs in the contact region can be averaged and is therefore equivalent to the force reduction in a single spring of the same stiffness as the macroscopic contact.

However, this reasoning is only applicable if the amplitude is small and the influence of the zone of intermittent contact is therefore negligible. For large amplitudes this is not the case, and numerical simulation is required. The results of such a simulation for a parabolic contact are presented in Figs. P4-7 and P4-8.

Influence of System Dynamics

Publication 5 examines the role of system dynamics in the proposed model. All other publications in this thesis are based on the assumption of quasi-staticity. This is a convenient approximation for elucidating basic mechanisms, but may not be sufficient for describing real tribological systems. Since the highly deformed contact region is usually very small (both in size and mass) compared to the entire system, its inertia can almost always be safely neglected, and propagation of elastic disturbances across the contact region can be considered instantaneous. However, the same cannot always be said of the *surrounding system*, and its dynamics in interaction with the contact forces should be described explicitly for realistic modeling. Due to the great diversity of possible systems this is ultimately the realm of numerical simulation and applied engineering. However, Publication 5 provides a very simple example of this hybrid approach, which nonetheless uncovers some qualitatively new behaviors.

The modeled scenario roughly corresponds to a pin-on-disc tribometer with an externally applied out-of-plane harmonic oscillation. The pin is considered to be rigid in the normal direction, but having a finite bending stiffness and mass. In the model these are represented with the system spring k_x and system mass m (Fig. P5-1b). All other aspects of the model are the same as in P4, including the displacement-controlled normal oscillation (only *in-plane* dynamics is simulated).

Since the oscillation is still displacement-controlled, the static COF remains unchanged. The critical velocity differs significantly, however, and is given by Eq. (P5-12):

$$v_c = \frac{v_0}{\mu_0 \omega A_z} \frac{k_{x,c}}{k_{z,c}} \frac{|k_x - m\omega^2|}{|k_{x,c} + k_x - m\omega^2|} < 1 \tag{4.12}$$

Note that P5 defines the critical velocity in a slightly different manner (as an actual dimensional velocity). In keeping with the notation established in P4 and later papers, it has been rewritten in the dimensionless form given above.

Of particular interest is the inertial factor $|k_x - m\omega^2|/|k_{x,c} + k_x - m\omega^2|$. When the system stiffness is very high ($k_x \to \infty$) this factor tends towards 1, and the critical velocity reduces to Eq. (4.7). (Note that the stiffness ratio $k_{x,c}/k_{z,c}$ of a flat-ended contact is equal to the Mindlin ratio G^*/E^*). In the opposite limit of a very soft system and stiff contact ($k_x \ll m\omega^2 \ll k_{x,c}$), the critical velocity reduces to:

$$v_c = \frac{v_0 m\omega}{\mu_0 A_z k_{z,c}} < 1 \tag{4.13}$$

This is equivalent to the condition $v_0 < \mu_0 \Delta F_N / m\omega$ previously reported by Teidelt et al. [78].

Eq. (4.12) also implies the presence of two resonant cases: If $k_{x,c} + k_x - m\omega^2 \approx 0$, the inertial factor tends to infinity, meaning that the condition $v_c < 1$ becomes unsatisfiable even at very small v_0, which further implies that reduction of friction is prevented at all sliding velocities. On the other hand, if $k_x - m\omega^2 \approx 0$, the inertial factor tends to zero, and the stick-slip condition is satisfied even at very high sliding velocities. At large v_0, the coefficient of friction still approaches a plateau value, which is given by Eq. (P5-37):

$$\bar{\mu}_p = \mu_0 \left(1 - \frac{A_z}{2\bar{u}_z}\right) \tag{4.14}$$

Comparing this with Eq. (4.6), it is easily seen that this plateau is situated halfway between μ_0 and the static coefficient of friction.

The two resonances also inform the choice of two dimensionless parameters, α and β, which simplify the parametrization of the system (Eq. P5-20):

$$\alpha = \frac{k_x}{m\omega^2}, \qquad \beta = \frac{k_x + k_{x,c}}{m\omega^2} \tag{4.15}$$

The detailed dependence of $\bar{\mu}$ on v_c, α and β is in general highly nontrivial, with some parameter combinations resulting in multiple intermediate plateaus (Fig. P5-5b) and other features. Thus, a simple approximating formula cannot be given. Instead, a large part of Publication 5 is devoted to a numerical exploration of the (α, β) parameter plane. The main results are summarized graphically in Fig. P5-10.

An additional factor that can have a large impact on the dynamics of a frictional system is inherent damping in the material. This is particularly relevant in frictional contacts with polymers, which can be found, for example, in many types of automotive brake pads. In Publication 6, the critical velocity is derived for a simple viscoelastic material, the Kelvin body:

$$v_c = \frac{v_0}{\mu_0 \omega A_z} \frac{k_{x,c}}{k_{z,c}} \frac{|k_x - m\omega^2|}{\sqrt{\left(\frac{k_{x,c}\gamma_{z,c}\omega}{k_{z,c}}\right)^2 + \left(k_{x,c} + k_x - m\omega^2\right)^2}} < 1 \tag{4.16}$$

(Adapted from Eq. P6-15). The main difference compared to Eq. (4.12) is the presence of the factor $k_{x,c}\gamma_{z,c}\omega / k_{z,c}$, where $\gamma_{z,c}$ is the damping constant of the velocity-proportional dashpot element set in parallel with the "contact spring" (Fig. P6-2). This new addition acts as a damping factor for the resonance associated with β, and may suppress it entirely if the relaxation time $\tau = \gamma_{z,c} / k_{z,c}$ of the material is sufficiently large.

The static coefficient of friction can also be determined (Eq. P6-7):

$$\mu_s = \mu_0 \left(1 - \frac{A_z}{\bar{u}_z}\sqrt{1 + (\omega\tau)^2}\right) \tag{4.17}$$

According to the above equation, large relaxation times and high oscillation frequencies can substantially reduce the static COF from its reference value in the purely elastic problem (Eq. 4.6). However, this is for the most part an artifact of the displacement-controlled formulation, in which the delayed relaxation amounts to a reduction of the effective indentation depth. This is one of the few cases in the presented series of publications where a force-controlled formulation would likely produce qualitatively different results.

Longitudinal Oscillation and Frictional Drives

It has already been noted that vibration is affected not only by normal, but also by longitudinal and transverse oscillations. The longitudinal case, which is the topic of Publication 7, has both similarities and differences compared to the normal oscillation. In the reduction of sliding friction by longitudinal vibration (i.e., aligned with the sliding direction), stick slip once again plays an important role and there is a critical velocity above which stick slip disappears and the effective COF reaches the constant value of μ_0. The critical velocity takes the following particularly simple form (Eq. P7-22):

$$v_c = \frac{v_0}{\omega A_x} < 1 \tag{4.18}$$

In other words, stick slip happens if the velocity amplitude of the longitudinal oscillation exceeds the sliding velocity. When a normal oscillation is added, the combined critical velocity can be expressed as $(v_x^2 + 2v_x v_z \operatorname{sgn} v_0 \cos\varphi_0 + v_z^2)^{1/2}$, where v_x and v_z are the separate critical velocities associated with the tangential and normal oscillations, and φ_0 is the phase shift. Written out, this has the form (Eq. P7-8):

$$v_c = \frac{v_0}{\omega\sqrt{A_x^2 + 2\mu_0 \frac{k_z}{k_x} A_x A_z \operatorname{sgn} v_0 \cos\varphi_0 + \left(\mu_0 \frac{k_z}{k_x} A_z\right)^2}} \tag{4.19}$$

Note that the critical velocity is asymmetric with respect to the direction of motion.

The static coefficient of friction in the purely longitudinal case is given in Publication 9 (adapted from Eq. P9-6):

$$\mu_s = \mu_0 - \frac{k_x A_x}{k_z \bar{u}_z} \tag{4.20}$$

while the static COF in the combined longitudinal-normal case is derived in P7 under some simplifying assumptions. In particular, the case where a large tangential amplitude causes the contact point to reverse the direction of sliding is neglected. The result (Eqs. P7-18,19) is likewise asymmetric, this time depending on the direction of the applied force:

$$\frac{\mu_s}{\mu_0} = 1 - \sqrt{\left(\frac{A_z}{\bar{u}_z}\right)^2 + \frac{2k_x A_z A_x}{\mu_0 k_z \bar{u}_z^2} \operatorname{sgn} F_x \cos\varphi_0 + \left(\frac{k_x A_x}{\mu_0 k_z \bar{u}_z}\right)^2} \tag{4.21}$$

With these quantities established, a numerical parameter study is undertaken in Publication 7. For a pure longitudinal oscillation, the results are presented in Fig. P7-3. At low amplitudes, the velocity dependence of the COF looks nearly identical to the dependencies obtained for the normal case, and can in fact be approximated with the same empirical formula (Eq. 4.8, Eq. P7-21). But note that the appropriate critical velocity needs to be used!

Fig. P7-3 also shows two distinct operating modes: one where the velocity amplitude is moderately larger than the velocity and causes one stick event per cycle, and another where the velocity amplitude is large enough to cause an in-place back-and-forth motion with two stick phases in between. No such behavior is observed in Storck's earlier model [76], but Kapelke and Seemann [33] produced qualitatively similar results by adding elastoplastic friction. In the view of the author this is unnecessary, and is only mentioned here for completeness.

So long as the oscillation is purely normal or purely longitudinal, the apparent friction force is "ordinary", in that the friction vector is directed opposite to the direction of sliding and has the same magnitude in both directions. When both are combined, two notable symmetry-breaking modes are the result. The first one, termed a *dynamic ratchet* in the paper, is represented in Fig. P7-5a and means that the magnitude of the friction force depends on the direction. In the second mode, an *active frictional drive* (Figs. P7-4 and P7-5b) is realized, where the apparent friction force becomes negative, i.e., it acts *in the direction of motion*. The energy for this driving force is supplied by the external oscillation source.

Which of the two modes is present is mostly determined by the amplitude, while the degree of symmetry-breaking is determined by the phase shift. Conventional friction is always realized at maximum phase shift ($\pi/2$), while highest drive efficiency is achieved when the oscillations are in phase or counter-phase ($\varphi_0 = 0$ or π). It should also be stressed that the presented drive mode works under quasi-static conditions and Amontons friction. Usually stick-slip drives exploit inertial effects and the difference between static and dynamic coefficients of friction in their construction (but in turn can be driven by a purely longitudinal oscillation). Thus the approach presented in Publication 7 potentially enlarges the design space for ultrasonic motors and actuators.

Transverse Oscillation

Publication 8 explores the remaining case of *transverse* oscillation. The model is mostly the same as in the other publications, but the contact spring can be deflected in both of the in-plane directions (x and y). The spring is under constant normal load and slides in the x-direction with constant velocity. A harmonic displacement oscillation is applied transversely (in the y-direction).

This mode of operation demonstrates yet another qualitatively different mechanism of friction reduction. While normal oscillations actually reduce total frictional energy dissipation through the previously described walking-like mechanism, longitudinal oscillations only *apparently* reduce friction, by shifting some of the work to the oscillator. Finally, transverse oscillations affect friction by making the friction force vector oscillate in the plane. Since the magnitude of this vector is constant (at least during sliding), but only part of it is projected along the direction of motion, there is an apparent reduction of friction. The presence of stick slip complicates this view somewhat, but does not change it in essence. If the transverse amplitude is large, the macroscopic force of friction can be reduced almost to zero. However, this comes at the cost of ever-increasing energy expenditure that must be invested by the vibrating mechanism.

The reduction mechanism, as described above, does not depend on stick slip, and is therefore present in similar form in the precursor model by Storck et al. [76]. However, the explicit consideration of the contact stiffness still considerably extends the reach of the model. For one, it covers both static and sliding friction, and further exposes much more complex structure depending on the amplitude.

The static coefficient of friction derived in Publication 8 is given by (Eq. P8-16):

$$\mu_s = \mu_0 \sqrt{1 - \left(\frac{A_y k}{\mu_0 F_z} \right)^2} \tag{4.22}$$

where A_y is the transverse amplitude, F_z the average normal load and k the isotropic in-plane contact stiffness. While the static coefficient of friction is thus relatively simple, the critical velocity and coefficient of dynamic friction are somewhat more complex. In the analysis of these quantities, P8 makes the distinction between small and large amplitudes (relative to the typical in-plane spring deflection l_0).

The critical velocity for small amplitudes is given by (adapted from Eq. P8-24):

$$v_{c,\mathrm{lo}} = v_0 \left(\sqrt{\frac{1}{4} + \frac{1}{2} \tilde{y}_0{}^2} - \frac{1}{2} \right)^{-1} \tag{4.23}$$

where $\tilde{y}_0 = A_y / l_0$ is the ratio of the transverse amplitude and the aforementioned average spring deflection (Eq. P8-8). For large amplitudes no closed-form expression can be given, and an empirical approximation is provided instead (adapted from Eq. P8-26):

$$v_{c,\mathrm{hi}} \approx v_0 \sqrt{\frac{4.5}{\tilde{y}_0}} \tag{4.24}$$

A combined approximation for low and high amplitudes is given in Eq. (P8-27). However, it should be noted that the term "critical velocity" is a bit of a misnomer in the case of transverse oscillation. It still discriminates between the presence or absence of stick-slip, but does not—unlike in the previously discussed cases—indicate a qualitative transition in the behavior of the coefficient of friction. This is apparent from Figs. P8-7 and P8-8, in which the dependence of the COF on normalized velocity and amplitude is presented. No clear transitions are visible in these figures at the "critical line".

However, in the case of small amplitudes, the critical velocity is still associated with a plateau-like coefficient of friction that grows very slowly. It's value is given approximately by (Eq. P8-32):

$$\bar{\mu}_1 = 1 - \frac{\tilde{y}_0}{4} \tag{4.25}$$

Interestingly enough, the interpolation between the static case and $\bar{\mu}_1$ at the critical velocity can be accomplished by the same empirical approximation (Eq. 4.8) that was developed for the normal case and was found to be partly applicable in the longitudinal case as well (see also Eq. P8-28 and Fig. P8-9). In the large-amplitude-limit, the coefficient of friction can be determined as well (Eq. P8-35):

$$\bar{\mu}_2 = \frac{2}{\pi} K \left(i \frac{\tilde{y}_0}{\tilde{v}_0} \right) \tag{4.26}$$

where K is the complete elliptic integral of the first kind. In this limit, the model is fairly close to Storck et al. [76], who obtained a fairly similar result, although the parametrization is different (compare Eq. 5 in their paper).

The main results of Publication 8 are visually summarized in Fig. P8-11.

Some Generalizations

Many of the above results are summarized and integrated in Publication 9, from which the present discussion borrows much of its notation and structure. P9 also provides a more general treatment that removes some of the assumptions of earlier papers.

For example, the min-max principle (i.e., the force of static friction is the lowest value, taken over one cycle of oscillation, of the highest sustainable friction force) directly results in closed-form expressions for the static coefficient of friction under oscillation in any of the three directions (Eq. P9-4,6,8), without additional assumptions about contact geometry and oscillation waveform. The static friction condition under multi-directional vibration is also given (Eq. P9-9):

$$\left(F_x + A_{Fx} g_x(t)\right)^2 + \left(A_{Fy} g_y(t)\right)^2 < \mu_0^2 \left(F_z + A_{Fz} g_z(t)\right)^2 \tag{4.27}$$

where F_x is the static tangential load, F_z the static normal load, A_{Fi} are the force amplitudes and $g_i(t)$ the corresponding oscillation waveforms. Unfortunately, this inequality does not in general permit a closed-form solution for the maximum value of F_x, but numerical solution is straight-forward.

P9 also dispenses with the harmonic oscillation, which was assumed in all earlier papers. Instead, a general waveform w with zero mean, unit period and unit maximum value is introduced, in terms of which the oscillation is parametrized (Eq. P9-11):

$$u_z(t) = \bar{u}_z + A_z w(ft) \tag{4.28}$$

This permits decoupling the velocity amplitude from the shape of the waveform (which is equal to ωA for the harmonic oscillation, but not in general), which also allows the transition from the waveform-specific concept of critical velocity, to a fully general pair of dimensionless variables (Eq. P9-16,17):

$$\alpha = \frac{A_z}{\bar{u}_z}, \quad \beta = \frac{k_x v_0}{\mu_0 k_z A_z f} \tag{4.29}$$

Although β looks like the previously defined critical velocity for the normal oscillation, it is important to stress that the harmonic-specific factor $A_z\omega$ has been replaced by the general velocity amplitude $A_z f$. In the same step, the inequality $v_c < 1$ is replaced by $\beta < \beta_c$ where β_c is the maximal positive slope of the waveform w (Eq. P9-20).

With these preliminaries, a more general and abstract treatment of the normal oscillation case is presented, which gives the effective coefficient of friction in the compact form (Eq. P9-33):

$$\bar{\mu} = \mu_0 \left(1 - \alpha \Psi_w(\beta)\right) \tag{4.30}$$

where all non-linear behavior has been encapsulated in the dimensionless and waveform-specific "reduction function" Ψ_w (Eq. P9-31). This function has a number of useful properties that were stated in Publication 9 without proof due to space constraints. The complete development can be found in Appendix A of this thesis.

The generalized derivation makes it possible to compare the effectiveness of different waveforms for friction reduction, and also to determine Ψ_w explicitly for a number of simple waveforms (Eq. P9-34,35,36):

$$\Psi_{\mathrm{str}}(\beta) = 1 - \frac{\beta}{2} \tag{4.31}$$

$$\Psi_{\mathrm{stl}}(\beta) = \frac{2}{2+\beta} \tag{4.32}$$

$$\Psi_{\mathrm{sqr}}(\beta) = \begin{cases} 1 - \beta/8\,, & \text{for } \beta < 4 \\ 2/\beta\,, & \text{for } \beta > 4 \end{cases} \tag{4.33}$$

where "str" and "stl" are the right- and left-leaning sawtooth functions, respectively, and "sqr" is the square wave. It is notable that the effectiveness of the sawtooth wave strongly depends on the orientation. The right-leaning sawtooth produces a slow force increase and an abrupt release, which makes it the least effective waveform. The left-leaning sawtooth, on the other hand, increases the load abruptly—leading to immediate contact pinning—and releases it more slowly. This greatly improves the reduction potential especially at high sliding velocities. Generally speaking, a steep positive slope (reflected in high β_c) is desirable when choosing waveforms.

4.2 Frictional Phenomena: Micro or Macro?

The presented work has hopefully convinced the reader that macroscopic contact mechanics and dynamics is a viable approach for modeling the influence of vibration on friction. The same approach has also been employed by other authors to explain pre-slip and frictional hysteresis, as described in the introduction. Given this, one may be excused for supposing that the phenomenology of friction under arbitrary dynamic loading may be macroscopic in general. Of course, more work would be necessary to be able to state this with confidence.

But this also poses the question whether the same can also apply to other "intrinsic" properties of friction. Could the numerical difference between the coefficients of static and sliding friction, the velocity-dependence, kinetic effects and slow creep possibly be caused by processes taking place at the macro-scale? In the opinion of the author, the answer is affirmative, and there are multiple hints scattered throughout the literature that corroborate this view. But the following discussion should nonetheless be regarded as speculative.

One early example of this view comes from Richard Feynman, who, in his famous *Lectures on Physics* (1964), has the following to say about friction:

> To show that the coefficient μ is nearly independent of velocity requires some delicate experimentation, because the apparent friction is much reduced if the lower surface vibrates very fast. When the experiment is done at very high speed, care must be taken that the objects do not vibrate relative to one another, since apparent decreases of the friction at high speed are often due to vibrations. At any rate, this friction law is another of those semi-empirical laws that are not thoroughly understood, and in view of all the work that has been done it is surprising that more understanding of this phenomenon has not come about.

Feynman does not cite any original sources in the *Lectures*, but in 1967 Tolstoi [81] performed friction experiments using an extremely stiff and well-damped apparatus that strongly suppressed motion and vibration in the normal direction. It was found that no velocity-dependence of the coefficient of friction could be observed under such conditions, and conversely that a strong reduction of friction could be achieved by active vibration at the resonant frequency. This would seem to support Feynman's view that the velocity-dependence of the coefficient of friction is, at least in part, caused by interaction with self-excited vibration. In addition, Tolstoi found that the transition from static to sliding friction is accompanied by a minute displacement in the normal direction, and also that no difference between the static and sliding COF could be measured if this upward displacement was suppressed.

A similar hint of the importance of seemingly unrelated degrees of freedom in frictional experiments was recently provided by Nakano et al. [47]. This concerns the effect of slowly accelerating microscopic creep prior to a stick-slip transition, or "stiction", which has been previously attributed to Dietrich-style rate-state friction [28]. However, Nakano et al. argue that it can also be an artifact of the measurement apparatus. They consider a typical tribological setup, where the frictional sample is guided by a double leaf spring. The spring is very soft in the direction of motion, but very stiff in the normal and transverse directions. This is meant to ensure that the sample can only move longitudinally. However, upon closer inspection, it is shown that the transverse degree of freedom can meaningfully participate in the motion. Given a very small misalignment, which would be difficult to avoid in practice, the contact tends to "rotate out to the side" during the start-up phase. Due to the stiffness anisotropy of the spring this motion would be hard to perceive, but the associated rotation of the friction force vector is actually measurable [46]. When projected onto the direction of motion, this rotating-out looks exactly like the accelerated creep of stiction.

It would go too far, however, to claim that kinetic friction is generally caused by microscopic displacement in a non-principal direction. Other experiments point strongly towards the presence of thermally activated aging effects in the contact, the earliest of which were performed by Coulomb himself [11], who was first to notice that the magnitude of the break-away friction force depends (logarithmically) on prior resting time. Long-term dynamics related to wear are likewise clearly attributable to the micro scale.

Another interesting case is elastomer friction. Here it is generally accepted that the primary dissipation mechanism is due to internal losses in the viscoelastic material. This is corroborated by the famous master curve procedure that relates the velocity- and temperature dependence of elastomer friction. However, finer points remain open to interpretation. For example, in Persson's influential theory of rubber friction with rough surfaces [50], great emphasis is placed on the multiscale nature of rough surfaces, with the assumption that all scales contribute significantly to friction. However, other authors [62, 60, 37] have argued that there is in fact a scale separation, with the main contributors being the smallest corrugation scale on one hand, and macroscopic contact parameters such as radius of curvature and indentation depth on the other.

The mentioned works show that the interpretation of tribological experiments is at the very least highly non-trivial. Even the general scale at which the mechanism is situated is often not easy to narrow down. To rule out large-scale effects, it may be necessary to make three-dimensional displacement and orientation measurements with microscopic precision, and also record generated vibration at ultrasonic frequencies. Needless to say, tribological experiments do not usually go to this trouble. Conversely, ruling out microscopic effects is no less problematic, since direct observation of the contact zone is in general very difficult.

4.3 Limitations and Future Research

The model and methods presented in this thesis have a considerable amount of explanatory and unifying power, but are not without limitations. The most glaring omission of the present work is undoubtedly the current lack of experimental validation, which came about through the author's strong affinity towards theory at the expense of experiment. Nonetheless, a large number of testable predictions are made that can form the basis of future research:

- Quantitative results have been presented for damping in frictional couples under combined tangential/normal oscillation. Coefficients of friction have been calculated under all three directions of oscillation as a function of velocity, amplitude, frequency and other parameters. These results can be directly compared to friction force measurements.

- In addition, specific physical mechanisms have been proposed. For example, it would be interesting to directly observe contact pinning and static force increase during stick, as well as the disappearance of stick-slip near the critical velocity, in the case of normal oscillation. Or maybe the transition from single to dual stick-slip modes in the case of longitudinal oscillation.

- Alternatively, one may try to compare the predicted time-dependence of the lateral force in stick-slip mode (see for example Fig. P9-3), with high resolution force measurements. Such an experiment was in fact attempted by the author's colleague Lars Voll (private communication), but the apparatus turned out to have insufficient stiffness to isolate the deformation of the contact region, and the results were inconclusive.

Apart from experimental verification, there are many opportunities to use the presented theoretical framework for more accurate numerical modeling:

- More realistic contact geometry with indentation-dependent contact stiffness.

- Force-controlled (as opposed to displacement-controlled) boundary conditions.
- Non-quasistatic systems and accurate modeling of surrounding system dynamics.
- Additional research into waveforms and combined multi-directional oscillation.

The model also allows incorporating a more complex friction law than Amontons'. In the author's opinion this is not a very promising idea, as argued previously, but some of the simpler variations, such as using different coefficients for static and sliding friction, are probably worth exploring.

4.4 Conclusion

With this work, the author attempted to make a small contribution to the ongoing endeavor of figuring out the quantitative, specific details of dry friction, and especially friction under dynamic loading. The adopted methodology, developed from the prior work of multiple authors, mostly revolves around the nontrivial and under-appreciated role that macroscopic contact mechanics can play in friction. The influence of contact mechanics is studied in two closely related cases: 1) Active control of friction, where external vibration is used to reduce the force of sliding or static friction. 2) Frictional damping in oscillating contacts, especially with superimposed vibration in two directions.

But this distinction is somewhat artificial, as was shown in this thesis. The discussed phenomena can be understood as special or limiting cases of one and the same system, depending on whether the system moves macroscopically or not, whether the vibrations break symmetry or not, and depending on which physical quantities our attention is drawn to. This is one of the primary advantages of the presented model, that it is able to cover so much phenomenological ground both qualitatively and quantitatively. This is especially true since the presented studies cover only a very limited range of the possible variation of the model—enough to elucidate the main mechanisms and behaviors, but barely scratching the surface of all possible dynamics with regard to practical applications.

It was also the author's hope to convince the reader that the macro-scale can absolutely not be ignored in tribology in general. Coefficients of friction really are system properties, and not local constants. Maybe this view is not very productive for the practicing engineer, but the continued sweeping-under-the-rug of the macro scale even by the research-oriented parts of the tribological community is likely holding back progress in the field. On the positive side, treating friction as a system property does not always result in more complexity. As was shown in the present work, sometimes it is quite sufficient to take into account the contact stiffness or even just the Mindlin ratio.

Appendix A

Extended Discussion of the Normal Oscillation Case

Publication 9 of this thesis presents the most recent formulation of our model. However, being in part an overview article, it was constrained in scope and length, and some proofs and details had to be omitted. An extended analysis of friction under normal oscillation (without jumping) is therefore presented in this appendix.

Note that sections 1-4, describing the model and its basic dynamics, are substantially the same as in Publication 9. They are repeated here for the sake of convenience. The new material is contained in sections 5-6.

A.1 Model

Following Publication 9, we consider a displacement-controlled, quasi-static contact model with force-independent contact stiffness, so that the contact can be regarded as a single linearly elastic spring (Figure A.1). The spring slides over a plane under the action of a normal (not necessarily harmonic) oscillation. The generalization to real contacts of curved bodies is relatively straightforward, but requires numerical simulation. To demonstrate the qualitative behavior of the system, a single spring is quite sufficient.

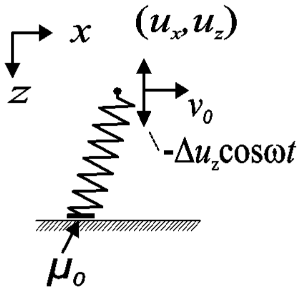

Figure A.1: A single massless spring, which serves as our model of a sliding frictional contact. The sliding velocity is constant, while the vertical coordinate oscillates. Amontons friction with a constant coefficient of friction μ_0 is assumed in the contact point.

The contact spring should not be thought of as a physical object, but rather as an abstract elastic element that maintains proportionality between displacement and force:

$$\begin{aligned} F_x &= k_x \left[u_x - u_{x,c}\right] \\ F_z &= k_z u_z \end{aligned} \tag{A.1}$$

Here F_x and F_z are the lateral and normal spring forces, and k_x and k_z the corresponding stiffnesses. u_z denotes the normal displacement (with the z-axis pointing into the plane). u_x is the nominal displacement of the spring in the tangential direction, relative to an arbitrary starting point. $u_{x,c}$ is the tangential displacement of the *contact point*, and $(u_x - u_{x,c})$ therefore represents the lateral stretch of the spring.

The spring is moved horizontally with a constant velocity v_0, while also being subjected to an arbitrary normal oscillation:

$$\begin{aligned} u_x(t) &= v_0 t \\ u_z(t) &= \bar{u}_z + A_z w(ft) \end{aligned} \tag{A.2}$$

Here $\bar{u}_z$ is the mean indentation, A_z is the amplitude and f the frequency of the oscillation. $w(\varphi)$ is a dimensionless function describing the shape of the oscillation, with $\varphi = ft$. The waveform w is normalized such that it is zero-mean, with a period of 1 and a minimum value of -1. This makes the definition of amplitude ($A_z = \bar{u}_z - \min_t u_z(t)$) consistent with its meaning in static friction. Note, however, that the chosen parametrization does not constrain the *maximum* of w: In general, $\max_t u_z(t) \neq \bar{u}_z + A_z$. Unless noted otherwise, w is assumed to be continuous and differentiable, although this requirement can be relaxed in many cases (e.g., to admit the sawtooth function). Note that, since u_x and u_z are given as explicit functions of time, the displacement $u_{x,c}$ of the contact point is the only unknown of the system.

In this analysis, we assume that the amplitude is less than the mean indentation, so that there is always contact between the spring and the plane, and the normal force is consequently always non-negative. Finally, Amontons' law of friction (with a constant coefficient of friction μ_0 that is the same for both static and sliding friction) is assumed in the contact point.

A.2 Slip state and slip-to-stick transition

While the contact is sliding, the spring force is in equilibrium with the friction force: $F_x = \mu_0 F_z$, which can also be written as:

$$k_x \left[u_x(t) - u_{x,c}(t)\right] = \mu_0 k_z u_z(t) \tag{A.3}$$

Substituting u_x and u_z from Eq. (A.2) and rearranging gives the position of the contact point:

$$u_{x,c}(t) = v_0 t - \mu_0 \frac{k_z}{k_x} \left[\bar{u}_z + A_z w(ft)\right] \tag{A.4}$$

The velocity of the contact point is therefore:

$$\dot{u}_{x,c}(t) = v_0 - \mu_0 \frac{k_z}{k_x} A_z f w'(ft) \tag{A.5}$$

Note that we use the common convention of denoting time derivatives with a dot (as in $\dot{u}_{x,c}(t)$) and other derivatives with a prime (as in $w'(\varphi)$).

To initiate stick, the velocity of the contact point must turn to zero. Applying this condition to Eq. (A.5), the point of stick onset can be determined:

$$ft_1 = \left(w'\right)^{-1}\left(\frac{k_x v_0}{\mu_0 k_z A_z f}\right) \tag{A.6}$$

Thus it becomes apparent that the time of stick onset is a function of a single compound variable, which combines all system parameters, *except* the mean indentation $\bar{u}_z$. To simplify further calculations, we introduce the dimensionless variables α (corresponding to amplitude), β (corresponding to velocity) and φ (phase):

$$\alpha = \frac{A_z}{\bar{u}_z} \tag{A.7}$$

$$\beta = \frac{k_x v_0}{\mu_0 k_z A_z f} \tag{A.8}$$

$$\varphi = ft \tag{A.9}$$

Using these variables, the static coefficient of friction for a single spring can be expressed as $\mu_s = \mu_0[1-\alpha]$, while Eq. (A.6) can be written as

$$\varphi_1 = \left(w'\right)^{-1}(\beta) \tag{A.10}$$

This equation can only have solutions if

$$\beta < \max_{\varphi} w'(\varphi) = \beta_c \tag{A.11}$$

where β_c is the critical value that separates the stick-slip regime from continuous sliding. As mentioned previously, active control of friction is only possible in the presence of stick-slip.

A.3 Stick state and stick-to-slip transition

During the stick phase the contact point stands still, while the upper point of the spring continues to move with the velocity v_0. The tangential force during stick therefore increases linearly with time:

$$F_{\text{stick}}(t) = \mu_0 F_z(t_1) + k_x v_0 \left[t - t_1\right] \tag{A.12}$$

The stick phase lasts while the condition for static friction is satisfied:

$$F_{\text{stick}}(t) < \mu_0 F_z(t) \tag{A.13}$$

and ends at some time t_2 such that $F_{\text{stick}}(t_2) = \mu_0 F_z(t_2)$. Expanding this condition yields

$$\mu_0 k_z u_z(t_1) + k_x v_0 \left[t_2 - t_1\right] = \mu_0 k_z u_z(t_2) \tag{A.14}$$

or, more conveniently,

$$\frac{v_0 k_x}{\mu_0 k_z}\left[t_2 - t_1\right] = u_z(t_2) - u_z(t_1) \tag{A.15}$$

Substituting the explicit form of u_z and $t = \varphi/f$, this can be rewritten as:

$$\beta\left[\varphi_2 - \varphi_1\right] = w(\varphi_2) - w(\varphi_1) \tag{A.16}$$

This gives the stick-to-slip transition in implicit form. Unfortunately, the equation cannot be solved symbolically for φ_2 except in the simplest cases (sawtooth, square wave, etc). E.g., in the case of a harmonic oscillation, Eq. (A.16) takes the form ($\cos x = a + bx$), which does not have a solution in terms of standard functions. Numerical solution is required in most cases. But note that φ_2 depends only on β (since φ_1 is itself a function of only β).

A.4 Macroscopic coefficient of friction

The macroscopic (as opposed to instantaneous) force of friction is simply the tangential force averaged over one period ($T = 1/f$) of oscillation:

$$\langle F_x \rangle = \frac{1}{T} \int_0^T F_x(t)\, \mathrm{d}t \tag{A.17}$$

However, it will become clear in a moment that it is more convenient to consider the difference or *reduction* of the force of friction relative to the state of continuous sliding:

$$\Delta F_x = \langle F_\mathrm{slip} \rangle - \langle F_x \rangle = \frac{1}{T} \int_0^T \left[F_\mathrm{slip}(t) - F_x(t) \right] \mathrm{d}t \tag{A.18}$$

Since F_x only differs from F_slip during the stick phase, we can tighten the integration bounds and rewrite the above as

$$\Delta F_x = \frac{1}{T} \int_{t_1}^{t_2} \left[\mu_0 F_z(t) - F_\mathrm{stick}(t) \right] \mathrm{d}t \tag{A.19}$$

This form is suitable for numerical solution. However, some additional properties can be gleaned by substituting the definitions of F_stick (Eq. A.12) and $u_z(t)$.

$$\begin{aligned}
\Delta F_x &= \frac{1}{T} \int_{t_1}^{t_2} \left[\mu_0 F_z(t) - \mu_0 F_z(t_1) - k_x v_0 \left[t - t_1 \right] \right] \mathrm{d}t \\
&= \frac{1}{T} \int_{t_1}^{t_2} \mu_0 k_z \left[\bar{u}_z + A_z w(ft) - \bar{u}_z - A_z w(ft_1) - \frac{k_x v_0}{\mu_0 k_z} \left[t - t_1 \right] \right] \mathrm{d}t \\
&= \mu_0 k_z A_z \int_{\varphi_1}^{\varphi_2} \left[w(\varphi) - w(\varphi_1) - \beta \left[\varphi - \varphi_1 \right] \right] \mathrm{d}\varphi
\end{aligned} \tag{A.20}$$

Note the use of the substitution ($\mathrm{d}t = T\, \mathrm{d}\varphi$) in the last step. This result shows that the expression for ΔF_x can be split into the dimensional factor $\mu_0 k_z A_z$ and a dimensionless function Ψ_w of a single variable:

$$\Delta F_x = \mu_0 k_z A_z \Psi_w(\beta) \tag{A.21}$$

where

$$\Psi_w(\beta) = \int_{\varphi_1}^{\varphi_2} \left[w(\varphi) - w(\varphi_1) - \beta \left[\varphi - \varphi_1 \right] \right] \mathrm{d}\varphi \tag{A.22}$$

This expression can often be integrated (depending on w), but a complete symbolic solution is usually precluded by the lack of an explicit solution for φ_2, as mentioned earlier.

As evidenced by (A.21), the *absolute reduction* of the friction force does not depend on the mean normal force / indentation. The same is not true for the *coefficient of friction*:

$$\bar{\mu} = \frac{\langle \mu_0 F_z \rangle - \Delta F_x}{\langle F_z \rangle} = \mu_0 - \frac{\Delta F_x}{k_z \bar{u}_z} \tag{A.23}$$

However, the dependence on $\bar{u}_z$ is incidental, merely reflecting the fact that ΔF_x is subtracted from different baselines of friction force. Using our dimensionless variables, the above can also be written in the following compact form:

$$\bar{\mu} = \mu_0 \left[1 - \alpha \Psi_w(\beta) \right] \tag{A.24}$$

A.5 General properties of Ψ_w

The reduction function $\Psi_w(\beta)$ has a number of useful properties that are (nearly) independent of the waveform w. In particular, it is strictly monotonously decreasing, convex, and has unit range. In the following, these properties are proved under the assumption that w is differentiable and that there is one stick phase per oscillation cycle. In practice, the listed properties usually hold even when w does not satisfy these criteria. However, a fully general proof seems to be more trouble than it is worth, so we confine ourselves to a single stick event and differentiable w.

Monotonicity is shown by taking the derivative of Ψ_w with respect to β. For this, we use Leibniz's formula for the derivative of a definite integral:

$$\frac{\mathrm{d}}{\mathrm{d}\xi}\int_{a(\xi)}^{b(\xi)} f(x,\xi)\,\mathrm{d}x = \int_a^b \frac{\partial f}{\partial \xi}\,\mathrm{d}x + f(b,\xi)\frac{\mathrm{d}b}{\mathrm{d}\xi} - f(a,\xi)\frac{\mathrm{d}a}{\mathrm{d}\xi} \tag{A.25}$$

Noting that the integrand in the definition of Ψ_w (Eq. A.22) is zero at both bounds, and assuming that the derivatives of φ_1 and φ_2 are finite, we can immediately discard the last two terms of Leibniz's formula and are left with:

$$\frac{\mathrm{d}\Psi_w}{\mathrm{d}\beta} = \int_{\varphi_1}^{\varphi_2} \frac{\partial}{\partial\beta}\left[w(\varphi) - w(\varphi_1) - \beta\left[\varphi - \varphi_1\right]\right]\mathrm{d}\varphi \tag{A.26}$$

$$= -\int_{\varphi_1}^{\varphi_2}\left[\varphi - \varphi_1\right]\mathrm{d}\varphi + \int_{\varphi_1}^{\varphi_2}\left[-w'(\varphi_1)\frac{\mathrm{d}\varphi_1}{\mathrm{d}\beta} + \beta\frac{\mathrm{d}\varphi_1}{\mathrm{d}\beta}\right]\mathrm{d}\varphi \tag{A.27}$$

Since $w'(\varphi_1) = \beta$ by definition of φ_1 (Eq. A.10), the second integral cancels, while the first one results in the pleasingly simple expression

$$\frac{\mathrm{d}\Psi_w}{\mathrm{d}\beta} = -\frac{1}{2}[\varphi_2 - \varphi_1]^2 = -\frac{\Delta\varphi^2}{2} \tag{A.28}$$

where $\Delta\varphi$ is the length of the stick phase. Since the resulting derivative is obviously negative for all w and β, this concludes the proof of monotonicity.

Convexity is shown by taking the second derivative:

$$\frac{\mathrm{d}^2\Psi_w}{\mathrm{d}\beta^2} = -\Delta\varphi\cdot\frac{\mathrm{d}\Delta\varphi}{\mathrm{d}\beta} \tag{A.29}$$

The duration of the stick phase $\Delta\varphi$ is positive by definition, while its derivative in β is negative, because the stick phase shrinks with increasing velocity[1]. The second derivative of Ψ_w is therefore positive for all w and β, which shows that the function is convex.

Since Ψ_w is monotonous, determining its range is just a question of considering two extreme points: In the static limit ($\beta = 0$), we have $\bar{\mu} = \mu_s$, and consequently:

$$\mu_0\left[1 - \alpha\,\Psi_w(0)\right] = \mu_0\left[1 - \alpha\right] \tag{A.30}$$

from which we immediately obtain $\Psi_w(0) = 1$. At the other extreme, when the system transitions to pure sliding ($\beta = \beta_c$), we have $\bar{\mu} = \mu_0$:

$$\mu_0\left[1 - \alpha\,\Psi_w(\beta_c)\right] = \mu_0 \tag{A.31}$$

[1]Formal proof of this is omitted. However, it is easy to see that the stick condition is met at a later time when velocity increases, while the transition back to slip comes earlier (because the tangential force increases faster during stick). Thus, the stick interval shrinks overall.

from which we obtain $\Psi_w(\beta_c) = 0$. Thus, we can conclude that Ψ_w decreases monotonously from 1 to 0, as β increases from 0 to β_c. In short, Ψ_w is a very well-behaved function that should be easy to approximate numerically, even if the underlying waveform w is complex or discontinuous. This is a very useful property considering that closed-form solutions for Ψ_w are usually not possible.

With these insights, we can also give an alternative definition for Ψ_w which is shorter than Eq. (A.22) and occasionally more convenient:

$$\Psi_w(\beta) = 1 - \frac{1}{2}\int_0^\beta \Delta\varphi^2 \,\mathrm{d}\beta \tag{A.32}$$

While Eq. (A.22) describes Ψ_w in terms of the difference between the potential sliding friction force and the actual static force, the new equation casts Ψ_w in terms of how increasing β progressively makes this difference smaller. (If we increase β by some small increment $\mathrm{d}\beta$, the integral of F_{stick} will increase by a thin triangular sliver with the base $\Delta\varphi$ and height $\Delta\varphi\,\mathrm{d}\beta$, while the integral of F_{slip} will not change).

Another interesting observation is that the coefficient of friction (Eq. A.24) can be rewritten as

$$\bar{\mu} = \mu_s + \mu_0\frac{\alpha}{2}\int_0^\beta \Delta\varphi^2 \,\mathrm{d}\beta \tag{A.33}$$

In other words, we can regard the coefficient of sliding friction under normal oscillation as consisting of a static friction term and a dynamic dissipation term, which for small β (and consequently $\Delta\varphi \approx 1$) takes the form

$$\frac{\mu_0\alpha\beta}{2} = \frac{k_x v_0}{2k_z\bar{u}_z f} \tag{A.34}$$

Note that in this form the dynamic contribution depends neither on amplitude or μ_0. It is a sort of “elastic friction”, closely related to the concept of relaxation damping presented in the first part of this thesis.

A.6 The fine print: Multiple stick events, periodicity, etc.

In the analysis so far, several tacit assumptions were made, namely that there is exactly one stick event per oscillation cycle, that it is entirely contained in said cycle and that it does not change from one cycle to the next. For the sake of completeness, these assumptions will be discussed here.

Let us begin with multiple stick phases per cycle. First we note that the onset of stick φ_1 is inherently ambiguous due to the periodicity of the oscillation. Therefore, the φ_1 in Eq. (A.10) should be understood as the smallest φ_1 greater than some arbitrary starting point φ_0. Likewise, φ_2 in Eq. (A.16) refers, strictly speaking, to the smallest φ_2 that is greater than φ_1. If a further stick phase is possible in the same cycle, we solve again for $\varphi_{1,a}$ that is greater than φ_2 and then for $\varphi_{2,a} > \varphi_{1,a}$. This process is repeated as necessary until all stick events have been identified. Note that this does not change the fact that the bounds of each stick phase are functions of β and are independent of $\bar{u}_z$. Therefore, the reduction function Ψ_w can be generalized for n stick events in a straightforward manner:

$$\Psi_w(\beta) = \sum_{i=1}^{n} \Psi_{w,i}(\beta) \tag{A.35}$$

where $\Psi_{w,i}$ is the reduction function for the i-th event only. In short, nothing changes qualitatively when there is more than one stick period per cycle of oscillation.

The number of stick events per cycle depends on β. In the static limit there is generally a single stick event lasting for almost the entire oscillation cycle. As β increases, this stick event may split into smaller separate stick phases. Each such "division event" has the interesting property that Ψ'_w changes discontinuously where they occur: If $\Delta\varphi$ is the length of the stick phase just before division, then $\Psi'_w = -\Delta\varphi^2/2$ (Eq. A.28). If the event is split into to halves of $\Delta\varphi/2$ each, Ψ'_w for each of them will be 1/4 as large as before, and the overall slope will be half as large. A less even split will have a less pronounced effect. One way to think about this behavior is that every split effectively increases the frequency of oscillation, thus making it more effective at reducing friction at high β.

Concerning the periodicity and stability of the stick-slip cycles, we first note that periodicity is only established after a certain run-in period, which depends on velocity. If an indenter is first pressed into the plane in the normal direction, and only then begins to move sideways, it needs to first build up a certain tangential force before it can begin to slide. In the limit of very low velocities this pre-loading might take long enough to have an impact on system dynamics. The run-in time can be estimated as

$$t_{\text{pre}} \approx \frac{\mu_0 k_z}{v_0 k_x} \cdot \min u_z \tag{A.36}$$

Once the system begins to slip, it becomes periodic, with the same period as the oscillation. This is intuitively clear, but for a formal argument, consider the point in the oscillation cycle at which the normal force is minimal. Assume for contradiction that the system is in a state of stick at this point. This implies that the tangential force $F_{x,1}$ on the spring is less than $(\mu_0 \cdot \min F_z)$. This is possible if the system started in stick (e.g. during run-in). However, if the current stick state was preceded by slip, the tangential force $F_{x,0}$ at the slip-stick transition must have been less than $F_{x,1}$, since F_x increases linearly during stick. This implies that at some point $(F_{x,0} < \mu_0 \cdot \min F_z)$ occurred in a sliding state, which is a contradiction. Thus, once slip sets in, it recurs at the point of minimal force/indentation in every oscillation cycle. Since the free variable of the system $u_{x,c}$ is uniquely determined at this point and evolves deterministically, we conclude that it is periodic.

Since the state of the system is periodic, with the same period as the oscillation, the "beginning" of the cycle can be chosen arbitrarily. In particular, it can be chosen such that all stick events are contained in the cycle and do not cross its "boundaries", which was implicitly assumed throughout the preceding analysis.

Bibliography

[1] Y. J. Ahn. "Relaxation damping and friction". *International Journal of Mechanical Sciences* 128 (2017), pp. 147–149.

[2] A. Akay. "Acoustics of friction". *The Journal of the Acoustical Society of America* 111.4 (2002), pp. 1525–1548.

[3] G. Amontons. "De la resistance cause'e dans les machines, tant par let frottements des parties qui les component, que par la roideur des cordes qu'on y employe, et la maniere de calculer l'un et l'autre". *Mem. l'Academie R* (1699), pp. 257–282.

[4] I. Argatov, V. Popov, T. Rademacher, and M. Zehn. "A model of a breathing crack with relaxation damping". *International Journal of Engineering Science* 93 (2015), pp. 46–50.

[5] Y. Ashida and H. Aoyama. "Press forming using ultrasonic vibration". *Journal of Materials Processing Technology* 187 (2007), pp. 118–122.

[6] J. R. Barber. *Contact mechanics*. Vol. 250. Springer, 2018.

[7] J. Benad, K. Nakano, V. L. Popov, and M. Popov. "Active control of friction by transverse oscillations". *Friction* 7.1 (2018), pp. 1–12.

[8] F. P. Bowden, F. P. Bowden, and D. Tabor. *The friction and lubrication of solids*. Vol. 1. Oxford university press, 2001.

[9] F. Carter. "On the action of a locomotive driving wheel/Proc. R. Soc. London: 112A" (1926).

[10] M. A. Chowdhury and M. Helali. "The effect of amplitude of vibration on the coefficient of friction for different materials". *Tribology International* 41.4 (2008), pp. 307–314.

[11] C. Coulomb. "Theorie des machines simple (Theory of simple machines, reprint)". *Bachelier, Paris* (1821).

[12] P. R. Dahl. *A solid friction model*. Tech. rep. Aerospace Corp El Segundo Ca, 1968.

[13] M. Davies, J. Barber, and D. Hills. "Energy dissipation in a frictional incomplete contact with varying normal load". *International Journal of Mechanical Sciences* 55.1 (2012), pp. 13–21.

[14] C. De Wit, H. Olsson, K. J. Astrom, and P. Lischinsky. "A new model for control of systems with friction". *IEEE Transactions on automatic control* 40.3 (1995), pp. 419–425.

[15] J. H. Dieterich. "Time-dependent friction and the mechanics of stick-slip". *Rock Friction and Earthquake Prediction*. Springer, 1978, pp. 790–806.

[16] J. H. Dieterich. “Modeling of rock friction: 1. Experimental results and constitutive equations”. *Journal of Geophysical Research: Solid Earth* 84.B5 (1979), pp. 2161–2168.

[17] P. Dupont, V. Hayward, B. Armstrong, and F. Altpeter. “Single state elastoplastic friction models”. *IEEE Transactions on automatic control* 47.5 (2002), pp. 787–792.

[18] A. Eaves, A. Smith, W. Waterhouse, and D. Sansome. “Review of the application of ultrasonic vibrations to deforming metals”. *Ultrasonics* 13.4 (1975), pp. 162–170.

[19] C. Edeler. *Modellierung und Validierung der Krafterzeugung mit Stick-Slip-Antrieben für nanorobotische Anwendungen*. Verlag Dr. Hut, 2011.

[20] C. Edeler, I. Meyer, and S. Fatikow. “Modeling of stick-slip micro-drives”. *Journal of Micro-Nano Mechatronics* 6.3-4 (2011), pp. 65–87.

[21] G. Eggers, J. Klein, J. Blank, and S. Hassfeld. “Piezosurgery: an ultrasound device for cutting bone and its use and limitations in maxillofacial surgery”. *British Journal of oral and maxillofacial surgery* 42.5 (2004), pp. 451–453.

[22] A. Erdemir and C. Donnet. “Tribology of diamond-like carbon films: recent progress and future prospects”. *Journal of Physics D: Applied Physics* 39.18 (2006), R311.

[23] H. D. Fridman and P. Levesque. “Reduction of static friction by sonic vibrations”. *Journal of applied physics* 30.10 (1959), pp. 1572–1575.

[24] H. A. Gaberson. “Particle Motion on Oscillating Conveyors—Part 2. Practical Solutions to the Equations of Motion and the Extension of the Theory to Beds of Granular Material”. *Journal of Engineering for Industry* 94.1 (1972), pp. 57–63.

[25] H. A. Gaberson. “Particle Motion on Oscillating Conveyors: The Equations of Motion and the Rules for Predicting Motion Form Transitions”. ASME. 1972.

[26] L. Gaul and J. Lenz. “Nonlinear dynamics of structures assembled by bolted joints”. *Acta Mechanica* 125.1-4 (1997), pp. 169–181.

[27] D. Godfrey. “Vibration reduces metal to metal contact and causes an apparent reduction in friction”. *ASLE transactions* 10.2 (1967), pp. 183–192.

[28] B. Grzemba. “New experimental investigations on the Dieterich-Ruina Law”. *Facta Universitatis, Series: Mechanical Engineering* 13.1 (2015), pp. 11–20.

[29] B. Grzemba, R. Pohrt, E. Teidelt, and V. L. Popov. “Maximum micro-slip in tangential contact of randomly rough self-affine surfaces”. *Wear* 309.1-2 (2014), pp. 256–258.

[30] T. Hanisch, I. Richter, and Q. Li. “Frictional energy dissipation in a contact of elastic bodies subjected to superimposed normal and tangential oscillations”. *Physical Mesomechanics* 23.6 (2020), pp. 556–561.

[31] M. A. Heckl and X. Huang. “Curve squeal of train wheels, part 3: active control”. *Journal of Sound and vibration* 229.3 (2000), pp. 709–735.

[32] K. L. Johnson. *Contact mechanics*. Cambridge university press, 1985.

[33] S. Kapelke and W. Seemann. “On the effect of longitudinal vibrations on dry friction: Modelling aspects and experimental investigations”. *Tribology Letters* 66.3 (2018), pp. 1–11.

[34] N. Kinkaid, O. M. O’Reilly, and P. Papadopoulos. “Automotive disc brake squeal”. *Journal of sound and vibration* 267.1 (2003), pp. 105–166.

[35] W. Lenkiewicz. “The sliding friction process—effect of external vibrations”. *Wear* 13.2 (1969), pp. 99–108.

[36] J. Li and J. Luo. “Advancements in superlubricity”. *Science China Technological Sciences* 56.12 (2013), pp. 2877–2887.

[37] Q. Li, M. Popov, A. Dimaki, A. Filippov, S. Kürschner, and V. L. Popov. “Friction between a viscoelastic body and a rigid surface with random self-affine roughness”. *Physical review letters* 111.3 (2013), p. 034301.

[38] X. Mao, V. L. Popov, J. Starcevic, and M. Popov. “Reduction of friction by normal oscillations. II. In-plane system dynamics”. *Friction* 5.2 (2017), pp. 194–206.

[39] N. Milahin and J. Starcevic. “Influence of the normal force and contact geometry on the static force of friction of an oscillating sample”. *Physical Mesomechanics* 17.3 (2014), pp. 228–231.

[40] N. Milahin. “Robuste Einflussparameter für Reibung und Oberflächenmodifizierung unter Einfluss von Ultraschall”. PhD thesis. Technische Universität Berlin, 2016.

[41] N. Milahin, Q. Li, J. Starcevic, et al. “Influence of the normal force on the sliding friction under ultrasonic oscillations”. *Facta Universitatis, Series: Mechanical Engineering* 13.1 (2015), pp. 27–32.

[42] R. Mindlin, W. Mason, T. Osmer, and H. Deresiewicz. “Effects of an oscillating tangential force on the contact surfaces of elastic spheres”. *Journal of Applied Mechanics-Transactions of the ASME*. Vol. 18. 3. ASME-AMER Soc Mechanical Eng 345 E 47TH ST, NEW YORK, NY 10017. 1952, pp. 331–331.

[43] M. Mracek and J. Wallaschek. “A system for powder transport based on piezoelectrically excited ultrasonic progressive waves”. *Materials chemistry and physics* 90.2-3 (2005), pp. 378–380.

[44] M. Müller and G. Ostermeyer. “Cellular automata method for macroscopic surface and friction dynamics in brake systems”. *Tribology International* 40.6 (2007), pp. 942–952.

[45] M. Murakawa and M. Jin. “The utility of radially and ultrasonically vibrated dies in the wire drawing process”. *Journal of Materials Processing Technology* 113.1-3 (2001), pp. 81–86.

[46] K. Nakano. “Several Aspects of Static Friction – Approach from Structural Asymmetry”. Presented at 9th International Forum on Fundamentals of Sliding Friction and Vibration. 2019.

[47] K. Nakano and V. L. Popov. “Dynamic stiction without static friction: The role of friction vector rotation”. *Physical Review E* 102.6 (2020), p. 063001.

[48] H. X. Nguyen, E. Teidelt, V. L. Popov, and S. Fatikow. “Dynamic tangential contact of rough surfaces in stick-slip microdrives: Modeling and validation using the method of dimensionality Reduction”. *Physical Mesomechanics* 17.4 (2014), pp. 304–310.

[49] G. Ostermeyer. “On the dynamics of the friction coefficient”. *Wear* 254.9 (2003), pp. 852–858.

[50] B. N. Persson, O. Albohr, U. Tartaglino, A. Volokitin, and E. Tosatti. “On the nature of surface roughness with application to contact mechanics, sealing, rubber friction and adhesion”. *Journal of physics: Condensed matter* 17.1 (2004), R1.

[51] R. Pohlman and E. Lehfeldt. “Influence of ultrasonic vibration on metallic friction”. *Ultrasonics* 4.4 (1966), pp. 178–185.

[52] M. Popov and Q. Li. “Multimode Active Control of Friction, Dynamic Ratchets and Actuators”. *Physical Mesomechanics* 21.1 (2018), pp. 24–31.

[53] M. Popov, V. L. Popov, and R. Pohrt. “Relaxation damping in oscillating contacts”. *Scientific reports* 5 (2015), p. 16189.

[54] M. Popov. “Non-frictional damping in the contact of two fibers subject to small oscillations”. *Facta Universitatis, Series: Mechanical Engineering* 13.1 (2015), pp. 21–25.

[55] M. Popov. “Critical velocity of controllability of sliding friction by normal oscillations in viscoelastic contacts”. *Facta Universitatis, Series: Mechanical Engineering* 14.3 (2016), pp. 335–341.

[56] M. Popov. “The influence of vibration on friction: a contact-mechanical perspective”. *Frontiers in Mechanical Engineering* 6.10.3389 (2020), p. 69.

[57] M. Popov. “Friction under large-amplitude normal oscillations”. *Facta Universitatis, Series: Mechanical Engineering* 19.1 (2021), pp. 105–113.

[58] M. Popov and V. L. Popov. “Relaxation damping in contacts under superimposed normal and torsional oscillation”. *Physical Mesomechanics* 19.2 (2016), pp. 178–181.

[59] M. Popov, V. L. Popov, and N. V. Popov. “Reduction of friction by normal oscillations. I. Influence of contact stiffness”. *Friction* 5.1 (2017), pp. 45–55.

[60] V. L. Popov. “What does friction really depend on? Robust governing parameters in contact mechanics and friction”. *Physical Mesomechanics* 19.2 (2016), pp. 115–122.

[61] V. L. Popov. “Oscillation-based methods for actuation and manipulation of nano-objects”. *AIP Conference Proceedings* 1882.1 (2017), p. 020056.

[62] V. L. Popov, A. Dimaki, S. Psakhie, and M. Popov. “On the role of scales in contact mechanics and friction between elastomers and randomly rough self-affine surfaces”. *Scientific reports* 5 (2015), p. 11139.

[63] V. L. Popov and M. Heß. *Method of dimensionality reduction in contact mechanics and friction*. Springer, 2016.

[64] V. L. Popov, J. Starcevic, and A. Filippov. “Influence of ultrasonic in-plane oscillations on static and sliding friction and intrinsic length scale of dry friction processes”. *Tribology letters* 39.1 (2010), pp. 25–30.

[65] V. Popov, B. Grzemba, J. Starcevic, and M. Popov. “Rate and state dependent friction laws and the prediction of earthquakes: What can we learn from laboratory models?” *Tectonophysics* 532 (2012), pp. 291–300.

[66] E. Popova and V. L. Popov. “The research works of Coulomb and Amontons and generalized laws of friction”. *Friction* 3.2 (2015), pp. 183–190.

[67] C. Putignano, M. Ciavarella, and J. Barber. “Frictional energy dissipation in contact of nominally flat rough surfaces under harmonically varying loads”. *Journal of the Mechanics and Physics of Solids* 59.12 (2011), pp. 2442–2454.

[68] J. R. Rice. “Constitutive relations for fault slip and earthquake instabilities”. *Instabilities in continuous media*. Springer, 1983, pp. 443–475.

[69] A. L. Ruina. “Slip instability and state variable friction laws”. *Journal of Geophysical Research: Solid Earth* 88.B12 (1983), pp. 10359–10370.

[70] J. P. Schmidt, P. Hagedorn, and M. Bingqi. “A note on the contact problem in an ultrasonic travelling wave motor”. *International journal of non-linear mechanics* 31.6 (1996), pp. 915–924.

[71] M. Schroeder and M. Herbich. “Fractals, chaos, power laws”. *Pure and Applied Geophysics* 147.3 (1996), pp. 601–601.

[72] K. Siegert and J. Ulmer. “Influencing the friction in metal forming processes by superimposing ultrasonic waves”. *CIRP Annals-Manufacturing Technology* 50.1 (2001), pp. 195–200.

[73] K. Siegert and J. Ulmer. “Superimposing ultrasonic waves on the dies in tube and wire drawing”. *Journal of Engineering Materials and technology* 123.4 (2001), pp. 517–523.

[74] A. Socoliuc, E. Gnecco, S. Maier, O. Pfeiffer, A. Baratoff, R. Bennewitz, and E. Meyer. “Atomic-scale control of friction by actuation of nanometer-sized contacts”. *Science* 313.5784 (2006), pp. 207–210.

[75] J. Starcevic and A. Filippov. “Simulation of the influence of ultrasonic in-plane oscillations on dry friction accounting for stick and creep”. *Physical Mesomechanics* 15.5 (2012), pp. 330–332.

[76] H. Storck, W. Littmann, J. Wallaschek, and M. Mracek. “The effect of friction reduction in presence of ultrasonic vibrations and its relevance to travelling wave ultrasonic motors”. *Ultrasonics* 40.1 (2002), pp. 379–383.

[77] E. Teidelt. “Oscillating contacts: Friction induced motion and control of friction”. PhD thesis. 2015.

[78] E. Teidelt, J. Starcevic, and V. L. Popov. “Influence of Ultrasonic Oscillation on Static and Sliding Friction”. *Tribology Letters* 48.1 (2012), pp. 51–62.

[79] E. Teidelt, E. Willert, A. Filippov, and V. L. Popov. “Modeling of the dynamic contact in stick-slip microdrives using the method of reduction of dimensionality”. *Physical Mesomechanics* 15.5 (2012), pp. 287–292.

[80] T. Thoe, D. Aspinwall, and M. Wise. “Review on ultrasonic machining”. *International journal of machine tools and manufacture* 38.4 (1998), pp. 239–255.

[81] D. Tolstoi. “Significance of the normal degree of freedom and natural normal vibrations in contact friction”. *Wear* 10.3 (1967), pp. 199–213.

[82] M. Urbakh, J. Klafter, D. Gourdon, and J. Israelachvili. “The nonlinear nature of friction”. *Nature* 430.6999 (2004), pp. 525–528.

[83] J. Wallaschek. “Contact mechanics of piezoelectric ultrasonic motors”. *Smart materials and Structures* 7.3 (1998), p. 369.

[84] R. Wetter and V. L. Popov. “The influence of system dynamics on the frictional resistance: insights from a discrete model”. *Tribology Letters* 61.2 (2016), p. 15.

[85] V. Zaloj, M. Urbakh, and J. Klafter. “Modifying friction by manipulating normal response to lateral motion”. *Physical review letters* 82.24 (1999), p. 4823.

[86] X. Zhou, E. Shin, K. Wang, and C. Bakis. “Interfacial damping characteristics of carbon nanotube-based composites”. *Composites Science and Technology* 64.15 (2004), pp. 2425–2437.

List of publications included in this thesis

This work was prepared in accordance with the rules for a cumulative thesis, i.e., based on prior publications. The following ten peer-reviewed papers, in the given order, form the core of the thesis. All papers are presented in the final pubslished version and in the publisher's original format.

Chapter 2

1. M. Popov, V. L. Popov, and R. Pohrt. "Relaxation damping in oscillating contacts". *Scientific reports* 5 (2015), p. 16189. https://doi.org/10.1038/srep16189

2. M. Popov. "Non-frictional damping in the contact of two fibers subject to small oscillations". *Facta Universitatis, Series: Mechanical Engineering* 13.1 (2015), pp. 21–25

3. M. Popov and V. L. Popov. "Relaxation damping in contacts under superimposed normal and torsional oscillation". *Physical Mesomechanics* 19.2 (2016), pp. 178–181. https://doi.org/10.1134/S1029959916020107

Chapter 3

4. M. Popov, V. L. Popov, and N. V. Popov. "Reduction of friction by normal oscillations. I. Influence of contact stiffness". *Friction* 5.1 (2017), pp. 45–55. https://doi.org/10.1007/s40544-016-0136-4

5. X. Mao et al. "Reduction of friction by normal oscillations. II. In-plane system dynamics". *Friction* 5.2 (2017), pp. 194–206. https://doi.org/10.1007/s40544-017-0146-x

6. M. Popov. "Critical velocity of controllability of sliding friction by normal oscillations in viscoelastic contacts". *Facta Universitatis, Series: Mechanical Engineering* 14.3 (2016), pp. 335–341. https://doi.org/10.22190/FUME1603335P

7. M. Popov and Q. Li. "Multimode Active Control of Friction, Dynamic Ratchets and Actuators". *Physical Mesomechanics* 21.1 (2018), pp. 24–31. https://doi.org/10.1134/S1029959918010046

8. J. Benad et al. "Active control of friction by transverse oscillations". *Friction* 7.1 (2018), pp. 1–12. https://doi.org/10.1007/s40544-018-0202-1

9. M. Popov. "The influence of vibration on friction: a contact-mechanical perspective". *Frontiers in Mechanical Engineering* 6.10.3389 (2020), p. 69. https://doi.org/10.3389/fmech.2020.00069

10. M. Popov. "Friction under large-amplitude normal oscillations". *Facta Universitatis, Series: Mechanical Engineering* 19.1 (2021), pp. 105–113. https://doi.org/10.22190/FUME201226017P